A TREATISE ON THE PLASTICALLY INTERACTED STRUCTURAL BEHAVIOR OF COLLAPSING BARS AND FRAMES

BY

TAIJIRO NONAKA

DECEMBER 1975

PREFACE

The contents of this treatise consist of the results obtained by the author in a series of studies on the plastic behavior of structures. Useful methods have been developed by predecessors to determine the plastic collaspe loads of structures, and are available in books, which have amounted to be next to uncountable up to date, first appearing from the end of the nineteen-fourties. The plastic collapse loads, as afforded by these books, are believed to provide a structural analyst with a design basis more reasonable than the conventional elastic design. The absolute pertinence of the plastic design, however, may not be established unless the post-collapse structural behavior is clarified. It is the objective of this treatise to contribute to better understanding of the behavior in the entire range of loading for plastically collapsing structures.

The structures considered herein are restricted to be of such a type that the constituent structural members can be regarded as one-dimensional continua with cross-sectional dimensions of the order of magnitude less than the axial dimensions. In teams of technical application, bars, beams, columns, braces, frames and trusses are comprised in this type of structures. We restrict ourselves to planar structural behavior; lying in a plane, structural members are assumed to deform in this plane without twisting. With these restrictions imposed on the structural type and deformation, the behavior of structures can be analysed in terms of a bending moment, axial force and shear, which play the role of generalized stresses.

When a ductile structure or a structure with overall toughness is loaded into a post-collapse range, it often undergoes a considerable amount of deformation or is subject to loads of large magnitude so that the use of a single generalized stress becomes irrelevant, and the interaction of the components of the generalized stresses plays an important role. Special attention is focused on such interaction effects in the plastic range. Efforts are directed to derive a closed-form analytic solution for each problem at the cost of minor effects, in order for the results to be of general application and also to serve as a basis of comparison with more elaborate numerical analyses. With these in mind perfect plasticity is employed as a fundamental assumption in most of the theoretical studies.

A brief sketch is made of the author's works to be presented, following the preparatory articles on the definitions of terminology and on the general plastic behavior of a typical structure discussed on the basis of the previously established theory of perfect plasticity for small deformation. The first chapter is concerned with the interaction effect of bending and axial loading on plastic collapse loads. The next five chapters are devoted to the hysteretic behavior of bars and frames under repeated loading in the light of the plastic interaction. In the last two chapters the interaction effects in the area of plastic dynamics are examined. Based on the papers with single authorship, each chapter deals with a particular topic and is self-contained with nomenclature, bibliography and formulation independent of one another. The contributive significance of these studies is left undiscussed until the general plastic behavior has been introduced. The results of the last chapter were obtained in the course of work directed toward a degree of Doctor of Philosophy, and are to be regarded as belonging to the Appendix. The treatise is also appended with the abstracts of papers by the author which are not covered in the text.

The author expresses his gratitude to Professors Yoshitsura Yokoo and Minoru Wakabayashi of Kyoto University for the continual encouragement and suggestive comments made in the course of the studies presented herein. He also wishes to thank Professor Paul S. Symonds of Brown University for valuable advice he received in his graduate work. Professor Masao Naruoka of Nagoya University and Dr. Tsuneyoshi Nakamura of Kyoto University gave the author the opportunity to make a contribution to their book; a part of the introductory chapter herein is taken from the author's participation in the book. He appreciates their encouragement as well as their interest in his work. The author feels indebted to many of his collaborators, to whom acknowledgements are made at the end of each chapter for their respective assistance.

T. Nonaka

Kyoto

December, 1975

CONTENTS

INTRODUCTION

This introductory chapter is intended to familiarize the reader with the terminology adopted in the content of the treatise as well as to illustrate the general behavior of an elastic-perfectly plastic structure under variable loading. With these as preparatory knowledge, a brief survey is made of the scope of the works to follow.

DEFINITIONS

The term perfectly plastic is meant to indicate the absence of the second order effects in the plastic range such as hardening and viscosity and at the same time implies the presence of ample ductility. Since the stresses in a structure of perfectly plastic material cannot exceed the yield limit anywhere, the loads applied to the structure cannot be increased indefinitely. When the loads attain certain critical magnitudes, the perfectly plastic structure collapses plastically and indefinitely increasing deformation makes the structure incapable of supporting any further increase of the loads, provided any change in geometry is negligible. Such a critical system of loads is termed a collapse or limit load system, and the distribution of the unlimited plastic flow is often called a collapse mechanism. The alternative definition is that the collapse load system is the system of the loads at which the structure of rigid-plastic material begins to undergo deformation.

In the limit or collapse analysis the loads are assumed to be applied statically, monotonously, proportionally or simultaneously. A structure is often subjected to several loads each of which can be applied repeatedly and can vary independently of one another, within certain prescribed limits. Such a load system, referred to as variable repeated loading, can lead a structure to a state of plastic failure, even if no single application of any load combination causes plastic collapse or instantaneous collapse. The failure by cyclic plastic deformation can take place in one of two ways. If the loads are essentially alternative in character, one or more of the members might be subject to yielding in tension and compression alternately or bent back and forth repeatedly, indicating a possibility of rupture. Such behavior is termed alternating plasticity or yield. In the other type of failure, plastic deformation is built up incrementally in each cycle, eventually leading to unacceptably large deformation by a number of critical combinations of loads following one another in fairly definite cycles. The structure is then said to have failed by incremental collapse, deflection instability or progressive plastic deformation.

In a statically indeterminate structure, being accompanied by some plastic deformation, a state of residual stress or of self-stress or self-equilibrated state of stress can exist, which keeps the structure in equilibrium without any external loads. It is possible for the structure to be free from the failure by cyclic plastic deformation, if, at an early stage of the loading program, such a state of residual stress is built up so that the stress due to elastic response of the structure to subsequent loads within the prescribed limits may be superimposed on these residual stresses without exceeding the yield limit at any point of the structure. The structure is then said to shake down to a state of residual stress and the corresponding state of permanent deformation. It is recognized that the plastic collapse and shake-down loads are determined independently of the past history or path of the loading within the restrictions of perfect plasticity and the absence of change in geometry.

EXAMPLE OF ELASTIC-PLASTIC BEHAVIOR*

Let us consider a simple structure and visualize the elastic-perfectly plastic type of behavior in which the afore-defined phenomena can occur. A singly indeterminate truss is subjected to a load P with fixed direction and slowly varying intensity as shown in Fig. 1. Three members ($i = 1, 2, 3$) are assumed to carry only axial forces and to have an elastic-perfectly plastic property. In the elastic range the axial elongations Δ_i are related linearly to the tensile forces N_i through $\Delta_i = c_i N_i$ with the compliance c_i as the proportional factors, where the subscripts refer to particular members. The yield limit is specified by $Y_i > 0$ for tension, and $Y_i' < 0$ for compression. Infinitesimal deformation is assumed with change in geometry neglected so that no instability phenomena take place.

We regard N_i as the sums of the elastic components N_i^e which would be caused if the truss were perfectly elastic without limit and the residual components N_i^r so that $N_i = N_i^e + N_i^r$. The elastic response is determined by the instantaneous load as

$$N_i^e = p_i P \tag{1}$$

where the proportionality factors p_i are given from the distribution of c_i and overall geometry. The residual forces N_i^r, on the other hand, depend on the entire history of loading because of the history-dependent or irreversible nature of plasticity, and are equal to the axial forces which are attained

* The material presented in this section is based on the author's article, Reference [1] on page 15.

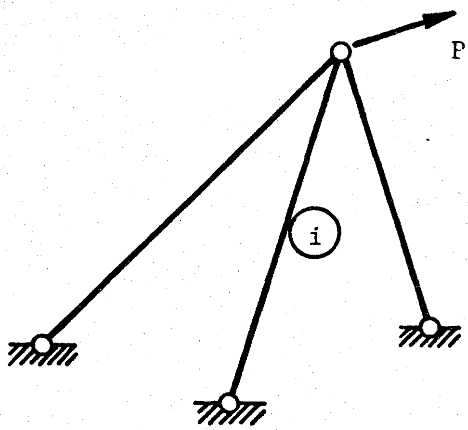

Fig. 1 Example

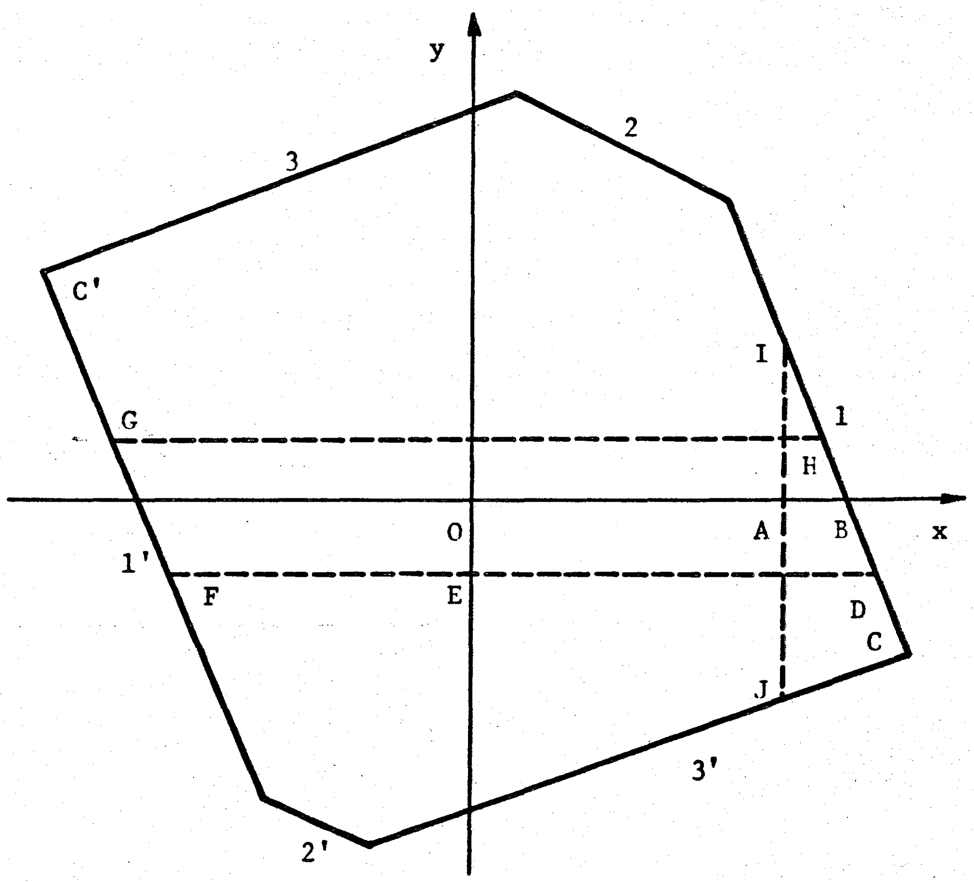

Fig. 2 Stress plane

by the complete removal of the load if the unloading process is elastic. The set of the components N_i^r forms a state of self-stress. We introduce the fictitious strain energy E corresponding to the axial forces N_i as

$$E=\frac{1}{2}\sum_{i=1}^{3}c_iN_i^2=\frac{1}{2}\sum_{i=1}^{3}c_i(N_i^e)^2+\sum_{i=1}^{3}c_iN_i^eN_i^r+\frac{1}{2}\sum_{i=1}^{3}c_i(N_i^r)^2. \tag{2}$$

The second term in the extreme-right side of Eq.(2) can be interpreted as the sum of the work done by the internal forces N_i^r on the elastic elongations $c_iN_i^e$. Since N_i^r are in equilibrium with P=0 and since $c_iN_i^e$ are compatible with a displacement at the joint of load application, the principle of virtual work gives the sum to be equal to the work done by the zero load on the joint displacement. The second term vanishes therefore. The first and third terms are rewritten by noting that N_i^e are related to P through Eq.(1) and that the two independent equations of equilibrium at the joint are combined to express the three forces N_i^r (i = 1, 2, 3) in terms of a parameter R in the form $N_i^r = r_iR$, where r_i are given from the geometry of the truss, whereas R depends on the loading history. With x and y, being proportional to P and R respectively, defined from

$$x=P\cdot\left\{\frac{1}{2}\left(\sum_{i=1}^{3}c_ip_i^2\right)\right\}^{1/2},\qquad y=R\cdot\left\{\frac{1}{2}\left(\sum_{i=1}^{3}c_ir_i^2\right)\right\}^{1/2} \tag{3}$$

it follows that

$$E=\frac{P^2}{2}\sum_{i=1}^{3}c_ip_i^2+\frac{R^2}{2}\sum_{i=1}^{3}c_ir_i^2=x^2+y^2. \tag{4}$$

Considering that

$$N_i=p_iP+r_iR \tag{5}$$

and taking note of Eq.(3), we see that the state of stress of the truss is represented by a point in the plane with x and y taken as the horizontal and vertical co-ordinate axes as shown in Fig. 2. It is also seen from

Eq.(4) that the energy E equals the square of the distance between the point and the origin of the co-ordinate axes. The perfect plasticity fixes the limits for the stress point by $Y_i' \leqq N_i \leqq Y_i$, i.e., by

$$Y_i' \leqq \left[p_i \Big/ \left\{ \frac{1}{2} \sum_{i=1}^{3} (c_i p_i^2) \right\}^{1/2} \right] x + \left[r_i \Big/ \left\{ \frac{1}{2} \sum_{i=1}^{3} (c_i r_i^2) \right\}^{1/2} \right] y \leqq Y_i \tag{6}$$

so that three pairs of parallel lines 1,1'; 2,2'; 3,3' enclose the convex allowable domain, which is symmetric with respect to the origin if $Y_i = -Y_i'$. It is found from Eqs.(3) and (5) that any states of stress in equilibrium with the load P have stress points on the equilibrium line IJ perpendicular to the x-axis. The actual stress point lies on this line segment, and has the ordinate corresponding to the true residual state of stress. If the truss is free from any previous plastic straining the principle of minimum strain energy determines the stress point to be located at point A, the intersection of the line of equilibrium with the x-axis. The stress point moves along the x-axis for the initial elastic response corresponding to the varying load, and member ① yields when the stress point arrives at point B, the truss becoming statically determinate. A further increase of the load is accompanied by a movement of the stress point along the line 1 until point C is reached, where the yield limit is also attained in member ③. There is no allowable state of equilibrium beyond this load, $P = P_c$. If the load reverses its direction at point D somewhere before reaching the point C, an elastic recovery takes place along line DF parallel to the x-axis, and the complete removal of the load, $P = 0$, leaves a residual state of stress as represented by point E. A further decrease in the load $P < 0$ causes a further shift of the stress point to the left, and the member ① is stressed to its yield limit at point F with the sign of the axial force opposite to that developed along the line 1. The arrival at point C' indicates the plastic collapse with $P = P_C' < 0$. Suppose the load can vary arbitrarily within the limits $P_G \leqq P \leqq P_D$, where the state G lies on the line 1' somewhere between the points F and C'. The repetition of particular cycles in the load

$$O \rightarrow P_D \rightarrow P_G \rightarrow P_D \rightarrow O$$

forces the stress point to move in a cyclic manner as in

$$O \rightarrow A \rightarrow B \rightarrow D \rightarrow E \rightarrow F \rightarrow G \rightarrow H \rightarrow B \rightarrow D \rightarrow E.$$

The member ① undergoes yielding in tension and compression alternately, and a large number of repetitions may lead to failure by alternating plasticity. If it is prescribed that the load varies in $P_F \leqq P \leqq P_D$, then the stress point travels along the line segment DF, indicating the elastic response; shake-down takes place after undergoing the plastic straining corresponding to the line segement BD in early ranges of the loading program.

Let us consider the example of changes in temperature at the load $P = P_A$. The stress point is again allowed to move along the segment IJ; stresses built up by a temperature change constitute a state of self-stress. If the stress point reaches the point I, the intersection of the line IJ and the line 1, then the truss is turned into a statically determinate one with plastic straining in the member ① under constant axial forces on all the members. A similar situation arises at point J, the intersection of the lines 3' and IJ, with plastic straining in the member ③ . If such a cycle of temperature changes is repeated, plastic strains accumulate with the same sign in each of the members, and a large number of repetitions eventually may lead to the incremental collapse of the truss with the same collapse mechanism as at the plastic collapse of the point C. If, on the other hand, the range of the temperature variation corresponds to a length less than the length $\overline{IJ}$, a shake-down state is reached, possibly after some plastic straining, and subsequently the truss responds in an elastic manner. It may be of interest to note in this connection that the state of stress varies only in a restricted range, no matter how large the range of the temperature variation may be. Another interesting feature is that the state of stress depends only on the overall distribution of the temperature and not on the precise local distribution. It is not difficult to demonstrate the occurrence of the incremental collapse under load variation alone.

Since an elastic response to a temperature change causes a change in the ordinate or the state of self-stress, it is convenient to separate the components N_i^r into the components due to the elastic response to the temperature change and the remaining residual components $\overline{N_i^r}$ so that the axial forces N_i are the sums of the three components, viz., the components due to the fictious elastic response to the load, the components due to the fictitious elastic response to the temperature change, and the components $\overline{N_i^r}$. We rewrite the sums of the first two components as N_i^e in the new sense; N_i^e are identified with the axial forces which would be developed in the perfectly elastic truss due to the change in temperature as well as the load. It is then recognized from the discussions made above that <u>shake-down will occur if and only if a state of self-stress $\overline{N_i^r}$ can be found such that superposition $\overline{N_i^r} + N_i^e = N_i$ of this state and the purely elastic response N_i^e to the given variation of loads and temperature will at no point or instant lead to stresses at or above the yield limit of bounds Y_i and Y_i'</u>. This is the static or equilibrium theorem of shake-down formulated by Melan and Prager. This implied that the truss has an ability to withstand the loading by rearranging the internal forces to best advantage. The principle provides a means of determining a safe range for the limits of variation in loads and temperature in order for no failure by cyclic plastic deformation to occur without restrictions on the number of repetions; a trial distribution of the history-independent residual forces $\overline{N_i^r}$ gives a safe range.

It is seen from Fig. 2 that as the load increases, the allowable range of a temperature change becomes smaller. When the load is close to the collapse load P_c, a small change in temperature causes incremental plastic deformation in the two members alternately. At the limit state C no change in temperature is required in order for the two members to yield simultaneously, and an unlimited plastic flow can take place under the constant load and temperature. Thus the static or plastic collapse is recognized to be a limiting case of an incremental collapse occurring due to variable repeated loading. The plastic or limit load itself is independent of any change in temperature. The above considerations suggest that a theorem for the static collapse be derived from the shake-down theorem as an application to the limiting case. The absence of variation indicates that the axial forces need not be separated into the variable and constant components. It follows that plastic collapse will not or is just about to occur if and only if an equilibrated state of stress N_i (satisfying the equations of equilibrium and boundary conditions on forces) can be found which nowhere exceeds the yield limit of bounds Y_i and Y_i'. This is nothing but the static or lower-bound theorem of limit analysis.

An unsafe bound of the allowable range is found from kinematical considerations with the use of a collapse mechanism. Suppose in an incremental collapse mechanism the i'th member is subjected to plastic elongation Δ_i^p. Considering that the yield limit is supposed to be reached in this member at some loading stage, we take either the maximum or minimum elastic axial force, $(N_i^e)_{max}$ or $(N_i^e)_{min}$, and either of equations

$$\begin{aligned} &(N_i^e)_{max} + \overline{N}_i^r = Y_i, && \text{if} && \Delta_i^p > 0, \\ &(N_i^e)_{min} + \overline{N}_i^r = Y_i', && \text{if} && \Delta_i^p < 0 \end{aligned} \tag{7}$$

is multiplied by Δ_i^p. The summation over all the yielding members gives

$$\sum_{i=1}^{3} \begin{Bmatrix} (N_i^e)_{max} \\ (N_i^e)_{min} \end{Bmatrix} \Delta_i^p + \sum_{i=1}^{3} \overline{N}_i^r \Delta_i^p = \sum_{i=1}^{3} \begin{Bmatrix} Y_i \\ Y_i' \end{Bmatrix} \Delta_i^p. \tag{8}$$

It is clear that each term in the summation of the right-hand side of Eq.(8) is positive regardless of the sign of Δ_i^p. The sum of the second term in the left hand side vanishes, since it is interpreted as the work done by the internal forces $\overline{N_i^r}$, which are in equilibrium with the external load P = 0, on the elongations Δ_i^p, which are compatible with a displacement at the joint of load application, and hence is equal to the work done by the vanishing load, as given from the principle of virtual work. It is thus seen that <u>incremental collapse must occur if there are such collapse mechanism and loading that satisfy the equation</u>

$$\sum_{i=1}^{3} \begin{Bmatrix} (N_i^e)_{max} \\ (N_i^e)_{min} \end{Bmatrix} \Delta_i^p = \sum_{i=1}^{3} \begin{Bmatrix} Y_i \\ Y_i' \end{Bmatrix} \Delta_i^p. \tag{9}$$

This implies that if there is a path to failure, the truss gives up. <u>The conditions to prevent the failure by alternating plasticity is easily understood to be</u>

$$(N_i^e)_{max} - (N_i^e)_{min} \leqq Y_i - Y_i'. \tag{10}$$

The corresponding principle for the static collapse is found by noting the absence of variation. It is convenient to express the sum of the internal work in the left-hand side of Eq.(9) in terms of the work done by the external load by means of the virtual work principle. A useful form of the statement is that plastic collapse must occur if for any assumed collapse mechanism, the external work equals (or is greater than) the internal plastic work. This is the kinematical or upper-bound theorem of limit analysis.

Another instructive consideration is made of energy dissipation for the case of variable repeated loading without temperature variation. A characteristic feature of plastic failure under repeated loading lies in the cyclic changes in the states of the internal as well as external forces. In Fig. 2 the state of internal forces and that of internal residual forces change in a cyclic manner as in the variation along the parallelogram DHGF. The cyclic change in the internal residual forces is accompanied by plastic deformation, and hence by energy dissipation. The elastic strain energy being recovered after a complete cyclic change, the amount of the energy dissipation in each cycle is given from the area of the parallelogram. An unlimited number of repetitions of such a cycle may require an unlimited amount of energy to be dissipated in plastic deformation. Similarly at the state of plastic collapse an indefinitely large energy dissipation may be accompanied by an indefinitely large plastic deformation. Failure by plastic deformation may thus be characterized by the limitless property of energy dissipation or plastic work; it is seen as the counterpart of this statement that shake-down is defined properly by the limitedness in the amount of the total sum of the energy dissipation under limitless repetitions of loading. It follows that the truss will not shake down but will fail ultimately by cyclic plastic deformation if any cycle of plastic deformation and any external load within the prescribed limits can be found which correspond to such a finite energy dissipation as the area of the parallelogram, and that the truss will shake down if for all admissible cycles of plastic deformation, no external load can be found within the prescribed limits which corresponds to such a finite amount of energy dissipation. Formulation of this principle in a form applicable to three dimensional continua may lead to Koiter's kinematical theorem of shake-down.

The above discussions have been restricted to the singly indeterminate truss under a single load with fixed direction combined with thermal loading. The geometrical representation of the state of internal forces can be extended to the cases of more than single determinancy and/or of the application of many loads by taking appropriate variables for orthogonal co-ordinate axes. It can also be generalized for beams and frames in which members are subject to bending. This is also the case with the principles and results stated on the simple model without proof. The generalization for the bending action with an elastic-perfectly plastic type of moment-curvature relation is made simply by replacing the axial force by the bending moment and by understanding the i'th member as critical section i where the bending moment takes a local extremum so that a yield or plastic hinge can develop, and by replacing the elongation by relative rotation across the yield hinge.

REMARKS

The knowledge and principles introduced in the preceding section on the general elastic-plastic behavior of structures were developed by predecessors in the field of the theory of plasticity with a few exceptions contributed by the author [1].* One is the application of the method of collapse mechanism to the truss example under thermal loading as well as variable repeated loads. A similar method had been exploited for rigid frames under varying loads without temperature change [2]. Another exception is the interpretation of Koiter's kinematical theorem established for three dimensional continua [3], in the less precise language of the structural behavior of the truss cited. For the historical review of the advancement the reader is referred to a separate article [4] as well as to the pertinent literature and books in the field.

The afore-introduced structural behavior and principles have been based on three fundamental assumptions. One is the elastic-perfectly plastic behavior of members in the sole action of bending or of axial loading. Another basic assumption is that changes in geometry can be neglected altogether. The third is a quasi-static behavior with the inertia effect neglected. It has seemed important to the author to axamine the validity of these assumptions and to make the structural behavior clear in the post-collapse range, motivating him to start the studies whose results come out in the treatise as the contents of the chapters to follow.

It is true that bending action predominates in beams and members of rigid frames, but there are certain cases where axial forces affect their behavior and thereby reduce the plastic collapse loads. This effect of the plastic interaction on the collapse loads is studied for rectangular rigid frames in the first chapter.

In order for a reasonable method of design to be established, it is essential to be well acquainted with the structural behavior for the entire history of loading through the plastic failure or collapse up to the

* Numbers in brackets refer to the references at the end of each chapter.

contributed by the author [1].* One is the application of the method of collapse mechanism to the truss example under thermal loading as well as variable repeated loads. A similar method had been exploited for rigid frames under varying loads without temperature change [2]. Another exception is the interpretation of Koiter's kinematical theorem established for three dimensional continua [3], in the less precise language of the structural behavior of the truss cited. For the historical review of the advancement the reader is referred to a separate article [4] as well as to the pertinent literature and books in the field.

The afore-introduced structural behavior and principles have been based on three fundamental assumptions. One is the elastic-perfectly plastic behavior of members in the sole action of bending or of axial loading. Another basic assumption is that changes in geometry can be neglected altogether. The third is a quasi-static behavior with the inertia effect neglected. It has seemed important to the author to axamine the validity of these assumptions and to make the structural behavior clear in the post-collapse range, motivating him to start the studies whose results come out in the treatise as the contents of the chapters to follow.

It is true that bending action predominates in beams and members of rigid frames, but there are certain cases where axial forces affect their behavior and thereby reduce the plastic collapse loads. This effect of the plastic interaction on the collapse loads is studied for rectangular rigid frames in the first chapter.

In order for a reasonable method of design to be established, it is essential to be well acquainted with the structural behavior for the entire history of loading through the plastic failure or collapse up to the

---

* Numbers in brackets refer to the references at the end of each chapter.

ultimate state where the structure ceases to serve its function as such. Deflections of a structure may become large after its critical state or the load-carrying capacity is reached, so that changes in geometry should be taken into account; viz., finite deformation has to be considered. Chapters from 2 to 6 are concerned with this effect with allowance for the repetition of loading. A portal frame under a constant gravity and varying horizontal load is investigated in Chap. 2. Chapters 3 and 4 treat the hysteretic behavior of a bar under repeated axial loading as in bracing or truss members. The analysis in the former is based on the piecewise-linear yield condition for the interaction of bending moment and axial force, and the piecewise linearity is modified in the latter, both being restricted to the range of finite but small deformation. In Chapts. 5 and 6 are examined the effects of large finite deformation on the behavioral characteristics of the bar. The former is devoted to the derivation of basic formulae, followed by the application and a comparative study on the small and large deformation theories in the latter.

If a structure happens to be subject to a load greater than its load carrying capacity, then the structure cannot be in a state of equilibrium, but is forced into an accelerated motion. If such a load continues long to be applied, excessive deformation may result and make the structure unserviceable. If, however, the load is applied for a sufficiently short period of time, the inertial resistance of the structure may restrict the deformation to a certain amount. The last two chapters deal with the determination of the permanent deformation for such a case. A load of large magnitude, as in the plastic dynamics of this kind, brings about the significance of shear effect, which is theorized in Chap. 7. Since the deflection often becomes large because of the severe loading, a finite deflection may come into effect, leading to the study in Chap. 8 where attention is paid to the interaction effect due to stretching.

The asbtracts appended are intended to introduce the scope of the past activities of the author, containing papers with joint as well as sole authorship.

REFERENCES

[1] T. Nonaka, "7.2 Example" in T. Nonaka and S. Morino, "7. Failure by Plastic Deformation in Structures under Repeated Loading", Survey on Analytical Methods of Frames (ed. M. Naruoka and T. Nakamura), Baifukan Pub. Co., Tokyo, to be published (in Japanese).

[2] P.S. Symonds and B.G. Neal, "Recent Progress in the Plastic Methods of Structural Analysis, Part II,"Jour. Franklin Institute, Vol. 252, 1951, pp. 469-492.

[3] W.T. Koiter, "A New General Theorem on Shakedown of Elastic-Plastic Structures", Proc. Koninklijke Nederlandse Akademie van Weteschappen, Series B, Vol. 59, 1956, pp. 24-34.

[4] T. Nonaka, "7.4 Review on the Development of Theorems", and S. Morino, "7.6 Survey on Related Studies", op. cit. in [1].

CHAPTER 1

PLASTIC COLLAPSE LOAD WITH CONSIDERATION OF AXIAL FORCES

ABSTRACT This chapter presents a method of determining the plastic collapse load of a frame with consideration of the effect of axial forces existing in the frame members on plastic limit moments. The method does not require iteration, based on a kinematical consideration, and gives a smaller upper bound than simple bending theory. The concept of an extensible yield hinge is utilized when applying the upper bound theorem of plastic limit analysis.

Application of the method is exemplified for some plane rectangular frames by making use of a linearized and non-linear yield conditions. With restrictions imposed on the order of magnitude of certain depth-length ratios, the results are approximately expressed in a closed simple analytic form, from which the effect of axial forces is estimated.

SOURCE The contents of Chapter 1 are based on the following paper: Taijiro NONAKA, "A Kinematic Approach to the Plastic Collapse Load of a Rectangular Frame with Consideration of Axial Forces", Proc. Symposium on Plastic Analysis of Structures, Vol. II, Jassy, 1972, pp. 193-220; Theoretical and Applied Mechanics, Vol. 23, Proc. 23rd Japan National Congress for Applied Mechanics(1973), University of Tokyo Press, Tokyo, 1975, pp. 301-315.

Notation

Physical symbols

- a cross-sectional constant
- c linearity constant
- D energy dissipation rate
- H horizontal load
- h storey height
- l span
- M bending moment
- m number of bays
- N axial force
- n number of stories
- r reduction factor
- v linear volocity
- w angular velocity

Dimensionless symbols

$\alpha \equiv \sqrt{2a}\, M_0/(N_0 l)$

$\beta \equiv 2c M_0/(N_0 l)$

$\gamma \equiv M_0/M_0'$

$\rho \equiv \sqrt{a/2}\, P/N_0$

$\nu \equiv N/\ (N_0 \sqrt{2/a}.)$

Subscripts

- c plastic collapse
- i i'th span
- j j'th storey
- u upper bound

Primes indicate reference to beams.

Bars over and under a letter indicate reference to the top and bottom of a column.

1. INTRODUCTION

It is widely known that the plastic behavior of structural frame cannot necessarily be well predicted by an analysis which completely neglects the effects of axial forces existing in the frame members. One important unfavourable effect is the instability caused by the compressive axial forces together with the accompanying deflections. Apart from the instability effect, the existence of axial forces in the frame members, tensile or compressive, reduces the plastic limit moment, whose distribution primarily determines the plastic collapse load of a rigid-jointed frame. The plastic collapse load is to be understood here, as is customary, to mean the system of loads which either would just cause a distortion on the frame of rigid-plastic material, or would cause unlimited plastic deformation on the frame of elastic-perfectly plastic material when the change in geometry is neglected.

The usual method for the determination of the plastic collapse load of a frame with consideration of the effect of axial forces on plastic limit moments is an iterative one, in which the frame is first analysed by neglecting this effect. The axial forces found from the first trial solution are then used for the evaluation of the limit moments in the second trial, and the frame is again analysed with the reduced values of the limit moments. This procedure is repeated until the necessary accuracy is reached. Onat and Prager proposed a method which does not require iteration [1]. The plastic collapse load of a frame in which axial forces were to be considered was found to equal the collapse load of a slightly modified frame in which axial forces could be neglected. In the modified frame, yield hinges in a member with nonzero axial force were supposed to locate off the center line of the member. Linearization of the yield condition relating the limit moment to the axial force led to the determination of the location of an off-center hinge. Ono and Tanaka employed an iterative approach in finding the positions of the neutral axes in cross-sections [2]. This was, in effect, to locate the positions of the off-center hinges with recourse to trial-and-error. The upper- and lower-bounding techniques of plastic limit analysis were combined to find the collapse loads of portal frames. Hodge analysed a portal frame on the basis of statical considerations, and set the limit on the stress profile not to lie outside the yield curve in the stress-resultant plane [3].

In an earlier paper on the limit analysis of arches, Onat and Prager also showed that the presence of axial forces requires the use of yield hinges that allow not only relative rotation but also relative axial displacement of adjacent cross-sections [4]. This concept of an extensible or contractible yield hinge is to be applied in the this chapter in connection with the upper-bound or kinematical theorem for the determination of the plastic collapse loads of plane rectangular frames. The approach is based on a similar but slightly different point of view from that of Onat and Prager. Some quantitative discussions of this effect will also be given based on the results of analysis for several examples.

2. OUTLINE OF PRINCIPLES

Suppose a collapse mechanism is known from the simple bending theory in which only relative rotations can occur across yield hinges.

In order to account for the effect of the axial forces on the limit moments, the hinges are allowed to extend or contract as well as to relatively rotate, upon kinematical considerations. In the following, contraction is taken as negative extension and compression likewise as negative tension, and the repetition of alternatives will be omitted. The extension is related to the rotation across the extensible yield hinge by the plastic flow rule which states that the plastic flow vector with two cartesian components proportional to the rates of change of extension and of rotation is in the direction of the outward normal to the yield condition represented geometrically in the stress-resultant plane with cartesian components proportional to the axial force and the bending moment [4].

If the yield condition is linearized, the direction of the plastic flow vector is independent of the axial force (and of the bending moment), and the rate of extension is proportional to that of rotation at an extensible yield hinge. In the case of a piecewise-linear yield condition, there is a need to specify as to which regime the flow vector is associated with. In the problems to be considered, this involves specifying whether the axial deformation is extension or contraction. An insight into the sign of the corresponding axial force from statical considerations or from some physical considerations of the pattern of deformation can help to judge this. If the judgement is not possible or difficult, both alternatives should be considered and the resulting upper bounds should be compared, as will be exemplified later. The rate of internal energy dissipation at the hinge, regarded as a function of the plastic flow in the collapse mechanism under consideration, is expressed in terms of rotation (or more conveniently in terms of extension in certain exceptional cases). This is done at each yield hinge. In the case of rectangular frames, the relation among rotations at yield hinges is given without much difficulty from kinematical considerations together with the flow rule, so that the rate of total internal energy dissipation can be expressed in terms of a single linear or angular velocity for a given collapse mechanism with a single degree of freedom. The rate of change of the work done by external loads can also be expressed in terms of the same velocity. The two rates are then equated to give an upper bound of the plastic collapse load. The upper bound thus obtained is smaller than the corresponding one from the simple bending theory, and equals the exact value of the collapse load to the accuracy of the linearized yield condition, provided the assumed collapse mechanism with extensible yield hinges is correct. There is a possibility, however, that the extensible yield hinges form in the correct collapse mechanism at positions different from those of the simple bending theory, so that the correct collapse mechanism in the light of bending-extension interaction may be entirely different from that in the simple bending theory. In order to ensure that the upper bound thus obtained is in fact equal to the correct collapse load, the lower-bounding technique or statical consideration should also be utilized, or alternatively, all possible collapse mechanisms must be considered to give the lowest upper bound.

For any real cross-sections, the yield condition is not exactly linear with respect to bending moment and axial force. In the case of a nonlinear yield condition, the relation between the rates of rotation and extension at an extensible yield hinge depends on the axial force existing in the member. The rate-of-energy balance gives an upper bound of the collapse load which includes the axial forces as parameters. Any values less in magnitude than the plastic limit axial force can be given for independent axial forces. Differentiation of the upper bound with respect to the independent axial forces gives the lowest upper bound among collapse mechanisms with definite positions of extensible yield hinges.

It turns out that when certain restrictions are imposed on the order of magnitude of parameters concerning the depth-length ratios, the collapse load (upper bound) of a rectangular frame can be approximately expressed in a relatively simple closed form, without recourse to an iterative procedure. The effect of the axial forces on the collapse load can be evaluated in terms of these parameters.

3. EXAMPLES FOR LINEAR YIELD CONDITION

Following Onat and Prager [1], let us first use a piecewise-linear yield condition. By assuming that $|N/N_0|$ is small in comparison with unity, the exact yield curve, such as the one shown in a dashed line in Fig.1, is approximated by

$$\left|\frac{M}{M_0}\right| + c \left|\frac{N}{N_0}\right| = 1 \tag{1}$$

where M is bending moment, N is tensile axial force, M_0 and N_0 are their limiting values in pure bending and pure tension, respectively, and c is a constant. To c an appropriate value between zero and unity is to be assigned, depending upon the shape of cross-section and upon the range of the value of N/N_0. c = 1 provides the exact yield condition for an ideal I-section with indefinitely thin web and flanges. It is noted that the simple bending theory would assume the yield belt $|M/M_0| = 1$, which is equivalent to taking c = o in Eq. (1). Let ω and v be the rates of change of relative rotation and displacement, respectively, across an

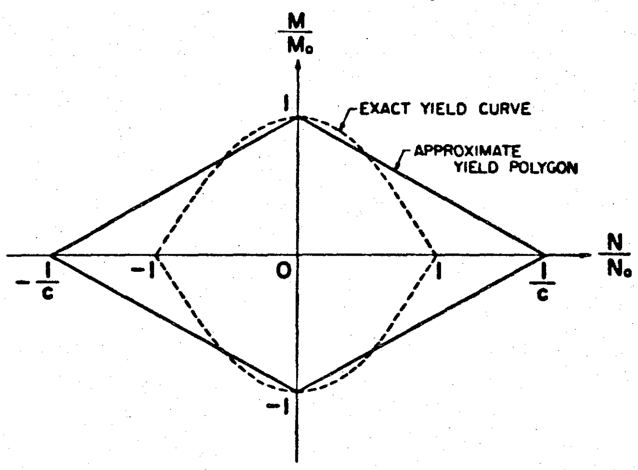

Fig. 1.

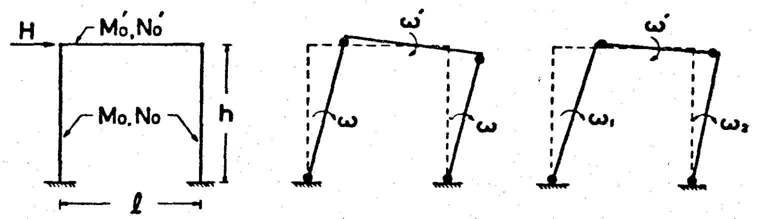

(a) (b) (c)

Fig. 2.

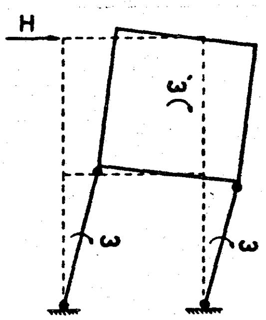

Fig. 3.

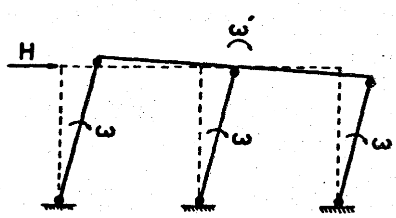

Fig. 4.

extensible yield hinge. In other words, they are the relative angular velocity and the rate of change of extension, respectively, at the hinge. From the flow rule associated with the yield condition, Eq. (1), it follows except for the singular points, $M = \pm M_o$ and $N = \pm N_o/c$, that

$$N_o \; |v| \; = cM_o \; |\omega| \tag{2}$$

The signs of v and ω are to be such that they are compatible with the corresponding N and M. Eq. (2) should be kept in mind when picking a collapse mechanism or a kinematically admissible plastic velocity field. The rate of internal energy dissipation D at a yield hinge is given by

$$D = M\,\omega + N\,v = \left|\frac{M}{M_o}\right| M_o\,|\omega| + \left|\frac{N}{N_o}\right| No\;|v| \tag{3}$$

and hence, with the aid of Eqs. (1) and (2),

$$D = \left(\left|\frac{M}{M_o}\right| + c\left|\frac{N}{N_o}\right| \right) M_o\;|\omega| = M_o\;|\omega| \tag{4}$$

unless* $M_o \; |\omega| < N_o \; |v| \; /c$.

Using Eqs. (2) and (4), let us determine the plastic collapse load or its upper bound for several examples of plane rectangular frames, in which all columns have the same uniform cross-section with plastic-limit stress-resultants M_o, N_o, constant c and the common height h, and all beams have M_o', N_o', c' and the length or span ℓ.

The first example is the portal frame shown in Fig. 2 (a). If $M_o < M_o'$ the simple bending theory predicts a side-sway collapse mechanism with yield hinges at the top and the foot of each column, and

---

* In the case of $M_o \; |\omega| < N_o \, |v| /c$, corresponding to the singular points $N = \pm N_o/c$, Eq. (4) should be replaced by $D = N_o \, |v| \,/c$.

gives the collapse load H_c for the horizontal load H, as

$$H_c = \frac{4M_0}{h} \tag{5}$$

In order to account for the effect of the axial forces on the collapse load, the yield hinges are supposed to be subject to extension as well as rotation, their relation satisfying Eq. (2). It is found from a statical consideration that a tensile force exists in the left column and a compressive in the right. A physical consideration of the pattern of frame deflection indicates that the left column elongates and the right contracts. Either of these considerations suggests a collapse mechanism such that the hinges in the left column extend and those in the right contract, so that the beam as well as the columns rotate in the clockwise direction. It is convenient to illustrate this collapse mechanism as shown in Fig. 2 (b). Since the length of the beam does not change, the two columns have the same angular velocity ω. The angular velocity of the beam is denoted by ω'. By making use of Eq. (4), the kinematical theorem of limit analysis [5, 6, 7, 8] provides the rate-of-energy balance

$$H_u \omega h = 2 M_0 [\omega + (\omega - \omega')] \tag{6}$$

for an upper bound H_u of the plastic collapse load, where it is assumed that

$$\omega - \omega' > 0 \tag{7}$$

for $\omega > 0$. Let $\underline{v}$ and $\bar{v}$ denote the rates of extension at the lower and upper yield hinges, respectively, of the left column. Eq. (2) gives the relations

$$N_0 \underline{v} = c M_0 \omega, \quad N_0 \bar{v} = c M_0 (\omega - \omega') \tag{8}$$

The rates of contraction at the yield hinges in the right column are equal numerically to $\underline{v}$ and $\bar{v}$ which satisfy Eq. (8). The change in geometry being ignored, there is the kinematical condition

$$\omega' \ell = 2\ (\underline{v} + \bar{v}) \tag{9}$$

Substitution for $\underline{v}$ and $\bar{v}$ in Eq. (9) from Eq. (8) expresses ω' in terms of ω as

$$\omega' = \frac{2\beta}{1 + \beta}\ \omega \tag{10}$$

where $\beta \equiv 2cM_o/(N_o\ell)$ is a parameter indicating the importance of the effect of the column axial forces. The value of β depends on the cross-sectional shape of the columns and the ratio of the column depth to the span as well as on the value of c. For an ideal I-section, β is identical with the depth-span ratio. β cannot be greater but is much smaller than unity. Eq. (10) thus confirms the assumption (7). Combination of Eqs. (6) and (10) determines H_u. When the result is expressed in the form

$$H_u = H_c\ (1 - r) \tag{11}$$

the factor r of the reduction due to axial forces becomes in this example

$$r = \frac{\beta}{1 + \beta} \tag{12}$$

In order for H_u, which is given by the combination of Eqs. (5), (11) and (12), to be the correct collapse load, a statically admissible distribution of the axial force and the bending moment which does not violate the yield condition must exist under this load. Evidently this is so provided the inequality

$$\left|\frac{M'}{M_o'}\right| + c' \left|\frac{N'}{N_o'}\right| \leqq 1 \tag{13}$$

is satisfied at the beam ends, where the primes denote reference to the beam. It turns out that condition (13) leads to

$$\frac{M_o}{M_o'} \leqq \frac{1 + \beta}{1 + \beta'} \tag{14}$$

where $\beta' \equiv 2\, c'M_o'/(N_o'h)$ is a counterpart of β, and is proportional to the ratio of the beam depth to the column height, indicating the importance of the beam axial force as becomes clear later. It is worth noting that the assumption of contraction at the yeild hinges in the left column and extension in the right would have resulted in an upper bound, $H_u = H_c\,(1 + r)$, larger than the collapse load H_c of the simple bending theory, where r is again given by Eq. (12).

If the inequality (14) is violated, the yield hinges at the top of the columns should be replaced by hinges at the beam ends as shown in Fig. 2 (c). For this case the simple bending theory gives the collapse load

$$H_c = \frac{2\,(M_o + M_o')}{h} \tag{15}$$

The hinges in the beam are now subject to contraction in addition to rotation. When multiplied by the span ℓ, the angular velocity ω' of the beam is equal to the sum of the rate of extension at the yield hinge of the left column and the rate of contraction at the right. These rates, in turn, are related to the angular velocities ω_1 and ω_2 of the left and right columns, respectively, through the flow rule Eq. (2) at the yield hinges. It follows that

$$\omega' = \frac{\beta}{2}\,(\omega_1 + \omega_2) \tag{16}$$

Similarly, the product of the height h and the difference between ω_1

and ω_2 is equal to the sum of the rates of contraction at the left and right yield hinges in the beam, which are proportional to the relative angular velocity $\omega_1 - \omega'$ and $\omega_2 - \omega'$, respectively, according to Eq. (2). Thus,

$$\omega_1 - \omega_2 = \frac{\beta'}{2} (\omega_1 + \omega_2 - 2\omega') \qquad (17)$$

Eqs. (16) and (17) are combined to express ω_2 and ω' in terms of ω_1 as

$$\omega_2 = \frac{2 - \beta' (1 - \beta)}{2 + \beta' (1 - \beta)} \omega_1 \qquad (18)$$

$$\omega' = \frac{2\beta}{2 + \beta' (1 - \beta)} \omega_1 \qquad (19)$$

Substitution of Eqs. (18) and (19) into the relation

$$H_u \omega_1 h = M_o (\omega_1 + \omega_2) + M_o' [(\omega_1 - \omega') + (\omega_2 - \omega')] \qquad (20)$$

gives the reduction factor

$$r = \frac{2\beta + \beta' (1 - \beta)(1 + \gamma)}{(2 + \beta' - \beta\beta') (1 + \gamma)} \qquad (21)$$

where $\gamma \equiv M_o/M_o'$. It is evident from the statical consideration that the upper bound thus obtained is also equal to the correct collapse load. This is confirmed by the fact that the value of H_u given by the combination of Eqs. (11), (15) and (21) is smaller than that of Eqs. (5), (11) and (12) when inequality (14) is violated.* In the examples which follow, only upper bounds are to be sought.

---

* It is worth mentioning that when the load H of Fig. 2 (a) is applied at the top of the right column instead of the left, the collapse mechanism in which the yield hinges at the beam ends expand leads to the same result as in Eq. (21).

Fig. 3 shows the application of the mechanism in Fig. 2 (b) to a two-storied frame. The simple bending theory again gives H_c of Eq. (5), but does not show whether failure occurs in the first story or in the second. When axial forces are accounted for, it must occur in the first, if yield hinges are to appear only in columns. Eqs. (7) to (11) are again valid; the replacement of ωh in the left hand side of Eq. (6) by $\omega h + \omega' h$ gives

$$r = \frac{3\beta}{1 + 3\beta} \tag{22}$$

A similar mechanism is considered for a frame with two bays in Fig. 4. The yield hinges in the middle column are subject to rotation alone, since the flow vectors corresponding to these hinges must be ruled out from Eq. (2) which is stipulated for the sides of the yield polygon, Fig. 1, and the generalized-stress points compatible with these flow vectors must be on the corners $|M| = M_o$. If there were any nonzero rates of axial deformation at these hinges, they should in magnitude be identical with those in either the left or the right column, since the relative angular velocities across the upper and lower yield hinges are common, respectively, to all columns. For this mechanism, manipulation similar to afore-mentioned examples gives the upper bound H_u as in Eq. (11) where

$$H_c = \frac{6M_o}{h}, \quad r = \frac{\frac{\beta}{2}}{1 + \frac{\beta}{2}} \tag{23 a,b}$$

Comparison of Eq. (12) with Eqs. (22) and (23b) makes it certain that when yield hinges appear only in columns the reduction of the collapse load due to axial forces increases with the number of stories and decreases with the number of bays. In the case of a single bay, n-storied frame subjected to a horizontal load H at the top, the collapse mechanism with hinges in the columns of the lowest story gives

$$r = \frac{(2n - 1)\beta}{1 + (2n - 1)\beta} \tag{24}$$

with H_c of Eq. (5). For instance, $\beta = 1/20$ and $n = 10$ indicate a 49 % reduction owing to the axial forces in columns.

On the other hand, the reduction due to the axial forces in beams, as in Fig. 2 (c), increases with the number of bays. Fig. 5 shows a collapse mechanism for a frame with m bays. The simple bending theory gives for this case

$$H_c = \frac{1}{h} \left[(m + 1) M_o + 2m M_o' \right] \tag{25}$$

A statical consideration indicates that all of the column axial forces are tensile except for the rightest column. This suggests a collapse mechanism in which extension takes place at the hinges in the former and contraction in the latter. The yield hinges in the beams are of, course, subject to contraction as well as rotation. Let subscripts refer to the members with consecutive numbering from the left as shown in the figure. The kinematical theorem of limit analysis provides

$$H_u \omega_1 h = M_o \sum_{i=1}^{m+1} \omega_i + M_o' \sum_{i=1}^{m} \left[(\omega_i - \omega_i') + (\omega_{i+1} - \omega_i') \right] \tag{26}$$

Considerations directed to derive Eqs. (16) and (17) now give

$$\left.\begin{aligned} \omega_i' &= \frac{\beta}{2} (\omega_i - \omega_{i+1}) \quad \text{for } i = 1, 2, \ldots, m - 1 \\ \omega_m' &= \frac{\beta}{2} (\omega_m + \omega_{m+1}) \end{aligned}\right\} \tag{27}$$

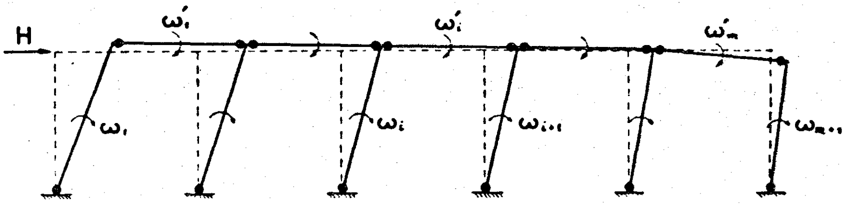

Fig. 5.

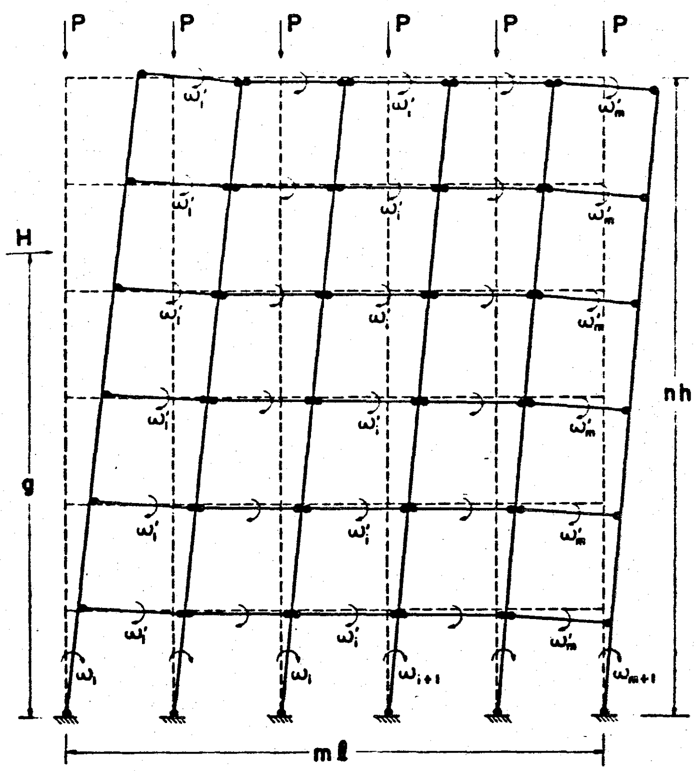

Fig. 6.

$$\omega_i - \omega_{i+1} = \frac{\beta'}{2} (\omega_i + \omega_{i+1} - 2\,\omega_i') \text{ for } i = 1, 2, \ldots m \qquad (28)$$

From these equations $\omega_2, \omega_3, \ldots\ldots, \omega_{m+1}$ and $\omega_1', \omega_2', \ldots\ldots, \omega_m'$ are expressed by ω_1. If β, β' and $m\beta'$ are of magnitude of the order less than unity, Eqs. (27) and (28) give the simple approximate relations

$$\omega_{i+1} \cong (1 - i\beta')\,\omega_1 \quad \text{for} \quad i = 1, 2, \ldots, m \qquad (29)$$

$$\left.\begin{aligned} \omega_i' &\cong 0 \quad \text{for} \quad i = 1, 2, \ldots, m-1 \\ \omega_m' &\cong \beta\,\omega_1 \end{aligned}\right\} \qquad (30)$$

to the first order with respect to β and β'. Substitution of Eqs. (29) and (30) into Eq. (26) gives

$$r \cong \frac{\frac{m(m+1)}{2}\,\beta'\,\gamma + m^2\,\beta' + 2\,\beta}{(m+1)\,\gamma + 2\,m} \qquad (31)$$

It is checked that substitution of $m = 1$ in Eq. (31) gives r identical with that from Eq. (21) within the first order approximation. The additional restriction on the order of magnitude that $m^2 \gg 2\,\beta/\beta'$ simplifies Eq. (31) further, viz.,

$$r \cong \frac{\beta' m}{2} \qquad (32)$$

For an example of $\beta' = 1/20$ and $m = 4$, Eq. (32) indicates a 10 % reduction approximately.

4. EXAMPLE FOR NONLINEAR YIELD CONDITION

Let us next consider a nonlinear yield condition of the form

$$\left|\frac{M}{M_o}\right| + \frac{a}{2} \left(\frac{N}{N_o} \right)^2 = 1 \qquad (33)$$

where "a" is a positive constant depending on the shape of the cross-section. Eq. (33) holds exactly for a rectangular cross-section when $a = 2$ is taken. This holds also for an I-section under strong-axis bending combined with axial loading when the neutral axis lies within the web; in this case "a" takes a value larger than 2. At an extensible yield hinge the associated flow rule becomes except for $N = \pm N_0 \sqrt{2/a}$

$$N_0 \, v = a \frac{N}{N_0} M_0 \, |\omega| \qquad (34)$$

and the rate of internal energy dissipation at the hinge is given from Eqs. (3), (33) and (34) as *

$$D = \left[1 + \frac{a}{2} \left(\frac{N}{N_0}\right)^2 \right] M_0 \, |\omega| \qquad (35)$$

Eq. (34) shows that the proportion of the rate of extension to that of rotation can vary among hinges, depending on the value of N, as against the linearized yield condition. To an arbitrary proportion there corresponds a value of N, and D is determined from Eq. (35) if $|N| < N_0 \sqrt{2/a}$, i.e., if $N_0 |v| < \sqrt{2a} \, M_0 |\omega|$, upon choosing a collapse mechanism. A choice of this proportion is equivalent to a choice of N.

Let us suppose a plane rectangular frame with m bays and n stories is subjected both to the system of vertical loads which is equipollent to P acting downward on each column and to the system of horizontal loads which is equipollent to a single force H acting from the left at a height g from the ground level. An upper bound H_u of H is to be sought under given P. The collapse mechanism to be considered is shown in Fig. 6 where yield hinges form at the foot of each column and at the left and

---

* For the cases $N = \pm N_0 \sqrt{2/a}$, the flow rule gives $\sqrt{2a} \, M_0 \, |\omega| \leqq N_0 |v|$. For these cases Eq. (35) should be replaced by $D = N_0 |v| \sqrt{2/a}$.

right ends of each beam in each span. The simple bending theory gives the plastic collapse load H_c, when so modified that the reduction of limit moments is only due to the direct vertical load P, as

$$H_c = \frac{1}{g}\left[(m + 1)(1 - \rho^2) M_o + 2\,m\,n\,M_o' \right] \tag{36}$$

where $\rho = \sqrt{a/2}\ P/N_o$.

As shown in the figure, all beams in the ith span have the common angular velocity ω_i', and the ith column from left has ω_i independent of stories. Let v_i denote the rate of extension at the yield hinge of the i th column from the left. ν_i is the ratio of the tensile force there to $N_o\sqrt{2/a}$. Let $\nu_{i,j}'$ be the tensile force of the beam in the ith span from the left on the jth story devided by $N_o'\sqrt{2/a'}$. "a" and a' are the constants for the column and beam cross-sections, respectively. With Eq. (35), the kinematical theorem of limit analysis gives

$$H_u\,\omega_1\,g - P\sum_{i=1}^{m+1} v_i = M_o\sum_{i=1}^{m+1}\left[(1+\nu_i^2)\,\omega_i\right]$$
$$+ M_o'\sum_{i=1}^{m}\sum_{j=1}^{n}\left\{\left[1+(\nu_{i,j}')^2\right]\left[(\omega_i-\omega_i')+(\omega_{i+1}-\omega_i')\right]\right\} \tag{37}$$

where it is assumed that

$$\omega_i - \omega_i' > 0, \quad \omega_{i+1} - \omega_i' > 0 \qquad \text{for} \quad i = 1, 2, \dots, m \tag{38}$$

Among 3m + 2 velocities, v_1, v_2, ... v_{m+1}, ω_1, ω_2, ..., ω_{m+1}, ω_1', ω_2', ..., ω_m', 3m+1 are now to be expressed by the rest, e.g., ω_1. This is done by making use of the flow rule and kinematical conditions as follows. First, Eq. (34) relates v_i to ω_i as follows:

$$v_i = \alpha\,\ell\,\nu_i\omega_i \qquad \text{for} \quad i = 1, 2, \dots, m + 1 \tag{39}$$

where $\alpha \equiv \sqrt{2a}\, M_o/(N_o \ell)$. Hence,

$$\omega_i' = \frac{v_i - v_{i+1}}{\ell} = \alpha \, (\nu_i \, \omega_i - \nu_{i+1} \, \omega_{i+1}) \tag{40}$$

for

$$i = 1, 2, \ldots., m$$

The difference $\omega_{i+1} - \omega_i$ of the angular velocities of the columns adjacent to the ith span is equal to the sum of the rates of extension of the left and right hinges in the beam of the ith span, jth story divided by jh. When these rates of extension are related to the relative angular velocities by Eq. (34), in a manner similar to that leading to Eq. (17) or (28), it is found that

$$\omega_{i+1} - \omega_i = \alpha' \frac{\nu'_{i,j}}{j} (\omega_i + \omega_{i+1} - 2\,\omega_i') \tag{41}$$

for

$$i = 1, 2, \ldots, m \,; \quad j = 1, 2, \ldots, n$$

where $\alpha' \equiv \sqrt{2a'}\, M_o'/(N_o' h)$. Consequently

$$\nu'_{i,1} = \frac{\nu'_{i,2}}{2} = \ldots\ldots. = \frac{\nu'_{i,j}}{j} = \ldots.. = \frac{\nu'_{i,j}}{n} \tag{42}$$

and

$$\omega_{i+1} - \omega_i = \alpha' \nu'_{i,1} \, (\omega_i + \omega_{i+1} - 2\,\omega_i') \tag{43}$$

for

$$i = 1, 2, \ldots.., m$$

The total of 2m linear homogeneous equations, Eqs. (40) and (43), is adequate for the determination of 2m ratios

$$\frac{\omega_2}{\omega_1}, \frac{\omega_3}{\omega_1}, \ldots, \frac{\omega_{m+1}}{\omega_1} \,; \frac{\omega_1'}{\omega_1}, \frac{\omega_2'}{\omega_1}, \ldots, \frac{\omega'_m}{\omega_1}$$

each ratio including 2m+1 parameters, viz., $\nu_1, \nu_2, \ldots, \nu_{m+1}, \nu_{1,1}'$, $\nu_{2,1}', \ldots\ldots, \nu_{m,1}'$. With these in mind, Eq. (37) provides an upper bound H_u for each choice of the parameters, which can take any values smaller than unity in magnitude, independently of one another (It should not be overlooked that all ν's are not independent because of Eq. (42)). The lowest upper bound is obtained by differentiation with respect to these parameters. It is noted that the modified simple bending theory would assume $\nu_1 = \nu_2 = \ldots. = \nu_{m+1}$, $\nu_{i,j}' = 0$, and hence lead to a larger value than the correct collapse load.

In order to derive the result in a simple form, let us impose the restrictions

$$\alpha, \alpha' \ll 1, \quad \alpha n = 0(1) \tag{44}$$

and assume that $\nu_{i,1}'$ is at most of the order of α' for i = 1, 2, ..., m. To first order terms, Eq. (43) gives the approximation $\omega_{i+1} - \omega_i \cong 0$ or

$$\omega_1 \cong \omega_2 \cong \ldots. \cong \omega_{m+1} \tag{45}$$

It follows from Eq. (40) that

$$\omega_i' \cong \alpha\,(\nu_i - \nu_{i+1})\,\omega_1 \quad \text{for} \quad i = 1, 2, \ldots, m \tag{46}$$

Eqs. (37), (39), (42), (45) and (46) are combined to give

$$\begin{aligned} H_u\, g \cong{}& P\, \alpha\, \ell \sum_{i=1}^{m+1} \nu_i + M_o \sum_{i=1}^{m+1} (1 + \nu_i^2) \\ &+ 2M_o' \sum_{i=1}^{m} \sum_{j=1}^{n} \{ [1 + (j\, \nu_{i,1}')^2][\, 1 - \alpha(\nu_i - \nu_{i+1})\,] \} \end{aligned} \tag{47}$$

Setting the differentiation of H_u in Eq. (47) with respect to $\nu_{1,1}'$, $\nu_{2,1}', \ldots\ldots, \nu_{m,1}'$ equal to zero, it is found that

$$\nu_{1,1}' \cong \nu_{2,1}' \cong \ldots\ldots \cong \nu_{m,1}' \cong 0 \tag{48}$$

After substitution of Eq. (48) into Eq. (47), the right hand side of Eq. (47) is differentiated with respect to ν_1, ν_2, ..., ν_{m+1} and set equal to zero to give

$$\begin{aligned} \nu_1 &\cong -\rho + \frac{\alpha n}{\gamma} \\ \nu_2 &\cong \nu_3 \cong \cdots\cdots \cong \nu_m \cong -\rho \\ \nu_{m+1} &\cong -\rho - \frac{\alpha n}{\gamma} \end{aligned} \tag{49}$$

Incidentally, Eqs. (46) and (49) are combined to give

$$\begin{aligned} \omega_1' &\cong \omega_m' \cong \frac{\alpha^2 n}{\gamma}\, \omega_1 \\ \omega_2' &\cong \omega_3' \cong \cdots \cong \omega_{m-1}' \cong 0 \end{aligned} \tag{50}$$

which confirms assumption (38), in view of the restrictions imposed by Eq. (44). Eq. (48) also shows the validity of the assumptions made apriori on the magnitude of $\nu_{i,1}'$. Combination of Eqs. (47) to (49) finally gives the reduction factor

$$r \cong \frac{2(\alpha n)^2}{\gamma\,[2\,mn + \gamma\,(m+1)\,(1-\rho^2)]} \tag{51}$$

r in this equation indicates the reduction of the collapse load (upper bound) due to axial forces as compared with H_c of Eq. (36) of the modified simple bending theory. To cite an instance, values $\alpha = 1/10$, $m = 2$, $n = 20$, $\gamma = 2$, $\rho = 1/2$ lead nearly to a 5 % reduction.

The author has suggested Hayashi to apply the kinematical approach stated in this section to a variety of frames of wide-flange sections. The effect of axial forces seems to be successfully estimated by the formulation exemplified for a nonlinear yield condition, even when the frames and loading are under more realistic conditions [9].

5. CONCLUDING REMARKS

The kinematical approach presented in this paper has been shown to be an effective tool to find upper bounds of the collapse loads of rectangular frames with consideration of the effect of axial forces on plastic limit moments. The basis of the approach lies in allowing yield hinges in a collapse mechanism to deform in axial direction in addition to relative rotation upon the application of the upper bound theorem of limit analysis. Use of a linearized yield condition is convenient and simplifies the analysis when the sign of the axial deformation or of the corresponding axial forces can be judged. If this judgement is difficult to be done, both alternatives should be considered to give a lower upper bound. Use of a nonlinear yield condition, which has not a singularity for zero axial forces, does not require this judgement apriori, and leads to an upper bound with axial forces as parameters. Minimization of the upper bound requires differentiation with respect to these axial forces. The differentiation procedure, however, does not assure the load thus obtained is equal to the exact collapse load, unless all possible collapse mechanisms are considered. There is a possibility that extensible yield hinges in the light of bending-extension interaction form at positions different from the simple bending theory.

The effect of axial forces is estimated in terms of certain depth-length ratios. The effect of column axial forces depends on the ratio of the column depth to the span, and that of beam axial forces depends on the ratio of the beam depth to the story height. Upper bounds of collapse loads have been derived in a closed simple analytic form by imposing certain restrictions on the order of magnitude of these ratios.

REFERENCES

[1] E. T. Onat and W. Prager, "The Influence of Axial Forces on the Collapse Loads of Frames", Proc. 1st Midwestern Conference on Solid Mechanics, Urbana, 1953, pp. 40-42.

[2] K. Ono and H. Tanaka, "Limit Design of Rigid Frames with Consideration of Axial Forces", Proc. Architectural Institute of Japan, Vol. 50, 1955, pp. 32-38 (in Japanese).

[3] P. G. Hodge, Jr., "Plastic Analysis of Structures", McGraw-Hill, 1959, pp. 177-182.

[4] E. T. Onat and W. Prager, "Limit Analysis of Arches", Jour. Mechanics and Physics of Solids, Vol. 1, 1953, pp. 77-89.

[5] H. J. Greenberg and W. Prager, "Limit Design of Beams and Frames", Proc. ASCE, Vol. 77, Separate No. 59, 1951.

[6] D. C. Drucker, W. Prager and H. J. Greenberg, "Extended Limit Design Theorems for Continuous Media", Quarterly of Applied Mathematics, Vol. 9, 1952, pp. 381-389.

[7] R. Hill, "On the State of Stress in a Plastic-Rigid Body at the yield Point", Phil. Mag. (7), Vol. 42, 1951, pp. 868-875.

[8] W. Prager, "The General Theory of Limit Design", Proc. 8th International Congress of Applied Mechanics, Istanbul (1952), Vol. 2, 1956, pp. 65-72.

[9] K. Hayashi, "On the Effects of Axial Forces on the Plastic Collapse Loads of Rectangular Frames" Thesis Sc. M., Kyoto University, in preparation.

CHAPTER 2

HYSTERETIC BEHAVIOR OF A PORTAL FRAME WITH AXIAL FORCE VARIATION

ABSTRACT Theoretical study is made of the hysteretic behavior of a portal frame under constant gravity and variable horizontal loading. Special account is taken of the variation of axial forces in the columns, the model simulating the plastic interaction of the overall shearing and bending in tall rectangular frames and battened columns. The assumed elastic-perfectly plastic behavior of columns makes mathematical formulation feasible, and detailed examination is given of the cyclic alternate displacement loading with P-Δ effect taken into consideration. Through this example are clarified characteristic features of repeated loading such as shake-down, incremental collapse and alternating plasticity, under the combined action of bending moment and axial force existing in a frame member.

SOURCE The contents of Chapter 2 are based on the following paper: Taijiro NONAKA, "Elastic-Perfectly Plastic Behavior of a Portal Frame with Variation in Column Axial Forces", to be published.

Notation

Physical symbols

- C coefficient of stability
- E Young's modulus
- F factor on column stiffness
- H horizontal load
- h height
- I cross-sectional moment of inertia
- l span
- M bending moment
- N axial force
- P gravity load per column
- Q shearing force of column
- V shearing force of beam in absence of gravity load
- Δ frame deflection
- Θ hinge rotation
- Φ angle defined in Fig. 5
- Ψ angle defined in Fig. 5

Dimensionless symbols

$$a \equiv \frac{12EI}{N_o h^2}$$

$$m \equiv \frac{M}{M_o}$$

$$n \equiv \frac{N}{N_o}$$

$$r \equiv \left(\frac{2EI}{M_o h}\right) \text{ (beam rotation)}$$

$$v \equiv \frac{Vl}{2M_o}$$

$$\alpha \equiv \frac{2M_o}{N_o l}$$

$$\beta \equiv \frac{2M_o}{N_o h}$$

$$\delta \equiv \frac{N_o \Delta}{2M_o}$$

$$\eta \equiv \frac{Hh}{4M_o}$$

$$\rho \equiv \frac{P}{N_o}$$

Subscripts indicate particular values with

- O full plasticity
- a amplitude
- e elastic limit
- l left column
- m fictitious elastic limit
- P axial load of P
- p plastic-mechanism state
- r right column
- A,B,C, ... states defined in Figs. 4 and 6
- 1, 1', 2, 2', ... states defined in Fig. 8

Bars over and under a letter indicate the top and bottom of a column.

1. INTRODUCTION

It is true that the behavior of ordinary building frames is governed by bending of their constituent members, but there are cases in which axial forces as well as bending moments play important role in the structural behavior. Apart from a braced frame typical of such a case, axial forces are induced in the columns of an unbraced rectangular frame due to gravity loads and to the shear forces existing in the beams. A characteristic feature of the gravity load is to cause direct compression of primarily constant magnitude, whereas the beam shear causes both tension and compression in the adjoining columns, with magnitude varying in the course of horizontal loading as in winds, earhquakes, etc. Since in the elastic range tention brings about a stiffening effect and compression weakening, the tension-induced column carries more of the horizontal load than the compression-induced one. On account of the nonlinearity of this effect, the variation of axial forces may affect the buckling load of a frame with slender columns. Having analysed the elastic sway-buckling of a single-bay multi-storied frame for various ratios of the distribution of the vertical load between the two columns, Salem asserts that the variation of the axial forces in the columns of an unbraced multi-storied frame can be neglected in the elastic stability analysis and the frame treated as though the columns in each story carry equal loads [1]. Shirahama and Mukudai have also concluded from the results of the experiment and numerical analysis on beam-columns under varying axial forces that the variation hardly affects the elastic-plastic stability limit [2].

Besides the effect on the stability, which is concerned with change in geometry, the existence of axial forces reduces the plastic limit moment of the frame members and hence reduces the plastic collapse load. The reduction takes place in the range of infinitesimal as well as finite deformation, and occurs both for tension and compression [3-6]. In view of the history dependence of plastic behavior, the effect of the variation of axial forces in this phenomenon is still complicated by the repeated action of loads. König proposed an approximate method of shake-down analysis, including the influence of axial forces [7]. Laying great emphasis on the circumstances where the columns of a rigid frame undergo variation in the axial forces due to bracing in the plane intersecting perpendicularly to the frame in question, Suzuki, et al. have demonstrated that tension and compression-induced columns exhibit quite different hysteretic behavior [8-10]. The aspects of this kind may become significant also in lower stories of multi-storied frames, where columns are stubby enough to carry large axial forces owing to the accumulation of the beam shear as well as the gravity loads in the upper stories. A similar situation can arise in a battened column, which may well be idealized as a multi-storied frame, when subjected to repeated lateral loading.

The objective of this chapter is to study theoretically the hysteretic behavior of an unbraced frame with consideration of the variation of the axial forces in the columns. In other words, special attention is focused on the plastic interaction of the overall shearing and bending of a rigid frame under repeated lateral loading. In order to formulate this complex behavior mathematically, drastic simplification is made as to the model of the frame and material behavior; a portal frame is taken to be composed of elastic-perfectly plastic columns and a beam with negligible deformability, and equilibrated with the simultaneous action of a variable horizontal load and constant gravity load, with due account of the overall frame instability. The modelling being intended to simulate the structural characteristics of a tall rectangular frame and a battened column, the span and height of the frame are not necessarily of the same order of magnitude, but it is allowed for the span to be as small as comparable with the depth of the columns.

2. STATEMENT OF THE PROBLEM

Let us examine the elastic-plastic behavior of a symmetric rectangular portal frame as shown in Fig. 1. The rigid beam of length l is rigidly connected at its ends to two identical columns of height h, each column being clamped at the foot. The frame is initially stress-free and is subjected to a constant vertical load, which may be concentrated or distributed and is equipollent to the force $2P$ acting downward at the center of the displaced beam. Account is taken of the destabilizing effect (P-Δ effect) caused by the vertical load through the frame deflection. A horizontal load H is also applied repeatedly with slowly varying intensity at the top of a column. If the effect of variation in the column axial forces were neglected, the behavior of the frame could be determined from that of a single column with the end rotation constrained, under the constant axial force P and the variable transverse load $H/2$. The hysteretic frame behavior is to be examined herein, by taking care of this effect in the plastic interaction between bending moments and axial forces. Primary interest is on the relationship between the load H and the corresponding horizontal displacement (sidesway) Δ of the frame in equilibrium.

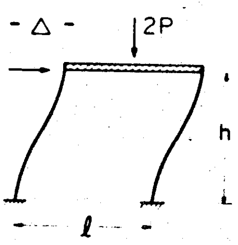

Fig. 1 Frame under consideration

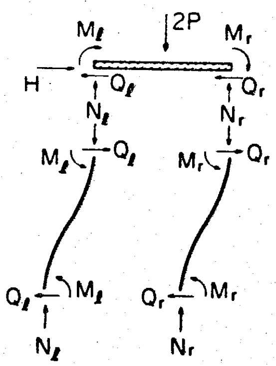

Fig. 2 Resultant forces at member ends

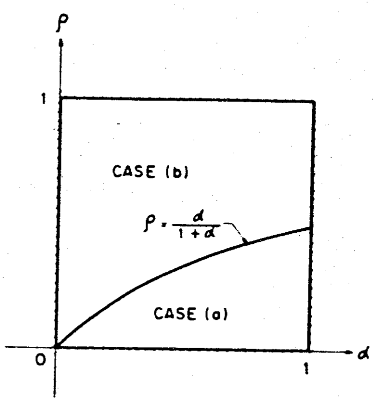

Fig. 3 Allowable domain

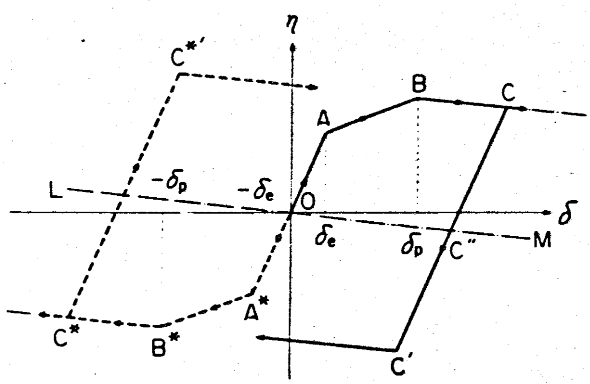

Fig. 4 Example of η-δ relation

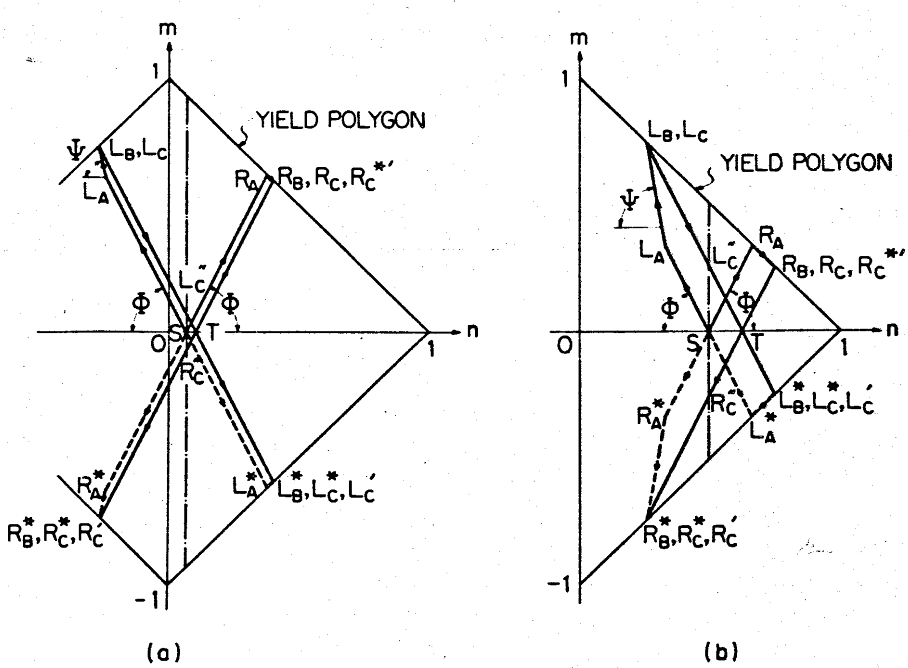

Fig. 5 Example of stress trajectory

3. ASSUMPTIONS

Among assumptions to be made about the columns, the most important ones are itemized below.

1. A column can be considered as a one-dimensional continuum with an elastic-perfectly plastic property under the combined action of axial force and bending moment, shear effects being completely negligible.
2. The yield condition is approximated as the one for an ideal I-section, which is composed of indefinitely thin web and flanges of ductile material with the same property in tension and compression (sandwich cross section).
3. Despite the significance of the overall P-Δ effect, no allowance needs be made for the consequence on column stiffness exerted through geometric change by the axial force present in an element of the column.*
4. Change in the length of a column can be neglected in comparison with the original length,** and deformation is of such magnitude that the square of slope in the deflection curve is negligible as compared with unity.
5. No anomaly takes place such as twisting, out-of-plane deformation, or local instability.

As regards nomenclature, the columns have the flexual rigidity EI of linear elasticity, plastic limit moment M_o in pure bending, and limit force N_o in pure tension.

---

* The change in the stiffness is small unless the column is very slender, as clarified in Appendix 1.

** The change in the length exerts a higher order effect, as discussed at length in Appendix 2.

4. EQUILIBRIUM RELATIONS

Fig. 2 shows the resultant forces and their positive directions at the ends of members. Symmetry and elementary equilibrium considerations have been utilized; M and Q are the bending moment and the shearing force, respectively, at the top and bottom of a column, and N is the compressive axial force. Subscripts l and r indicate reference to the left and right columns, respectively. It is to be understood that the forces, moments and displacements are taken as negative when their sense is opposite to that shown in Figs. 1 and 2.

Equilibrium of each member in the deflected state requires the following relations to be satisfied:

$$H = Q_l + Q_r \tag{1}$$

$$2P = N_l + N_r \tag{2}$$

$$M_l + M_r = (N_r - N_l)l/2 \tag{3}$$

$$2M_l = N_l\Delta + Q_l h \tag{4}$$

$$2M_r = N_r\Delta + Q_r h\,. \tag{5}$$

The vertical equilibrium of the beam, Eq.(2), is automatically satisfied by introducing V such that $N_l = P - V$ and $N_r = P + V$. It is noted that V indicates the deviation of the column axial forces from P, and that it becomes identical with the shearing force of the beam in the absence of the vertical load. In addition, the following dimensionless quantities are introduced:

$$m \equiv \frac{M}{M_o},\quad n \equiv \frac{N}{N_o},\quad v \equiv \frac{Vl}{2M_o},\quad \alpha \equiv \frac{2M_o}{N_o l},\quad \delta \equiv \frac{N_o\Delta}{2M_o},\quad \eta \equiv \frac{Hh}{4M_o},\quad \rho \equiv \frac{P}{N_o}\,. \tag{6}$$

It turns out that the importance of the axial force variation depends on the parameter α. For the ideal I-section α is equal to the ratio of the column depth to the span, and hence $0<\alpha<1$ in order to form the portal frame. It is allowed herein that α gets close to unity, but with the tacit restriction that $\alpha^2<<1$ on account of assumption 4. The variable δ is the ratio of the displacement Δ to the column depth; η is the ratio of the horizontal load H to the plastic collapse load of simple bending theory. It is supposed, of course, that the vertical load is such that* $0\leqq\rho\leqq1$.

With above notation, the column axial forces are give by

$$n_l = \rho - \alpha v, \qquad n_r = \rho + \alpha v. \tag{7a,b}$$

Equation (3) becomes

$$v = (1/2)(m_l + m_r). \tag{8}$$

Equations (1), (4), (5), (6), (7) and (8) are combined to give

$$\eta = v - \rho\delta. \tag{9}$$

It is of interest to note from the equations in (7) that the deviation of the column axial forces from the direct vertical compression becomes greater as the geometrical parameter α does. The second term in the right-hand side of Eq.(9) is caused by the change in overall geometry.

5. BEHAVIORAL CHARACTERISTICS

5.1 MONOTONOUS LOADING

Let us first consider the case in which the horizontal displacement

---

* The case $-1\leqq\rho<0$ could be incorporated in the analysis without complication, but is omitted here because of little practical interest.

increases monotonously from zero, and seek for the expression of v in terms of δ.

When δ is sufficiently small, the elementary beam theory of linear elasticity gives the relations

$$m_l = a\delta, \qquad m_r = a\delta; \qquad a \equiv 12EI/(N_o h^2) \tag{10a,b,c}$$

on the basis of assumptions 3 and 4. It follows from Eqs.(8) and (10) that

$$v = a\delta. \tag{11}$$

This relation ceases to hold when $\delta = \delta_e$ and $v = v_e$, at which the state of stress at the top and bottom of the right column reaches the yield limit. At still larger values, $\delta = \delta_p$, and $v = v_p$, the yield limit is reached at the ends of the left column as well, and the frame is converted into a mechanism. The yield limit at a cross section is given for the combined action of bending moment and axial force by

$$|m| + |n| = 1, \tag{12}$$

in conformity with the assumptions 1 and 2. Since it is clear that $m_r > 0$ and $n_r > 0$, the yield condition

$$m_r + n_r = 1 \tag{13}$$

is satisfied at the ends of the right column for $\delta \geqq \delta_e$. For $\delta_e \leqq \delta \leqq \delta_p$, Eqs. (7b), (8), (10a) and (13) are combined to give.

$$v = (1 - \rho + a\delta)/(2 + \alpha). \tag{14}$$

To analyze the case of $\delta \geqq \delta_p$ two alternatives, $n_l \geqq 0$ and $n_l < 0$, need to be treated in turn, since both are possible depending upon the intensity of the vertical load while $m_l \geqq 0$. By supposing first that $n_l \geqq 0$, the yield condition

$$m_1 + n_1 = 1 \tag{15}$$

is combined with Eqs.(7), (8), and (13) to give $v = 1-\rho$. The condition $n_1 \geqq 0$ is therefore satisfied if $\rho \geqq \alpha/(1+\alpha)$. If $0 \leqq \rho \leqq \alpha/(1+\alpha)$, then $n_1 \leqq 0$ and the reversion of the sign of n_1 in Eq.(15) leads to the relation $v=1/(1+\alpha)$. These results indicate that inspite of change in geometry, v, and hence m and n as well, remain constant after the initiation of the mechanism state.* Thus,

$$v = v_p \qquad \text{for} \qquad \delta \geqq \delta_p, \tag{16a}$$

where

$$v_p \equiv \begin{cases} 1/(1+\alpha) & \text{if} \quad 0 \leqq \rho \leqq \alpha/(1+\alpha) \\ 1 - \rho & \text{if} \quad \alpha/(1+\alpha) \leqq \rho \leqq 1. \end{cases} \tag{16b}$$

After obtaining these relations it is quite easy to show that

$$a\delta_e = v_e = (1-\rho)/(1+\alpha) \tag{17}$$

$$a\delta_p = \begin{cases} \rho + 1/(1+\alpha) & \text{if} \quad 0 \leqq \rho \leqq \alpha/(1+\alpha) \\ (1-\rho)(1+\alpha) & \text{if} \quad \alpha/(1+\alpha) \leqq \rho \leqq 1. \end{cases} \tag{18}$$

In Fig. 3 is shown the allowable domain in the plane with co-ordinates α and ρ. This domain is divided into two cases $0 \leqq \rho \leqq \alpha/(1+\alpha)$ and $\alpha/(1+\alpha) \leqq \rho \leqq 1$, which will in what follows be referred to as case (a) and case (b), respectively.

---

* The limit analysis of perfectly plastic solids shows that loads and stresses remain constant for the collapsed state under increasing deformation, when change in geometry is disregarded. The constancy of stresses despite change in geometry in the present analysis comes from piecewise linearity of the yield condition, Eq.(12)

The horizontal load-displacement relation is found from Eq.(9) in which v is given, under the condition of monotonously increasing displacement, from Eqs.(11), (14) and (16). An example of such a relation is illustrated by the solid line OABC in Fig. 4.

The variation of the state of stress is observed as a trajectory in the stress plane (m, n); (a) and (b) in Fig. 5 are associated with the cases (a) and (b), respectively. The ends of the left and right columns have the stress points L and R, respectively, which move as

$$S \rightarrow \left\{{L_A \atop R_A}\right\} \rightarrow \left\{{L_B \atop R_B}\right\} \rightarrow \left\{{L_C \atop R_C}\right\}$$

corresponding to $O \rightarrow A \rightarrow B \rightarrow C$ in Fig. 4. From the equations in (7), it is seen that at each stage, L and R have the same distance $\alpha|v|$ to the chain line, $n = \rho$, passing through point S. It has been confirmed that in Fig. 5(b) R does not reach the right corner before L arrives somewhere on the yield polygon, since for the mechanism state of case (b), Eqs.(7b) and (16b) are combined to give $n_r = \rho + \alpha(1-\rho) \leqq 1 + \alpha(1-1) = 1$. It is worthy of note from Eqs.(8) and (9) that the ordinate of a stress point in Fig. 5 is indicative of the capability to resist the sidesway of the frame. Thus, during the process $A \rightarrow B \rightarrow C$, the left column carries more of the horizontal load than the right. The slope dm/dn of a line segment in the stress trajectory of Fig. 5 is found from the foregoing relations; for angles Φ and Ψ defined in the figure, $\tan\Phi = 1/\alpha$, and $\tan\Psi = 1 + 2/\alpha$.

In the case of monotonously decreasing displacement from zero, the η-δ relation is represented by the dashed line OA*B*C* in Fig. 4, and the corresponding stress trajectory is shown in Fig. 5 as

$$S \to \left\{ \begin{matrix} L_A^* \\ R_A^* \end{matrix} \right\} \to \left\{ \begin{matrix} L_B^* \\ R_B^* \end{matrix} \right\} \to \left\{ \begin{matrix} L_C^* \\ R_C^* \end{matrix} \right\} .$$

On the line segments BC and B*C* in Fig. 4, which are referred to as mechanism lines, $v = v_p$ and $v = -v_p$, respectively. In Fig. 5, the stress points L_A^*, R_A^*, $L_B^* \equiv L_C^*$ and $R_B^* \equiv R_C^*$ are the reflections, through the horizontal co-ordinate axis, of the points R_A, L_A, $R_B \equiv R_C$ and $L_B \equiv L_C$, respectively.

It is noted that when the load-desplacement point in Fig. 4 lies on the line AB, the right column has its stress point on the yield polygon in the first quadrant in Fig. 5, while the left column has its stress point inside the yield polygon. It is also noted that when the load-displacement point lies on the line A*B*, the left column has its stress point on the yield polygon in the fourth quadrant while the right column has its stress point inside the yield polygon; these are true for both cases of (a) and (b) of Fig. 5.

5.2 UNLOADING FROM MECHANISM STATE

Let us next consider the case of reversed displacement from the mechanism state. It is supposed that the load-displacement point has reached C after the process 0 → A → B → C in Fig. 4. The process of the reversed displacement starts elastically so that the stress points in Fig. 5 move from L_C and R_C on the lines L_CL_C' and R_CR_C' which are parallel to the initial loading lines SL_A and SR_A, respectively. It has been confirmed that by these movements the stress points do not go outside of the yield polygon, until one or both of the stress points reach somewhere on the yield polygon in the lower half of the stress plane, since $\tan\Phi = 1/\alpha$ and $0 < \alpha < 1$, and since each segment of the yield polygon has the slope of magnitude unity. Equations (8) and (10) are rewritten in the incremental form,

$$dm_l = a\ d\delta, \qquad dm_r = a\ d\delta, \qquad dv = a\ d\delta. \qquad (19a,b,c)$$

By assuming that one of the columns remains elastic when the other reaches the yield limit, the equations in (19) are combined, after integrations, with Eqs.(7) and (12), to produce the results that the change in v during the process from the mechanism state to the termination of the elastic behavior is equal to $-2v_p$. This is true for whichever column may be assumed to first reach the yield limit, and is true for both cases (a) and (b), provided the proper alternative is taken for v_p in Eq.(16b). It follows that the left and right columns reach the yield limit simultaneously, and in Fig. 4 the load-displacement point moves on the line CC' parallel to OA*, unitl it reaches the point C', with $v = -v_p$, which is on the mechanism line B*C*. As a consequence, the corresponding stress points L_C' and R_C' in Fig. 5 coincide with $L_B^* \equiv L_C^*$ and $R_B^* \equiv R_C^*$, respectively. It is seen that lines L_CL_C' and R_CR_C' intersect at the point T on the horizontal co-ordinate axis. It is also seen from Eqs.(7) and (8) that when the stress point L is located at L_C'', the stress point R is at R_C'', the points L_C'' and R_C'' being on the line $n = \rho$ at the same distance from the point S. Since $v = 0$ at this state, Eq.(9) indicates that the corresponding load-displacement point C" lies on the line LM which represents the relation $\eta = -a\delta$ in Fig. 4. In Fig. 5, the stress points L and R which move along the lines L_CL_C' and R_CR_C', respectively have the same speed, since $dm_l = dm_r$ and $-dn_l = \alpha dv = dn_r$. The fact that in the stress plane $\overline{L_CL_C'} = \overline{R_CR_C'}$ complies with the fact that the left and right columns reach the yield limit simultaneously.

From these considerations it is clear that once the stress points fall on the lines $L_C L_C'$ and $R_C R_C'$, they remain on these lines for any later variation of δ or η and that plastic action can occur only at $\{{L_C \atop R_C}\}$ or $\{{L_C' \atop R_C'}\}$; in the former case the load-displacement point in Fig. 4 can move on the upper mechanism line and for the latter on the lower, in the sense shown by arrow heads in each case. Except for these end points in the stress plane, the frame behaves completely elastically, so that the corresponding load-displacement point can move with either sense on a line parallel to the line OA, between the two mechanism lines. The above is adequate to determine the subsequent behavior of the portal frame.

The situation of the case with the load-displacement trace of $0 \rightarrow A^* \rightarrow B^* \rightarrow C^* \rightarrow C^{*\prime}$ is clear from the above statements.

5.3 UNLOADING FROM A PARTIALLY PLASTIC STATE

Consider now the case of reversed displacement from a partially plastic state. The load-displacement point has such a trace as $0 \rightarrow A \rightarrow 1 \rightarrow 1'$ in Fig. 6, where the point 1 is an arbitrany point on the line AB. It is clear that the early reversing process is completely elastic so that the line 11' is parallel to the line OA; the corresponding stress trajectory is represented in Fig. 7 by

$$S \rightarrow \{{L_A \atop R_A}\} \rightarrow \{{L_1 \atop R_1}\} \rightarrow \{{L_1' \atop R_1'}\}.$$

This situation in the stress plane together with the equality in the speeds of the stress points for the left and right columns indicate that in the course of the reversed displacement the left column reaches the yield limit before the right. This can be confirmed easily by comparing the changes in v or δ occurring during the process form the state 1 to the termination of the elastic behavior, state 1', between the case where one of the columns yields before the other and the reversed case.

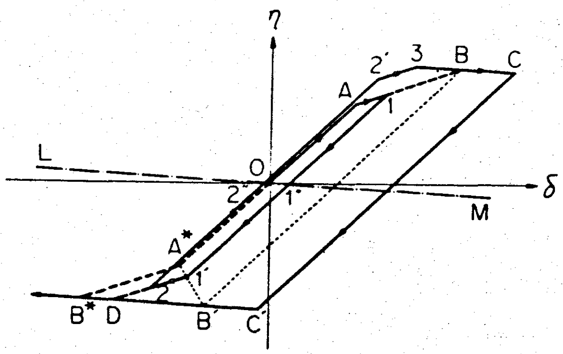

Fig. 6 Trace of load-displacement point

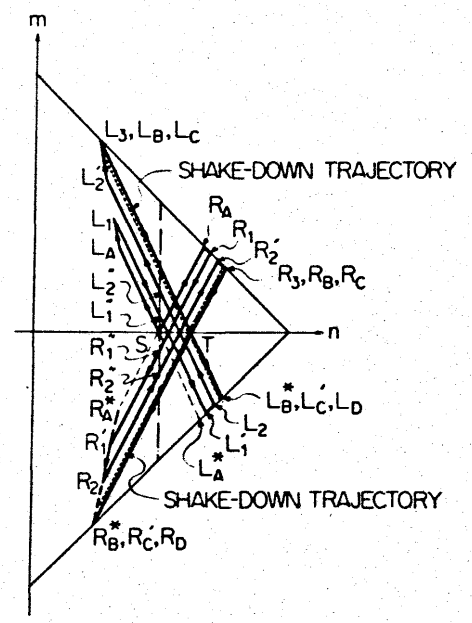

Fig. 7 Stress trajectory of Fig. 6, case (b)

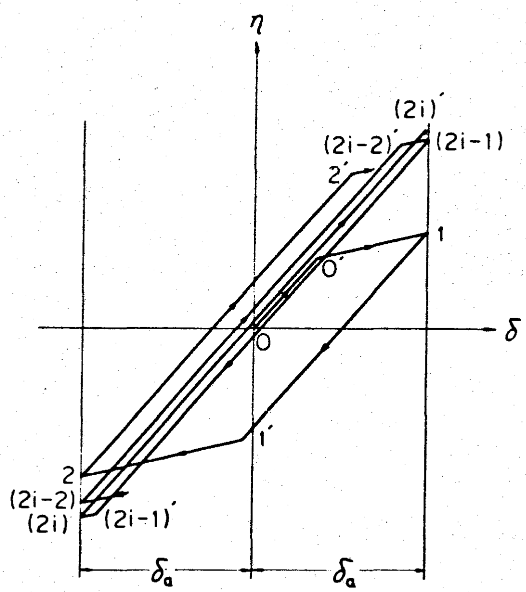

Fig. 8 Consecutive numbering

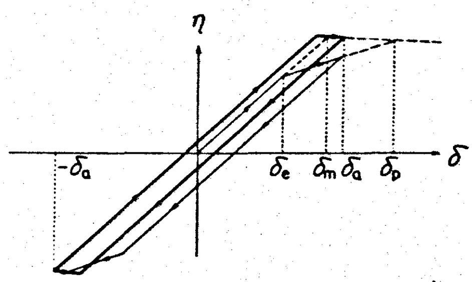

Fig. 9 Cyclic alternate loading, $\delta_m < \delta_a < \delta_p$

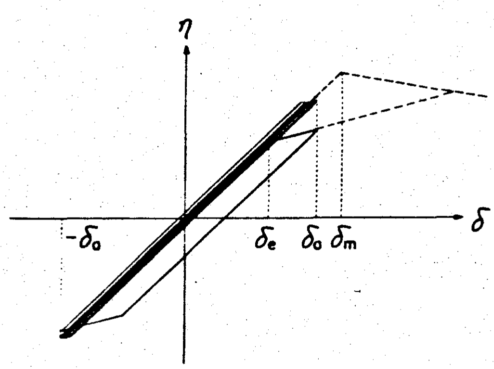

Fig. 10 Cyclic alternate loading, $\delta_e < \delta_a < \delta_m$

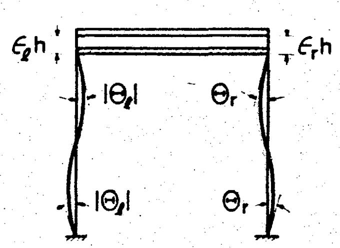

Fig. 11 Permanent Deformation,

$\delta_e < \delta_a < \delta_m$

In order to investigate the state 1', Eq.(19c) is integrated from the state 1 to 1', to give

$$v_1' - v_1 = a(\delta_1' - \delta_1), \tag{20}$$

where the numerals in the subscripts refer to the states defined in Fig. 6 (For the purpose of designating quantities for the states of primed numbers, primes are annexed to the quantities, instead of annexing them to the numbers). By noting that the left column is not subjected to previous plastic straining, Eqs.(7a), (10a) and (12) are combined to give

$$-a\delta_1' + (\rho - \alpha v_1') = 1. \tag{21}$$

In addition, the combination of Eqs.(7b), (8), (10a) and (13) gives

$$2v_1 = a\delta_1 + [1 - (\rho + \alpha v_1)] . \tag{22}$$

From Eqs.(20) to (22) it follows that

$$v_1' = -v_1. \tag{23}$$

This indicates that in Fig. 7 points L_1' and R_1' are the reflections of points R_1 and L_1, respectively, and that lines L_1L_1' and R_1R_1' intersect with each other on the horizontal co-ordinate axis. It is thus seen that state 1", the intersection of the line LM and 11' in Fig. 6, has the stress points in Fig. 7 at L_1'' and R_1'', on the line $n = \rho$, such that $\overline{L_1''S} = \overline{SR_1''}$. From Eq.(9), it is seen that v_1 is equal to the length of the projection of the line segment $\overline{1''1}$ to the vertical axis in Fig. 6; the terminal point 1' of elastic behavior is determined by the condition that $\overline{11''} = \overline{1''1'}$. If, in particular, the reversing starts from the state B, the elastic process proceeds up to point B' on the lower mechanism line, and it is clear from Eqs.(9) and (23) that the point 1' lies on the line A*B'.

If the displacement is decreased beyond 1', the right column behaves elastically, while plastic action occurs at the left column ends. For this process, Eq.(19b) is combined vith Eqs.(7a), (8) and (12) in their incremental form, to give

$$dv = [a/(2 + \alpha)]d\delta. \tag{24}$$

Accordingly, the corresponding line 1'2 of η-δ relation in Fig. 6 has the same slope, $a/(2+\alpha) - \rho$, with the lines AB and A*B*, as is seen by comparing Eq.(24) with Eq.(18). Equation(24) ceases to be valid when the state D is reached, whence both columns yield with $v = -v_p$, both for cases (a) and (b); the point D lies on the lower mechanism line C'B*. The stress points $\{{}^{L_D}_{R_D}\}$ for the state D coincide with those for the states B* and C'. The subsequent behavior needs no further discussions.

5.4 RELOADING FROM A PARTIALLY PLASTIC STATE

Suppose that the displacement is again increased from the state 2 between the states 1' and D in Fig. 6. The frame behaves in an elastic manner up to the state 2' whence plastic action again takes place at the ends of the right column. Equations in (19) apply to the precess $2 \rightarrow 2'$, to give

$$v_2' - v_2 = a(\delta_2' - \delta_2). \tag{25}$$

The deviation in m_l at the state 2' from the value, $(\rho - \alpha v_2) - 1$, at the state 2 is $a(\delta_2' - \delta_2)$. At the state 2', the value of m_r is given from Eq.(13) to be $1 - (\rho + \alpha v_2')$, since m_r and n_r are then positive, both in cases (a) and (b). It follows from Eq.(8) that

$$2v_2' = a(\delta_2' - \delta_2) - \alpha(v_2 + v_2'). \tag{26}$$

When Eqs.(25) and (26) are combined, it is found that $v_2 = -v_2'$. Concequently in Fig. 6, the elastic limit, the state 2', is determined by the relation $\overline{2''2'} = \overline{22''}$.

If the displacement is further increased, the mechanism state is reached at state 3, and continues along $3 \rightarrow B \rightarrow C$. Needless to say, Eq.(24) is again valid for the process $2' \rightarrow 3$, and Eq.(16) for the process beyond 3. It is noted that

$$v_e < |v_1| = |v_1'| < |v_2| = |v_2'| < |v_3| = v_p. \qquad (27)$$

It is also worth noting that the abscissa of the point 3 is smaller than that of the point B, and hence that the displacement at which the mechanism state is reached is reduced by the plastic straining during a cycle of loading and unloading. Behavior of the frame under decreasing displacement from the state C is characterized by the process $C \rightarrow C' \rightarrow D$ as before. The stress trajectory for the above processes is included in Fig. 7. The stress points approach to the stable lines $L_BL_B^*$ and $R_BR_B^*$. Incidentally, $\overline{L_1L_1''} = \overline{L_1''L_1'}$, $\overline{R_1R_1''} = \overline{R_1''R_1'}$; $\overline{L_2L_2''} = \overline{L_2''L_2'}$, $\overline{R_2R_2''} = \overline{R_2''R_2'}$; $\overline{SL_1''} = \overline{SR_1''}$, $\overline{SL_2''} = \overline{SR_2''}$.

It is now clear that the foregoing statements and equations are adequate for the determination of the elastic-plastic behavior of the frame under any history of loading and unloading.

6. EXAMPLES OF CYCLIC LOADING

6.1 ASYMPTOTIC BEHAVIOR

Let us consider several examples of cyclic loading with constant amplitude. When the amplitude of the horizontal load is specified, the resulting static behavior is simple; for load cycling within the load carrying capacity, the frame behaves elastically, either from the outset or after some plastic straining in the first cycle. When the displacement amplitude is specified and the loading is restricted in the same sign of the displacement, then the load-displacement curve becomes stable and fixed in a definite loop within the first cycle. These cases need no further discussion.

Alternate loading with a constant displacement amplitude is of practical interest, and worth close examination. With the restriction of zero mean, if the amplitude δ_a is smaller than δ_e of Eq.(17) or larger than δ_p of Eq.(18), the frame behavior is clear from Fig. 4. In the former, the frame remains elastic; in the latter, the $\eta - \delta$ raltion is similar to that of OABCC'C*C*'C, and the loop becomes stable by undergoing the mechanism state in the first cycle. The case $\delta_e \leqq \delta_a \leqq \delta_p$ is to be scrutinized in the following. The load-displacement relation is typified in Fig. 8. Its trace is represented, when started with positive direction of δ, by

$$0 \rightarrow 0' \rightarrow 1 \rightarrow 1' \rightarrow 2 \rightarrow 2'$$

in the first cycle. For the i'th cycle it is represented by

$$(2i - 2) \rightarrow (2i - 2)' \rightarrow (2i - 1) \rightarrow (2i - 1)' \rightarrow (2i) \rightarrow (2i)'$$

and there are conditions that

$$\delta_{2i-2} = -\delta_a, \qquad \delta_{2i-1} = \delta_a, \qquad \delta_{2i} = -\delta_a \tag{28a,b,c}$$

$$v'_{2i-2} = -v_{2i-2}, \quad v'_{2i-1} = -v_{2i-1}, \quad v'_{2i} = -v_{2i} \tag{29a,b,c}$$

for i = 2, 3, 4, ... In order to determine $\eta - \delta$ relation for the i'th cycle, the relation between δ'_{2i} and δ'_{2i-2} first has to be sought, by assuming that the mechanism state is not reached. Either of the piecewise-linear relations, Eqs.(19c) and (24), holds for each change of states. For the changes between (2i-2) and (2i)', these relations are integrated and combined with Eqs.(28) and (29) to give

$$-2v_{2i-2} = a(\delta'_{2i-2} + \delta_a) \tag{30}$$

$$(2 + \alpha)(v_{2i-1} + v_{2i-2}) = a(\delta_a - \delta'_{2i-2}) \tag{31}$$

$$-2v_{2i-1} = a(\delta'_{2i-1} - \delta_a) \tag{32}$$

$$(2 + \alpha)(v_{2i} + v_{2i-1}) = a(-\delta_a - \delta'_{2i-1}) \tag{33}$$

$$-2v_{2i} = a(\delta'_{2i} + \delta_a) \tag{34}$$

for i = 2, 3, 4, ... Elimination of the unknowns v_{2i-2}, v_{2i-1}, v_{2i} and δ'_{2i-1} from Eqs.(30) to (34) gives the recurrence formula

$$\delta'_{2i} = (\frac{\alpha}{2+\alpha})^2\delta'_{2i-2} + \frac{4(1+\alpha)}{(2+\alpha)^2}\delta_a. \tag{35}$$

Repeated use of Eq.(35), either directly or after rewriting into a geometric series

$$\delta'_{2i} - \delta_a = (\frac{\alpha}{2+\alpha})^2(\delta'_{2i-2} - \delta_a), \tag{36}$$

gives

$$\delta'_{2i} - \delta_a = (\frac{\alpha}{2+\alpha})^{2i-2}(\delta'_2 - \delta_a), \tag{37}$$

in which δ'_2 is determined through a similar manipulation for the first cycle. Equations (32) to (34) remain valied for i = 1, and Eqs.(30) and (31) are replaced by $v_e = a\delta_e$ and

$$(2 + \alpha)(v_1 - v_e) = a(\delta_a - \delta_e), \tag{38}$$

respectively. It follows that

$$\delta'_2 = [\frac{2-\alpha}{2+\alpha} + \frac{2\alpha}{(2+\alpha)^2}]\delta_a + \frac{2\alpha(1+\alpha)}{(2+\alpha)^2}\delta_e. \tag{39}$$

Equations (37) and (39) are combined to give

$$\delta'_{2i} = \delta_a - (\frac{\alpha}{2+\alpha})^{2i-1} \frac{2(1+\alpha)}{2+\alpha} (\delta_a - \delta_e) \tag{40}$$

for i = 2, 3, 4, ... It is found from Eqs.(29c), (34), (39) and (40) that

$$v'_2 = [\frac{2}{2+\alpha} + \frac{\alpha}{(2+\alpha)^2}]a\ \delta_a + \frac{\alpha(1+\alpha)}{(2+\alpha)^2}\ a\ \delta_e \tag{41}$$

and

$$v'_{2i} = a\ \delta_a - (\frac{\alpha}{2+\alpha})^{2i-1} \frac{1+\alpha}{2+\alpha}(a\ \delta_a - a\ \delta_e) \tag{42}$$

for i = 2, 3, 4, ...

Similar treatments for the changes between the states (2i-3) to (2i-1)' lead to the recurrence formula

$$\delta'_{2i-1} = (\frac{\alpha}{2+\alpha})^2\ \delta'_{2i-3} - \frac{4(1+\alpha)}{(2+\alpha)^2}\ \delta_a$$

and result in

$$\delta'_1 = \frac{\alpha}{2+\alpha}\ \delta_a - \frac{2(1+\alpha)}{2+\alpha}\ \delta_e \tag{43}$$

$$\delta'_{2i-1} = -\delta_a + (\frac{\alpha}{2+\alpha})^{2i-2} \frac{2(1+\alpha)}{2+\alpha} (\delta_a - \delta_e) \tag{44}$$

$$v'_1 = -\frac{1}{2+\alpha}\ a\delta - \frac{1+\alpha}{2+\alpha}\ a\ \delta_e \tag{45}$$

$$v'_{2i-1} = -a\ \delta_a + (\frac{\alpha}{2+\alpha})^{2i-2} \frac{1+\alpha}{2+\alpha}(\ a\ \delta_a - a\ \delta_e) \tag{46}$$

for i = 2, 3, 4, ... The complete history of load-displacement relation is found from the piecewise linearity and from Eqs.(9), (28), (29) and (39) to (46).

The above is valid until the absolute value of v attains the value v_p which is realized on the upper or lower mechanism lines. It is seen from Eq.(42) or (46) that there is such a value of i that this condition is satisfied in the i'th cycle, provided

$$\delta_a > \delta_m, \tag{47}$$

where $\delta_m \equiv v_p/a$, indicating the fictious elastic limit, is the magnitude of δ which would be attained at the mechanism state during the initial loading by disregarding the partially plastic states, as shown in Figs. 9 and 10.

In Fig. 9 is shown an example of η-δ relation for which Inequality (47) is satisfied. Once the mechanism state is reached, the loop becomes stable as shown in thick solid lines. Fig. 10 shows an example of the counter case $\delta_a \leqq \delta_m$. In this case the loop becomes slender as i increases, and shrinks to the initial elastic line $\eta = (a - \rho)\delta$ as i tends to infinity. This is comfirmed by the fact that Eqs. (40), (42), (44) and (46) give limits

$$\lim_{i\to\infty} \delta'_{2i} = -\lim_{i\to\infty} \delta'_{2i-1} = \delta_a, \qquad \lim_{i\to\infty} v'_{2i} = -\lim_{i\to\infty} v'_{2i-1} = a\delta_a.$$

Thus, the shake-down state is attained asymptotically, if $\delta_e < \delta_a \leqq \delta_m$. It is seen on inspection of Fig. 4 that the shake-down condition $\delta_a \leqq \delta_m$ is not altered by shifting the mean of the sidesway to either direction. The asymptote of the stress trajectory is typified by dotted lines in Fig. 7.

6.2 PERMANENT DEFORMATION

Let us examine the permanent deformation the frame undergoes due to the repeated displacement loading considered above. In the case of $\delta_e < \delta_a \leq \delta_m$, it is seen from Fig. 7 [for case (a), see Fig. 5(a)] that plastic action takes place in each cycle, the ends of the right column having stress points in the first quadrant on the yield polygon and the left in the fourth quadrant. This indicates the accumulation of plastic deformation. Let us first determine the plastic-hinge rotation θ developed at the ends of each column. The positive direction of $\dot{\theta}$ is taken to accord with the positive direction of the bending moment defined in Fig. 2. In the i'th cycle, plastic deformation develops in the right column from the state (2i - 2)' to the state (2i - 1); the increment of the joint translation angle $\Delta/h \equiv \beta\delta$ consists of the elastic component $dM_r h/(6EI)$ and the plastic component $d\Theta_r$, and hence

$$d\delta = dm_r/a + d\Theta_r/\beta, \tag{48}$$

where $\beta \equiv 2M_o/(N_o h)$ is the depth-height ratio of the columns and is equal to $\alpha l/h$. The increment dm_r in this equation is given from Eqs.(13) and (7b) to be $-\alpha dv$, where dv is to be rewritten from Eq.(14) in terms of $d\delta$. It follows that

$$d\Theta_r = [2\beta(1+\alpha)/(2+\alpha)]\, d\delta. \tag{49}$$

After the first k cycles, therefore,

$$\Theta_r = \frac{2(1+\alpha)}{2+\alpha}\, \beta \sum_{i=1}^{k} (\delta_{2i-1} - \delta'_{2i-2}), \tag{50}$$

in which $\delta_{2i-1} = \delta_a$, and δ'_{2i-2} is given for i = 1 by δ_e of Eq.(17), for i = 2 by Eq.(39), and for i = 3, 4, 5, ..., k by Eq.(40). In consequence

$$\Theta_r = (1+\alpha)[1-(\tfrac{\alpha}{2+\alpha})^{2k-1}]\ \beta(\delta_a - \delta_e) \tag{51}$$

for k = 3, 4, 5, ...

From the states (2i-1)' to 2i, the left column undergoes plastic deformation with negative bending moment at the plastic hinges. Starting from Eq.(48), with r in the subscripts replaced by l, manipulation similar to the right column finally gives the hinge rotation after the first k cycles to be

$$\Theta_l = -(1+\alpha)[1+(\tfrac{\alpha}{2+\alpha})^{2k}]\ \beta(\delta_a - \delta_e) \tag{52}$$

for $k = 2, 3, 4, \ldots$. It is noted from Eqs.(51) and (52) that the hinge rotations for $k \to \infty$, when the frame shakes down, tend equally in magnitude to the product of the quantity, $1 + \alpha$, and the difference, $\beta\delta_a - \beta\delta_e$, between the amplitude and the elastic limit, of the joint translation angle. The plastic deformation at the end of each loading cycle is greater in the left column than in the right.

The plastic axial deformation is also developed at each plastic hinge in each cycle. This is a contraction, since the axial forces at the hinges are compressive in both the cases (a) and (b). Let the total plastic contraction of each column be $h\varepsilon$. It is found from the flow rule associated with the yield condition of Eq.(12) that $Nh\,d\varepsilon = 2M_o|d\theta|$ for each plastic action, and hence that

$$\varepsilon = \beta|\theta| \tag{53}$$

where θ is to be substituted from Eqs.(51) and (52) for the right and left columns, respectively. The plastic deformation gives rise to such a shape of the permanent deformation as the one shown in Fig. 11. It is easily found, on account of the piecewise linearity of the yield condition, that the total plastic work equals $2M_o(\theta_r - \theta_l)$.

If the displacement amplitude is so large that $\delta_p \leqq \delta_a$, then the load-displacement relation becomes stable in the first cycle as seen in Fig. 4, and plastic action takes place in a cyclic manner. As is found from Fig. 5, the bending moments reverse their signs alternately in each cycle at the plastic hinges, indicating the danger of rupture due to alternate plastic bending. In the case of (a), the axial forces also reverse their signs, whereas in the case of (b) they remain compressive in both columns. From the flow rule, therefore, it is seen that the plastic deformation does not accumulate in bending; axial deformation does not accumulate in the case of (a), and does in the case of (b) as a contraction. The amount of the plastic contration is determined by noting that the abscissae of the states C and C*' in Fig. 4 are give in this cyclic loading to be δ_a and $-\delta_a + 2\delta_m$, respectively, and that the frame deforms in a perfectly plastic manner at a mechanism state without any chnage in the resultant stresses. Equation (48) gives the change $d\Theta$ of the plastic hinge rotation between the two states to be

$$d\Theta = 2\beta(\delta_a - \delta_m). \tag{54}$$

This holds for the plastic hinges in the left column as well as in the right. From the state C' to the State C* the hinge rotation undergoes in magnitude the same amount of change as that in Eq.(54). The increment $h\,d\varepsilon$ of the plastic contraction of a column in half a cycle is found by making use of Eq.(53) in its incremental form and of Eq.(54), as

$$d\varepsilon = 2\beta^2(\delta_a - \delta_m) \tag{55}$$

except for the first half cycle. The plastic work done in each cycle is given by $8\ M_o d\Theta$. Suppose, for example, $\beta = 1/10$ and that the joint translation angle, $\beta\delta_a - \beta\delta_m$, is 1/100 radian. After 10 cycles, the plastic contraction of the columns amounts approximately to 4% of the original length.

In the case of $\delta_m<\delta_a<\delta_p$, the behavior of the frame is determined by the equations for the case $\delta_e<\delta_a\leqq\delta_m$ until the mechanism state is reached, and henceforth by the equations for the case $\delta_p\leqq\delta_a$.

7. SUMMARY

Based on the drastic assumptions of perfect plasticity for columns and infinite rigidity for the beam the hysteretic behavior of a portal frame has been formulated and determined for the combined action of a gravity load and variable repeated horizontal loading. The specification of the history of the sidesway uniquely determines the variation of the horizontal load, of the state of stress, and of the deformation of the frame in equilibrium. Special consideration has been paid to the effect of the variation in the axial forces existing in the columns. Allowance has also been made for the P-Δ effect. Picewise-linear approximation of the yield condition has made feasible for the interaction of the bending moment and axial force to be treated mathematically. Representation of the stress path as a trajectory in the stress plane has been of great help in visualizing the hysteretic characteristics.

As a result of the analysis it has been found that the importance of the variation in the column axial forces depends on the parameter α; as the column depth becomes greater relative to the span, the effect of the variation gets more significant. In order to neglect this effect it suffices to set $\alpha = 0$ in the foregoing equations. A fundamental feature of this effect is the addition of turns and hence of smoothness in the load-deflection curve (Figs. 4 and 6). The range of the elastic response to load changes is expanded by plastic straining until the left- or right-swayed mechanism state is reached (Fig. 6). Due to the plastic straining, the stress path shifts steadily in the definite direction (to the right in Fig. 7), complying with the direct compression due to the gravity load, and finally the stress point moves with the stable locus bridging between the two limiting states of mechanism. No subsequent loading alters the path nor reverses shifting. Each mechanism state has the path-independent state of stress, despite the instability of P-Δ effect, whereas the corresponding load and deformation depend on the past history (Figs. 4-7). Worth noting also is the fact that the effect of the axial force variation is of magnitude of the order of α as against the effect of axial deformation of the order of α^2. Another feature of the existence of the axial forces is to reduce the load carrying capacity [Eq.(16b)]. It is a general characteristic of rectangular frames that the reduction in the plastic collapse load depends on parameters similar to α; the ratio of column depth to span and the ratio of beam depth to story height determine the importance of the variation in the axial forces existing in the column and the beam, respectively [5].

From the investigation into the case of cyclic alternate displacement loading it has been seen that the frame shakes down with almost symmetrical plastic deformation in columns (Fig. 11), when the amplitude is less than a certain limit. When the amplitude is larger [Eq.(47)], the frame collapses plastically; alternating plasticity takes place in bending, and either alternating plasticity or strain accumulation (incremental collapse) in axial deformation, depending upon the magnitude of the vertical load. It is interesting to note the similarity of the herein theorized frame behavior to the actual material behavior of uniaxially loaded mild steel, which exhibits strain accumulation or cyclic creep in the direction of mean stress when subjected to stress cycles around the mean; the load-deformation characteristics of Fig. 6 somewhat resembles the hysteretic stress-strain relationship often observed.

It is concluded by way of caution that the results obtained herein are based on perfect plasticity and piecewise-linear idealization of the yield condition, and hence that they may hold only approximately for actual material behavior and/or actual cross section. Other restrictions are that the beam has to be sufficiently rigid relative to the columns, and that the columns have to be of length long enough in comparison with the cross-sectional dimensions in order for the one-dimensional idealization to be valid and for the shear effects in the individual columns to be negligible, but short enough so that the instability of the individual columns and the effect of axial deformation can both be ignored. The results are fruitful only when the column depth is not negligibly small, as compared with the span, but small enough so that $\alpha^2 \ll 1$. Accounting for the change in the overall geometry, the analysis presented ceases to hold in such a range of large deformation that deflections or displacements reach a magnitude of the order of the original dimensions of the model frame.

REFERENCES

[1] A. H. Aalem, "Satability of Unbraced Single-Bay Multistory Frames," Journal of the Structural Division, Proc. ASCE, ST2, February, 1973, pp. 223-241.

[2] K. Shirahama and J. Mukudai, "Elastic-plastic Behavior of Columns in Rigid Frames Subjected to Varying Axial Forces," Abstracts, Annual Meeting of Architectural Institute of Japan, 1973, pp. 963-964 (in Japanese).

[3] E.T. Onat and W. Prager, "The Influece of Axial Forces on the Collapse Loads of Frames," Proc. 1st Midwestern Conf. Solid Mechanics, Urbana, 1954, pp. 40-42.

[4] K. Ono and H. Tanaka, "Limit Design of Rigid Frames with Consideration of Axial Forces," Proc. Architectural Institute of Japan, Vol. 50, 1955 pp. 32-38, (in Japanese).

[5] T. Nonaka, " A Kinematical Approach to the Plastic Callapse Load of a Rectangular Frame with Consideration of Axial Forces", Proc. Symposium on Plastic Analysis of Stractures, Jassy, Rumania, Vol. II, 1972, pp. 193-220; Theoretical and Applied Mechanics, Vol. 23, University of Tokyo Press, 1975, pp. 301-315; Chap. 1 of this treatise.

[6] M.Z. Cohn and T. Rafay, "Collapse Load Analysis of Frames Considering Axial Forces", Journal of the Structural Division, Proc. ASCE, EM4, August, 1974, pp. 773-794.

[7] J.A. König, "A Method of Shakedown Analysis of Frames and Arches", International Journal of Solids and Structures, Vol. 7, 1971, pp. 327-344.

[8] T. Suzuki and K. Tamamatsu, "On the Variation of Column Axial Forces in Low-Rise Steel Frames", Abstracts, Annual Meeting of Architectural Institute of Japan, 1973, pp. 965-966, (in Japanese).

[9] T. Suzuki, K. Tamamatsu and K. Okuda, "On the Behavior of Columns Subjected to Variable Axial Forces", Abstracts, Annual Meeting of Architectural Institute of Japan, 1973, pp. 967-968, (in Japanese).

[10] T. Suzuki, K. Tamamatsu, I. Kubodera and K. Okuda, "Experimental Studies on the Elastic-Plastic Behavior of Frames with Tension Bracing - Investigation into Earthquake Resistance of Low-Rise Steel Frames, Part 1", Trans., Architecteral Institute of Japan, Vol. 228, February,1975, pp. 57-64, (in Japanese).

[11] See, e.g., M.R. Horne and W. Merchant, "The Stability of Frames",

Pergamon Press, 1965, pp. 50-55.

[12] T. Nonaka, "An Elastic-Plastic Analysis of a Bar under Repeated Axial Loading", International Journal of Solids and Structures, Vol. 9, No. 5 with Erratum in No. 10, 1973, pp. 569-580; Chap. 3 of this treatise.

[13] T. Nonaka, "An Analysis for Large Deformation of an Elastic-Plastic Bar under Repeated Axial Loading", to be published; Chaps.5&6 of this treatise.

APPENDIX 1. Effect of the axial force on column stiffness.

The equations in (10) have been used as the elastic constitutive relations, relating the end moment M linearly with the deflection Δ of a column with end rotation constrained, by disregarding the axial force existing in a column element. The presence of the axial force modifies the equilibrium relation of a deformed element through change in geometry, to result in

$$M_l = F_l(6EI/h^2)\Delta, \qquad M_r = F_r(6EI/h^2)\Delta, \tag{A1}$$

where the factor F indicates this influence and is a function of the axial force N [11]. Since N varies with Δ, the moment-deflection relations are nonlinear. However, by considering that $N_l = P - V$ and $N_r = P + V$, the factor F, involving triangular or hyperbolic functions, is linearized with respect to N about N = P in the form

$$F_l = F_P(1 - CV), \qquad F_r = F_P(1 + CV) \tag{A2}$$

in which F_P designates the value of F at N = P, and C is a coefficient, independent of V. In view of Eq.(8), the nonlinearity in the restoring-force representation due to the axial force variation is cancelled between the two columns, and the dependence of stiffness on the axial force appears in the reduction of F_P from unity owing to the direct compression P. This reduction is negligible when P is sufficiently small as compared with the elastic buckling load $P_E = \pi^2 EI/h^2$; for example, $P = 0.04P_E$ affords $F_P = 0.993$. It is pointed out in this connection that the effect is independent of deformation to the accuracy of the linearization of F in the assumed range of small deformation, whereas the P-Δ effect on the overall frame behavior is significant if the sidesway is large, even if the vertical load is small in itself.

If the variation V attains such a magnitude as comparable with the buckling load P_E, then the column behavior becomes highly nonlinear, and a more rigorous treatment is necessary as presented elsewhere for an isolated bar [12,13].

APPENDIX 2. Effect of axial deformation

Apart from large deformation, unequal axial deformation in the two columns gives rise to rotation of the beam, and consequently the inclusion of this effect distiguishes the magnitudes of the top- and bottom-end moments in each column. Equilibrium relations, Eqs.(1) to (5), remain valid, provided the moments in Eq.(3) are understood as designating those at the top end and left-hand sides of Eqs.(4) and (5) as the sums of the moments at both ends. With this in mind, Eqs.(1), (2), (4) and (5) are combined and expressed in terms of dimensionless symbols to give

$$\eta = (1/4)(\bar{m}_l + \underline{m}_l + \bar{m}_r + \underline{m}_r) - \rho\delta, \tag{A3}$$

replacing the equation afforded by combining Eqs.(8) and (9), where the bars over and under a letter indicate the top and bottom of a column, respectively. For purely elastic response, equations in (10) are replaced by

$$\bar{m}_l = \bar{m}_r = a\delta - 2r \tag{A4}$$

$$\underline{m}_l = \underline{m}_r = a\delta - r \, , \tag{A5}$$

where r is the multiple of the clockwise rotation of the beam with the factor $2EI/(M_0 h)$, and is related to the difference, $N_r - N_l$, of the axial forces by the linearly elastic law. Since this difference in turn is related to the top-end moments through Eq.(3), the substitution of these moments from Eq.(A4) gives the relation between r and δ. For the ideal I-section this becomes

$$r = [2\alpha^2/(1 + 4\alpha^2)] \; a\delta. \tag{A6}$$

It follows from Eqs.(A3) to (A6) for the elastic behavior that

$$\eta = [1 - 3\alpha^2/(1 + 4\alpha^2)] \; a\delta - \rho\delta. \tag{A7}$$

The second term in the brackets indicates the effect of the column axial deformation. It is seen that the axial deformation reduces the elastic stiffness, but with the effect only of the order of α^2.

The plastic action at yield hinges also causes a change in the axial deformation. When this happens in a partially plastic state with either column remaining elastic, the change is contained within a magnitude of the order of elastic deformation. In a mechanism state the state of stress does not depend on the development of deformation, and consequently the axial deformation brings no effect, unless the change in length reaches a magnitude of the order of the original length, which is beyond the scope of this study as stated in assumption 4. It follows that the effect of the axial deformation can be neglected so long as α^2 is small in comparion with unity.

CHAPTER 3

HYSTERETIC BEHAVIOR OF AN AXIALLY LOADED BAR WITH IDEALIZED YIELD CONDITION

ABSTRACT An elastic-perfectly plastic analysis of a bar under repeated axial loading is herein presented. The bar is taken as a one-dimensional continuum with both ends simply supported. The plastic interaction is considered for the combined action of bending and axial deformation, based on a piecewise-linear yield condition. The solution is derived in a closed form, and can describe the hysteretic behavior of a bar, such as a structural brace or a truss member, under any given history of tension and/or compression or of corresponding displacements. An example is illustrated, and some implications of the analytical results are discussed. The chapter is concluded with critical comments on the basic assumptions adopted in the course of the analysis.

SOURCE The contents of Chapter 3 are based on the following paper: Taijiro NONAKA, "An Elastic-Plastic Analysis of a Bar under Repeated Axial Loading", International Journal of Solids and Structures, Vol. 9, No. 5 with Erratum in No. 10, 1973, pp. 569-580.

Notation

Physical symbols

- A cross-sectional area
- E Young's modulus
- l length
- M bending moment
- N load
- x coordinate along bar axis
- y deflection
- Δ relative displacement

Dimensionless symbols

- $m \equiv M/M_o$
- $n \equiv N/N_o$
- $v \equiv \eta$ at $\xi=1$
- $\alpha \equiv (A/I)(M_o/N_o)^2$
- $\delta \equiv (EA/N_o l)\Delta$
- $\eta \equiv (N_o/M_o)y$
- $\theta \equiv d\eta/d\xi$ at $\xi = 1-0$
- $\nu \equiv \sqrt{(Nl^2/4EI)}$
- $\xi \equiv 2x/l$

Subscripts indicate particular values with

- A amplitude
- E Euler load
- O full plasticity
- 1, 2, 3, ...states in order

Superscripts indicate components due to

- e elasticity
- g change in geometry
- p plastic hinge
- t plastic extension

Dots indicate rates of change; primes indicate differentiation

1. INTRODUCTION

The role of bracing in the structural behavior of a frame cannot be overemphasized. A great deal of contribution is normally anticipated from braces to the strength and rigidity of a braced frame. The structural functions of braces are represented by their capabilities to sustain axial loads. Therefore the knowledge of the axial load-displacement relationships is essential in finding the structural performance of a braced frame. This is also the case with a trussed structure. The overall behavior of a truss cannot be revealed without clarifying the axial load-displacement characteristics of each constituent member. Such a knowledge is prerequisite to the determination of the load-carrying capacity of a redundant structure.

When a structure is subjected to a repeated load as in an earthquake, a bracing or a truss member is likewise subjected to tension and/or compression repeatedly. An initially straight bar under compression may be forced into a plastically deformed configuration due to instability effects, with its axial-load carrying capacity much decreased. A subsequent tension may decrease the deflection and the bar will recover some strength and rigidity. This bar may again be subjected to compression before recovering its full strength. Repetition of this kind of loading complicates the hysteretic behavior of the bar.

There are some experimental data on the hysteretic behavior of steel braces under alternately repeated axial loading, their axial load-displacement relation indicating the afore-mentioned characteristics [1-3]. Theoretical investigations, however, seem to be scarce.

Fujimoto, Segawa and Matsumoto [4], Wakabayashi, Matsui, Minami and Mitani [5], and Igarashi and Kibayashi [6] analyzed a braced portal frame under alternately repeated loading on the basis of a modified simple plastic theory. The effects of axial forces were considered in the yield condition for the braces, but it was not taken into account that at a yield hinge plastic action takes place in the axial deformation as well as in bending [7, 8]. In fact, plastic axial deformation at a yield hinge plays an important role in the load-deformation characteristics of a bar when subjected to a large axial force as in a brace or in a truss member.* Reference should be made in this connection to the work of Matsui, Mitani and Tsumadori [11]. The results of their numerical analysis on the post-buckling behavior of a compressed steel brace indicate, in effect, that the axial displacement cannot be evaluated properly by the plastic hinge method which neglects the plastic axial deformation at a yield hinge.

In this chapter, the hysteretic behavior of an elastic-plastic bar is to be studied theoretically for repeated action of axial loading, following the general principles of perfect plasticity. A few implications of the analytical results are also to be discussed.

2. BASIC RELATIONS AND ASSUMPTIONS

Suppose an initially straight bar with uniform cross-section is subjected to an axial load. The load is repeatedly applied and varied

---

* Based on the author's early notes [9], which constitute a basis for the present paper, Shibata took this plastic interaction effect into consideration in his analysis of braced frames, neglecting elastic flexural deformation of braces [10], and found a reasonable agreement with experimental results from a previous test.

quasi-statically. The hysteretic behavior of the bar in equilibrium is to be analyzed. The relationship between the load N and the axial displacement Δ is of primary interest. The effective length is taken from the bar so that the bar of length ℓ can be considered as being simply supported at its ends. It is supposed that the cross-section has an axis of symmetry, and that the bar deflects only in the plane of symmetry. N is taken positive when tensile, and Δ, defined as the relative displacement between the ends, is taken positive when the distance increases.

For mathematical simplicity, analysis is to be based on the following assumptions:

1. The bar can be considered as a one-dimensional continuum.
2. It has an elastic-perfectly plastic property, under the combined action of an axial force N and a bending moment M, shear effects being negligible. The yield condition is idealized as the one for an ideal I-section with indefinitely thin web and flanges,

$$\left|\frac{N}{N_0}\right| + \left|\frac{M}{M_0}\right| = 1 \qquad (1)$$

   where N_0 is the limit load in pure tension and M_0 the limit moment in pure bending.
3. Although change in geometry is taken into account, the deflections are sufficiently small so that the square of the slope can be neglected in comparison with unity. Change in the length of the bar is also negligibly small when compared with the original length.
4. When the load is compressive, the bar cannot carry a load greater in magnitude than the Euler's elastic buckling load $N_E = \pi^2 EI/\ell^2$, where E is the Young's modulus and I is the moment of inertia of

the cross-section. In case $N_E < N_0$, the bar deflects transversely in an elastic and quasi-static manner sustaining the buckling load until the yield limit, Eq. (1), is reached at the critical section in the deflected configuration.

5. When subjected to the compression of magnitude N_0, a straight-shaped bar cannot remain straight, but deflects transversely. This assumption excludes an extremely stubby bar, which can contract plastically without appreciable deflection under the axial load N_0.

6. The bar is composed of ductile material, and no local instability takes place.

Let the dimensionless axial load n and displacement δ be defined by

$$n \equiv \frac{N}{N_0} \quad , \qquad \delta \equiv \frac{\Delta}{\ell} \; \frac{EA}{N_0} \tag{2}$$

where A is the cross-sectional area. δ is equal to the ratio of the fictitious strain Δ/ℓ to the yield point strain N_0/EA, original yield displacement corresponding to $\delta = \pm 1$. On the basis of above assumptions, δ is made up of four components,

$$\delta = \delta^e + \delta^g + \delta^p + \delta^t \tag{3}$$

where δ^e is due to uniform elastic axial deformation, δ^g to change in geometry caused by lateral deflection, δ^p to plastic axial deformation at a yield hinge, and δ^t to plastic elongation distributed along the bar axis.

The first component δ^e is related to the axial force by the elastic linear law

$$\delta^e = n \tag{4}$$

Deflection $y(x)$ in the transverse direction reduces the relative displacement Δ by the amount

$$\int_0^{\ell} \frac{1}{2} \left(\frac{dy}{dx} \right)^2 dx$$

in conformity with assumption 3, where x is the coordinate taken along the original bar axis from an end. With notation

$$\xi \equiv \frac{2x}{\ell}, \quad \eta \equiv \frac{N_o\, y}{M_o}; \qquad \alpha \equiv \frac{A}{I} \left(\frac{M_o}{N_o} \right)^2, \quad n_E \equiv \frac{N_E}{N_o} \tag{5}$$

and with symmetry consideration in Fig. 1, the second component δ^g in Eq. (3) is therefore evaluated from

$$\delta^g = - \frac{2\alpha n_E}{\pi^2} \int_0^1 (\eta')^2\, d\xi \tag{6}$$

where the prime indicates differentiation with respect to ξ. The parameter α is a number depending only on the shape of the cross-section, and is equal to the square of the ratio of plastic section modulus to the product of cross-sectional area and radius of gyration. For an ideal I-section, $\alpha = 1$, and for a rectangular cross-section, $\alpha = 3/4$. Thus, α takes a value close to unity for most structural steel sections.

The dimensionless deflection $\eta(\xi)$ which satisfies both the equilibrium differential equation

$$\eta'' - \nu^2 \eta = 0 \tag{7}$$

and the boundary condition at the bar end $\eta(0) = 0$ must be of the form

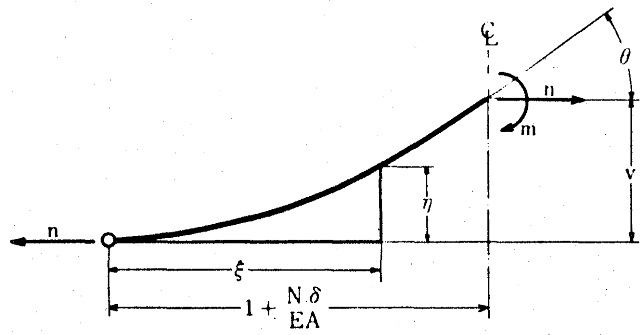

Fig. 1 Deflected half bar and dimensionless quantities

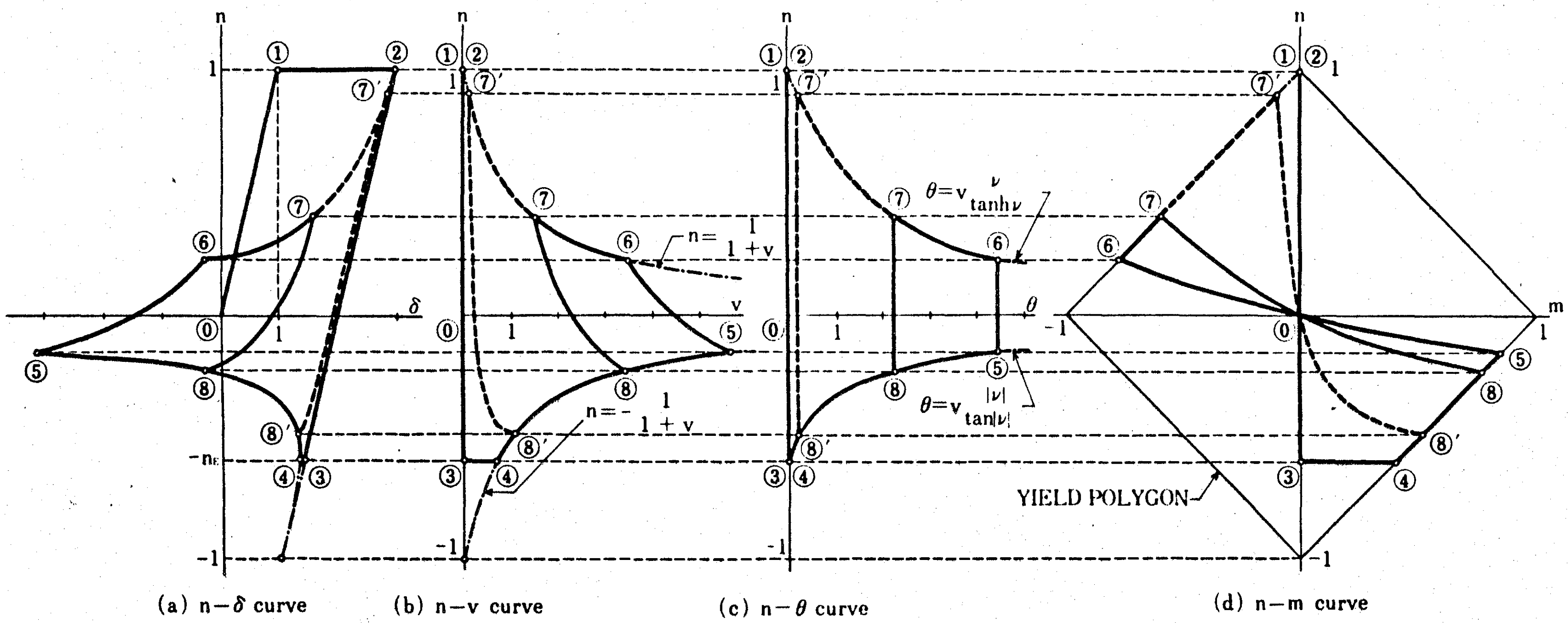

Fig. 2 Behavioral diagrams of a bar under repeated axial loading

$$\eta = a \sinh (\nu \xi) \tag{8}$$

where

$$\nu \equiv \sqrt{\frac{N\ell^2}{4EI}} = \frac{\pi}{2}\sqrt{\frac{n}{n_E}} \tag{9}$$

The constant of integration "a" appearing in Eq. (8) is determined from the other boundary condition at the bar center, i.e., either

$$\eta(1) = v \qquad \text{or} \qquad \eta'(1-0) = \theta \tag{10 a,b}$$

according to whether plastic action takes place there or not, respectively. It is noted that v and θ have necessarily the same sign in our problem, and that the sense of η-axis is so taken that v and θ are nonnegative.

Plastic action can take place at the bar center when the yield condition, Eq. (1), is satisfied.* Let m denote the ratio of the bending moment M at the center to M_0, its positive direction being shown in Fig. 1. The equilibrium relation for the half bar

$$m + n\,v = 0 \tag{11}$$

along with Eq. (1) give the relation

$$n = \pm \frac{1}{1+v} \tag{12}$$

if it is noted from Eq. (11) that m and n have opposite signs. It follows from Eqs. (6), (8) and (10 a) that

$$\delta g = -\alpha n_E \left(\frac{v}{\pi} \frac{\nu}{\sinh \nu} \right)^2 \left[\frac{\sinh(2\nu)}{2\nu} + 1 \right] \tag{13}$$

---

* Although the present formulation expresses δ explicitly in terms of n, owing to the irreversibility of a plastic process the uniqueness of the solution is not assured by the specification of the history of n; the history of δ determines the history of n uniquely.

Combination of Eqs. (9), (12) and (13) expresses δ^g in terms of n. The plastic action causes discontinuity in slope at the center. The slope angle θ at just next to the center of the dimensionless deflection curve is found from Eqs. (8) and (10) to be

$$\theta = v \frac{\nu}{\tanh \nu} \tag{14}$$

When the state of stress is such that $|m| + |n| < 1$, the bar behaves in an elastic manner, and θ remains constant, whose value is determined by the preceding plastic action through Eq. (14). In this case δ^g is given from Eqs. (6), (8) and (10 b) to be

$$\delta^g = -\alpha n_E \left(\frac{\theta}{\pi \cosh \nu} \right)^2 \left[\frac{\sinh (2\nu)}{2\nu} + 1 \right] \tag{15}$$

The central dimensionless deflection v varies with the axial force, and is found by recourse to Eqs. (8) and (10) to be

$$v = \theta \frac{\tanh \nu}{\nu} \tag{16}$$

When the axial force is compressive, n is negative, and ν and "a" are imaginary. In order to express δ^g in terms of real functions, ν simply has to be replaced by its modulus $|\nu|$, and the hyperbolic functions by the corresponding trigonometric functions in Eqs. (13) and (15). A similar manipulation in Eqs. (14) and (16) gives θ and v, respectively, in terms of real functions.

The third component δ^p in Eq. (3) varies in value when plastic action takes place at the central yield hinge. Due to the presence of axial force, plastic deformation occurs there in axial direction as well as in bending [7, 8]. Their relation is provided by the flow rule associated with the yield condition, Eq. (1). In geometric terms, the flow rule states that when the state of stress is represented by a point on the yield polygon, the plastic flow vector is in the direction of the outward normal to the yield polygon at the corresponding stress point [12]. By representing the yield polygon in the dimensionless stress plane (m, n), and by recalling that m and n have opposite signs [see Fig. 2 (d)], it is found that, except for corners $m = \pm 1$ and $n = \pm 1$, two components of the plastic flow vector, viz., M_o times the rate of change of the slope discontinuity and N_o times the rate of change of the plastic elongation, are equal and opposite. With dots denoting the rates, it follows that

$$\dot{\delta}^P = - \left(\frac{2}{\pi} \right)^2 \alpha \, n_E \, \dot{\theta} \qquad (17)$$

It should be noted that the cases $m = \pm 1$ are not encountered in our problem, and that consideration of plastic action for $n = -1$ is not required due to assumption 5. If the conditions $n = 1$ and $\dot{n} = 0$ are simultaneously satisfied, Eq. (14) gives in conjunction with Eqs. (9) and (12) that $\dot{\theta} = 0$, and it is seen from Eq. (17) that $\dot{\delta}^P = 0$. The plastic deformation for this case* is accounted for in the component δ^t. Eq. (17) is still valid when the bar behaves elastically, because then θ remains constant and Eq. (17) leads to $\dot{\delta}^P = 0$. Consequently, Eq. (17) holds throughout the history, and integration with the initial condition $\delta^P = 0$ for $\theta = 0$ gives the relation

$$\delta^P = - \left(\frac{2}{\pi}\right)^2 \alpha \, n_E \, \theta \qquad (18)$$

---

* When $n = 1$ and $\dot{n} < 0$, plastic action does not occur, and hence $\dot{\theta} = 0$. Assumption of perfect plasticity does not allow the case of $n = 1$, $\dot{n} > 0$. With these in mind it is found that $\dot{\theta} = \dot{\delta}^P = 0$ whenever $n = 1$.

The last term δ^t in the right-hand side of Eq. (3) can take any nonnegative value. The only restrictions are that $\dot{\delta}^t \geqq 0$ during the simultaneous satisfaction of $n = 1$ and $\dot{n} = 0$, which can be attained solely in a straight configuration, and that $\dot{\delta}^t = 0$ otherwise. Evidently this is allowed by the generalized flow rule stipulated for the corner of the yield polygon that the plastic flow vector lies between the outward normals to the adjacent line segments [13].

Worth noting is that $\delta^g \leqq 0$, $\delta^p \leqq 0$ and $\delta^t \geqq 0$, whereas δ^e can have either sign.

3. EXAMPLE

Let us consider an example, in which the bar is first subjected to elongation from the straight virgin state until the yield limit $n = 1$ is reached. The behavior in this process is obvious, the $n-\delta$ relation being represented by the trace ⓪ → ① → ② in Fig. 2 (a). It is instructive to illustrate the corresponding history of deformation and the state of stress at the critical section; in (b), (c) and (d) of Fig. 2, v, θ and m are taken, respectively, for the abscisae as against the common ordinate of n.

After undergoing the deformation

$$\delta_2 = \delta^e_2 + \delta^t_2 = 1 + \delta^t_2 \qquad (19)$$

at state ②, the bar is subjected to a decreasing load up to the load carrying capacity in compression. The subscripts refer to the states with encircled consecutive numbers in Fig. 2. If the bar is so slender that $n_E \leqq 1$, it will buckle at $n = -n_E$, under which the deflection increases elastically from zero until the yield limit is reached at the bar center, according to assumption 4 . This process is represented in Fig. 2 by states ② → ③ → ④. For ② → ③, $\delta = n + \delta_2^t$ with vanishing δ^g and δ^p. δ^g contributes to the relative axial displacement from state ③, caused by the lateral deflection, and δ_4^g, whose magnitude gives the length of the plateau ③ → ④ in Fig. 2 (a), is determined from Eq. (13)in conjunction with Eq. (12) by setting $n_4 = -n_E$ and $|\nu_4| = \pi/2$, to be $\delta_4^g = -\alpha\,(1-n_E)^2/(4n_E)$.

In the case of $n_E \geqq 1$, assumption 5° stipulates that the bar buckles at $n = -1$, and states ③ and ④ coincide. The treatment for this case is simpler, and the subsequent behavior is clear from the case $n_E < 1$. The latter case is assumed in the illustration of Fig. 2 (Particular curves used for demonstration in Figs. 2 to 4 are drawn for $\alpha = 1$ and $n_E = 0.6$).

After state ④, equilibrium is maintained under decreasing compression, and increasing deflection is accompanied by plastic hinge formation. For states ④ → ⑤, the state of stress at the bar center has a trajectory on the yield polygon in the fourth quadrant of the stress plane as shown in Fig. 2 (d). Due to the plastic action the slope becomes discontinuous at the bar center, θ being given by Eq. (14). v is determined from Eq. (12) with the negative sign in the right-hand side. Each component of δ in Eq. (3) now has a nonvanishing value. δ^e, δ^g and δ^p are found as functions of n or ν from Eqs. (4), (13) and (18), respectively, and $\delta^t = \delta_2^t$.

The variation of the states ⑤ → ⑥ is characterized by elastic recovery with increasing n and δ. θ remains constant at θ_5 and so do δ^p as well as δ^t, i.e., $\delta^p = \delta_5^p$, $\delta^t = \delta_5^t = \delta_2^t$. δ^e and δ^g

are given by Eqs. (4) and (15), respectively, where v is determined through Eq. (16).

Elastic behavior ceases to continue at state ⑥, at which the yield limit is reached with positive n. The values n_6 and v_6 are found, as functions of the history dependent quantity θ_5 and the parameter n_E, by making use of Eqs. (9), (12) and (16), i.e., by solving the simultaneous equations

$$n_6 = \frac{1}{1+v_6}\ , \qquad v_6 = \theta_5 \frac{\tanh\left(\frac{\pi}{2}\sqrt{\frac{n_6}{n_E}}\right)}{\frac{\pi}{2}\sqrt{\frac{n_6}{n_E}}} \tag{20}$$

Plastic action again takes place along ⑥ → ⑦ with the stress point on the yield polygon in the second quadrant. θ as well as v decrease. Each component of δ in Eq. (3) can be determined from the foregoing equations in a manner similar to ④ → ⑤, having in this case positive values of n. If the load is kept increasing and $n = 1$ is attained, then Eqs. (12) and (14) indicate that $v = \theta = 0$, so that $\delta^g = \delta^p = 0$, and δ amounts to $1 + \delta_2^t$, which is nothing but δ_2 according to Eq. (19). As a consequence, it is observed that the extension of the curve ⑥ → ⑦ leads to ②, as shown in dashed-and-dotted lines in Fig. 2. The bar is not straightened and does not recover its full strength, until elongated beyond $\delta = 1 + \delta_2^t$. Within the limitation of small deformation setted in assumption 3, this cycle of loading and unloading, from and to state ②, has no influence whatsoever on the subsequent behavior of the bar.*

---

* If the elongation attains the order of magnitude of the original bar length, the buckling strength becomes smaller than the original, to cite an instance.

Unloading from state ⑦ gives rise to elastic behavior and can be treated in a way similar to ⑤ → ⑥. The yield limit is again reached at ⑧. The ensuing plastic action is associated with $n < 0$, and δ^e, δ^g and δ^p are determined by the same equations as for ④ → ⑤; δ^t still remains constant at δ_2^t. Accordingly, it is seen that state ⑧ falls on a certain point between ④ and ⑤ in each curve of Fig. 2. The subsequent behavior is therefore clear from the foregoing descriptions. If the unloading point ⑦' is close to ②, the traces corresponding to ⑦' → ⑧' tend to curve sharply near $n = -n_E$, except for n-θ curve of (c), as depicted in dashed lines in Fig. 2. The qualitative behavior, however, is not different from the case ⑦ → ⑧.

From this example it is evident that the foregoing equations are adequate for the explicit representation of the load-deformation characteristics of a bar under any history of axial loading.

4. FURTHER REMARKS

Among the components of δ in Eq. (3), δ^t can take any positive value, as already mentioned. δ^t is controlled by displacement constraints. δ^e is, of course, independent of the history. When plastic action takes place at the yield hinge, it is revealed from Eqs. (9), (12), (13), (14) and (18) that δ^g and δ^p are also independent of history; they are functions only of the current value of the axial force for a given bar. Consequently, it turns out that $\delta - \delta^t$ can be expressed as a function of n alone for the parameters α and n_E given, as far as plastic action occurs. This relation is shown in thick solid lines in Fig. 3. Irreversible nature of the plastic process restricts the variation in the direction shown by arrows, i.e., in the direction $\dot{n} > 0$. The variation along the lower curve is associated with increasing θ, and the upper decreasing θ. Analytically the difference in shape between the two curves results from that between trigonometric and corresponding hyperbolic functions.

Bridging between these curves is associated with elastic behavior and is reversible. $\delta - \delta^t$ depends not only on n but also on the previous history. This is because in an elastic process δ^g and δ^p depend on θ, as seen from Eqs. (15) and (18), θ remaining constant in each elastic process. These relations are shown in thin solid lines in Fig. 3. The slope of these curves becomes larger as θ decreases, and takes the maximum and constant value unity for $\theta = 0$. Along each curve, the slope increases as n does.

With these in mind it is seen that the curves in Fig. 3 suffice for the completion of the hysteretic n-δ relation for any given history of axial loading. For instance, if the bar is subjected to cyclic displacement changes between $\delta = -\delta_A$ and $\delta = \delta_A$ ($\delta_A > 1$) with contraction first, the hysteretic n-δ relation is determined as in Fig. 4 by simple translation of curves in Fig. 3. The trace of n-δ relation falls on the final loop, the thick solid-lined curve, and becomes stable before the end of the first cycle.

5. CONCLUSIONS

The closed-form solution has been found for the hysteretic behavior of an elastic-perfectly plastic bar with moderate slenderness

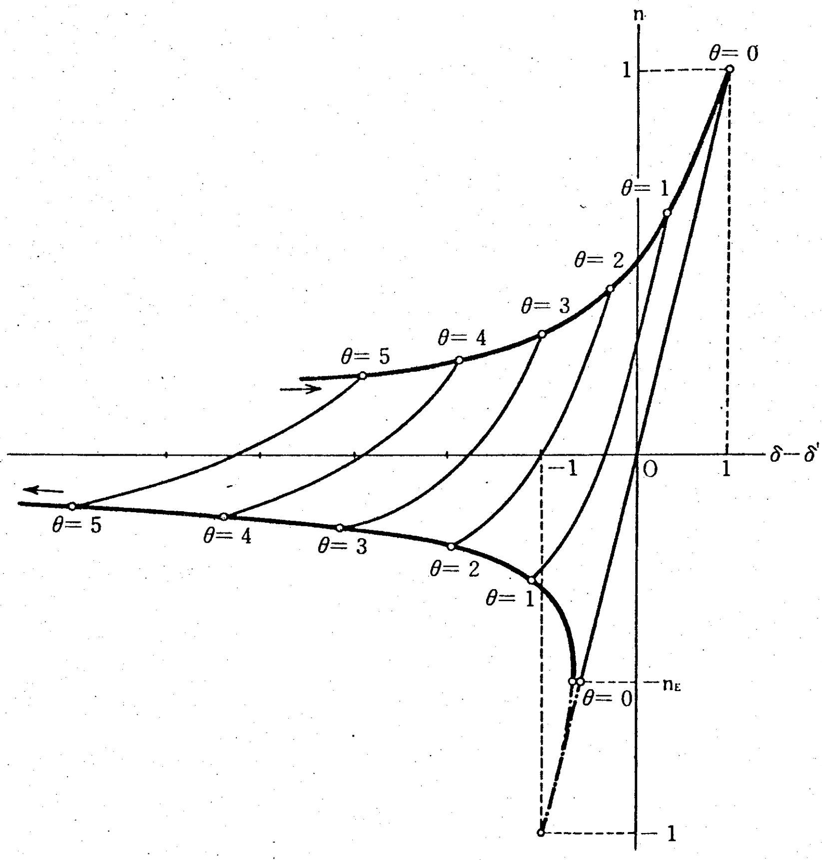

Fig. 3 n versus $\delta - \delta^{t}$ relation

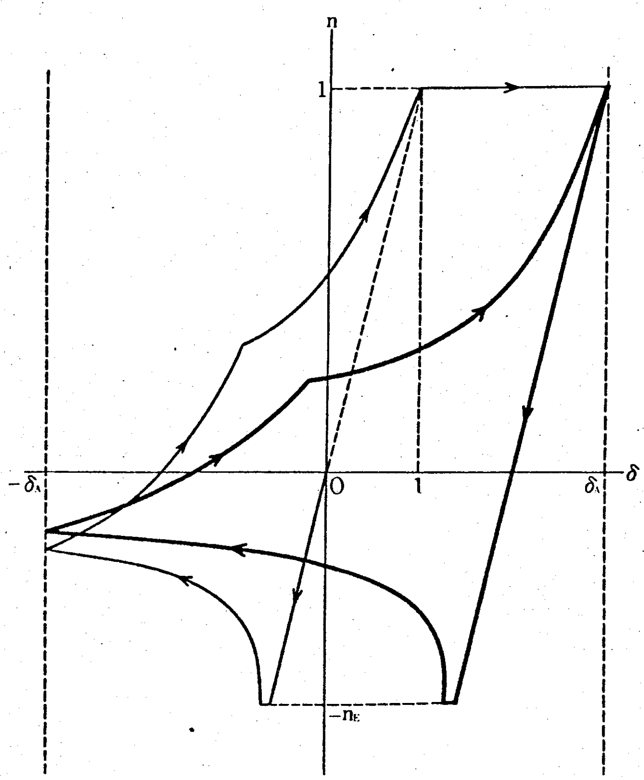

Fig. 4 Example of cyclic loading with constant displacement amplitude

under repeated axial loading, based on the piecewise-linear yield condition, Eq. (1), for the combined action of axial force and bending moment. The solution is complete in the sense that the load-deformation characteristics can be found uniquely whenever the history of the end displacements is specified. The dimensionless relative axial displacement δ is expressed as a function of the history of the dimensionless axial load n, with the cross-sectional factor α and the dimensionless Euler buckling load n_E as parameters.

As a result of the analysis, it is observed how a bar plastically deformed due to instability recovers its strength and rigidity during the course of the subsequent elongation. The analysis also demonstrates the feature that a bar gets loosened due to plastic elongation, and the bar cannot exhibit the full strength subsequently, until it undergoes the maximum relative displacement that it has experienced. A cycle, from and to this maximum displacement, has no influence on the subsequent behavior of the bar.

It seems pertinent to conclude with critical comments on some of the basic assumptions adopted in this chapter. The assumption of perfect plasticity in the use of stress resultants and the corresponding kinematical quantities neglects the stage of partial yielding in a cross-section. It is impossible therefore for the residual nature of plastic deformation to be strictly taken into consideration by the theory which has a basis on this assumption. This will cause some error in the prediction of the behavior of actual sections with a web and/or finite flange thickness under repeated loading, in addition to the error usually observed in the case of monotonic loading. To draw an instance from Fig. 2, an actual bar with elastic-perfectly plastic stress-strain relationship, after being subjected to the loading program like (1) to (7), would not acquire full recovery by the attainment of the maximum relative displacement that the bar has previously experienced; that is, $n < 1$ at $\delta = \delta_2$. There would still remain some residual deflection at $\delta = \delta_2$ due to nonuniform residual strain distribution in a cross-section, and the load carrying capacity in the subsequent compression would be lower than that for the original state, n_E. The full strength in tension, $n = 1$, would be reached at a still larger displacement than δ_2. In order to gain access to the real behavior of an actual steel brace or a truss member, a more realistic hysteretic constitutive relation may have to be used. Nevertheless, the analysis presented in this paper has a merit in its simplicity, and will serve as a reasonable first order approximation. It is worth mentioning that for the purpose of determining the post-buckling deformation characteristics of a bar the piecewise-linear approximation of the yield condition is reasonable even for a rectangular cross-section [14]. The shape of the exemplified curves in Figs. 2 and 4 indicates qualitative agreement with the experimental results obtained from bar specimens with rectangular cross-section [1-3]. Details of the comparison between the theory presented and the experimental observations shall be discussed in Chapters 4 and 6.

For very stubby bars to which the present analysis is not accomodated because of assumption 5, the shear effect may also come into play unless the bar has a compact cross-section, or it may be too stocky to be treated as a one-dimentional continuum. If the bar is extremely slender and flexible, and forced into large deflection, assumption 3 of small deformation may not be appropriate. Such a bar, however, may well be treated as incapable of carrying compression, and can be analyzed in a very simple manner.

ACKNOWLEDGMENTS

The work presented in this chapter has been supported by a grant from the Matsunaga Science Foundation awarded to the author. Encouragement by Professors Y. Yokoo and M. Wakabayashi of Kyoto University are gratefully acknowledged. The author is especially indebted to Mr. M. Shibata of Osaka Institute of Technology for stimulating discussions. Mr. N. Yoshida, student of Kyoto University, also contributed by preparing the figures.

REFERENCES

[1] M. Wakabayashi, T. Nonaka, O. Koshiro and N. Yamamoto, "An Experiment on the Behavior of a Steel Bar under Repeated Axial Loading", Disaster Prevention Research Institute Annuals, Kyoto University, No. 14A, 1971, pp. 371-381 (in Japanese).

[2] M. Yamada, B. Tsuji and K. Takeda, "Experimental Studies on Elasto-Plastic Behavior of Steel Bracings under Cyclic Loading", Abstracts, Annual Meeting of Kinki Branch, Architectural Institute of Japan, 1971, pp. 391-394 (in Japanese).

[3] M. Wakabayashi, T. Nonaka, T. Nakamura, S. Morino and N. Yoshida, "Experimental Studies on the Behavior of Steel Bars under Repeated Axial Loading", Disaster Prevention Research Institute Annuals, Kyoto University, No. 16B, 1973, pp. 113-125 (in Japanese).

[4] M. Fujimoto, T. Segawa and Y. Matsumoto, "An Elastic-Plastic Analysis of a Braced Frame under Repeated Loading", Abstracts, Annual Meeting of Architectural Institute of Japan, 1969, pp. 1213-1214 (in Japanese).

[5] M. Wakabayashi, C. Matsui, K. Minami and I. Mitani, "Inelastic Behavior of Full Scale Steel Frames", Disaster Prevention Research Institute Annuals, Kyoto University, No. 13A, 1970, pp. 329-369 (in Japanese).

[6] S. Igarashi and M. Kibayashi, "Restoring-Force Characteristics of a Braced Frame", Abstracts, Annual Meeting of Architectural Institute of Japan, 1971, pp. 393-394 (in Japanese).

[7] E. T. Onat and W. Prager, "Limit Analysis of Arches", Jour. Mechanics and Physics of Solids, Vol. 1, 1953, pp. 77-89.

[8] E. T. Onat and W. Prager, "The Influence of Axial Forces on the Collapse Loads of Frames", Proc. 1st Midwestern Conference on Solid Mechanics, Urbana, 1953, pp. 40-42.

[9] T. Nonaka, Notes on Braces under Repeated Loading, unpublished, 1968 (in Japanese).

[10] M. Shibata derived the theoretical curves for braces and braced frames in the paper, "M. Wakabayashi, The Behavior of Steel Frames with Diagonal Bracings under Repeated Loading, Japan-U.S. Seminar on Earthquake Engineering with Emphasis on the Safety of School Buildings, Sendai, Japan, 1970".

[11] C. Matsui, I. Mitani and J. Tsumadori, "Elastic-Plastic Analysis of a Compressed Steel Brace", Abstracts, Annual Meeting of Architectural Institute of Japan, 1971, pp. 365-366 (in Japanese).

[12] W. Prager, "The General Theory of Limit Design", Proc. 8th International Congress of Applied Mechanics, Istanbul (1952), Vol. 2, 1956, pp. 65-72.

[13] W. T. Koiter, "Stress-Strain Relations, Uniqueness and Variational

Theorems for Elastic-Plastic Materials with a Singular Yield Surface", Quarterly of Applied Mathematics, Vol. 11, 1953, pp. 350-354.

[14] M. Shibata, T. Nonaka and M. Wakabayashi, "A Theoretical Study on the Post-Buckling Behavior of Braces", in preparation.

CHAPTER 4

HYSTERETIC BEHAVIOR OF AN AXIALLY LOADED BAR WITH MODIFIED YIELD CONDITION

ABSTRACT This chapter is concerned with the hysteretic behavior of a prismatic bar subjected to repeated axial loading. Elastic-perfectly plastic behavior is assumed in the analysis under the combined action of axial force and bending moment. The fully plastic states in pure bending and in pure tension and compression are bilinearly interpolated to serve as the yield condition; linearly interacted regimes are combined with interactionless regimes of pure bending to form the yield hexagon, which is a modification of a previously assumed yield quadrangle. Basic equations are derived through the analysis, expressed in a simple analytic closed form, and are able to determine the load-deformation relationship of the bar for any specified history of axial loading.

As a result of the analysis it follows that due to the load cycle of tension and compression an initially straight and plastically bent bar undergoes a plastic extension upon the recovery of the straight configuration. This is the balanced axial deformation at a yield hinge between extension and contraction, taking place during the cycle of hinge rotation. Another characteristic feature found is that cyclic alternate displacement loading with large amplitude leads to a steady state after some repeated deterioration of processes. Comparison is made of the load-axial displacement relation between the analytical and experimental results to show reasonable agreement, with discussions extended to the appropriateness of the form of the yield condition.

SOURCE The contents of Chaper 4 are based on the following paper: Taijiro NONAKA, "Approximation of Yield Condition for the Hysteretic Behavior of a Bar under Repeated Axial Loading", to be published.

Notation

Physical symbols

A	cross-sectional area
c	constant
E	Young's modulus
L	length
M	bending moment
N	load
V	middle deflection
x	coordinate along bar axis
y	deflection
Δ	relative displacement
Θ	one-half of hinge rotation

Dimensionless symbols

$m \equiv M/M_O$

$n \equiv N/N_O$

$v \equiv (N_O/M_O)V$

$\alpha \equiv (A/I)(M_O/N_O)^2$

$\delta \equiv (EA/N_OL)\Delta$

$\eta \equiv (N_O/M_O)y$

$\theta \equiv (N_OL/2M_O)\Theta$

$\nu \equiv \sqrt{(NL^2/4EI)}$

Subscripts indicate particular values with

A	amplitude
E	Euler load
O	full plasticity
1, 2, 3, ...	states in order

Superscripts indicate components due to

e	elasticity
g	change in geometry
p	plastic hinge
t	plastic longation

1. INTRODUCTION

Axially loaded members play an important role in such structures as trusses and braced frames. Clarification of the performance of these structures under repeated loading requires the knowledge of the hysteretic load-deformation characteristics of axially loaded members. Recently in Italy and Japan much effort has been directed to the formulation of the elastic-plastic axial load-displacement relation of steel braces, in relation to the response of tall braced frames to earthquake excitation; the static relationship is useful for the determination of dynamic behavior, since braces have relatively small mass. It is worthy of note that plastic action in axially loaded members ordinarily takes precedence of flexurally loaded members because of the predominance in stiffness of the former over the latter. Some results of numerical analyses are reported in the form of charts [1-7], and a successive approach is proposed on the basis of simple plastic theory established for beams and unbraced frames, which does not take account of plastic axial deformation [8,9].

The author has formulated a general elastic-plastic solution for the hysteretic behavior of a prismatic bar subject to repeatedly applied loads in the axial direction [10]. The assumption of perfect plasticity together with the one-dimensional idealization of the bar has led to basic equations which have been shown to be adequate for the behavior to be determined for any history of axial loading in the range of small deformation. This theory describes how a bar, after deforming plastically due to instability during compression, recovers in a subsequent tension, and describes how the bar as a structural member gets loosened by plastic elongation, reducing the overall stiffness of the structure. The usefulness of the theory as a first order approximation being confirmed experimentally [11, 12], it has possessed a significant defect. The analysis has been based on the assumption that the fully plastic states in pure bending and in purely axial loading can be linearly interpolated to serve as the yield condition for the interaction of bending moment and axial force. The piecewise linearity in the yield condition is the idealization for an I-section with thin web and flanges, and is rather a crude approximation of commercially available cross sections. As a consequence, the solution has had a merit in simplicity but a demerit in the prediction that a plastically deformed bar completely restores its full strength and initial straightness upon the reversion of the axial displacement, as against the actual observation that a plastically deformed bar hardly becomes straight again through mere extension. A nonlinear yield condition replacing the piecewise-linear one corrects the defect of this kind to a certain extent, and an attempt to use a parabolic yield condition has resulted in better agreement with the experimental behavior of a rectangular prism [13]. Then, however, the basic equations have not been able to be expressed in a finite number of analytic functions. The objective of the discussions in this chapter is to obviate the two shortecomings found in the use of the piecewise-linear and parabolic yield conditions, and to develop an analysis which still leads to a closed-form analytic solution. This is accomplished by modifying the form of the yield condition. The analytical results are then compared with the experimental, and discussions extend to the pertinence of the modification.

2. ASSUMPTIONS

An initially straight bar of uniform material and cross section is subjected to a repeatedly applied load, which is a pair of equal and opposite forces acting centroidally at the ends of the bar with slowly varying intensity. The effective length L is taken so that the bar can be regarded as being simply supported at its ends. The main interest lies in the hysteretic relationship between the load N, positive for tension, and the relative displacement Δ, positive for separation, of the bar ends in the direction of loading. In this chapter there is the restriction that deformation may be finite but small enough so that change in the length of the bar is negligible when compared with the original and so that the square of the slope of the deflection curve can be neglected in comparison with unity. It is assumed that the cross section has axes of symmetry and that the bar deflects only in the plane of symmetry without twist, having cross-sectional area A and moment of inertia I. The bar is idealized as a one-dimensional continuum, having the property of linear elasticity with Young's modulus E followed by perfect plasticity under combined action of the axial force N and bending moment M.

The yield condition for the M-N interaction is approximated by bilinearly interpolating the fully plastic state $|M| = M_o$ in pure bending and the fully plastic state $|N| = N_o$ in pure tension and compression. This is represented in the dimensionless stress-resultant plane $(M/M_o, N/N_o)$ to form the yield hexagon, as shown by solid lines in Fig. 1. Yielding is stipulated by linking interactionless regimes of pure bending with linearly interacted regimes, having a corner at (1, 1-c) in the first quadrant, and having double symmetry with respect to the co-ordinate axes. This form of the yield condition is selected as the simplest with a single parameter c among bilinear representations in one quadrant, while still furnishing a reasonable prediction for the overall hysteretic behavior of an axially loaded bar; c is to be chosen properly between

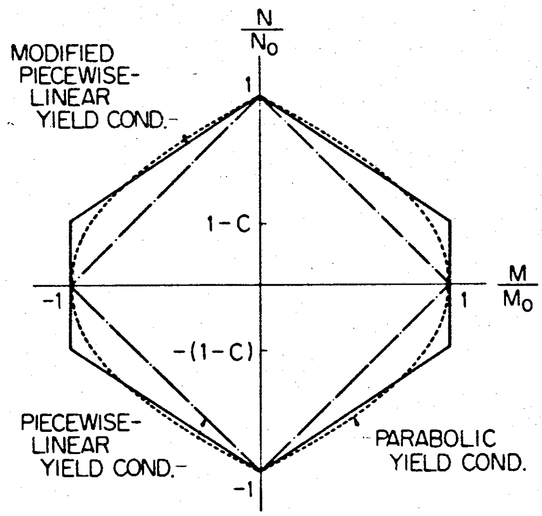

Fig. 1 Yield curves

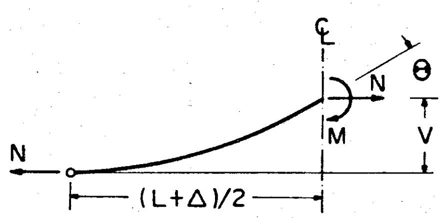

Fig. 2 Notation

zero and unity, according to the shape of the cross section and the dominant range of the load intensity. The choice $c = 1$ would be identical with the previously assumed piecewise-linear yield condition which is represented by the square as drawn in dotted-and-dashed lines in Fig. 1. If it is specified that the same area of elastic domain be enclosed by the hexagon of the modified piecewise-linear yield condition and by the pair of parabolas drawn in dotted lines which correspond to the fully plastic condition for a rectangular cross section, then it follows that $c = 2/3$. It is worth noting that the modified piecewise linearity is equivalent to assuming the cross section to consist of three concentrated areas, two as flanges and the other as the center web.

It is also assumed that a compressed straight bar buckles when the compression reaches either the Euler load $N_E = \pi^2 EI/L^2$ or the crush load N_O. Investigation is focused on bars of moderate slenderness such that N_E and N_O are of the same order of magnitude. The effects of shear are completely neglected.

3. FORMULATION

While taking note of the fact that the history of the axial displacement has to be specified in order for the behavior of the bar to be determined, it is convenient to express the displacement in terms of the load. Some of the basic relations established previously remain valid [10]. The dimensionless displacement δ, the ratio of the relative axial displacement to the yield point displacement, is composed of four components, viz.,

$$\delta \equiv (EA/N_O L)\Delta = \delta^e + \delta^g + \delta^p + \delta^t.$$

where δ^e is due to elastic axial deformation, $\delta^g \leqq 0$ to change in geometry associated with transverse deflection, $\delta^p \leqq 0$ to plastic axial deformation at a yield hinge, and $\delta^t \geqq 0$ to plastic elongation in a straight configuration. Among these it is clear that δ^e is equal to the dimensionless load $n \equiv N/N_o$, and that δ^t can increase when n equals unity and remains constant otherwise. The component δ^g is caused by the difference in length between the arc and chord of the deflection curve two halves of which are symmetric and determined from the equilibrium and elasticity of the bar. Each half is expressible in terms of hyperbolic function, as shown in Fig. 2. At the middle the deflection $V \equiv (M_o/N_o)v \geqq 0$ is related to the slope angle $\Theta \equiv (2M_o/N_oL)\theta \geqq 0$ by

$$\theta = (\nu/\tanh\nu)\ v. \tag{1}$$

Integration of the square of the slope along the bar axis provides the component

$$\delta^g = -\alpha n_E\left(\frac{\theta}{\pi\cosh\nu}\right)^2\left[\frac{\sinh(2\nu)}{2\nu} + 1\right], \tag{2}$$

where $\alpha \equiv (A/I)(M_o/N_o)^2$ is a cross-sectional constant, $n_E \equiv N_E/N_o$ is a slenderness constant, and $\nu \equiv (NL^2/4EI)^{1/2} = (\pi/2)(n/n_E)^{1/2}$ is a dimensionless axial force. When the load is negative, ν is imaginary and in order to express the results in terms of real functions, it suffices to replace ν by its modulus and to replace the hyperbolic functions by the corresponding trigonometric functions. The above relations are unchanged by the modification of the yield condition.

Plastic action can take place with a yield hinge at the middle of the bar when the deflection attains such a value that the yield condition is satisfied. In order to relate this deflection to the load, it is first noted from the equilibrium relation

$$m + nv = 0 \tag{3}$$

that the bending moment $M \equiv mM_0$ at the middle has the opposite sign to the load when the positive moment is defined to be compatible with an increase in the hinge rotation 2θ as shown in Fig. 2. It follows that the state of stress at the middle cross section has a stress point somewhere in the second or fourth quadrant in the stress plane of Fig. 1, and for the relevant regimes the yield condition reads

$$|m| = 1 \qquad \text{for} \qquad |n| \leqq 1 - c, \tag{4a}$$

$$|n - cm| = 1 \qquad \text{for} \qquad 1 - c \leqq |n| \leqq 1. \tag{4b}$$

Combination of Eqs.(3) and (4) gives

$$v = \begin{cases} 1/|n| & \text{for} \quad |n| \leqq 1 - c \\ (1/c)(1/|n| - 1) & \text{for} \quad 1 - c \leqq |n| \leqq 1. \end{cases} \tag{5a,b}$$

As long as Eq.(5) is kept satisfied, there can be a change in the hinge rotation at the middle. It is accompanied by a change in the plastic axial deformation, their relation being determined by the normality of the flow rule associated with Eq.(4). It follows for the increments that

$$d\delta^p = \begin{cases} 0 & \text{for} \quad |n| \leqq 1 - c \\ -(2/\pi)^2(\alpha n_E/c)d\theta & \text{for} \quad 1 - c < |n| \leqq 1. \end{cases} \tag{6a,b}$$

The hinge rotation to be substituted in Eqs.(2) and (6) is related to the load by combining Eqs.(1) and (5) for an plastic process.

When the deflection is smaller than is given by Eq.(5), then the bar behaves in an elastic manner and

$$d\delta^p = d\theta = 0. \tag{7}$$

If v is to be determined for an elastic process, Eq.(1) may be used with

θ kept constant and specifed by the preceding plastic action. It is worthy of note that because of the incremental relation of Eq.(6) the hereditary nature of plasticity is comprised not only in δ^t and θ but also in δ^p, appearing as an integral constant, which has not been the case with the piecewise-linear yield condition assumed previously [10].

4. ILLUSTRATION

Figure 3 serves to illustrate the behavioral characteristics of a bar under a varying axial load. In (a), (b), (c) and (d) of Fig. 3, δ, v, θ and m are taken, respectively, for the abscissae as against the common ordinate of n. The variation in the states of deformation and stress is indicated by orderly numbering in circles. It is assumed in this illustration that $1 - c < n_E < 1$. After being subjected to plastic yielding in tension, the bar is compressed until it buckles at $n = -n_E$ as in ⓪→③. A yield hinge is formed at the middle of the bar in ④→⑥, with the stress point moving first along an interacted regime and transferring at ⑤ to an interactionless regime of the yield hexagon as shown in Fig. 3(d). During the process ④→⑤ the yielding causes plastic flow of contraction in the axial direction besides a relative rotation across the yield hinge, whereas no change takes place in the axial plastic deformation in ⑤→⑥. The process ⑥→⑦ is characterized by elastic recovery, and is followed by hinge action with a tensile force in ⑦→⑨, until the bar restores straightness, $v = \theta = 0$, with $n = 1$ at ⑨. The plastic axial deformation developed at the yield hinge in ⑧→⑨ is an extension, and the balanced hinge extension remaining at ⑨ is given through Eqs.(6) and (7) from

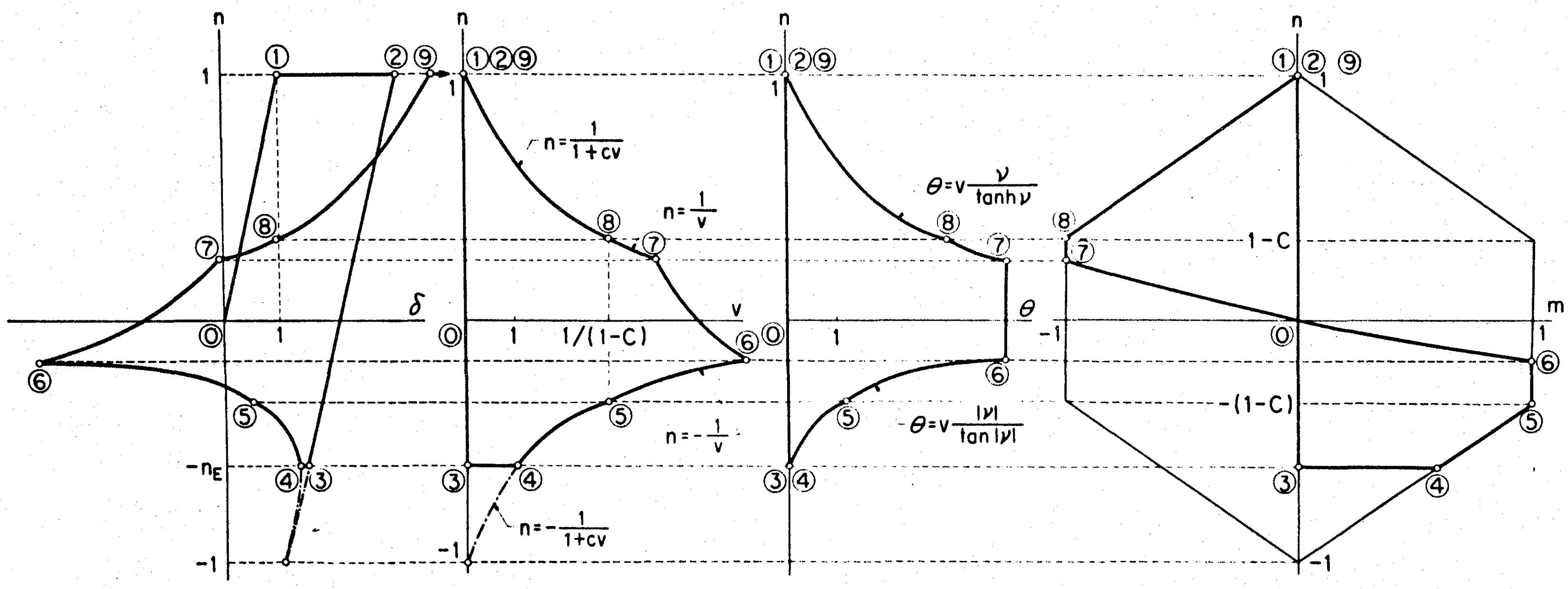

(a) n-δ curve (b) n-v curve (c) n-θ curve (d) n-m curve

Fig. 3 Behavioral diagrams of an axially loaded bar

$$\delta_9^p = -(2/\pi)^2(\alpha n_E/c)[(\theta_9 - \theta_8) + (\theta_5 - \theta_4)], \tag{8}$$

where subscripts refer to the states defined above. With $\theta_9 = \theta_4 = 0$, $n_8 = -n_5 = 1 - c$, and with Eq.(5), it is found that $v_8 = v_5 = 1/(1-c)$, and hence Eqs.(1) and (8) are combined to give

$$\delta_9^p = \frac{2}{\pi}\frac{\alpha}{c}\left(\frac{n_E}{1-c}\right)^{1/2}\{1/\tanh[\tfrac{\pi}{2}(\tfrac{1-c}{n_E})^{1/2}] - 1/\tan[\tfrac{\pi}{2}(\tfrac{1-c}{n_E})^{1/2}]\} > 0. \tag{9}$$

The fact $\delta_9^p > 0$ follows from the inequality $\theta_8 > \theta_5$, which is visualized by noting that there is a change in the hinge rotation without a change in the plastic axial deformation between the states 5 and 8 , the middle deflection returning to the identical value, and by noting that the actual deflection curve is hyperbolic-sine for tension and is sine for compression in each half with the co-ordinate origin at the end, as shown in Fig. 4. It is thus seen that the yield hinge undergoes extension through the rotation cycle caused by the load cycling from and to $n = 1$. Therefore, the n-δ curve of Fig. 3(a) does not close in 2 $\rightarrow$ 9; since the changes in δ^e, δ^g and δ^t between 2 and 9 all vanish, the difference $\delta_9 - \delta_2$ equals δ_9^p of Eq.(9). For a rectangular cross section, $\alpha = 3/4$, and specification $c = 2/3$, $n_E = 3/5$, for example, leads to $\delta_9 - \delta_2 = 0.76$. It is reminded that in the previous case of the piecewise-linear yield condition the accumulation phenomenon in hinge extension has not occurred, but the n-δ curve has closed at the attainment of $n = 1$, because of the complete proportionality of the hinge rotation and plastic axial deformation [10].

Let us examine a case of cyclic displacement loading. It is again assumed that $1 - c < n_E < 1$. The loading is started with contraction and is repeated alternately with the same amplitude δ_A in the separation and approach. If δ_A is sufficiently large, the hysteretic n-δ relation traces

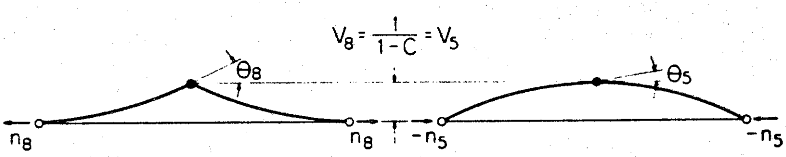

Fig. 4 Dimensionless deflection curves

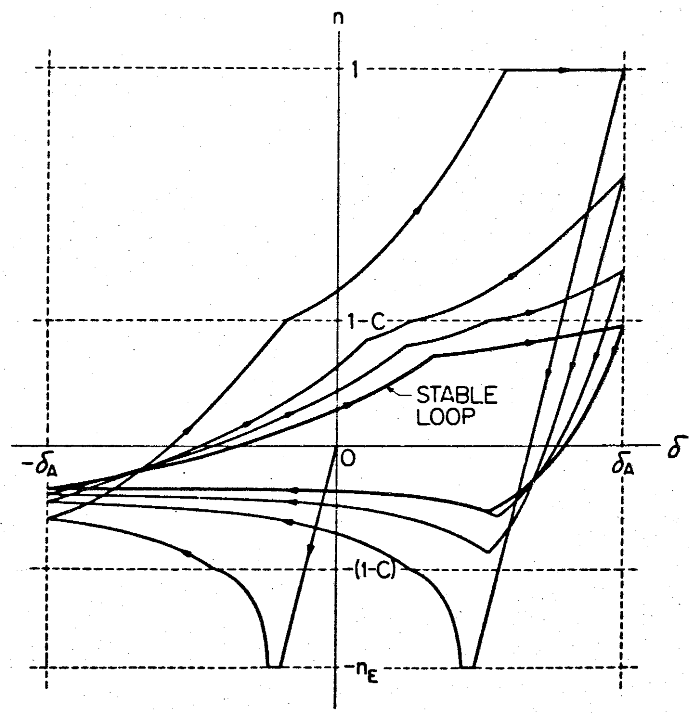

Fig. 5 Cyclic alternate displacement loading

such loops as shown in Fig. 5. The behavior of the bar deteriorates with the number of repetition of loading cycles until the load magnitude is reduced into the range $|n| \leqq 1 - c$. Henceforth the loop becomes stable as drawn in thick lines, and the behavior reaches a steady state. The previous piecewise linearity in the yield condition has indicated for a steady state to be attained before the end of the first cycle [10], and the use of the parabolic yield condition never leads to a steady state, predicting everlasting deterioration [13].

5. COMPARISON AND CONCLUSIONS

Comparison is made of the n-δ relation between the theoretical and experimental results in Fig. 6. The solid lines are drawn for the modified piecewise-linear yield condition with $c = 2/3$, dotted lines for the parabolic yield condition [13], dotted-and-dashed lines for the piecewise-linear yield condition [10], and dashed lines for experiment [14, 15]. The tests were carried out with mild steel specimens of square cross section (15 x 15 cm). The particular specimen cited had the slenderness of $n_E = 1.13$. The loading program was controlled by the axial displacement, with regard to which discretion is exercised in comparing with theoretical prediction. Starting with contraction, the loading was not successfully regulated in the early post-buckling region because of the rapid variation in the load and deformation. This is seen to cause a marked discrepancy with the theories in this region. For another discrepancy observed near the second buckling region the theories may be responsible; all the theories introduced herein predict the complete

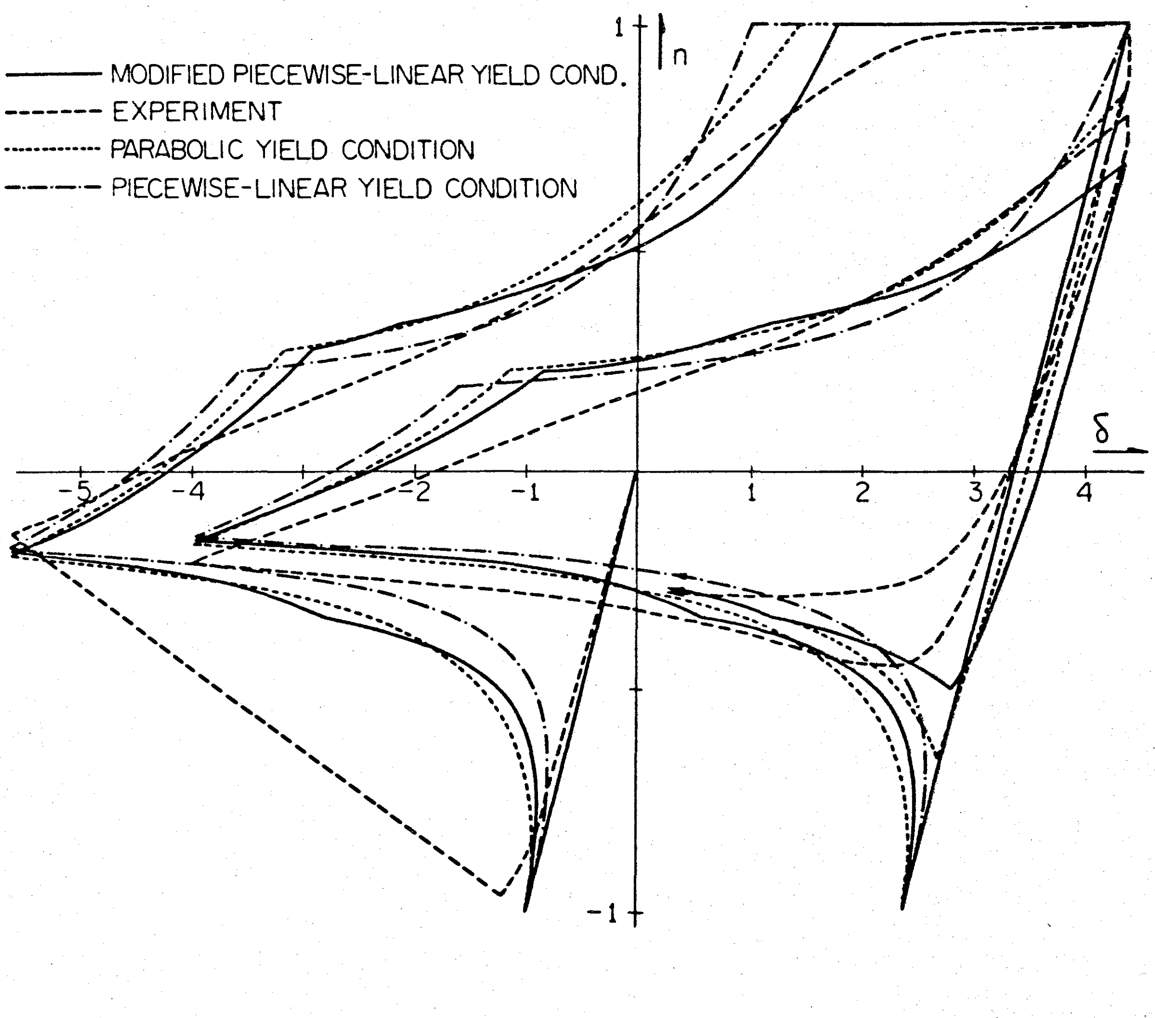

Fig. 6 Comparison between theories and experiment

recovery of straightness upon the attainment of $n = 1$, material hardening in the plastic range being ignored, whereas the actual bar hardly becomes straight through mere extension after being plastically deformed into a crooked configuration. Except for these regions and for other minor diserepancies occurring due to the theoretical negligence of partial yielding in cross sections, general agreement is seen between the theoretical and experimental results. Difference in the theoretical prediction due to the various forms of the yield condition is rather remarkable. It is seen that the parabolic or modified piecewise-linear yield condition with $c = 2/3$ better fits the experimental behavior of the mild steel square prism than the piecewise-linear yield condition, which corresponds to a state of stress lying somewhere between the initial yield and full plasticity for many practical cross sections. The difference in fitness between the modified piecewise-linear and parabolic yield conditions is not significant in this figure, but an advantage in the use of the former lies in the simplicity of analysis. Another advantage is concerned with the experimental observation that steel bars tend visibly to arrive at a steady state, which can be reached in the prediction by the former but not by the latter, within the first few cycles when subjected to cyclic displacement loading, unless local instabilities or twisting occurs [15]. Within the framing of this series of theoretical investigation, therefore, it seems advisable to use the modified piecewise-linear yield condition with a proper choice of the parameter c according to the cross-sectional shape and the dominant loading range.

REFERENCES

[1] S. Igarashi, K. Inoue, M. Kibayashi and M. Asano, "Hysteretic Characteristics of Steel Braced Frames - Part 1, The Behaviors of Bracing Members under Cyclic Axial Forces", Transactions of the Architectural Institute of Japan, Vol. 196, June, 1972, pp. 47-54 (in Japanese).

[2] A. Di Tommaso and A. La Tegola, "Double-Layer Space Frame Shells", Preliminary Report, IIIc, IABSE, Amsterdam, May, 1972, pp. 517-522.

[3] A. La Tegola, "Analisi incrementale di strutture reticolari metalliche in campo plastico con aste in regime post-critico", Giornale del Genio Civile, Vol. 110, n. 7-8-9, Roma, 1972, pp. 233-246.

[4] B.Tsuji and M. Yamada, "Elasto-Plastic Behavior of Bracings under The Cyclic Axial Forces, Part I: Analysis", Transactions of the Architectural Institute of Japan, Vol. 205, March, 1973, pp. 31-35 (in Japanese).

[5] S. Igarashi, K. Inoue, M. Asano and K. Ogawa, "Restoring Force Characteristics of Steel Diagonal Bracings", Fifth World Conference on Earthquake Engineering, Preprint No. 270, Rome, June, 1973.

[6] M. Fujimoto, A. Wada, K. Shirakata and R. Kosugi, "Nonlinear Analysis for K-Type Braced Steel Frames", Vol 209, July, 1973, pp. 41-51 (in Japanese).

[7] G. Oliveto, "Influenza della non perfetta rettilinearitâ delle aste sul comportamento delle strutture reticolari elasto-plastiche", Giornale del Genio Civile, n. 7-8-9, Roma, 1974, pp. 299-307.

[8] M. Wakabayashi, C. Matsui, K. Minami and I. Mitani, "Inelastic Behavior of Full Scale Steel Frames," Disaster Prevention Research Institute Annuals, Kyoto University, Vol. 13A, 1970, pp. 329-363 (in Japanese).

[9] A.B., Higginbotham, "The Inelastic Cyclic Behavior of Axially-Loaded Steel Members", Ph.D. Dissertation, University of Michigan, 1973.

[10] T. Nonaka, "An Elastic-Plastic Analysis of a Bar under Repeated Axial Loading", International Journal of Solids and Structures, Vol. 9, No. 5 with Erratum in No. 10, 1973, pp. 569-580; Chapter 3 of this treatise.

[11] M. Shibata, T. Nakamura, N. Yoshida, S. Morino, T. Nonaka and M. Wakabayashi, "Elastic-Plastic Behavior of Steel Braces under Repeated Axial Loading", Fifth World Conference on Earthquake Engineering, Preprint No. 100, Rome, 1973, Proceedings (1974), pp. 845-848.

[12] M. Wakabayashi, C. Matsui, K. Minami and I. Mitani, "Inelastic Behavior of Steel Frames Subjected to Constant Vertical and Alternating Horizontal Loads", Fifth World Conference on Earthquake Engineering, Preprint No. 146, Rome, 1973, Proceedings (1974), pp. 1194-1197.

[13] N. Yoshida, T. Nonaka, et al., "Use of the Parabolic Yield Condition in the Analytic Behavior of Axially-Loaded Members", in preparation (in Japanese).

[14] M. Wakabayashi, T. Nonaka, O. Koshiro and N. Yamamoto, "An Experiment on the Behavior of a Steel Bar under Repeated Axial Loading", Disaster Prevention Research Institute Annuals, Kyoto University, No. 14A, 1971, pp. 371-381 (in Japanese).

[15] M. Wakabayashi, T. Nonaka, T. Nakamura, S. Morino and N. Yoshida, "Experimental Studies on the Behavior of Steel Bars under Repeated Axial Loading", Disaster Prevention Research Institute Annuals, Kyoto University, No. 16B, 1973, pp. 113-125 (in Japanese).

CHAPTER 5

LARGE DEFORMATION ANALYSIS OF AN AXIALLY LOADED BAR

ABSTRACT A brief summary is first made of the hysteretic behavior, analytical and experimental, of a prismatic bar under variable repeated axial loading, based on earlier studies for small deformation. Basic equations are then derived in a closed form through an elastic-perfectly plastic type of analysis in conformity with one-dimensional idealization, by extending previously obtained principles into the range of large deformation, for determining the load-deformation characteristics of a moderately long bar. Account is taken of changes in geometry due to large transverse deflection and changes in bar dimensions due to plastic elongation.

SOURCE The contents of Chapter 5 are based on the following paper: Taijiro NONAKA, "An Analysis for Large Deformation of an Elastic-Plastic Bar under Repeated Axial Loading, Part 1 Derivation of Basic Equations", to be published.

Notation

A cross-sectional area

E Young's modulus

$F(k,\theta)$, $E(k,\theta)$ elliptic integrals of the first and second kinds with modulus k, amplitude θ

$f \equiv (1/2)\,(|N|/EI)^{1/2}$

I cross-sectional moment of inertia

$k \equiv \cos(\Psi/2)$; $k' \equiv \sin(\Psi/2)$

L length

M bending moment

N load

s arc length

V middle deflection

x coordinate along original bar axis

y deflection

Δ relative displacement

ε strain

Θ one-half of hinge rotation

θ, θ' values of ϕ at $\Phi = \Theta$ for $N > 0$ and $N < 0$

σ stress

ϕ defined by Eq.(15)

Φ slope angle

Ψ end slope angle

<u>Subscripts</u> indicate particular values with

E Euler load

O original value

p full plasticity

y yielding

<u>Superscripts</u> indicate components due to

e elasticity

g change in geometry

p plastic hinge

t plastic extension

1. INTRODUCTION

A column has long been the subject of investigation in the field of structural theory, and its instability phenomena seem to be well understood as long as it is axially compressed in a monotonous manner. An axially resistant member in such a structure as a truss or braced frame is often subjected to variable repeated loading; loads due to winds, earthquakes, cranes, transportation vehicles and some machine parts are applied repeatedly in nature, and they may act in different or opposite directions.

Suppose an initially straight prismatic bar, of structural material such as steel, is subjected to tension and/or compression repeatedly. If the bar is very stubby, i.e., short and compact, its behavior is determined, in theory, directly from the axial stress-strain relationship. If the bar is extremely long and slender, its strength in compression is much smaller than in tension, and it may well be treated as a tension-resistant member for practical purposes; or it may be feasible for compression to be taken into consideration since such a bar most likely remains elastic with large transverse deflection upon buckling. The combined effects of instability and plasticity, however, complicate the behavior of a bar with moderate slenderness, and this is the case most frequently confronted with. It is also noted that plastic action in axially loaded members often precedes and predominates over that in flexurally loaded members, because of the difference in stiffness between the two kinds of members, when they are coexistent in a structure such as a braced frame. These considerations motivated the author to investigate the behavior of an elastic-plastic bar under variable repeated axial loading. In spite of the dynamic nature of actual repeated loading, the inertia of an axially loaded member can in general be neglected as compared with that of other heavy portions such as floors, walls, etc., indicating the usefulness of its static load-deformation characteristics in determining the overall behavior of a dynamically loaded structure. A previous theoretical study resulted in a general analytic solution of the problem in a simple closed form [1]. This theory has been confirmed experimentally so as to predict the hysteretic behavior of actual steel bars with a first order accuracy [2]. The basic equations of this theory have been derived through a quasi-linear analysis of small deformation. The objective of the discussions of this chapter is to extend this theory to the range of large deformation.

Large deformation in the compression side is accompanied by the post-buckling transverse deflection. For the elastic behavior of this problem the closed-form solution is available in terms of elliptic integrals, the deflection curve being referred to as the "elastica" [3-8]. A numerical analysis has also been carried out by Oden and Childs to take material nonlinearity into consideration [9]. Since an elastic process is reversible, the repeated or varying nature of the load causes no additional difficulty. Based implicitly on the assumption of pure bending, Monasa took account of partial yielding in cross sections and obtained numerical results for the case of monotonously increasing deflections [10]. Since the completion of the work presented here, Higginbotham's dissertation has been brought to the author's attention [11]. He analyses the cyclic behavior of steel braces, and combines the equations of the "elastica" with the yield condition of full plasticity in a cross section. Plastic rotation is considered at a yield hinge but not plastic axial deformation, and hence to the present author its validity seems to be limited to very long bars or thin rods.

The effect of large deformation in the tension side is equally important, though not considered as yet. Finite elongation causes changes in bar dimensions, reducing the stiffness and increasing the flexibility of the bar. In this chapter general basic equations are derived which can determine the hysteretic behavior of the bar under repeated axial loading, admitting large deformation in the tension side as well as the compression. The derivation is preceded by a brief summary on the theoretical behavior of an axially loaded bar on the basis of the previous work, together with its correlation to experimental observations.

2. PREVIOUS RESULTS

It is supposed that an initially straight bar of uniform material and cross section is subjected to repeated loading. The load is composed of a pair of equal and opposite forces acting at the ends of the bar in the direction of its original axis. The effective length is taken so that the bar can be considered as being simply supported at its ends. Theoretical study is made of the hysteretic behavior of the bar in equilibrium with the load which varies in a quasi-static manner. The main interest lies in the hysteretic relationship between the load N and the relative displacement Δ of the bar ends in the direction of loading; N is taken as positive when tensile, and correspondingly Δ is taken as positive for seperation so that the distance between the bar ends, originally L_o, becomes $L_o + \Delta$ after deformation. It is assumed that the cross section has axes of symmetry and that the bar deflects only in the plane of symmetry without twist, having cross-sectional area A_o and moment of inertia I_o. The bar is idealized as a one-dimensional continuum, with the property of linear elasticity followed by perfect plasticity under the combined action of the axial force and bending moment. The fully plastic state in pure bending, with limit moment M_o, and that in purely axial loading, with limit force N_o, are interpolated linearly to serve as the yield condition for interaction. The shear effects are neglected altogether. It is also assumed that a compressed straight bar buckles when the compression reaches either the crush load N_o or the Euler load $N_E = \pi^2 EI_o/L_o^2$, where E is the Young's modulus. Two restrictions of small deformation are added in the previous work [1]. They are that change in the length of the bar is negligible when compared with the original length and that the square of the slope of the deflection curve can be neglected in comparison with unity. A quasi-linear analysis has been carried out on the basis of such assumptions, leading to basic equations, which are adequate for the determination of the hysteretic behavior in the range of small deformation. According to this theory, the relative displacement is given by the sum of four components. The first component Δ^e is due to elastic axial deformation and determined directly from the instantaneous load, to be $\Delta^e = NL_o/(EA_o)$. The second component Δ^g is due to change in geometry associated with transverse deflection, which is symmetric with respect to the middle with a kink caused by plastic rotation. The assumption of small deflection permits the linear approximation of curvature, and the slope angle $\Theta \geqq 0$ of the deflection curve at just next to the middle is related to the maximum deflection $V \geqq 0$ at the middle through the relation

$$\Theta = \frac{[N/(EI_o)]^{1/2}}{\tanh\,[(L_o/2)(N/EI_o)^{1/2}]}\,V. \tag{1}$$

Plastic action can take place with a yield hinge at the middle, when the deflection attains the value

$$V = M_o\ (1/|N| - 1/N_o). \tag{2}$$

When V is smaller, the bar behaves in an elastic manner, with Θ remaining constant. Integration of the square of the slope allows Δ^g to be expressed in terms of N and Θ as

$$\Delta^g = -L_o\{\frac{\Theta}{2\cosh[(L_o/2)(N/EI_o)^{1/2}]}\}^2\ \{1 + \frac{\sinh\,[L_o(N/EI_o)^{1/2}]}{L_o(N/EI_o)^{1/2}}\}. \tag{3}$$

Equations (1) and (3) involve imaginary functions when $N < 0$. Expressions in terms of real functions can be obtained simply by taking the absolute value for N and replacing hyperbolic functions by the corresponding trigonometric functions in these equations. The third component Δ^p is the plastic axial deformation at the yield hinge, and given by the flow rule to be $\Delta^p = -2\Theta M_o/N_o$. The fourth component Δ^t is the plastic elongation the bar undergoes in a straight configuration under $N = N_o$, and controlled only by the displacement constraints. Worth noting is that, apart from the influence of Δ^t, hereditary nature is retained only in Θ and that in a plastic process the deformation characterstics are determined explicitly from the instantaneous load, since Θ is then expressed in terms of N through Eqs. (1) and (2).

In Fig. 1 is illustrated an example of the analytic behavior for the case $N_E = 0.6\ N_o$, $(M_o/N_o)^2 = I_o/A_o$. Fig. 1(a) shows the load-axial displacement

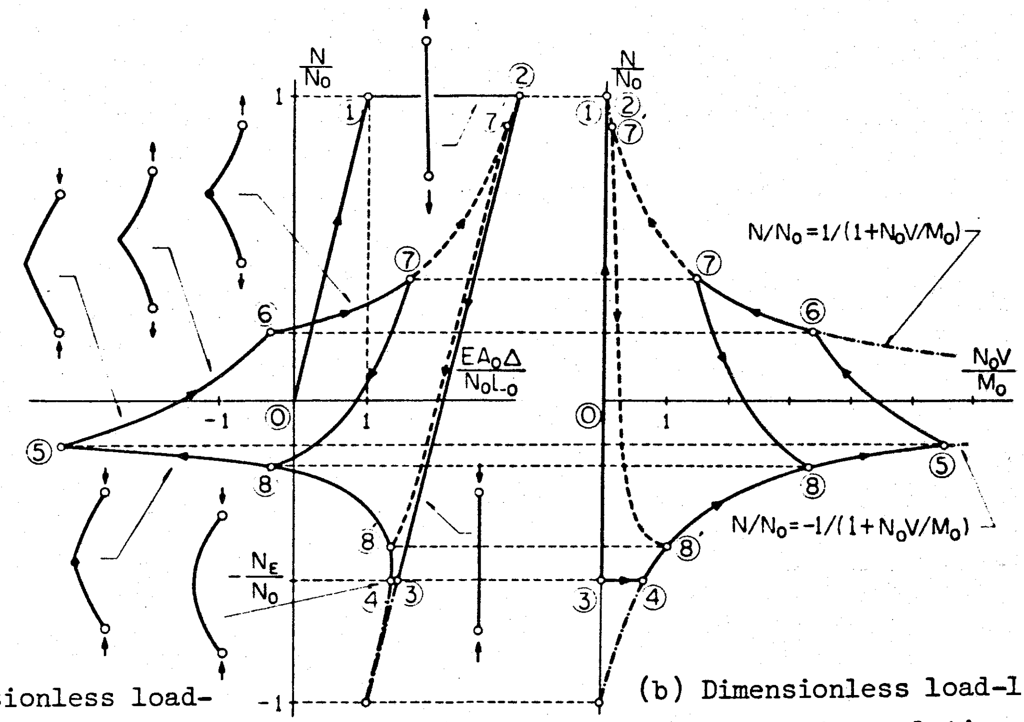

(a) Dimensionless load-axial displacement relation

(b) Dimensionless load-lateral deflection relation

Fig. 1 Load-deformation characteristics of an axially loaded bar

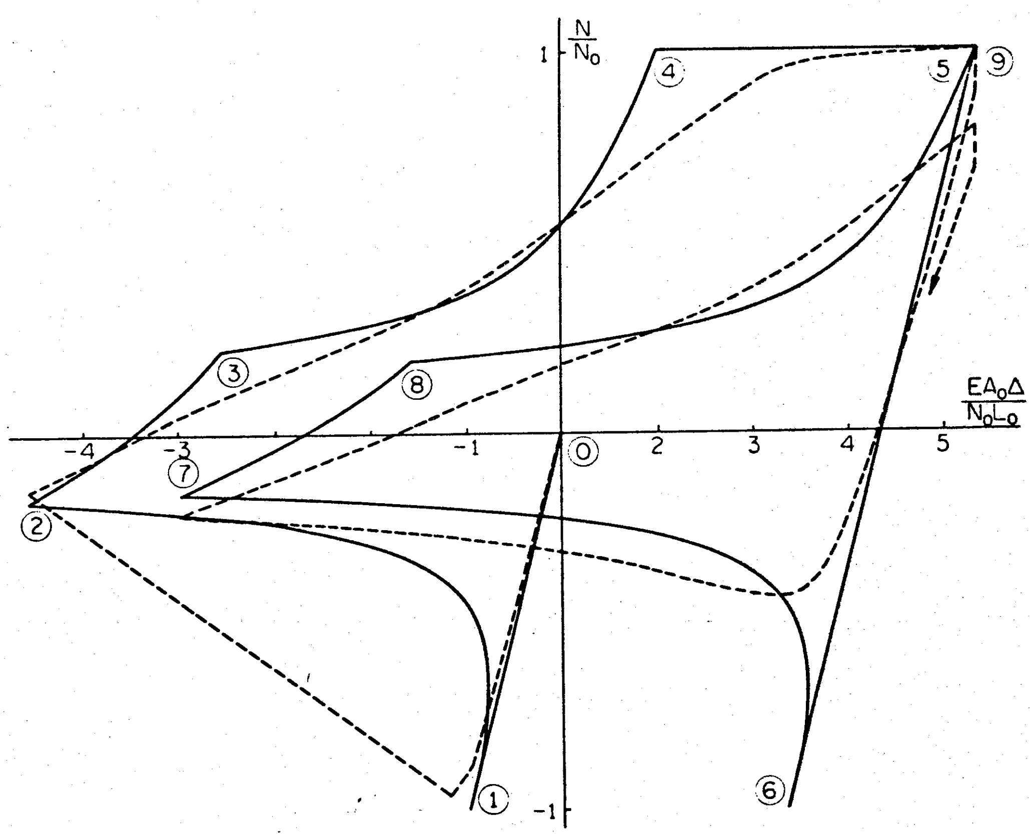

Fig. 2 Comparison between theory and experiment

relationship. When an initially straight bar is subjected to a compression after reaching the yield limit in tension, as in ⓪→①→②→③, it buckles at $N = -N_E$. Fig. 1(b) shows the variation of the deflection V. The deflection develops abruptly at the buckling load. As the deflection keeps increasing, the yield limit is reached at state ④, and a further increase in the deflection is accompanied with plastic action in the yield hinge. The axial load decreases in magnitude as in ④→⑤. If the bar ends begin to separate anywhere along the curve ④→⑤, such as at state ⑤, the yield hinge disappears, leaving a kink at the middle of the deflection curve. The variation ⑤→⑥ is characterized by elastic recovery with decreasing deflection. The deflected shape in each of the two halves is represented by a sine curve for $N < 0$, by a straight line for $N = 0$ and by a hyperbolic-sine curve for $N > 0$. At state ⑥, the yield hinge again forms with a tensile axial force, and the kink angle 2θ decreases subsequently. The bar restores its straight configuration at $N = N_o$; it turns out that the curve ⑥→⑦ leads to ②, closing the hysteretic curve. Unloading from ⑦ or ⑦', before the complete recovery at ②, gives rise to elastic behavior and the yield limit is again reached at state ⑧ or ⑧' somewhere along ④→⑤. It is indicated that there is a tendency for a bar to adjust itself toward a steady state whenever possible.

The above theory is compared with the experimental observation in Fig. 2 for the axial load-displacement relation. The solid line refers to the theory and dashed line to the experiment. The experimental result cited here was obtained with a mild steel specimen of square cross section for $N_E = 1.13\ N_o$ [12, 13]. Having started with compression, the loading was controlled by axial displacements, from which the first few cyles are shown in ⓪ to ⑨. The initial post-buckling behavior was not recorded successfully in this test, because of the abrupt changes in states; the straight segment in the figure is the linear interpolation between the well recorded terminal points, ① and ②*. It is seen that the above theory serves as a first order approximation for the overall behavior [2], despite the rather drastic assumptions of perfect plasticity** and the piecewise linear yield condition.*** The most significant discrepancy is seen near ⑥; the experimentally observed strength in compression is much reduced by the preceding loading cycle, whereas the theory predicts the constant buckling load. This may be attributed principally to the Bauschinger

---

* Paris attributes the difference, between the experimental straight segment and the theoretical prediction in the early plastic buckling range such as in ① → ②, to an increase in yield stress due to high rates of strain, giving the name "plastic dynamic buckling" [14].

** Inclusion of the existence of second order plastic strains can lead to instabilities of a prismatic bar under a large number of loading cycles in the plastic range, taking account of cyclic creep due to stress cycling and cyclic relaxation due to strain cycling. Cyclic tensile strain accumulation can give rise to necking and have precedence over fatigue in causing fracture; during displacement-controlled cyclic loading of a column, the load limits decrease from cycle to cycle, indicating a gradual reduction in critical compressive load for instability [15, 16]. The present work is not intended to include long term cycling.

*** Simple modification of the yield condition can lead to better agreement with experimental observations, depending on the shape of cross section. For a rectangular cross section as in this test, use of the parabolic yield condition of full plasticity [17] or of an approximate hexagon representing the yield curve seems to be adequate [18]. The flow rule associated with such a yield condition does not come to the result that in Fig. 2 the curve corresponding to ⑧ → ⑨ points to ⑤, but to the result that the extension of that curve points to the right of ⑤; the maximum load N_o is attained at a relative displacement larger than that of ⑤, because of the eventual expansion consequent on the loading cycle, and the load at ⑨ with the same displacement as ⑤ is smaller than the load N_o of ⑤.

effect and to the fact that an actual bar hardly becomes straight again, once it is bent plastically. Discrepancy is also seen near 3, 4 and 9; the theory predicts sharp changes in slope because of elastic-plastic transitions, as against the smoothly varying curve of the experiment, the assumption of the elastic-perfectly plastic property in the one-dimensional idealization may chiefly be responsible for this discrepancy, neglecting phases of partial yielding in a cross section.

The application of this theory to braced frames has also been attempted and resulted in close agreement with the experimental behavior of full-scale steel frames [19].

While the assumption of small deformation on which this theory is based is pertinent to most practical cases, deflection of a long flexible bar may become so large, due to compression, that the square of the slope of the deflection curve attains a magnitude of the order of unity. Such large deflection is accompanied by the relative axial displacement of the order of the original length of the bar. A similar situation can arise in tension as well; elongation of the order of the length requires the consequent changes in the dimensions of the bar to be taken into account. These effects of large deformation are incorporated in the analysis which follows.

3. ASSUMPTIONS

If a bar remains elastic, its post-buckling behavior is stable, and the theory of "elastica" is applicable to the large deflection behavior. When the load is a pair of mutually facing terminal forces without couples as in the problem under consideration, a possible curve of deflection of an initially straight prismatic bar has equally spaced inflections along the line of loading with both ends among inflections. That portion of the bar contained between two consecutive inflections is taken again to be analysed with the original length L_o. It is also noted that among deflection curves having a number of inflections, the stable one is that having the least possible inflections. The analysis to follow is intended to hold until the ends of the bar touch eath other*. The signs of the load are redefined so as to allow for large deflection: positive N means the terminal forces directing opposite to each other, causing tension in the central portion of the deflected bar.

Changes in bar dimensions require the current values L, A, I, N_p and M_p of the length, cross-sectional area, cross-sectional moment of inertia, limit load in pure tension and limit moment in pure bending, to be distinguished from their original values L_o, A_o, I_o, N_o and M_o, respectively. In order to facilitate the analysis with allowance for the changes, further assumptions are made in addition to those for the case of small deformation.

---

* In the classical theory of "elastica", allowance is made for the deflection curve to form loops or partly overlap in a plane. It is possible to extend the results of the present paper to such a case without modification, with only additional care to be taken for the signs of the load and relative displacement. On the basis of elasticity, the load magnitude keeps increasing with deflection slopes, and its increase brings about a reduction in the size of the loop. Zajac points out that as the loop is made smaller, a state of instability is reached at which the planar loop pops out into a spatial configuration, and eventually the bar assumes a straight shape containing one complete twist [20]. However, overlapping of a planar curve is not physically possible in the case of an actual bar with finite cross-sectional dimensions, but contact phenomena take place [21]. In the problem under consideration, the end touching would occur with the end slope angle of 131°, provided the bar remained linearly elastic [22, 23].

None of these phenomena are likely to occur with steel bars of moderate slenderness due to the onset of yielding, leading to the investigation reported herein.

Important assumptions are itemized as follows:

1. When subjected to uniform tension with allowance for large elongation, the bar behaves in an elastic-perfectly plastic manner, having constant limit axial force N_p.
2. The bar retains the elastic-perfectly plastic property under the combined action of the axial force N and bending moment M, with the linearized yield condition

$$|N/N_p| + |M/M_p| = 1. \tag{4}$$

3. Changes in bar dimensions due to elastic deformation are negligibly small in comparison with the original dimensions.
4. The cross section remains geometrically similar to the original.
5. A straight-shaped bar cannot remain straight, but buckles transversely, when the load is compressive and it reaches in magnitude either the current Euler load $\pi^2 EI/L^2$ or crush load N_p.
6. Local stability and sufficient ductility in the material behavior are assumed.

It is noted that assumption 1, when combined with assumption 3 and with plastic incompressibility, is equivalent to taking the relationship between the Eulerian stress σ and logarithmic strain ε in monotonic uniaxial tension to be

$$\sigma = \begin{cases} \sigma_y \varepsilon/\varepsilon_y & \text{for} \quad \varepsilon \leqq \varepsilon_y \\ \sigma_y \exp(\varepsilon - \varepsilon_y) & \text{for} \quad \varepsilon \geqq \varepsilon_y, \end{cases}$$

together with taking $\varepsilon_y << 1$, where the subscript y indicates the yield limit. This stress-strain relation in the plastic range is rewritten as $\sigma = \sigma_y L/L_y$

for $L \geqq L_y$. Propriety of assumption 2 depends on the shape of cross section as well as on the material used. Equation (4) is exact for an ideal I-section with indefinitely thin web and flanges, and a reasonable approximation for many structural steel sections, corresponding to a yield curve lying within the area bounded by initial yielding and full plasticity of a cross section. Assumption 4 results from the idealization of the uniformly uniaxial state of stress and isotropy in a cross section.

4. FUNDAMENTAL RELATIONS

Let cartesian coordinates (x,y) represent the deflection curve $y(x)$, s the arc length, and Φ the slope angle, as shown in Fig. 3. The origin of the coordinates is taken at the left end, and the positive directions are so taken that s, $y \geqq 0$ and $0 \leqq \Phi \leqq \pi$ for the left half. In view of symmetry, it suffices to analyse only one-half of the bar. By noting the relation

$$\Delta \equiv 2\int_0^{(L_0+\Delta)/2} dx - L_0 = (2\int_0^{L/2} \cos\Phi \, ds - L) + (L - L_0), \tag{5}$$

it is seen that the relative displacement Δ consists of two constituents. When the straight bar of length L is deflected transversely, the bar ends approach each other giving rise to the first constituent

$$\Delta^g = 2\int_0^{L/2} \cos\Phi \, ds - L \leqq 0 . \tag{6}$$

The second constituent, $L - L_0$, is identified as the change in the length of the bar, and brought about by three distinct actions. They are elastic axial deformation Δ^e, plastic axial deformation Δ^p at a yield hinge, and plastic

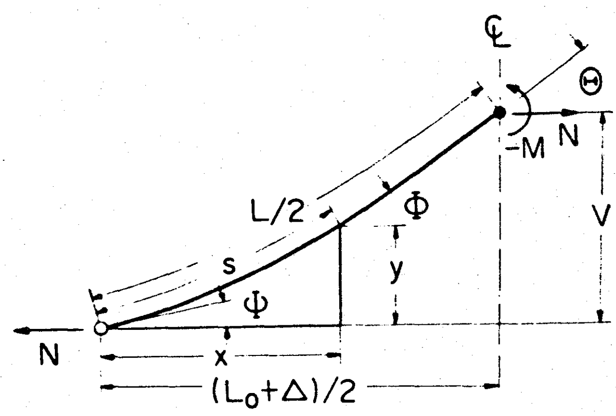

(a) $N \geqq 0$; $\Psi \leqq \Phi \leqq \Theta$, $M \leqq 0$

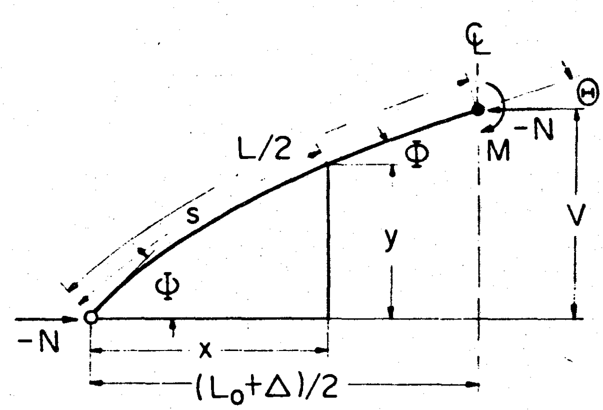

(b) $N \leqq 0$; $\Psi \geqq \Phi \geqq \Theta$, $M \geqq 0$

Fig. 3 Deflected bar and symbols

elongation $\Delta^t \geqq 0$ in a straight configuration with $N = N_p$. It is thus justified to still write

$$\Delta = \Delta^e + \Delta^g + \Delta^p + \Delta^t \tag{7}$$

with allowance for large deformation. Among three components affecting the length of the bar, Δ^e can be neglected when compared with the original length L_o owing to assumption 3; Δ^p is of magnitude of the order of the depth* and is also negligible: Δ^t is the principal cause of the change in length, viz., approximately

$$L = L_o + \Delta^t. \tag{8}$$

The consequent changes in the cross-sectional properties are determined from the plastic incompressibility and from assumtions 1, 3 and 4, to give

$$A = A_o\ (L_o/L), \quad I = I_o\ (L_o/L)^2, \quad N_p = N_o, \quad M_p = M_o\ (L_o/L)^{1/2} \tag{9a,b,c,d}$$

The first three components in Eq.(7) are determined in the following sections by treating the load N as the independent variable for convenience, in spite of the fact that the behavior of the bar is not uniquely specified by N but by the history of Δ. For the last component Δ^t, there is a restriction only that its increment $d\Delta^t$ is non-negative when $N = N_p$ and zero otherwise.

---

* In order to show this, it is convenient to follow the concept of an off-center yield hinge [24]. The cross sections rotate relatively across the yield hinge about the neutral axis, causing a relative displacment along the bar axis.

5. DERIVATION OF Δ^e

On the basis of linear elasticity, the axial force N cosΦ increases the length ds of an element by amount N cosΦ ds/(EA). The equilibrium of the bar requires constancy of the resultant force N in the x-direction (see Fig. 3). With recourse to Eq (6), it is found that

$$\Delta^e = \frac{2N}{EA} \int_0^{L/2} \cos\Phi \, ds = \frac{N}{EA} (L + \Delta^g). \tag{10}$$

6. DERIVATION OF Δ^g

The component Δ^g of Eq.(6) arises from the difference in lengths between the chord and arc of the deflection curve, which is given when $N < 0$ from the classical theory of the "elastica" as long as the bar remains elastic. Since plastic action takes place only at the middle of the deflected bar, the "elastica" is applicable to the half bar with the plastic rotation properly taken into the boundary condition. It turns out that the case of $N \geqq 0$ can be treated along similar lines. By considering that the load takes either sign in the problem under consideration, analysis is carried out in a unified manner, and the results are to be formulated in the form of dual expressions.

The equilibrium equation $EI(d^2\Phi/ds^2) = N \sin\Phi$ is once integrated with the boundary condition that $d\Phi/ds = 0$ and $\Phi = \Psi$ at $s = 0$, to give

$$(d\Phi/ds)^2 = (2N/EI)(\cos\Psi - \cos\Phi), \qquad 0 \leqq s < L/2 \tag{11}$$

where Ψ is the slope angle at the left end. The curvature $d\Phi/ds$ is positive or negative according to $N > 0$ or $N < 0$, respectively (see Fig. 3). It is also seen from Eq.(11) that $\Psi \lesseqgtr \Phi$ according to $N \gtreqless 0$. It follows with the notation

$$f \equiv (1/2)\,(|N|/EI)^{1/2} \tag{12}$$

that

$$ds = \begin{cases} (2f)^{-1}\,[2(\cos\Psi - \cos\Phi)]^{-1/2}\,d\Phi & \text{for} \quad N > 0 \\ -(2f)^{-1}\,[2(\cos\Phi - \cos\Psi)]^{-1/2}\,d\Phi & \text{for} \quad N < 0. \end{cases} \tag{13a,b}$$

Use is made of the trigonometric identities

$$\cos\Phi = \begin{cases} 2\cos^2(\Phi/2) - 1 & \text{for} \quad N > 0 \\ 1 - 2\sin^2(\Phi/2) & \text{for} \quad N < 0 \end{cases} \tag{14a,b}$$

and of the change of variables from Φ to ϕ such that*

$$\sin\phi = \begin{cases} [\cos(\Phi/2)]/[\cos(\Psi/2)] & \text{for} \quad N > 0 \\ [\sin(\Phi/2)]/[\sin(\Psi/2)] & \text{for} \quad N < 0. \end{cases} \tag{15a,b}$$

Let

$$k \equiv \cos(\Psi/2), \qquad k' \equiv \sin(\Psi/2) \tag{16a,b}$$

---

* Considerations which have led to the dual transformation of Eq.(15), of which (a) is known in the "elastica", are indicated in the Appendix of the next chapter.

and $k^2 + k'^2 = 1$; k and k' play the role of the modulus and the complementary modulus of elliptic integrals, respectively. It follows from Eqs. (13) through (16) that

$$ds = \begin{cases} -(2f)^{-1}(1-k^2\sin^2\phi)^{-1/2}\,d\phi & \text{for} \quad N > 0 \\ -(2f)^{-1}(1-k'^2\sin\phi\;)^{-1/2}\,d\phi & \text{for} \quad N < 0. \end{cases} \tag{17a,b}$$

In addition, it is found that

$$dx = \cos\phi\; ds = \begin{cases} \dfrac{1-2k^2\sin^2\phi}{2f(1-k^2\sin^2\phi)^{1/2}}\,d\phi = \dfrac{1}{f}(1-k^2\sin^2\phi)^{1/2}d\phi + ds & \text{for} \quad N > 0 \\ \dfrac{2k'^2\sin^2\phi - 1}{2f(1-k'^2\sin^2\phi)^{1/2}}\,d\phi = -\dfrac{1}{f}(1-k'^2\sin^2\phi)^{1/2}d\phi - ds & \text{for} \quad N < 0 \end{cases} \tag{18a,b}$$

$$dy = \sin\Phi\; ds = \begin{cases} -(k/f)\sin\phi\; ds & \text{for} \quad N > 0 \\ -(k'/f)\sin\phi\; ds & \text{for} \quad N < 0, \end{cases} \tag{19a,b}$$

where in the derivation of the latter, Eq.(19), use is also made of the identities

$$\sin\Phi = 2\sin(\Phi/2)\cos(\Phi/2) = \begin{cases} 2[1-\cos^2(\Phi/2)]^{1/2}\cos(\Phi/2) & \text{for} \quad N > 0 \\ 2[1-\sin^2(\Phi/2)]^{1/2}\sin(\Phi/2) & \text{for} \quad N < 0. \end{cases} \tag{20a,b}$$

Equations (17) to (19) are integrated from $s = 0$ to $s = L/2$, with the boundary condition that $\phi = \pi/2$ at $s = 0$ and that $\phi = \theta$ or θ' at $s = L/2 - 0$ according to $N > 0$ or $N < 0$, respectively, where θ and θ', both representing Θ, half the hinge rotation at the middle, are defined by

$$k\sin\theta = \cos(\Theta/2), \qquad k'\sin\theta' = \sin(\Theta/2). \tag{21a,b}$$

With $F(k,\theta)$ and $E(k,\theta)$ denoting the Legendre elliptic integrals* of the first and second kinds, respectively, with modulus k, amplitude θ, it follows that

$$fL = \begin{cases} F(k,\pi/2) - F(k,\theta) & \text{for} \quad N > 0 \\ F(k',\pi/2) - F(k',\theta') & \text{for} \quad N < 0 \end{cases} \tag{22a,b}$$

$$L + \Delta^g = \begin{cases} -(2/f)[E(k'\pi/2) - E(k'\theta)] + L & \text{for} \quad N > 0 \\ (2/f)[E(k',\pi/2) - E(k',\theta')] - L & \text{for} \quad N < 0 \end{cases} \tag{23a,b}$$

$$fV = \begin{cases} k\cos\theta & \text{for} \quad N > 0 \\ k'\cos\theta' & \text{for} \quad N < 0. \end{cases} \tag{24a,b}$$

Plastic action can take place with a yield hinge at the middle, when the yield condition of Eq.(4) is satisfied, in which N and M are to be understood as the axial force and bending moment at the middle cross section. The positive M is defined to cause tension in the upper fibres, as shown in Fig. 3(b), so that an increment in the hinge rotation is compatible with the bending moment. The equilibrium condition $M + NV = 0$ along with Eq.(4) give the middle deflection

$$V = M_p\,(1/|N| - 1/N_p), \tag{25}$$

as far as the plastic action proceeds. Equations (21), (22) and (24) are then combined to determine three unknowns k, θ and Θ, or, k', θ' and Θ, according to $N > 0$ or $N < 0$, respectively.

For a state of stress whithin the yield limit, the bar behaves elastically with constant Θ determined from the preceding plastic action. Combination

---

* For the definition of Legendre elliptic integrals, see Appendix of Chapt. 6.

of Eqs. (21) and (22) gives k and θ or their primed quantities, and Eq.(24) then determines V, if necessary, giving a value smaller than that of Eq. (25).

Substitution of k and θ or their primed quantities into Eq.(23) gives Δ^g both for the plastic and elastic processes. In order to determine the entire deflection curve, it suffices to take proper limits of integration in the elliptic integrals (see Appendix of Chapter 6).

7. DERIVATION OF Δ^p

Upon the formation of a yield hinge, plastic action causes a change $d\Delta^p$ in the plastic axial deformation as well as a change $d(2\Theta)$ in the relative rotation across the hinge, due to the presence of the axial force. By noting from equilibrium that M and N have opposite signs, the flow rule gives the normality condition, $N_p\, d\Delta^p = -M_p\, d(2\Theta)$, associated with Eq.(4), except for the singular points $M = \pm M_p$ and $N = \pm N_p$ [24]. The cases $M = \pm M_p$ and $N = -N_p$ need not be considered here because of the bounded deflection and assumption 5, respectively. The condition $N = N_p$ is maintained only under vanishing deflection, and the above relation of normality remains valid, since $\Theta = d\Theta = 0$ leads to $d\Delta^p = 0$; the plastic deformation for this case is taken into account in the component Δ^t. It may be worth noting that the normality indicates the physically acceptable fact that $d\Delta^p \gtrless 0$ according to $N \gtrless 0$ since alternatives $d\Theta \lessgtr 0$ follow from $N \gtrless 0$. The normality relation can be still used during an elastic process, since the constancy of Θ again leads to $d\Delta^p = 0$. The validity of the incremental normality throughout the history and the initial straightness are combined to establish the relation

$$\Delta^p = -(2M_p/N_p)\Theta \leqq 0. \tag{26}$$

8. RELATIONS FOR N = 0

The dual expressions derived in the preceding sections must yield single relations when the limit $N \to 0$ is taken both for the case $N > 0$ and $N < 0$. In fact, setting $f = 0$ in Eq.(22) leads to $\theta = \theta' = \pi/2$, and consequently combination of Eqs.(16) and (21) leads to $\Psi = \Theta$. The deflection curve for $N = 0$ is composed of two straight segments with a kink at the middle. By noting from Eq.(22) that

$$(\partial f/\partial\theta)L = -(1 - k^2\sin^2\theta)^{-1/2}, \quad (\partial f/\partial\theta')L = -(1-k'^2\sin^2\theta'^2)^{-1/2},$$

it follows from Eqs.(16), (23) and (24) that

$$\lim_{f\to 0}(L+\Delta^g) = \begin{cases} 2\lim_{\theta\to\pi/2}\left[\dfrac{(1-k^2\sin^2\theta)^{1/2}}{\partial f/\partial\theta}\right] + L & \text{for} \quad N > 0 \\ -2\lim_{\theta'\to\pi/2}\left[\dfrac{(1-k'^2\sin^2\theta')^{1/2}}{\partial f/\partial\theta'}\right] - L & \text{for} \quad N < 0 \end{cases}$$

$$= 2L\lim_{\Psi\to\Theta} k^2 - L = L\cos\Theta, \tag{27}$$

$$\lim_{f\to 0} V = \begin{cases} \lim_{\theta\to\pi/2}\left(k\,\dfrac{-\sin\theta}{\partial f/\partial\theta}\right) & \text{for} \quad N > 0 \\ \lim_{\theta'\to\pi/2}\left(k'\,\dfrac{-\sin\theta'}{\partial f/\partial\theta}\right) & \text{for} \quad N < 0 \end{cases}$$

$$= L\lim_{\Psi\to\Theta}(k\,k') = (L/2)\sin\Theta. \tag{28}$$

Thus, continuity of the solution is assured by supplementing the results of this section for N = 0.

9. FINAL REMARKS

Basic equations have been derived to determine the large deformation behavior of an elastic-perfectly plastic bar in equilibrium with a pair of terminal forces applied repeatedly along its original axis. Allowance is made for changes in dimensions and in geometry due to large plastic elongation and transverse deflection, both or either of which can attain a magnitude of the order of the length of the bar. It is clear from the discussions presented on the analytical behavior in the small deformation range that the basic equations obtained herein are adequate to describe the hysteretic behavior of the bar for any history of loading; specification of the history of the relative displacement between the ends uniquely determines the load variation and deformation characteristics. The large deformation theory will be compared with the small deformation theory in the next chapter, as to both the basic eauations and a numerical example of the hysteretic behavior.

Finally a word of caution may be in order. Representing a portion between adjacent inflections, the bar analysed has to be long enough to assure the validities of the one-dimensional idealization, notion of a yield hinge, neglect of shear effects, and neglect of uniform plastic contraction under the compressive yield load.

ACKNOWLEDGEMENTS

An early phase of this work was supported by Matsunaga Science Foundation awarded to the author. Thanks are due to Dr. S. Morino and Mr. N. Yoshida of Kyoto University, and Mr. M. Shibata of Osaka Institute of

Technology for helpful discussions during the preparation of this chapter.

REFERENCES

[1] T. Nonaka, "An Elastic-Plastic Analysis of a Bar under Repeated Axial Loading". International Journal of Solids and Structures, Vol. 9, No. 5 with Erratum in No. 10, 1973, pp. 569-580 ; Chapter 3 of this treatise.

[2] M. Shibata, T. Nakamura, N. Yoshida, S. Morino, T. Nonaka and M. Wakabayashi, "Elastic-Plastic Behavior of Steel Braces under Repeated Axial Loading", Fifth World Conference on Earthquake Engineering, Preprint No. 100, Rome, 1973, Proceedings (1974), pp. 845-848.

[3] A.E. Love, "A Treatise on the Mathematical Theory of Elasticity", Fourth Edition, Dover, 1944, pp. 401-405.

[4] T.P. Mitchell, "The Nonlinear Bending of thin Rods", Journal of Applied Mechanics, March, 1959, pp. 40-43.

[5] S.T. Tomoshenko and J.M. Gere, "Theory of Elastic Stability", Second Edition, McGraw-Hill, 1961, pp. 76-82.

[6] R. Frisch-Fay, "A New Approach to the Analysis of the Deflection of Thin Cantilevers", Journal of Applied Mechanics, March, 1961, pp. 87-90.

[7] G.E. Sliter and A.P. Boresi, "Elastica Supported at Midpoint by a Spring", Journal of the Engineering Mechanics Division, Proceedings of ASCE, Vol. 90, No. EM2, April, 1964, pp. 1-15.

[8] S.J. Britvec, "The Theory of Elastica in the Non-linear Behaviour of Plane Frameworks", International Journal of Mechanical Sciences, Vol. 7, 1965, pp. 661-684.

[9] J.T. Oden and S.B. Childs, "Finite Deflections of a Nonlinearly Elastic Bar", Journal of Applied Mechanics, March, 1970, pp. 48-52.

[10] F.E. Monasa, " Deflections and Stability Behavior of Elasto-Plastic Flexible Bars", Journal of Applied Mechanics, Brief Notes, June, 1974, pp. 537-538.

[11] A.B. Higginbotham, "The Inelastic Cyclic Behavior of Axially-Loaded Steel Members", Ph.D. Dissertation, University of Michigan, 1973.

[12] M. Wakabayashi, T. Nonaka, O. Koshiro and N. Yamamoro, "An Experiment on the Behavior of a Steel Bar under Repeated Axial Loading", Disaster Prevention Research Institute Annuals, Kyoto University, No. 14A, 1971, pp. 371-381 (in Japanese).

[13] M. Wakabayashi, T. Nonaka, T. Nakamura, S. Morino and N. Yoshida, "Experimental Studies on the Behavior of Steel Bars under Repeated Axial Loading", Disaster Prevention Research Institute Annuals, Kyoto University, No. 16B, 1973, pp. 113-125 (in Japanese).

[14] P.C. Paris, "Limit Design of Columns", Journal of the Aeronautical Sciences, January, 1954, pp. 43-49.

[15] K. Neale and J. Schroeder, " Instability under Cycles of Plastic Deformation", Instability of Continuous Systems, edited by H. Leipholz, Springer-Verlag, 1971, pp. 329-333.

[16] T.M. Mulcahy and E.M. Shoemaker, "Column Instabilities Caused by Cyclic Loading", International Journal of Solids and Structures, Vol. 6, 1970, pp. 1011-1019.

[17] N. Yoshida, T. Nonaka, et al., "Use of the Parabolic Yield Condition in the Analytic Behavior of Axially-Loaded Members", in preparation.

[18] Nonaka, T., "An Elastic-Plastic Analysis with a Modified Yield Condition for Bar under Repeated Axial Loading", to be published; Chapter 4 of this treatise.

[19] M. Wakabayachi, C. Matsui, K. Minami and I. Mitani, "Inelastic Behavior of Steel Frames Subjected to Constant Vertical and Alternating

Horizontal Loads", Fifth World Conference on Earthquake Engineering, Preprint No. 146, Rome, 1973, Proceedings (1974), pp. 1194-1197.

[20] E.E. Zajac, "Stability of Two Planar Loop Elasticas", Journal of Applied Mechanics, March, 1962, pp. 136-142.

[21] J.E. Flaherty and J.B. Keller, "Contact Problems Involving a Buckled Elastica", SIAM Journal on Applied Mathematics, Vol. 24, No. 2, March, 1973, pp. 215-225.

[22] op.cit. in [3], p. 403.

[23] J. Prescott, "Applied Elasticity", Dover, 1961, p. 104.

[24] See, e.g., P.G. Hodge, Jr., "Plastic Analysis of Structures", McGraw-Hill, 1959, pp. 175-191.

CHAPTER 6

LARGE AND SMALL DEFORMATION BEHAVIOR OF AN AXIALLY LOADED BAR

ABSTRACT This chapter contains the second phase of theoretical studies on the hysteretic behavior of an elastic-plastic bar subjected to large deformation under variable repeated axial loading. Basic equations obtained in the first phase of the studies are summarized, and they are approximated by assuming that changes in bar dimensions can be neglected and that the square of the slope of the deflection curve is negligibly small in comparison with unity, to yield the basic equations obtained previously for small deformation. By making use of the basic equations, a numerical example is presented for the load-deformation characteristics of the bar from the large and small deformation theories for comparison purposes. The chapter is concluded with discussion on the effects of large deformation, based on the order of magnitude and the results of the example.

SOURCE The contents of Chapter 6 are based on the following paper: Taijiro NONAKA, "An analysis for Large Deformation of an Elastic-Plastic Bar under Repeated Axial Loading, Part 2 Correlation with Small Deformation Theory", to be published.

Notation

A cross-sectional area

E Young's modulus

$F(k,\theta)$, $E(k,\theta)$ elliptic integrals of the first and second kinds with modulus k, amplitude θ ,

h integral constant

$f \equiv (1/2)\,(|N|/EI)^{1/2}$

I cross-sectional moment of inertia

$k \equiv \cos(\Psi/2)$; $k' \equiv \sin(\Psi/2)$

$P(\eta) \equiv (1-\eta^2)|h-\eta|$

L length

M bending moment

N load

s arc length

V middle deflection

x coordinate along original bar axis

y deflection

Δ relative displacement

$\eta \equiv h - Ny^2/(2EI)$

Θ one-half of hinge rotation

θ, θ' values of ϕ at $\Phi = \Theta$ for $N > 0$ and $N < 0$

ϕ defined by Eq.(A8)

Φ slope angle

Ψ end slope angle

Subscripts indicate particular values with

E Euler load

O original value

p full plasticity

l large deformation theory

s small deformation theory

Superscripts indicate components due to

e elasticity

g change in geometry

p plastic hinge

t plastic extension

Notation

A cross-sectional area

E Young's modulus

$F(k,\theta)$, $E(k,\theta)$ elliptic integrals of the first and second kinds with modulus k, amplitude θ

h integral constant

$f \equiv (1/2)\ (|N|/EI)^{1/2}$

I cross-sectional moment of inertia

$k \equiv \cos(\Psi/2)$; $k' \equiv \sin(\Psi/2)$

$P(\eta) \equiv (1-\eta^2)|h-\eta|$

L length

M bending moment

N load

s arc length

V middle deflection

x coordinate along original bar axis

y deflection

Δ relative displacement

$\eta \equiv h - Ny^2/(2EI)$

Θ one-half of hinge rotation

θ, θ' values of ϕ at $\Phi = \Theta$ for $N > 0$ and $N < 0$

ϕ defined by Eq.(A8)

Φ slope angle

Ψ end slope angle

Subscripts indicate particular values with

E Euler load

O original value

p full plasticity

l large deformation theory

s small deformation theory

Superscripts indicate components due to

e elasticity

g change in geometry

p plastic hinge

t plastic extension

1. INTRODUCTION

This series of investigation is concerned with the hysteretic behavior of a prismatic bar subjected principally to repeated axial loading, tension and/or compression. In the preceding chapter, an elastic-perfectly plastic type of analysis has been presented to derive the basic equations which can describe theoretically the large deformation characteristics of the bar [1]. Geometrical nonlinearities as well as the material have been strictly taken into account, including the effects of large deflection and of changes in bar dimensions due to plastic elongation. In Chapter 3, the basic equations were derived through quasi-linear analysis, which neglected these effects of large deformation, based on otherwise similar assumptions [2]. The small deformation theory was confirmed experimentally to predict the elastic-plastic behavior of actual steel bars with first order accuracy [1]. The objective of the discussions of this chapter is twofold: to derive the basic equations for small deformation from those for large deformation, the process of the approximation being instructive and helpful for better understanding of the large deformation equations, and to present a numerical example for the load-deformation characteristics from both theories for comparison purposes. They are preceded by a brief summary of the results obtained in Chapter 5.

2. BASIC EQUATIONS OF LARGE DEFORMATION

It is supposed that an initially straight uniform bar is in equilibrium with the load of a pair of equal and opposite forces varying slowly and applied repeatedly along the original axis. The bar deflects only in a definite plane without twisting and shearing with the current cross-sectional dimensions of area A and moment of inertia I, having the current length L contained between the two adjoining inflections. In order to determine the load-deformation characteristics, it suffices to relate the load N to the relative displacement Δ between the ends with hereditary nature in plastic hinge rotation and in bar dimensions due to plastic elongation. The positive directions of N and Δ are so taken that they accord, in the case of small deformation, with the sign convention of positive N for tension and positive Δ for separation. With allowance for large elongation, the elastic-perfectly plastic type of properties are assumed under combined action of axial force N and bending moment M on the basis of the one-dimensional idealization of the bar, having constant limit axial force N_p in pure tension, current plastic limit moment M_p in pure bending and the yield condition $|N/N_p| + |M/M_p| = 1$. Among other important assumptions are moderately large bar slenderness, negligible elastic changes in bar dimensions, cross-sectional shape remaining similar to the original, and that a compressed straight bar buckles when the compression reaches either the crush load N_p or Euler load π^2EI/L^2, where E is the Young's modulus.

Just as in the case of small deformation, the relative displacement is composed of four components, viz., $\Delta = \Delta^e + \Delta^g + \Delta^p + \Delta^t$, where Δ^e is the elastic change in the length, $\Delta^g \leqq 0$ is a component caused by change in geometry associated with transverse deflection, $\Delta^p \leqq 0$ is the plastic axial deformation at a yield hinge, and $\Delta^t \geqq 0$ is the plastic elongation acquired in a straight configuration. The components Δ^g and Δ^t can reach a magnitude of the order of the length. The latter adds to the original length L_o to give nearly $L = L_o + \Delta^t$, accordingly reducing cross-sectional dimensions so that the current values A, I, N_p and M_p are related to their original volues A_o, I_o, N_o and M_o, respectively, through equations

$$A = A_o(L_o/L), \qquad I = I_o(L_o/L)^2, \qquad N_p = N_o, \qquad M_p = M_o(L_o/L)^{1/2}. \tag{1}$$

The plastic elongation Δ^t can increase indefinitely under $N = N_p$, being controlled by the displacement constraints. By treating the load as the independent variable, the other components of Δ are given from

$$\Delta^e = (N/EA)\ (L+\Delta^g) \tag{2}$$

$$\Delta^g = \begin{cases} -(2/f)[E(k,\pi/2) - E(k,\theta)] & \text{for} \quad N > 0 \\ (2/f)[E(k',\pi/2) - E(k',\theta')] - 2L & \text{for} \quad N < 0 \end{cases} \tag{3a,b}$$

$$\Delta^p = -(2M_p/N_p)\Theta \tag{4}$$

and, in addition, from the nature of the deflection curve it follows that

$$fL = \begin{cases} F(k,\pi/2) - F(k,\theta) & \text{for} \quad N > 0 \\ F(k',\pi/2) - F(k',\theta') & \text{for} \quad N < 0 \end{cases} \tag{5a,b}$$

$$fV = \begin{cases} k\cos\theta & \text{for} \quad N > 0 \\ k'\cos\theta' & \text{for} \quad N < 0 \end{cases} \tag{6a,b}$$

among the deflection $V \geqq 0$ at the middle and slope angles $\Psi \geqq 0$ and $\Theta \geqq 0$ at an end and at just next to the middle, respectively, where $F(k,\theta)$ and $E(k,\theta)$ are the Legendre elliptic integrals of the first and second kinds (defined in the Appendix), respectively, with modulus k, amplitude θ;

$f \equiv (1/2)(|N|/EI)^{1/2}$, and

$$k \equiv \cos(\Psi/2), \quad k' \equiv \sin(\Psi/2); \quad \theta \equiv \arc\sin\frac{\cos(\Theta/2)}{k}, \quad \theta' \equiv \arc\sin\frac{\sin(\Theta/2)}{k'} . \tag{7a,b; 8a,b}$$

A yield hinge forms at the middle with the deflection

$$V = M_p \,(1/|N| - 1/N_p) . \tag{9}$$

Equations (5), (6) and (8) are then combined to find k, θ and Θ for $N > 0$ and to find k', θ' and Θ for $N < 0$. The bar behaves elastically with a deflection smaller than that of Eq.(9), with Θ remaing constant, and with k and θ, or, their primed quantities, according to $N > 0$ or $N < 0$, respectively, determined from Eqs.(5) and (8). The behavior at $N = 0$ is elastic, and the deflection curve consists of two straight segments intersecting at the middle with angle 2Θ, so that $\Psi = \Theta$, $\theta = \theta' = \pi/2$, and $\Delta^g = -L(1 - \cos\Theta)$.

3. REDUCTION TO SMALL DEFORMATION

If the elongation is sufficiently small as compared with the original length of the bar, then the bar dimensions can be approximated by their original values.

If deflections are so small that the square of the slope is negligible in comparison with unity, then quasi-linear analysis holds as presented previously [2]. In order to derive approximate formulae for small deformation from the results summarized in the preceding section, two cases $N > 0$ and $N < 0$ are considered below one after the other. Noting from Eq.(7) that

$$k = 1 - \Psi^2/8 + O(\Psi^4), \qquad k' = \Psi/2 + O(\Psi^3), \tag{10a,b}$$

let us first consider the case $N > 0$.

Eqs.(8a) and (10a) are combined to give $\sin\theta \simeq 1 - (\Theta^2 - \Psi^2)/8$ to the second order in slope angles. By combining this relation with the identity $\sin\theta = \cos(\pi/2 - \theta) \simeq 1 - (1/2)(\pi/2 - \theta)^2$, it follows that $\pi/2 - \theta \simeq (\Theta^2 - \Psi^2)^{1/2}/2$. Another trigonometric identity $\cos\theta = \sin(\pi/2 - \theta) \simeq \pi/2 - \theta$ will be used repeatedly. The relation between Ψ and Θ is approximated from Eq.(5a), in which the integral $F(k,\theta)$ is singular at $\theta = \pi/2$ for $k = 1$, but the manipulation

$$\int_\theta^{\pi/2} \frac{d\phi}{(1-k^2 \sin^2\phi)^{1/2}} \simeq \int_\theta^{\pi/2} \frac{d\phi}{[k'^2+(\pi/2-\phi)^2]^{1/2}} = \int_0^{\pi/2-\theta} \frac{dt}{(k'^2+t^2)^{1/2}}$$

$$= \sinh^{-1}[(\pi/2-\theta)/k'] = \cosh^{-1}[1 + (\pi/2-\theta)^2/k'^2]^{1/2} = \cosh^{-1}(\Theta/\Psi) \tag{11}$$

yields

$$\Theta \simeq \Psi \cosh(fL). \tag{12}$$

Consequently,

$$\pi/2 - \theta \simeq (\Theta/2)\tanh(fL). \tag{13}$$

It follows from Eq.(6a), when combined with Eqs.(10a) and (13), that

$$V \simeq (\Theta/2f)\tanh(fL). \tag{14}$$

The component Δ^g of Eq.(3a) is approximated through the relation

$$\int_\theta^{\pi/2} (1-k^2\sin^2\phi)^{1/2}\, d\phi \simeq \int_\theta^{\pi/2}[k'^2+(\pi/2-\phi)^2]^{1/2}\, d\phi = \int_0^{\pi/2-\theta}(k'^2 + t^2)^{1/2}\, dt, \quad (15)$$

in which the last integral is evaluated with the change of variables, $t = k'\sinh\tau$, viz., with the relation

$$(k'^2+t^2)^{1/2}\, dt = (k'^2/2)[1 + \cosh(2\tau)]\,d\tau = (k'^2/2)d(\tau + \sinh\tau\, \cosh\tau)$$

$$= (k'^2/2)\, d\{\sinh^{-1}(t/k') + (t/k')[1 + (t/k')^2]^{1/2}\}. \quad (16)$$

It follows, after use is also made of Eqs.(10b), (12) and (13), that

$$\Delta^g \simeq - L \left[\frac{\Theta}{2\cosh(fL)} \right]^2 \left[1 + \frac{\sinh(2fL)}{2fL} \right]. \quad (17)$$

For the case $N < 0$, integration is carried out through the binomial expansion of the integrands in Eqs.(3b) and (5b), giving

$$\Delta^g \simeq (2/f)\{(\pi/2-\theta')-(k'/2)^2[(\pi/2-\theta')+\sin\theta'\, \cos\theta']\} - 2L \quad (18)$$

$$fL \simeq (\pi/2 - \theta') + (k'/2)^2[(\pi/2 - \theta') + \sin\theta'\, \cos\theta'] \quad (19)$$

to the second order in k'. To the first order, Eq.(19) provides

$$\pi/2 - \theta' \simeq fL, \quad \therefore \sin\theta' \simeq \cos(fL), \quad \cos\theta' \simeq \sin(fL), \quad (20a,b,c)$$

and from Eqs. (6b), (8b), (10b) and (20b,c) it follows that

$$\Theta \simeq \Psi \cos(fL), \quad V \simeq (\Theta/2f) \tan(fL). \quad (21a,b)$$

The second order approximation for $\pi/2 - \theta'$ is obtained from Eq.(19) as the first parenthesized quantity by substituting Eq.(20) into the brackets. It follows from Eq.(18), with the second order approximation for the quantity within the second pair of parentheses and with the first order within the brackets, that

$$\Delta^{g} \simeq - L \left[\frac{\Theta}{2 \cos(fL)} \right]^{2} \left[1 + \frac{\sin(2fL)}{2fL} \right]. \tag{22}$$

When $\Theta = 0$, Δ^{g} can take a nonvanishing value only if $\cos(fL) = 0$, whose smallest root corresponds to Euler load, i.e., $N = -\pi^{2}EI/L^{2}$

When comparison is made of corresponding equations between the cases $N > 0$ and $N < 0$, i.e., between Eqs.(12) and (21a), Eqs.(14) and (21b), Eqs.(17) and (22), it is seen that there exists a simple correspondence for small deflection. Namely, hyperbolic functions in the case of $N > 0$ become the corresponding trigonometric functions in the case of $N < 0$. This is due to the simple relations between these functions in the use of complex numbers. The component Δ^{g} is thus expressed explicitly in terms of L, f and Θ.

It is seen by combining Eq.(12) with Eq.(17), and combing Eq.(21a) with Eq.(22), that the assumption $\Psi^{2} \ll 1$ leads to $|\Delta^{g}| \ll L$. As a consequence, Eq.(2) is reduced to $\Delta^{e} \simeq NL/(EA)$.

The results of this section coincide with what have been obtained previously [1] and summarized in Chap. 5, provided changes in bar dimensions are neglected on the basis of the assumption $\Delta^{t} \ll L$. It has been shown in Chap. 3 through treatment in terms of dimensionless quantities, that in the general case of small deformation each component of Δ is of the comparative order of magnitude for bars with moderate slenderness.

4. EXAMPLE

A numerical example is given for a bar of material with the yield point strain $N_o/(EA_o) = 1.143 \times 10^{-3}$ (experimental value [3]) and initial slenderness such that the Euler load $N_E \equiv \pi^2 EI_o/L_o^2$ equals the crush load N_o. The loading program is specified by the relative displacement as follows:

$$\Delta/L_o = 0 \rightarrow -0.1 \rightarrow 0.1 \rightarrow -0.1 \rightarrow 0.2 \rightarrow -0.2 \rightarrow 0.2$$

Fig.1 shows the load-deformation characteristics and stress trajectory for the mid-section; Δ/L_o, V/L_o, Θ, Ψ and M/M_o are taken for the abscissae in (a), (b), (c), (d) and (e), respectively, as against the common ordinate of N/N_o. The variation of these quantities from the large deformation theory is shown by solid lines with numbers in order enclosed by circles. Dashed lines are also drawn from the small deformation theory for comparison. It is seen that on the whole the small deformation theory predicts somewhat larger magnitudes of the load for the displacement controlled loading. The weakening effect of changes in dimensions is remarkable; plastic elongation in ④ → ⑤ causes a reduction in the buckling strength as observed by the change in the ordinates, from ① to ⑥, and elongation ⑨ → ⑩ causes change from ⑥ to ⑪. On the other hand, the effect of large deflection looks invisible in this illustration with the same extremum $|\Delta/L_o| = 0.2$ in separation and approach. In order to observe this effect, post-buckling behavior is examined under monotonously decreasing displacment. Fig. 2 shows the variation of the ratio of the difference $|N_l| - |N_s|$ in the

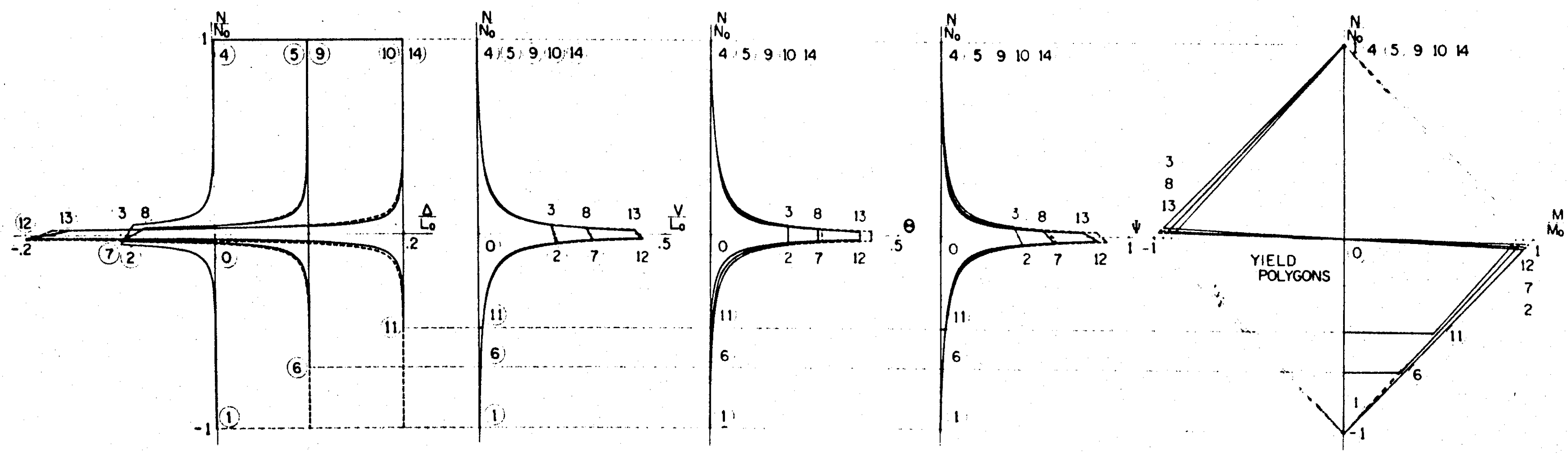

(a) Load vs displacement

(b) Load vs deflection

(c) Load vs central rotation

(d) Load vs end rotation

(e) Mid-section stress trajectoy

Fig. 1 Behavioral diagrams of an axially loaded bar from large (thick solid lines) and small (thick dashed lines) deformation theories

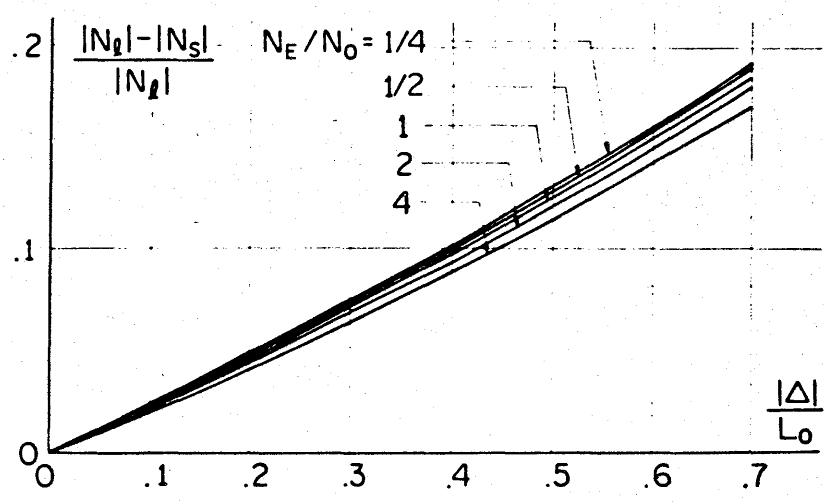

Fig. 2 Effect of large deflection in post-buckling

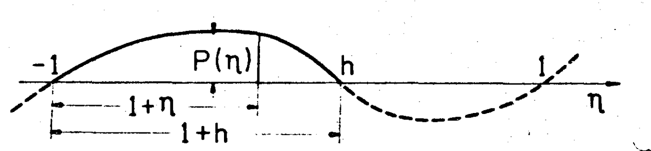

(a) $N \geqq 0;\ -1 \leqq \eta \leqq h \leqq 1,\quad P(\eta) = (1-\eta^2)(h-\eta)$

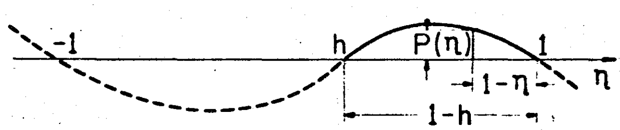

(b) $N \leqq 0;\ -1 \leqq h \leqq \eta \leqq 1,\quad P(\eta) = (1-\eta^2)(\eta-h)$

Fig. 3 Considerations on elliptic integrals load magnitudes between the large and small deformation theories to the former $|N_1|$ as a function of the ratio $|\Delta|/L_o$, with slenderness parameter N_E/N_o ranging between 1/4 and 4. It is seen that the assumption of small deflection underestimates the post-buckling strength. The relative error, determined by the quotient, increases with deformation and reaches about 10% when the approach displacement is 40% of the bar length; it does not depend seriously on slenderness within the range considered herein.

No experimental data seem to be available to date for the large deformatiom behavior in question.

5. CONCLUDING REMARKS

In the fundamental relation of large deformation, the four components of Δ can be of different order of magnitude. When need is strictly in the range of large deformation, two components, Δ^e and Δ^p, may be neglected as compared with the rest, Δ^g and Δ^t; the general formulation presented here is comprehensive for those cases where in the course of variable repeated loading, the bar is loaded into the range of large deformation for some time and subjected to small variation of the load or deformation for the rest.

The fact that Δ^g/L has the same order of magnitude as Ψ^2 indicates that if the decrease in the distance between the bar ends attains a magnitude of the order of the bar length, then the square of the slope cannot be neglected in comparison with unity and the large deflection analysis should be resorted to. Since the effect of changes in bar dimensions comes into play when the increase in the distance attains a magnitude of the order of the original length of the bar, both effects are equally important in such a case as alternately repeated loading with the displacement extrema of the order of the bar length in both directions. While these effects of large deformation may not be very important in most practical cases, it has been shown in the results of the example cited that the latter effect is rather significant with $|\Delta|/L_0$ in the range of 20%. Actual mild steel may be brought to rupture by extension of a greater range, whereas a long bar may be bent into large deflection without catastrophic or hereditary damage. In such a case, the former effect gains in importance.

If the bar is extremely long and slender, the component Δ^p, which is of the order of the depth, can be neglected in comparison; it may be even allowable to ignore the compressive strength altogether, and to regard the bar as a tension resistant member for practical applications.

Worth mentioning is that it is appropriate to approximate $\Delta^e \simeq NL_0/(EA)$, irrespective of the order of magnitude of deformation; by writing $\Delta^e = (N/EA)L_0 + (N/EA)\Delta^t + (N/EA)\Delta^g$ and considering that the factor N/EA is at most of the order of yield strain, it is seen when substituted into $\Delta = \Delta^e + \Delta^g + \Delta^p + \Delta^t$ that the second and third terms of Δ^e may be neglected in comparison with Δ^t and Δ^g themselves, respectively, and therefore is suggestive of keeping the first term alone.

Final comment is made upon the yield condition. The assumed linearized yield condition can be replaced by another, according to the shape of the cross section, without modification in the basic equations except for Δ^p. It follows from the flow rule associated with a nonlinear yield condition, as is the case for an actual cross section with finite web, that the plastic flow created at a yield hinge has a variable proportion between the rotation and axial deformation, depending upon the existing axial force or the load. As a consequence, the axial deformation at the yield hinge does not vanish in general after a complete cycle of plastic rotation. This adds another history-dependent property, agreeing with the tendency observed in the experimental observation [1, 4, 5].

ACKNOWLEDGEMENTS

The author is much indebted to Mr. N. Yoshida, graduate student of Kyoto University, for the numerical computation and preparing the figures.

REFERENCES

[1] T. Nonaka, "An Analysis for Large Deformation of an Elastic-Plastic Bar under Repeated Axial Loading, Part 1 Derivation of Basic Equations", to be published; Chapter 5 of this treatise.

[2] T. Nonaka, "An Elastic-Plastic Analysis of a Bar under Repeated Axial Loading", International Journal of Solids and Structures, Vol. 9, No. 5 with Erratum in No. 10, 1973, pp. 569-580 ; Chapter 3 of this treatise.

[3] M. Wakabayashi, T. Nonaka, T. Nakamura, S. Morino and N. Yoshida, "Experimental Studies on the Behavior of Steel Bars under Repeated Axial Loading", Disaster Prevention Research Institute Annuals, Kyoto University, No. 16 B, 1973, pp. 113-125 (in Japanese).

[4] T. Nonaka, "An Elastic-Plastic Analysis with a Modified Yield Condition for a Bar under Repeated Axial Loading", in preparation.

[5] N. Yoshida, T. Nonaka, et al., "Use of the Parabolic Yield Condition in the Analytic Behavior of Axially-Loaded Members", in preparation.

APPENDIX Derivation of Deflection Curve

The key to the closed-form solution presented herein lies in the analytic expression of the deflection curve. This has been done by integrating the equilibrium equation

$$(d\Phi/ds)^2 = (2N/EI)(\cos\Psi - \cos\Phi) \tag{A1}$$

through the dual transformation

$$\sin\phi = \begin{cases} [\cos(\Phi/2)]/k & \text{for} \quad N \geqq 0 \\ [\sin(\Phi/2)]/k' & \text{for} \quad N \leqq 0 , \end{cases} \tag{A2}$$

where s and Φ are arc length and slope angle, respectively, at a generic point of the deflection curve. This transformation enables the case $N \geqq 0$ to be treated in a way analogous to the case $N \leqq 0$ of the "elastica". Indication is herein made of the considerations which have led to Eq.(A2), as well as the determination of the entire deflection curve.

Let (x,y) be the cartesian coordinates, with $x \geqq 0$ taken along the original axis of the bar, and $y \geqq 0$ designating the deflection; the origin is taken at the end s = 0. Inclusion of the nonlinear term in the curvature expression $(d^2y/dx^2)\ [1 + (dy/dx)^2]^{-3/2}$ gives the once-integrated equilibrium equation

$$[1 + (dy/dx)^2]^{-1/2} + Ny^2/(2EI) = h, \tag{A3}$$

in the place of Eq.(A1), where h is an integral constant. Equation (A3) is combined with the relation $ds = [1 + (dx/dy)^2]^{1/2}\,dy$ and integrated to give

$$s = \int_0^y \frac{dy}{\{1-[h-Ny^2/(2EI)]^2\}^{1/2}}, \qquad x = \int_0^y \frac{[h-Ny^2/(2EI)]dy}{\{1-[h-Ny^2/(2EI)]^2\}^{1/2}}. \tag{A4}$$

The form of these integrals suggests the change of variables,

$$\eta = h - Ny^2/(2EI). \tag{A5}$$

It is noticed from Eqs.(A3) and (A5) that

$$h = \cos\Psi, \qquad \eta = \cos\Phi, \tag{A6}$$

and that $-1 \geqq h,\eta \leqq 1$. By considering that $h \gtreqless \eta$ according to $N \gtreqless 0$, it follows from Eqs.(A4) and (A5) that

$$2\sqrt{2}\,fs = \int [P(\eta)]^{-1/2}\,d\eta, \quad 2\sqrt{2}\,fx = \int \eta\,[P(\eta)]^{-1/2}\,d\eta, \tag{A7}$$

where $P(\eta) \equiv (1-\eta^2)\,|h-\eta|$, and the limits of integration are form η to h for $N \geqq 0$ and h to η for $N \leqq 0$. Examination of the ranges of integration in

Fig. 3 suggests another change of variables,

$$\sin^2\phi = \begin{cases} (1 + \eta)/(1 + h) & \text{for} \quad N \geqq 0 \\ (1 - \eta)/(1 - h) & \text{for} \quad N \leqq 0 \end{cases} \tag{A8}$$

Elliptic integrals in Eq.(A7)are thus converted into Legendre's form,

$$2fs = \begin{cases} F(k,\pi/2) - F(k,\phi) & \text{for} \quad N \geqq 0 \\ F(k',\pi/2) - F(k',\phi) & \text{for} \quad N \leqq 0 \end{cases} \tag{A9}$$

$$fx = \begin{cases} fs - [E(k,\pi/2) - E(k,\phi)] & \text{for} \quad N \geqq 0 \\ -fs + [E(k',\pi/2) - E(k',\phi)] & \text{for} \quad N \leqq 0 \end{cases} \tag{A10}$$

where

$$k^2 \equiv (1+h)/2 \leqq 1, \qquad k'^2 \equiv (1-h)/2 \leqq 1, \tag{A11}$$

$$F(k,\phi) \equiv \int_0^\phi (1-k^2 \sin^2\phi)^{-1/2}\, d\phi, \quad E(k,\phi) \equiv \int_0^\phi (1-k^2 \sin^2\phi)^{1/2}\, d\phi. \tag{A12}$$

Equation (A6) converts Eq.(A11) into Eq.(7) and converts Eq.(A8) into Eq.(A2), thus indicating the analysis presented in Chapter 5. Equations (A9) and (A10) are adequate to determine the entire curve of deflection. Alternatively the deflection curve can also be expressed in terms of Jacobian elliptic functions.

CHAPTER 7

DYNAMIC PLASTIC BEHAVIOR OF A BEAM WITH SHEAR AND BENDING DEFORMATION

ABSTRACT An analysis is presented of the dynamic behavior and permanent deformation of a rigid-perfectly plastic beam subjected to blast-type loading. The beam is simply supported at the ends, and the load is uniformly distributed over the span. The analysis is based on an approximate yield curve relating limiting values of shear force and bending moment. Various patterns of deformation are found to occur with combination of plastic bending and shear sliding depending upon the load magnitude and beam characteristics. The effects of shear and of the shape of the load pulse are examined, and the chapter is concluded with the results expressed in general terms for application to similar cases.

SOURCE The contents of Chapter 7 are based on the following paper: Taijiro NONAKA, "Shear and Bending Response of a Rigid-Plastic Beam to Blast-Type Loading", to be published.

Notation

d beam depth

E energy

I $\equiv \int_o^t \mu dt$

$\hat{I}$ total impulse

l half beam length

m mass per unit length

M bending moment

P load

Q shear force

q effective load intensity

t time

v velocity

x co-ordinate along beam

y deflection

δ permanent deflection

θ slope angle

κ curvature

μ $\equiv Pl/(4M_o)$

ν $\equiv Q_o l/(2M_o)$

ξ dimensionless length of rigid segment

τ load duration

ω angular velocity

Subscripts indicate:

b bending

d discontinuity

f finish

h yield hinge

m middle

o initiation, full plasticity or beam end

s shear sliding

1. INTRODUCTION

This chapter is concerned with the permanent deformation and the overall dynamic plastic behavior of beams under impact loads. A great number of studies have been made of bending response, and much effort has also been directed to the effect of extensional deformation arising from finite deflection [1]. Very few have treated the effect of shear, however. The shear effect is known not to be important in the static behavior of beams under normal conditions. According to recent papers bending of steel beams is not much affected by shear unless the shear span is smaller than thirty per cent of the span [2]. The shear effect even diminishes with increasing deflection in slender bars [3]. But in the problems of plastic beam dynamics loads are allowed to take instantaneous magnitudes of order greater than the static collapse loads. Large loads cause large shear forces and beams may deform plastically in shear as well as in bending.

Bleich and Shaw [4] showed from an elastic approach of Timoshenko beam that all beams, even those which are statically much stronger in shear than in bending, will begin to yield in shear before yielding in bending, when subjected to sufficiently high initial velocity distributions. Salvadori and Weidlinger [5] considered a simply supported rigid-perfectly plastic beam subjected to uniform pressure with exponential load-time relationship, and indicated that the beam may deform plastically by developing plastic slides at the supports in addition to the assumed single-hinge rotation at the mid-point due to yielding in bending. Karunes and Onat [6] examined the shear effects for a free-free, rigid-perfectly plastic beam subjected to point impact at the mid-point. They assumed the impact velocity to be kept constant during deformation, and found that the shear effects are of considerable importance when the ratio of the product of the beam length and the limit force in pure shear to the limit moment in pure bending is less than twenty. Nonaka found that the shear effect is ordinarily small for compact cross sections, and that this effect can become important when beams have non-compact cross sections such as an I-section and have small span-depth ratio when subjected to impulsive loading [7]. It was also found that this effect grows in significance as the loaded area gets small for the same total load [8]. Symonds discussed the potential importance of plastic shear deformations by introducing some analytical results including a part of the results to be presented herein [9].

Review of the literature outlined above indicates insufficiency in the quantitative knowledge about the shear effect in the dynamic plastic behavior of beams, and it is the purpose of this chapter to fully investigate and evaluate this effect. Examination is made of all the possibilities for deformation patterns under the combined plastic action of bending and shear. How they are affected by the load-time relation is also examined. A simply supported beam under a uniformly distributed, monotonously decreasing load is considered as an example, and is theoretically analysed on the basis of an approximate yield condition.

2. ASSUMPTIONS AND YIELD CONDITION

The rigid-perfectly plastic analysis to be presented herein ignores elastic deformation, strain rate sensitivity, strain-hardening and delay time effects of yield. It is known that the effect of elasticity is to increase the permanent deformation of a beam for a small ratio of the load magnitude to the plastic collapse load and to decrease for a large ratio, when the loading has the same total impulse [10]. However, the elasticity effect is believed to be negligible if the energy absorbed in plastic deformation is sufficiently large as compared with the maximum strain energy that the beam could absorb in an elastic manner [11, 12]. The effect of high rates of strain is to raise the yield stress of the material and is known to be of considerable importance in impact problems. An approximate inclusion of this effect is to note that the bulk of the kinetic energy is dissipated before the stresses and strain rates depart appreciably from their initial values, and to utilize a rate-insensitive material with constant yield stress equal to the initial dynamic yield stress [13]. This can be done by making use of the results of the rate-insensitive analysis to be presented herein.

The material is assumed to have ample ductility so that brittle fracture does not occur. We also assume small deformation and strong lateral supports so that the change in geometry is negligible and no instability phenomena take place.

In simple bending theory for perfectly plastic beams plastic action can take place in bending at a beam element only when the bending moment M of that element reaches the limit moment M_o in magnitude, regardless of the shear force present at the beam element. When strength in shear is considered, the shear force Q cannot be greater in magnitude than the limit force Q_o. With M_o and Q_o understood as the limiting values of M and Q in pure bending and in pure shear, respectively, plastic action may occur in shear as well as in bending, when M and Q are coexistent at the beam element and they satisfy a certain interaction relation interpolating the two limiting states. It is recognized that such a unique relation does not really exist as a local condition [14]; M and Q are not independent of each other but Q equals the rate of change of M with respect to the co-ordinate along the beam axis. Nevertheless, we approximately make use of such a relation for the formulation of our problem and assume the yield condition

$$(|M/M_0|-1)(|Q/Q_0|-1)=0 \,. \tag{1}$$

This relation is represented as a yield polygon in Fig. 1. For comparison the interaction curve

$$|M/M_0|+(Q/Q_0)^4-1=0 \tag{2}$$

suggested by Drucker for a rectangular cross section is also drawn in a thin dashed line [14]. In the case of an I-beam the limit force in shear can hardly exceed the shear force that is carried only by the web yielding in pure shear [15], except for very short beams which invalidate the concept of the beam with M and Q used as the generalized stresses. With this shear force taken for Q_0 Heyman suggests a practical ralation [16], which is written for positive M and Q as

$$M=M_f+[1-(Q/Q_0)^2]^{1/2}\,M_w \quad \text{for} \quad Q<Q_0, \tag{3a}$$

$$Q=Q_0 \qquad \text{for} \qquad M\leqq M_f, \tag{3b}$$

where M_f and M_w denote the contributions of the flanges and web respectively to the fully plastic moment ($M_f + M_w = M_0$). Equation (3) forms an interaction curve such as the one drawn in a thin dotted line in Fig. 1. The comparisons indicate that Eq.(1) is an unsafe approximation, but it turns out that the error in the yield condition does not play an important role in the particular

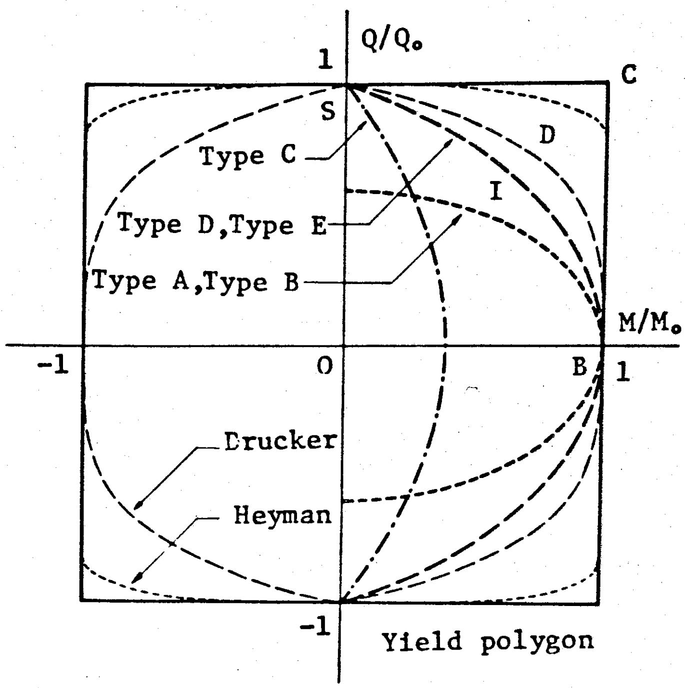

Fig. 1 Yield and stress Curves

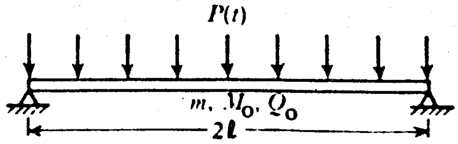

Fig. 2 Structure and loading

problem cosidered herein as will be discussed later, and the use of Eq.(1) as the yield condition for non-compact as well as compact cross sections is justified, provided Q_o is evaluated properly from the effective shear area for the former.

A generic element of the beam has to possess such a state of stress that it is represented by a point on or within the yield polygon, no point being allowed to lie outside the polygon in Fig. 1. On the basis of rigid-perfect plasticity no deformation takes place when the stress point lies within the fixed yield polygon, and the beam element can deform in a perfectly plastic manner when the stress point falls on the yield polygon according to the normality as stated in the flow rule associated with the assumed yield condition. It follows that if $|M| = M_o$, an indefinite change of curvature can occur; that if $|Q| = Q_o$, an indefinite change of shear slope can occur; and that if $|M| = M_o$ and $|Q| = Q_o$, then either or both of indefinite changes of curvature and shear slope can occur, the changes having directions compatible with M and Q existing at the element so that non-negative work is done both in bending and shear.

Further we restrict ourselves to blast-type loading, which is defined by the load $P(t) \geqq 0$ starting with the peak P_o at t=0 and decreasing monotonously with time t. This includes, in particular, a rectangular pulse, exponentially decreasing pulse, and impulsive load with indefinitely large magnitude and vanishingly small duration.

3. GENERAL ANALYSIS

Consider a simply supported uniform beam of limit moment M_o, limit shear Q_o, and mass per unit length m. The beam is subjected to a blast-type load P(t) uniformly distributed over the whole span $2l$ as shown in Fig. 2. The beam undergoes no deformation if P is so small that the bending moment and shear force developed in the beam are everywhere less in magnitude than M_o and Q_o, respectively. It may be supposed that in the case of a beam strong in shear pure bending deformation takes place if P is equal to or greater than the plastic collapse load in bending $P_b = 4M_o/l$, whilst pure shear deformation occurs in a beam weak in shear and strong in bending if P equals or is greater than the collapse load in shear $P_s = 2Q_o$. It turns out that deformation occurs in motion starting with one of five different patterns, depending upon the load magnitude and beam characteristics as shown in Fig. 3, where the relative shear strength $\nu \equiv P_s/P_b$ and relative load magnitude $\mu_o \equiv P_o/P_b$ are taken for the horizontal and vertical co-ordinate axes, respectively. Cases corresponding to the area below the inclined curves are not accompanied by shear deformation and have been analysed in detail by Symonds [17]. Recognizing that for the blast-type loading the interface which separates plastic and rigid zones moves only in one direction, he has obtained the analytic solution in a simple closed form. A brief review of his results first follows.

3.1 PURE BENDING MOTION

It is supposed that the beam is sufficiently strong in shear. If the load is such that $1 \leqq \mu_o \leqq 3$, then the beam engages in a motion with a yield-hinge rotation at the middle. Let it be referred to as Type A motion. With positive directions defined as in Fig. 4, the pattern of motion, distributions of q, Q and M, and final shape of permanent deformation δ are shown in Fig. 5, where q designates the effective load intensity per unit length in the sense of the d'Alembert principle. Because of the

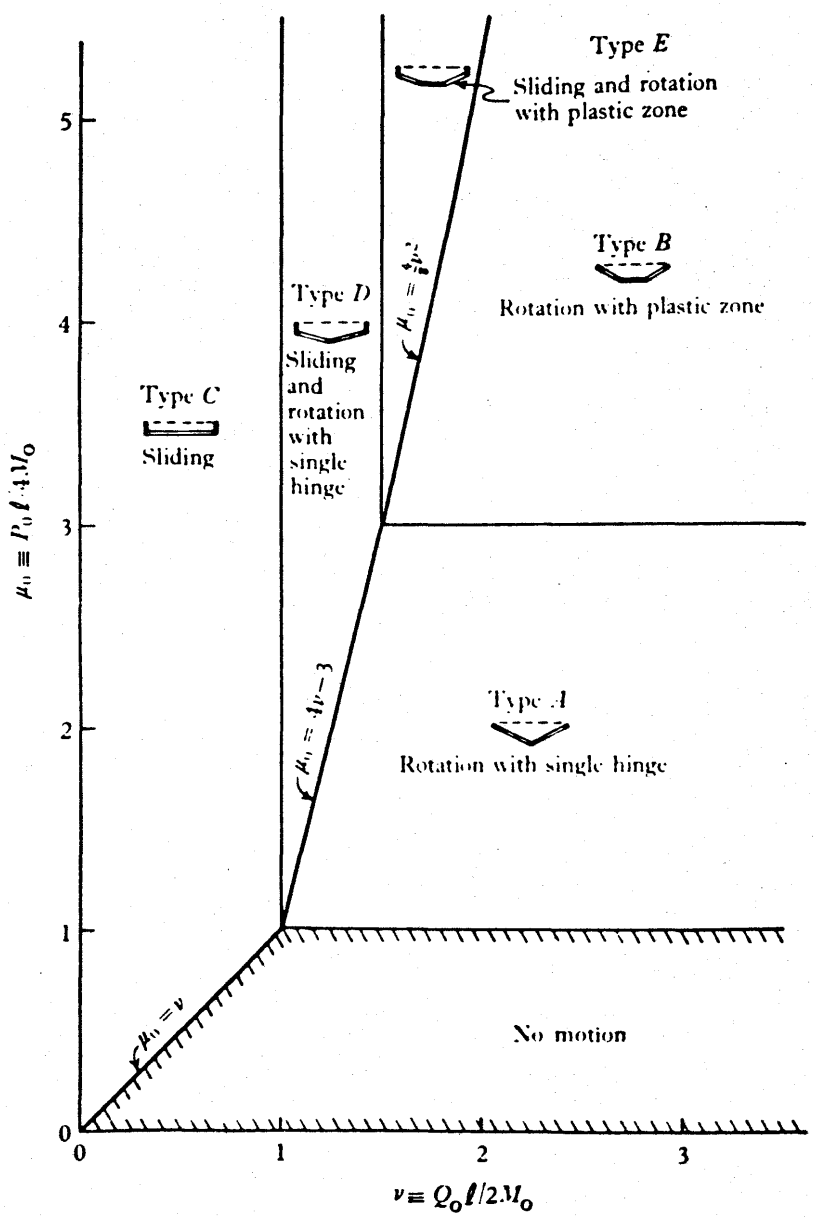

Fig. 3 Patterns of initial motion

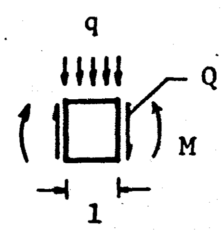

Fig. 4 Positive direction

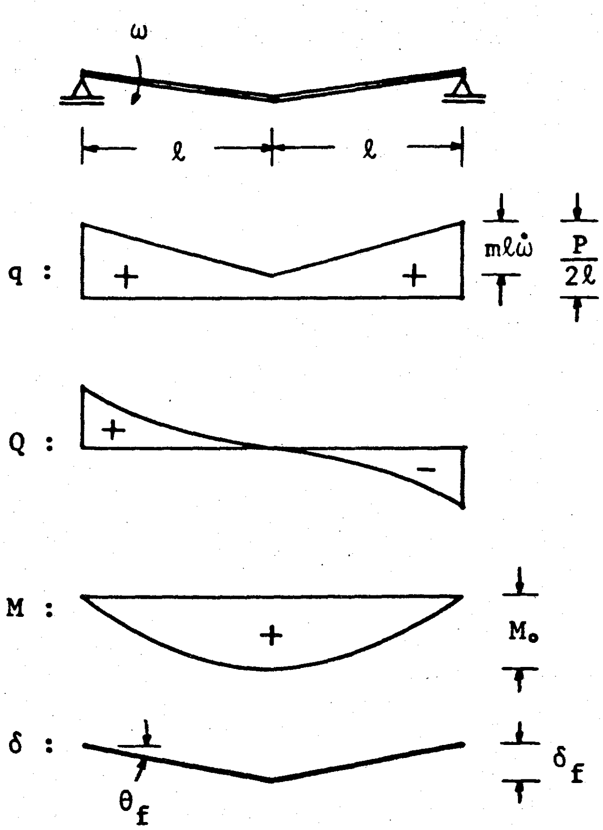

Fig. 5 Type A motion

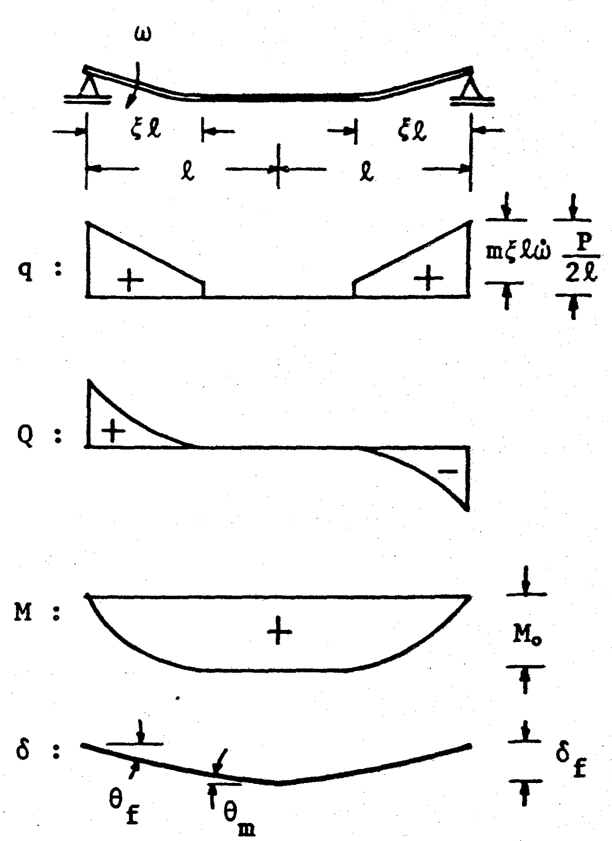

Fig. 6 Type B motion

symmetry of the problem under consideration we refer only to the left half beam in what follows except for discussions on the pattern of motion. The equation of motion is

$$(ml^3/M_0)\dot{\omega} = 3(\mu - 1), \tag{4}$$

where the dot denotes differentiation with respect to t, ω is the clockwise angular velocity, and $\mu \equiv P/P_b = Pl/(4M_0)$ is the dimensionless load. The final deformation is obtained by simple quadrature. With notation $I(t) \equiv \int_0^t \mu dt$, the final slope angle Θ_f of the beam axis and the final middle deflection δ_f are given by

$$\frac{ml^3}{M_0}\theta_f = \frac{ml^2}{M_0}\delta_f = 3\int_0^{t_f} I\,dt - \frac{3}{2}t_f^2, \tag{5}$$

where t_f, denoting the termination of motion, is determined from

$$t_f = I_f \equiv \int_0^{t_f} \mu\,dt. \tag{6}$$

For $\mu_0 > 3$ a finite plastic zone is first produced in the middle portion of the beam between two segments of length ξl which rotate as rigid bars as shown in Fig. 6. Let this pattern of motion be Type B. Equations of motion and velocity continuity across the rigid-plastic interface are combined to give

$$\xi^2 = 3t/I, \tag{7}$$

$$[(ml^3/M_0)\omega]^2 = 4I^3/(3t). \tag{8}$$

These equations apply until $t = t_h$ corresponding to $\xi = 1$, when the motion changes into Type A, Eq.(4) being valid for t such that $t_h \leqq t \leqq t_f$. Final deformation parameters are given by

$$\frac{ml^3}{M_0}\theta_f = 2\int_0^{t_h}\sqrt{\frac{I^3}{3t}}\,dt + 3\int_{t_h}^{t_f} I\,dt - \frac{3}{2}(t_f^2 - t_h^2), \tag{9}$$

$$\frac{ml^2}{M_0}\delta_f = 2\int_0^{t_h} I\,dt + 3\int_{t_h}^{t_f} I\,dt - \frac{3}{2}(t_f^2 - t_h^2), \tag{10}$$

$$\frac{ml^3}{M_0}\theta_m = 3\int_{t_h}^{t_f} I\,dt - \frac{3}{2}(t_f^2 - t_h^2), \tag{11}$$

where

$$3t_h = I_h \equiv \int_0^{t_h} \mu\,dt, \tag{12}$$

$$t_f = I_f, \tag{13}$$

and θ_f and θ_m are the final slope angles at the beam end and middle, respectively. The traveling interface with $\xi \geqq 0$ causes a curvature $\kappa(\xi)$ convex downward, which is determined from $\kappa = \omega\, dt/(l d\xi)$ and

$$(ml^4/M_0)\kappa = 4I^2/(3-\mu\xi^2). \tag{14}$$

It is interesting to note that the curvature can also be found from

$$(ml^4/4M_0)\kappa = I\,dt/d(\xi^2) = 3\,d(t^2)/d(\xi^4). \tag{14'}$$

We will now examine the state of stress in the light of bending-shear interaction. The stress points of the beam in Type A and B motions are distributed on such a curve as the one drawn in a thick-dotted line in Fig. 1. Point B represents the state of stress at the yield hinge in Type A motion and represents that in the plastic zone in Type B. The upper half of the curve stands for the left half of the beam. It is clear that the flow rule is satisfied by the pure bending deformation in these motions. Inasmuch as the strength in shear is taken into account, Symonds' solution summarized above ceases to hold when the shear force induced in the beam reaches Q_o in magnitude. In order for Type A motion to occur the condition, $P - ml^2\dot{\omega} < 2Q_o$, has to be kept satisfied, and hence, the condition

$$\mu_0 < 4\nu - 3 \tag{15}$$

must be added to the inequality $1 \leqq \mu_o \leqq 3$. In order to establish the shear condition for the validity of Type B motion, it is convenient to replace a similar static principle by the condition that the motion due to shear disappears in Type E motion to be studied later. This condition turns out to give

$$3 < \mu_0 < 4\nu^2/3. \tag{16}$$

3.2 PURE SLIDING MOTION

If a beam with strength relation $P_s < P_b$ is subjected to such a large load that $P_o \geqq P_s$, i.e., if the conditions

$$1 > \nu, \qquad \mu_0 \geqq \nu \tag{17a,b}$$

are both satisfied, then the yield limit $|Q| = Q_o$ is reached at the beam ends and it follows from the flow rule that shear sliding may develop at the supports, the beam part between the ends moving as a rigid body as shown in Fig. 7. Occurrence of a shear slide at any position other than the ends would violate the condition $|Q| \leqq Q_o$. The stress points of the beam lie on such a parabolic curve as the one drawn by a thick chain line in Fig. 1. The curve is similar to the bending moment diagram in Fig. 7, since the shear force varies linearly along the beam axis.

With y indicating the displacement in the direction of loading, the principle of linear momentum reads

$$(ml^2/M_0)\dot{y} = 2(I - \nu t). \tag{18}$$

The fact that inequality (17a) assures $|M| < M_o$ is seen from $q = P/(2\,l) - m\ddot{y}$. The sliding motion stops at time t_s which is determined from

$$\nu t_s = I_s \equiv \int_0^{t_s} \mu\, dt. \tag{19}$$

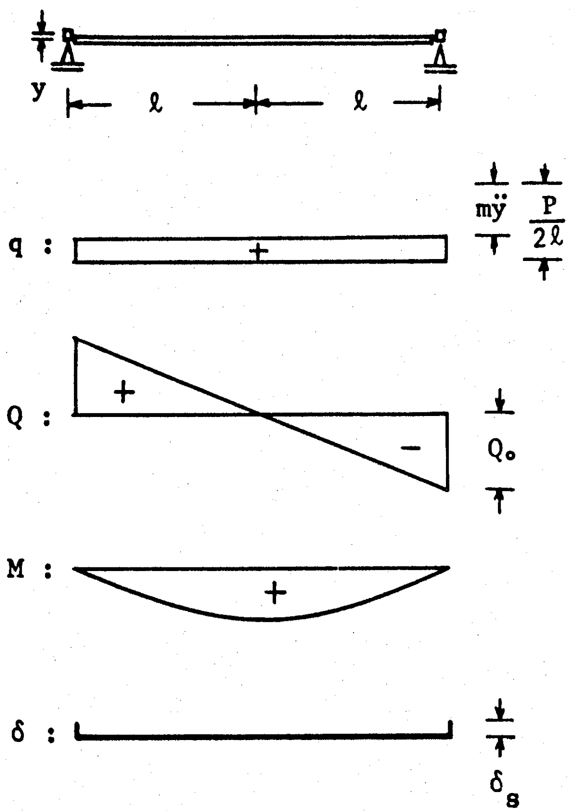

Fig. 7 Type C motion

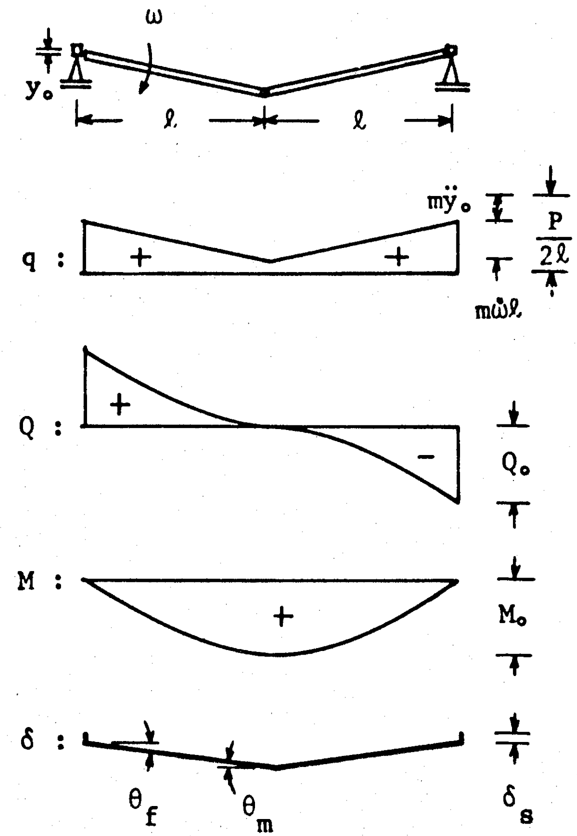

Fig. 8 Type D motion

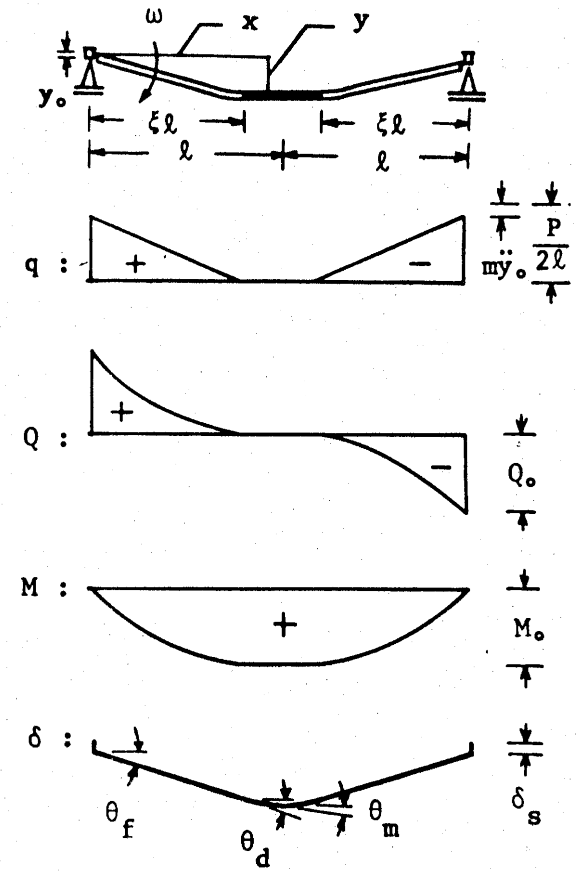

Fig. 9 Type E motion

The final deflection δ_s is produced uniformly over the beam length, and is given by*

$$\frac{ml^2}{M_0}\delta_s = 2\int_0^{t_s} I\,dt - \nu t_s^2. \tag{20}$$

It follows from our nomenclature that $t_f = t_s$, and $\delta_f = \delta_s$.

3.3 COMBINED SLIDING AND BENDING MOTION

If the maximum shear force reaches Q_o in Type A or B motion, or if the maximum bending moment reaches M_o in Type C motion, then a coupled motion of bending and sliding is supposed to occur. The beam becomes plastic in pure shear at the end and in pure bending at the middle portion. The state of stress of the beam is represented by such a curve as the one drawn by a thick-dashed line in Fig. 1. The maximum shear necessarily occurs only at the end which is supposed to engage in shear sliding, whereas the plasticized portion in bending possibly has a finite length. If we assume the latter to be a single yield hinge, the motion has a mechanism of two rigid segments connected with a hinge at the middle, having slides at both ends as shown in Fig. 8. Let this motion be referred to as Type D.

Principles of linear momentum and moment of momentum about the beam end are

$$(ml^2/M_0)\dot{y}_0 + (ml^3/2M_0)\omega = 2(I - \nu t), \tag{21}$$

$$(ml^2/2M_0)\dot{y}_0 + (ml^3/3M_0)\omega = I - t, \tag{22}$$

where y_o is the displacement of the end. Solving Eqs.(21) and (22) for

---

* The permanent shear deformation δ_s is assumed to be less than the beam depth, throughout the paper.

unknowns $\dot{y}_O$ and $\dot{\omega}$, we get

$$(ml^3/M_0)\,\omega = 12(\nu-1)t, \tag{23}$$

$$(ml^2/M_0)\,\dot{y}_0 = 2(I-4\nu t+3t). \tag{24}$$

These formulae show that the sliding first stops at time

$$t_s = I_s/(4\nu-3), \tag{25}$$

when the end displacement δ_s and end slope angle θ_s attain the values given by

$$(ml^2/M_0)\,\delta_s = 2\int_0^{t_s} I\,dt + (3-4\nu)t_s^2 \tag{26}$$

and

$$(ml^3/M_0)\,\theta_s = 6(\nu-1)t_s^2, \tag{27}$$

respectively. For t such that $t_s \leqq t \leqq t_f$, pure bending motion of Type A occurs so that Eq.(4) applies, which becomes, after integration from time t_s to t,

$$(ml^3/3M_0)(\omega-\omega_s) = (I-I_s)-(t-t_s), \tag{28}$$

where ω_s is the angular velocity at $t = t_s$, and is determined from Eq.(22) to satisfy

$$(ml^3/3M_0)\,\omega_s = I_s - t_s. \tag{29}$$

Adding Eq.(29) to Eq.(28), we obtain

$$(ml^3/M_0)\,\omega = 3(I-t). \tag{30}$$

Equation (30) could also have been derived either by integrating Eq.(4) from t = 0 to $t = t_s$ or by simply setting $\dot{y}_O = 0$ in Eq.(22). The reason for this is that the bending moment and shear force at the middle remain constant, regardless of the inequalities $t \lesseqgtr t_s$ and that the shear force at the end does not contribute to the angular momentum of the half beam with respect to the support. Motion stops at

$$t_f = I_f . \tag{31}$$

Final slope angle θ_f at the end is found from

$$\theta_f = \theta_s + \int_{t_s}^{t_f} \omega \, dt , \tag{32}$$

giving

$$\frac{ml^3}{M_0} \theta_f = \frac{ml^3}{M_0} \theta_m = 6(\nu - 1) t_s^2 + 3\int_{t_s}^{t_f} I \, dt - \frac{3}{2} (t_f^2 - t_s^2). \tag{33}$$

The final middle deflection $\delta_f = \delta_s + \theta_f l$ is obtained from

$$\frac{ml^2}{M_0} \delta_f = 2\int_0^{t_s} I \, dt + (2\nu - 3) t_s^2 + 3\int_{t_s}^{t_f} I \, dt - \frac{3}{2} (t_f^2 - t_s^2). \tag{34}$$

In order for the above to be valid, the maximum bending moment should not exceed M_0. It is seen from Fig. 8 that this condition is satisfied if at the middle $q \geqq 0$, i.e., if

$$P/(2l) - m\ddot{y}_0 - ml\dot{\omega} \geqq 0 . \tag{35}$$

which rejects the possibility that the plastic portion in bending has finite length. By means of Eqs.(23) and (24), Inequality (35) becomes

$$\nu \leqq 3/2. \tag{36}$$

Combining this with the counterparts of Inequalities (15) and (17a), we get the conditions for the motion to start with Type D as

$$1 \leqq \nu \leqq 3/2, \qquad \mu_0 \geqq 4\nu - 3. \tag{37a, b}$$

The remaining possibility is the simultaneous occurrence of shear sliding at the beam ends and finite plastic zone in bending at the middle portion of the beam. Two rigid segments of length ξl rotate about the ends and slide at the ends simultaneously as shown in Fig. 9. Let this motion be Type E. Assuming a priori $\dot{\xi} \geqq o$, we see that the plastic zone of length $2\,l\,(1-\xi)$ moves downward with velocity

$$\dot{y} = \int_0^t \frac{P}{2ml}\,dt \qquad \text{for} \qquad \xi l \leqq x \leqq l, \tag{38}$$

where the x-axis, indicating the position of an element, is taken along the beam from the left end. Against three unknowns ω, $\dot{y}_o$ and ξ, the principles of linear and angular momenta, and the continuity of velocity across the rigid-plastic interface provide

$$\int_0^t \frac{P}{2}\,dt - Q_0 t = m\xi l\,(\dot{y}_0 + \frac{1}{2}\,\omega\xi l) + (1-\xi l)\int_0^t \frac{P}{2l}\,dt, \tag{39}$$

$$\int_0^t \frac{Pl}{4}\,dt - M_0 t = \frac{1}{2}\,m(\xi l)^2\,\dot{y}_0 + \frac{1}{3}\,m(\xi l)^3\omega + \frac{1}{2}(l^2 - \xi^2 l^2)\int_0^t \frac{P}{2l}\,dt, \tag{40}$$

$$\dot{y}_0 + \xi l\omega = \int_0^t \frac{P}{2ml}\,dt, \tag{41}$$

reducing to

$$2I - (ml^2/M_0)\,\dot{y}_0 - (ml^3/2M_0)\,\omega\xi = 2\nu t/\xi, \tag{42}$$

$$I - (ml^2/2M_0)\,\dot{y}_0 - (ml^3/3M_0)\,\omega\xi = t/\xi^2, \tag{43}$$

$$2I - (ml^2/M_0)\,\dot{y}_0 - (ml^3/M_0)\,\omega\xi = 0. \tag{44}$$

It is of interest to compare Eq.(42) or

$$2I\xi - (ml^2/M_0)\,\dot{y}_0\xi - (ml^2/2M_0)\,\omega\xi^2 = 2\nu t \tag{42$'$}$$

with

$$\int_0^t 2\mu\xi\,dt - \int_0^t \frac{ml^2}{M_0}\,\ddot{y}_0\xi\,dt - \int_0^t \frac{ml^3}{2M_0}\,\dot{\omega}\xi^2\,dt = 2\nu t\,. \tag{42$''$}$$

The both equations are derived from the principle of linear momentum

$$\int_0^t\int_0^l m\ddot{y}\,dx\,dt = \int_0^t (\frac{P}{2} - Q_0)\,dt\,. \tag{42$'''$}$$

Equation (42)' is obtained by carrying out the integration, first with respect to t and then to x in the double integral of the left-hand side of Eq.(42)''' ; Eq. (42)" is obtained in the reversed order of integration.

Note that $\ddot{y}$ is at worst piecewise continuous along the x-axis with a jump discontinuity at $x = \xi l$. Equation (42)" reduces to Eq.(42)' after integration by parts only when $\dot{\xi} = 0$ or the velocity continuity Eq.(44) holds. A similar feature is seen for Eq.(43).

Combination of Eqs.(42) to (44) leads us to

$$(ml^3/M_0)\,\omega = (16\nu^3/9)\,t, \tag{45}$$

$$(ml^2/M_0)\,\dot{y}_0 = 2I - (8\nu^2/3)\,t, \tag{46}$$

$$\xi = 3/(2\nu). \tag{47}$$

Worth noting is that according to Eq.(47) the position of the rigid-plastic interface is independent of the load magnitude, depending only upon the beam dimensions, and it stays there, which confirms the a priori assumption $\dot{\xi} \geqq 0$, so long as this type of motion continues. Thus a discontinuity θ_d of the slope angle occurs at $x/l = 3/(2\nu)$ as well as a discotinuity θ_m at the middle caused by the subsequent motion. It follows from Eqs.(45) and (46) that the sliding first stops at time

$$t_s = [3/(2\nu)^2]\, I_s, \tag{48}$$

leaving

$$\frac{ml^2}{M_0}\,\delta_s = 2\int_0^{t_s} I\,dt - \frac{(2\nu)^2}{3}\,t_s^2, \tag{49}$$

$$(ml^3/M_0)\,\theta_s = (ml^3/M_0)\,\theta_d = [(2\nu)^3/9]\;t_s^2. \tag{50}$$

For t such that $t_s \leqq t \leqq t_h$ pure bending motion of Type B occurs, and similar considerations made in deriving Eq.(30) from Eq.(28) lead us to Eqs.(7) and (8). The rigid-plastic interface now moves inward,* starting

---

* It is, of course, possible that the interface remains at a position for some time interval for certain loads so that additional discontinuities in slope appear.

from $\xi_s = 3/(2\nu)$. Combination of Eqs.(7) and (48) checks this position as follows: $\xi_s^{\,2} = 3t_s/I_s = (3/2\nu)^2$. Angular velocity ω_s at this instant is also checked in a similar manner. The subsequent motion is analysed in the way discussed earlier. The plastic zone shrinks to a single hinge at $t = t_h$, and the single hinge motion of Type A follows, terminating at $t = t_f$. Permanent deformation parameters are determined from the addition of the deformation acquired during the motion of Type E, B and A, giving

$$\frac{ml^3}{M_0}\,\theta_f = \frac{8\nu^3}{9}\,t_s^2 + \int_{t_s}^{t_h}\sqrt{\frac{4I^3}{3t}}\,dt + 3\int_{t_h}^{t_f} I\,dt - \frac{3}{2}\,(t_f^2 - t_h^2), \tag{51}$$

$$\frac{ml^2}{M_0}\,\delta_f = 2\int_0^{t_h} I\,dt + 3\int_{t_h}^{t_f} I\,dt - \frac{3}{2}\,(t_f^2 - t_h^2), \tag{52}$$

$$\frac{ml^2}{M_0}\,\theta_m = 3\int_{t_h}^{t_f} I\,dt - \frac{3}{2}\,(t_f^2 - t_h^2), \tag{53}$$

where

$$t_h = I_h/3, \qquad t_f = I_f. \tag{54a,b}$$

Curvature is distributed from $x = \xi_s l$ to the middle by the amount given by Eq.(14) or (14)'.

To establish the validity of Type E, Inequality (36) gives the condition to its counterpart, viz., the spreading of plastic hinge. As mentioned earlier, the condition in shear is found from $\ddot{y}_o > 0$, to which Eq.(46) is substituted. We thus obtain the condition

$$\nu > 3/2, \qquad \mu_0 \geqq 4\nu^2/3 \tag{55a,b}$$

for the motion to start with Type E. Inequality (55b) rejects Type B motion which does not engage in shear sliding, and so giving the afore-introduced Inequality (16). Showing conditions for the occurrence of various types of motion, Fig. 3 also indicates the order of the transition of the types of motion. For a given beam the abscissa is fixed, and the type of the initial motion depends on the ordinate μ_o. The motion changes its pattern a later times to those corresponding to an ordinate as the ordinate decreases toward zero (The transition does not necessarily occur at the instant when μ attains the boundary value). For example, for $\nu = 2$, motion of Type E first develops if $\mu_o > 5.33$, being followed by Type B and then by Type A ; if $3 < \mu_o < 5.33$, starting with Type B, motion changes into Type A without sliding motion. This figure also shows the following interesing aspects:

For $\mu_o \to \infty$, as in the case of impulsive loading, sliding motion always occurs, the possibility of the types of motion C, D or E depending only on the beam dimensions, i.e., on ν. A beam with $\nu < 1$ never suffers bending deformation, and the plastic portion cannot have finite length in a beam with $\nu < 1.5$ however large the loading. The fact that the vertical line $\nu = 1.5$ separates two types of motion D and E implies the independence of the position of the rigid-plastic interface in the latter motion on μ value or on the magnitude of the load, because small deviation from $\nu = 1.5$ into $\nu > 1.5$ requires a small plastic zone however large μ_o.

It is seen from Eqs.(6), (13), (31) and (54b) that the motion stops after the same time duration in all types of motion, independent of the shear capacity, except for the case of pure sliding motion, in which the motion lasts longer, the duration depending on ν, as Eq.(19) indicates. This results from the fact that shear sliding always terminates first, and Type A motion comes last whenever bending deformation occurs and that governing equations are the same while the same types of motion hold *for the same time reference*, producting many similar terms in the deformation parameters. Comparison of Eqs.(10) and (52), for example, indicates that

δ_f has the same value in the deformations starting with Type E and Type B motion, i.e., regardless of the occurrence of sliding motion if a finite plastic zone has appeared. The same thing is true for θ_m.

The energy absorbed in plastic deformation may be of interest. The plastic work in shear deformation E_s equals $2Q_o\delta_s$. The plastic work in bending E_b is equal to $2M_o\theta_f$, whether or not the plastic portion in bending has a finite length; for instance, for the deformation starting with Type E motion, it is seen that

$$E_b = 2M_0(\theta_d + l\int_{\xi_s}^{1} \kappa\, d\xi + \theta_m) = 2M_0\theta_f \,. \tag{56}$$

The total energy absorbed is given by the sum $E_b + E_s$, which must be equal to the work done by the load or equal to the initial kinetic energy in the case of impulsive loading. Relative importance of the shear deformation to the bending may well be indicated by the ratio

$$E_s/E_b = (2\nu/l)(\delta_s/\theta_f). \tag{57}$$

4. EXAMPLES

Let us consider the cases of an impulsive, rectangular pulse and exponentially decreasing load as examples of blast-type loading.

4.1 IMPULSIVE LOADING

For impulsive loading with impulse $\hat{I}$

$$\mu = (\hat{I}\, l/4M_0)\,\delta(t), \quad I = (\hat{I}\, l/4M_0)\,H(t), \tag{58a, b}$$

where $\delta(t)$ is the Dirac delta function or unit impulse function and $H(t)$ is the Heavisides unit step function. Motion starts with Type C, D, or

E according to $\nu < 1$, $1 \leqq \nu \leqq 3/2$, or $3/2 < \nu$. Final deformation parameters are determined by substituting Eq.(58) into the results of the previous section.

When $\nu < 1$, it follows from Eqs.(19), (20) and (57) that

$$\frac{M_0}{\hat{I}l} t_s = \frac{1}{4\nu}, \quad \frac{mM_0}{\hat{I}^2}\delta_s = \frac{mM_0}{\hat{I}^2}\delta_f = \frac{1}{16\nu}, \quad \frac{E_s}{E_b} = \infty, \tag{59a, b, c}$$

respectively. When $1 \leqq \nu \leqq 3/2$, from Eqs. (25), (31), (26), (33), (34) and (57),

$$\frac{M_0}{\hat{I}l} t_s = \frac{1}{4(4\nu-3)}, \quad \frac{M_0}{\hat{I}l} t_f = \frac{1}{4}, \quad \frac{mM_0}{\hat{I}^2}\delta_s = \frac{1}{16(4\nu-3)}, \tag{60a, b, c}$$

$$\frac{mlM_0}{\hat{I}^2}\theta_f = \frac{mlM_0}{\hat{I}^2}\theta_m = \frac{3}{8}\,\frac{\nu-1}{4\nu-3}, \quad \frac{mM_0}{\hat{I}^2}\delta_f = \frac{6\nu-5}{16(4\nu-3)}, \quad \frac{E_s}{E_b} = \frac{\nu}{3(\nu-1)}. \tag{60d, e, f}$$

When $3/2 < \nu$, from Eqs. (48), (54), (49), (50), (51), (52), (53) and (57),

$$\frac{M_0}{\hat{I}l} t_s = \frac{3}{16\nu^2}, \quad \frac{M_0}{\hat{I}l} t_h = \frac{1}{12}, \quad \frac{M_0}{\hat{I}l} t_f = \frac{1}{4}, \tag{61a, b, c}$$

$$\frac{mM_0}{\hat{I}^2}\delta_s = \frac{3}{64\nu^2}, \quad \frac{mlM_0}{\hat{I}^2}\theta_d = \frac{1}{32\nu} \ \text{at} \ \frac{x}{l} = \frac{3}{2\nu}, \quad \frac{mlM_0}{\hat{I}^2}\theta_f = \frac{4\nu-3}{32\nu}, \tag{61d, e, f}$$

$$\frac{mM_0}{\hat{I}^2}\delta_f = \frac{1}{12}, \quad \frac{mlM_0}{\hat{I}^2}\theta_m = \frac{1}{24}, \quad \frac{E_s}{E_b} = \frac{3}{4\nu-3} \tag{61g, h, i}$$

Regardless of ν, the energy absorbed in the plastic deformation is

$$E_b + E_s = \hat{I}^2/(4ml). \tag{62}$$

Equations (23) and (45) show zero angular velocity at $t = 0$, which indicates that the initial velocity is distributed uniformly along the beam even if the rotational motion follows; Eqs. (18), (24) and (46) give the initial velocity $v_o = \hat{I}/(2m\,l)$ as it should be. Thus the initial kinetic energy $mlv_o^2 = \hat{I}^2/(4ml)$ confirms the energy balance with reference to Eq.(62). It is worthy of note that the energy is independent of ν, since the shear forces of finite magnitude do no work upon impulsive loading.

In order to obtain the permanent deformation for a beam with $\nu > 3/2$, Eq.(14) gives the curvature distribution by noting that $\mu = 0$ while the rigid-plastic interface traverses a position of interest, as

$$(ml^2M_0/\hat{I}^2)\kappa = 1/12 \qquad \text{for} \qquad 3/(2\nu) < x/l < 1 \tag{63}$$

The slope angle θ is obtained from

$$\theta = \begin{cases} \theta_f & \text{for} \quad 0 < \dfrac{x}{l} < \dfrac{3}{2\nu} \\ \theta_f - \theta_d - \int_{3l/(2\nu)}^{x} \kappa \, dx & \text{for} \quad \dfrac{3}{2\nu} < \dfrac{x}{l} < 1 \end{cases} \tag{64}$$

There is a discontinuity θ_d at $x/l = 3/(2\nu)$. The integration being carried out, Eq.(64) gives, in particular, θ at $x = l-0$, which is confirmed to coincide with θ_m of Eq.(61h). The final deflection is determined by integrating θ with respect to x, and provides δ_f with the substitution of $x/l = 1$, which again confirms Eq.(61g). The shape of the permanent deformation thus obtained is illustrated in Fig. 10 for $\nu = 1.5$ and 5.

In Figs. 11 and 12 dimensionless parameters are plotted as functions of ν. Small circles indicate the transition of deformation patterns. Clearly the limit $\nu \to \infty$ gives the pure bending deformation. From these figures we observe the following aspects:

The energy ratio E_s/E_b is a monotonously decreasing function of ν, with particular values 1 for $\nu = 1.5$ and 0.0811 for $\nu = 10$. It follows from this and the constancy of the total energy that the more bending deformation is diminished by the shear, the less ν is. This feature also appears in the fact that θ_f and the almost equivalent quantity $(\delta_f - \delta_s)/l$ increase with ν. At $\nu = 1.5$, θ_f takes just one-half of the value which is obtained by ignoring shear deformation; no bending deformation takes place for $\nu < 1$. The shear displacement δ_s as well as t_s monotonously decrease with ν, as would

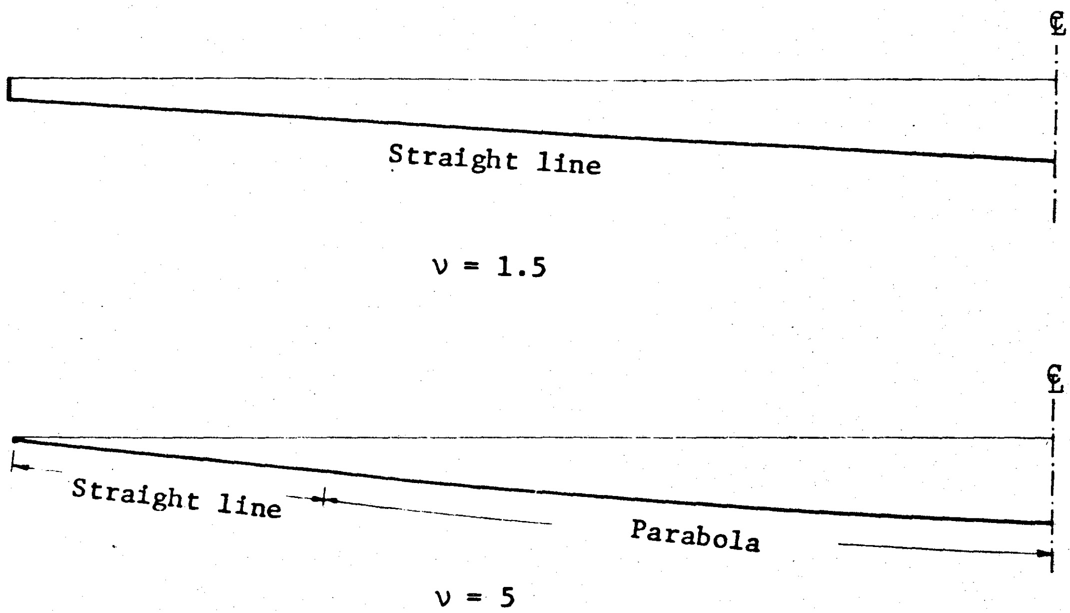

Fig. 10 Final shapes of beams with ν = 1.5 and ν = 5 for impulsive load

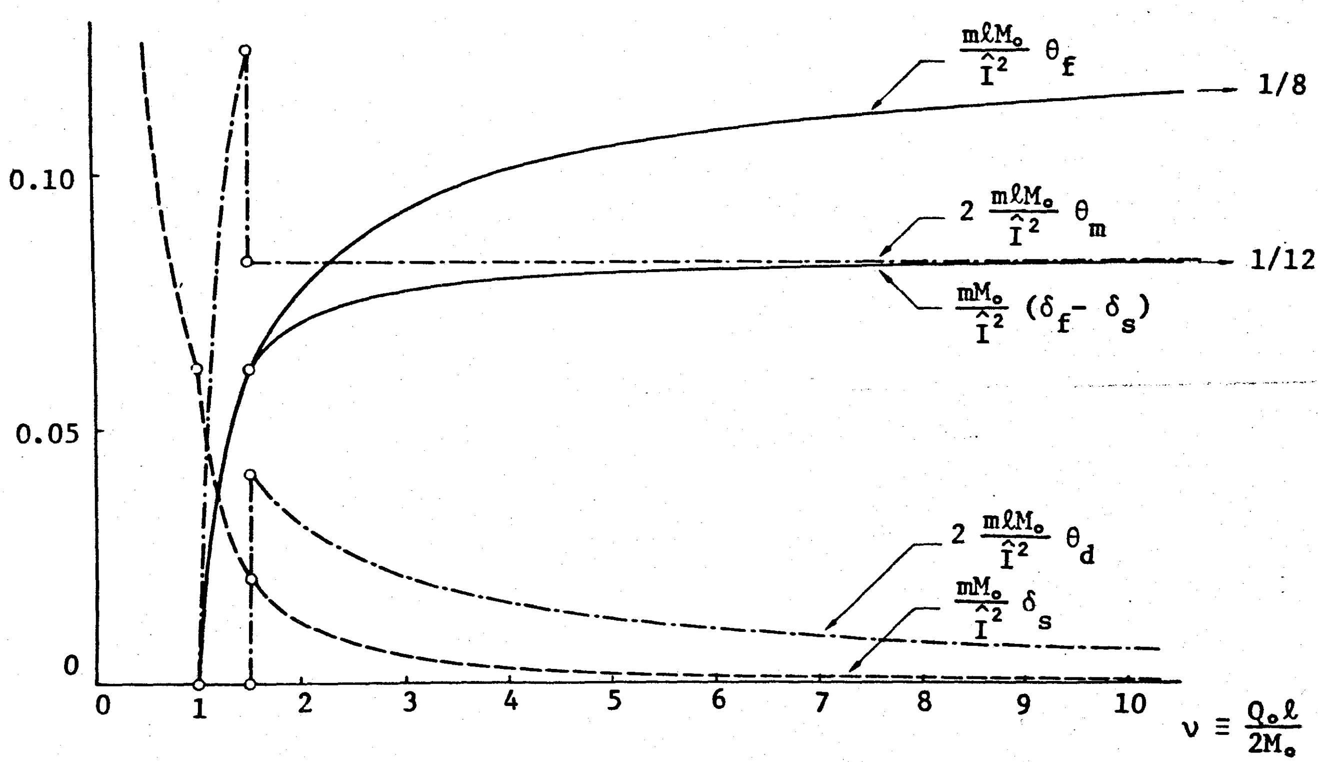

Fig. 11 Deformation parameters for impulsive load

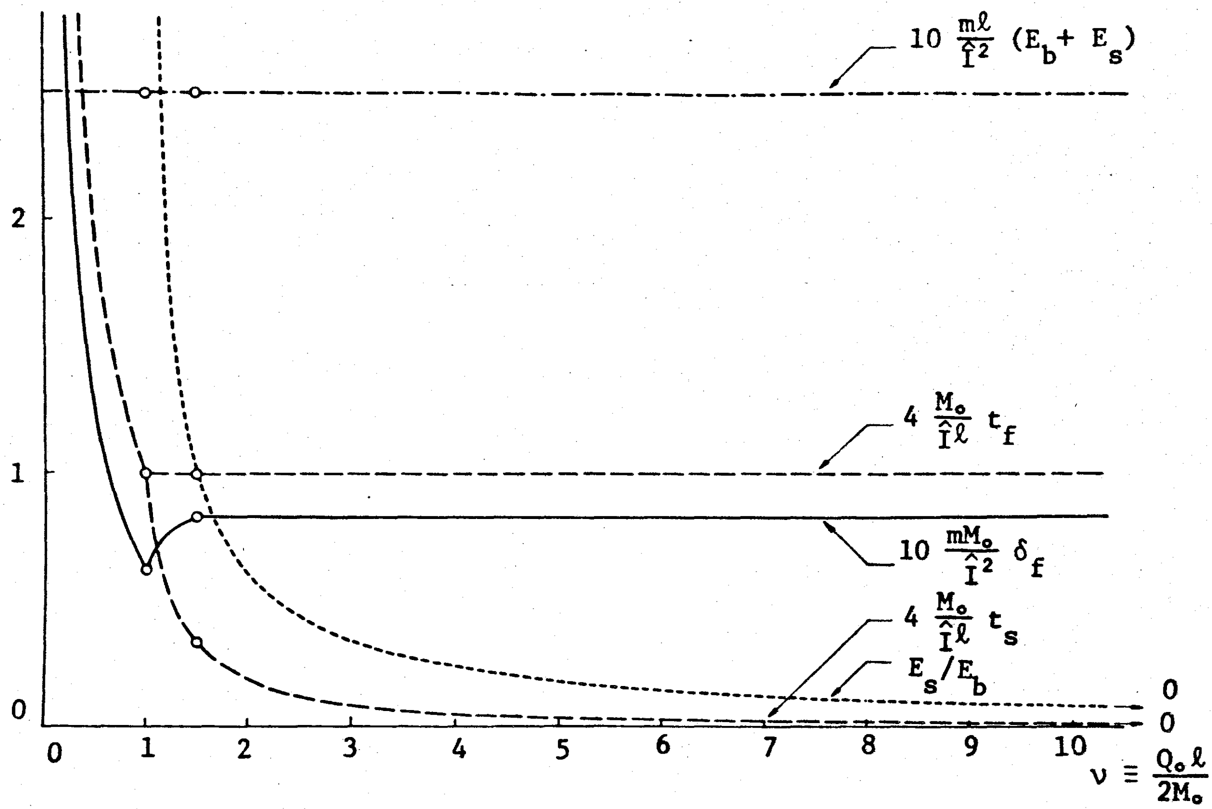

Fig. 12 Deformation parameters for impulsive load

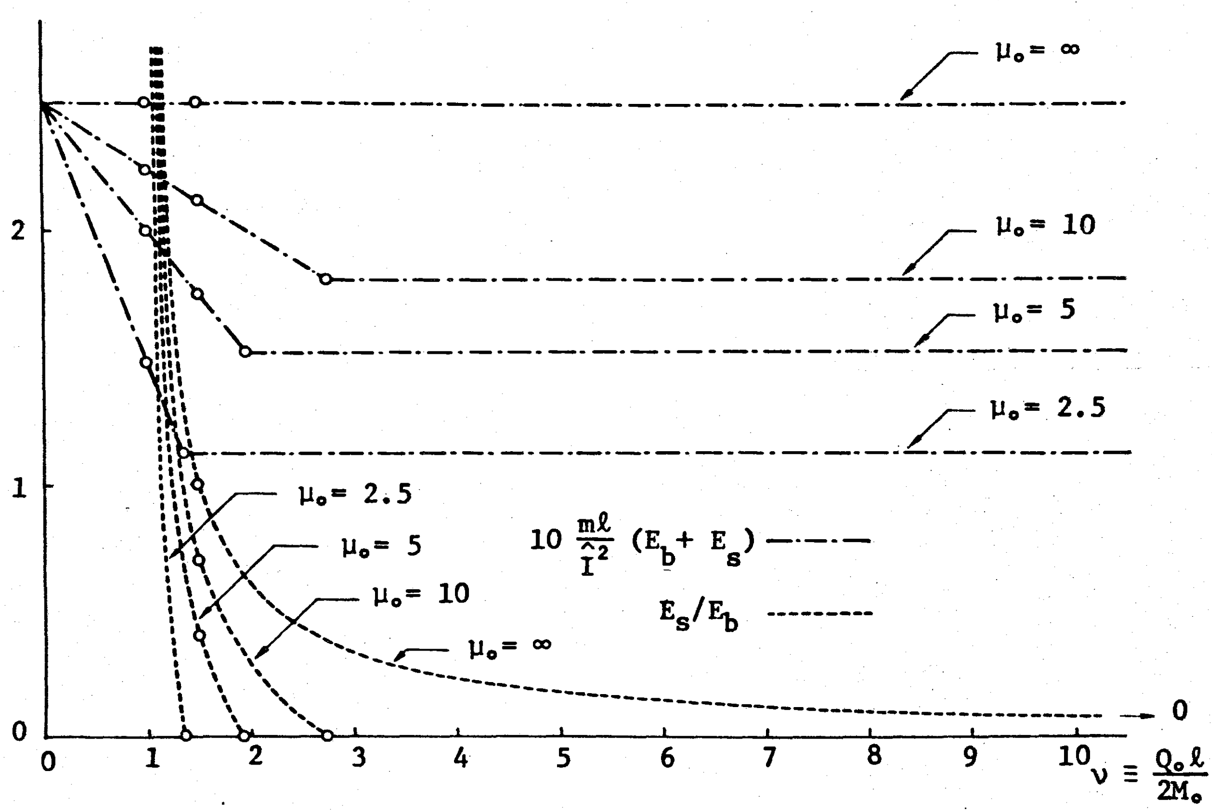

Fig. 13 Absorbed energy and energy ratio for rectangular pulse load

be expected. The middle deflection δ_f is relatively small near $\nu = 1$, and is not affected by the shear deformation when $\nu \geqq 1.5$. The finish time t_f is a monotonously decreasing function of ν, the duration of motion being independent of ν for $\nu \geqq 1.0$. The middle slope angle θ_m as well as θ_d are not continuous functions of ν. Their discontinuity at $\nu = 1.5$ results from the fact that a beam with $\nu > 1.5$ undergoes a discontinuity θ_d in slope angle at $x/l = 3/(2\nu)$ during Type E motion together with θ_m during the subsequent motion; whereas in a beam with $1 \leqq \nu \leqq 1.5$, θ_m is produced at the middle from $t = 0$ in the motion of Type D. Note that when $\nu = 1.5 + 0$, θ_d is located at $x/l = 1-0$. Thus the sum $\theta_m + \theta_d$ is continuous across $\nu = 1.5$. It is concluded for the impulsive loading that the deformation greatly depends on ν when ν is of the order of unity, but that the dependecne is not significant when ν is of the order of ten or greater.

4.2 RECTANGURAR PULSE LOADING

For a rectangular load pulse with amplitude P_o and duration τ,

$$\mu = (P_0 l/4M_0)[H(t) - H(t-\tau)], \qquad I = (P_0 l/4M_0)[t - (t-\tau)H(t-\tau)]. \qquad (65a, b)$$

Deformation is determined simply by substituting Eq.(65) into the formulae of the preceding section in the same way as for the impulsive loading. In order to examine the effect of the shape of the load pulse we express the results in terms of $\mu_o = (P_o l/4M_o)$ and $\hat{I} = P_o\tau$. The limit $\mu_o \to \infty$ corresponds to the impulsive loading. All types of motion can take place depending on μ_o as well as ν.

When $1 \leqq \mu_o \leqq 3$ and $\mu_o < 4\nu-3$, Type A motion occurs and

$$\frac{M_0}{\hat{I} l} t_f = \frac{1}{4}, \qquad \frac{mlM_0}{\hat{I}^2}\theta_f = \frac{mM_0}{\hat{I}^2}\delta_f = \frac{mlM_0}{\hat{I}^2}\theta_m = \frac{3}{32}\left(1 - \frac{1}{\mu_0}\right), \qquad (66a, b)$$

$$\frac{ml}{\hat{I}^2}(E_b+E_s)=\frac{3}{16}\left(1-\frac{1}{\mu_0}\right), \quad \frac{E_s}{E_b}=0. \tag{66c, d}$$

When $3 < \mu_0 < \frac{4}{3}\nu^2$, Type B motion first occurs, being followed by Type A motion. In this case,

$$\frac{M_0}{\hat{I}l}t_h=\frac{1}{12}, \quad \frac{M_0}{\hat{I}l}t_f=\frac{1}{4} \tag{67a, b}$$

$$\frac{mlM_0}{\hat{I}^2}\theta_d=\frac{mlM_0}{\hat{I}^2}\int_0^\tau \omega\,dt=\frac{1}{24}\sqrt{\frac{3}{4\mu_0}} \quad \text{at} \quad \frac{x}{l}=\sqrt{\frac{3}{\mu_0}}, \tag{67c}$$

$$\frac{mlM_0}{\hat{I}^2}\theta_f=\frac{1}{8}\left(1-\sqrt{\frac{3}{4\mu_0}}\right), \quad \frac{mM_0}{\hat{I}^2}\delta_f=\frac{1}{12}\left(1-\frac{3}{4\mu_0}\right), \quad \frac{mlM_0}{\hat{I}^2}\theta_m=\frac{1}{24}, \tag{67d, e, f}$$

$$\frac{ml}{\hat{I}^2}(E_b+E_s)=\frac{1}{4}\left(1-\sqrt{\frac{3}{4\mu_0}}\right), \quad \frac{E_s}{E_b}=0. \tag{67g, h}$$

When $\nu < 1$ and $\mu_0 \geqq \nu$, Type C motion occurs, and

$$\frac{M_0}{\hat{I}l}t_s=\frac{1}{4\nu}, \quad \frac{mM_0}{\hat{I}^2}\delta_s=\frac{mM_0}{\hat{I}^2}\delta_f=\frac{1}{16}\left(\frac{1}{\nu}-\frac{1}{\mu_0}\right), \tag{68a, b}$$

$$\frac{ml}{\hat{I}^2}(E_b+E_s)=\frac{1}{4}\left(1-\frac{\nu}{\mu_0}\right), \quad \frac{E_s}{E_b}=\infty. \tag{68c, d}$$

When $1 \leqq \nu \leqq 1.5$, $\mu_0 \geqq 4\nu-3$, Type D motion first occurs, being followed by Type A motion, and

$$\frac{M_0}{\hat{I}l}t_s=\frac{1}{4(4\nu-3)}, \qquad \frac{M_0}{\hat{I}l}t_f=\frac{1}{4}, \tag{69a, b}$$

$$\frac{mM_0}{\hat{I}^2}\delta_s=\frac{1}{16}\left\{\frac{1}{4\nu-3}-\frac{1}{\mu_0}\right\}, \qquad \frac{mlM_0}{\hat{I}^2}\theta_f=\frac{mlM_0}{\hat{I}^2}\theta_m=\frac{3}{8}\,\frac{\nu-1}{4\nu-3}, \tag{69c, d}$$

$$\frac{mM_0}{\hat{I}^2}\delta_f=\frac{1}{16}\left\{\frac{6\nu-5}{4\nu-3}-\frac{1}{\mu_0}\right\}, \tag{69e}$$

$$\frac{ml}{\hat{I}^2}(E_b+E_s)=\frac{1}{4}\left(1-\frac{\nu}{\mu_0}\right), \qquad \frac{E_s}{E_b}=\frac{\nu}{3(\nu-1)}\left(1-\frac{4\nu-3}{\mu_0}\right). \tag{69f, g}$$

When $\nu > 1.5$ and $\mu_0 \geqq \frac{4}{3}\nu^2$, Type E motion first occurs, being followed by Type B and then by Type A. In this case,

$$\frac{M_0}{\hat{I}l}t_s=\frac{3}{16\nu^2}, \qquad \frac{M_0}{\hat{I}l}t_h=\frac{1}{12}, \qquad \frac{M_0}{\hat{I}l}t_f=\frac{1}{4}, \tag{70a, b, c}$$

$$\frac{mM_0}{\hat{I}^2}\delta_s = \frac{1}{16}\left(\frac{3}{4\nu^2} - \frac{1}{\mu_0}\right), \qquad \frac{mlM_0}{\hat{I}^2}\theta_d = \frac{1}{32\nu} \quad \text{at} \quad \frac{x}{l} = \frac{3}{2\nu}, \tag{70d, e}$$

$$\frac{mlM_0}{\hat{I}^2}\theta_f = \frac{1}{8}\left(1 - \frac{3}{4\nu}\right), \quad \frac{mM_0}{\hat{I}^2}\delta_f = \frac{1}{12}\left(1 - \frac{3}{4\mu_0}\right), \quad \frac{mlM_0}{\hat{I}^2}\theta_m = \frac{1}{24}, \tag{70f, g, h}$$

$$\frac{ml}{\hat{I}^2}(E_b + E_s) = \frac{1}{4}\left(1 - \frac{\nu}{\mu_0}\right), \qquad \frac{E_s}{E_b} = \frac{3}{4\nu - 3}\left(1 - \frac{4\nu^2}{3\mu_0}\right). \tag{70i, j}$$

It is seen that the type of motion does not change during the load application, i.e., in any case t_s, t_h, $t_f \geq \tau$ and that these times are exactly the same as in the case of impulsive loading with the same impulse $\hat{I}$; thus motion stops after the same time duration as in impulsive loading. In the case of the rectangular pulse loading the work done by the applied load is given by the product of P_o and the displacement at $t = \tau$. The unchangeability of the motion type during the load application simplifies the time integration of velocity to give this displacement. The work thus determined is confirmed to be identical with the sum $E_b + E_s$ obtained above. Comparison of Eqs.(68c), (69f) and (70i) indicates the same work expression for the last three cases with the shear deformation accompanied. For these cases bending paramaters θ_f, θ_m and $\delta_f - \delta_s$ are independent of μ_o, and accordingly take the same values as for impulsive leading. When the motion starts with Type B, a discontinuity in slope angle occurs in addition to θ_m, since the rigid-plastic interface stands still during the load application due to the constancy of the load magnitude. In contrast to this discontinuity the discontinuity in Type E motion is produced during the interval $t = 0$ to t_s. The position and amount of the former depend on the load amplitude but not of the latter as seen in Eqs.(67c) and (70e). The curvature is again given by Eq.(63), and the permanent deflection can be determined with ease in the same way as for the impulsive loading.

Dimensionless parameters characteristic of the plastic deformation are plotted for a rectangular load pulse in Figs. 13 to 16. It should be emphasized that all comparisons are made for the same total impulse. While decreasing with increasing ν, the effect of shear keeps increasing with increasing μ_o and becomes maximum for impulsive loading, as seen, for example, from E_s/E_b in Fig. 13. The total energy $E_b + E_s$ grows with μ_o and diminishes or remains constant with ν, the dependence on ν getting less as μ_o gets greater. The case $\nu = 0$ gives the same amount of the total energy as in the impulsive loading. Figure 14 shows the dependence of δ_f on ν and μ_o. The dashed lines separate the different patterns of deformation, and the alphabetical letters enclosed by circles refer to the types of initial motion. The middle deflection increases with μ_o. It is not a monotonous function of ν but has a minimum at $\nu = 1$. It is seen from Figs. 13 and 14 that the plastic deformation depends considerably on the values of ν and μ_o when ν and/or μ_o is of the order of unity. Curves are drawn in Fig. 15 for the deformation paramaters of a particular beam with $\nu = 10$. For this beam the motion starts with Type A, B or E, according to $1 \leqq \mu_o \leqq 3$, $3 < \mu_o < 400/3$ or $\mu_o \geqq 400/3$, respectively. We see that for μ_o of the order of ten or greater, the deformation parameters do not depend much on μ_o, except for $E_b + E_s$ and θ_f. At $\mu_o = 10$, these two parameters take 72.6% of their limiting values of impulsive loading, but δ_f, for instance, takes 92.5% of its limiting value. Figure 16 shows for a beam with $\nu = 1.5$, for which if $1 \leqq \mu_o < 3$, the pure bending motion of Type A occurs, and if $\mu_o \geqq 3$, Type D motion first occurs, being followed by Type A. The deformation parameters E_s/E_b and δ_s concerning shear deformation depend significantly on μ_o. If $\mu_o = 10$ these parameters take 70% of their limiting values; the bending deformation approaches faster than shear to the limiting case of the impulsive loading,

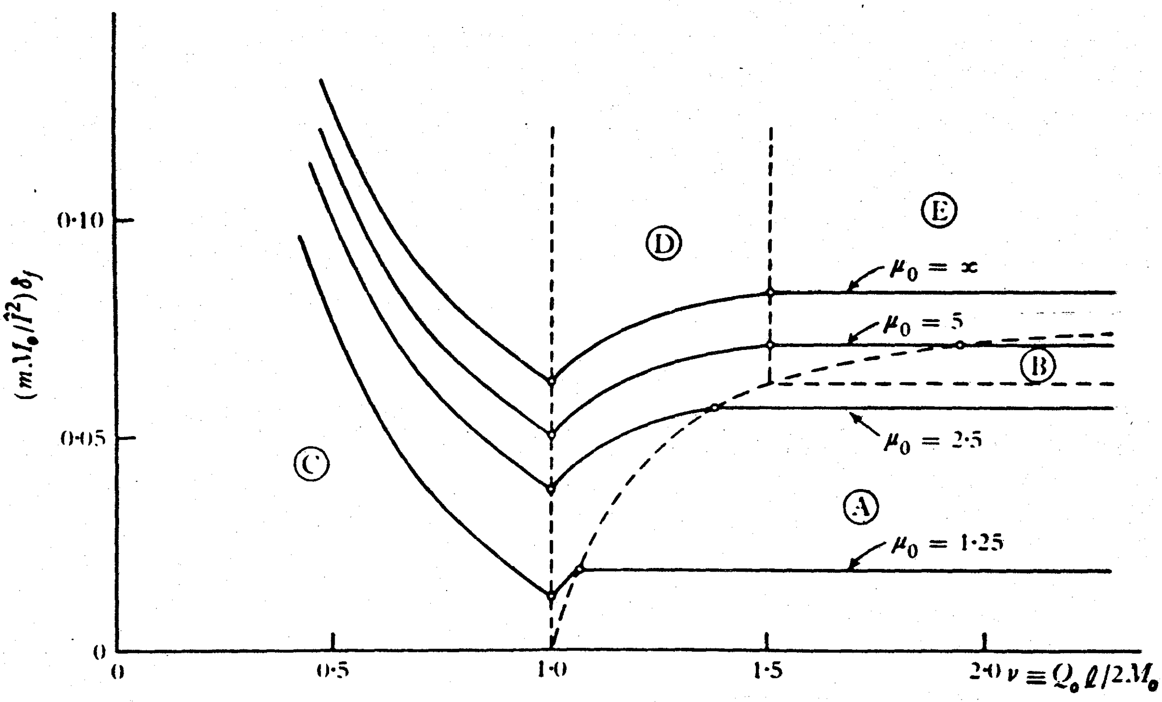

Fig. 14 $\frac{mM_o}{\hat{I}^2}\delta_f$ for rectangular pulse load

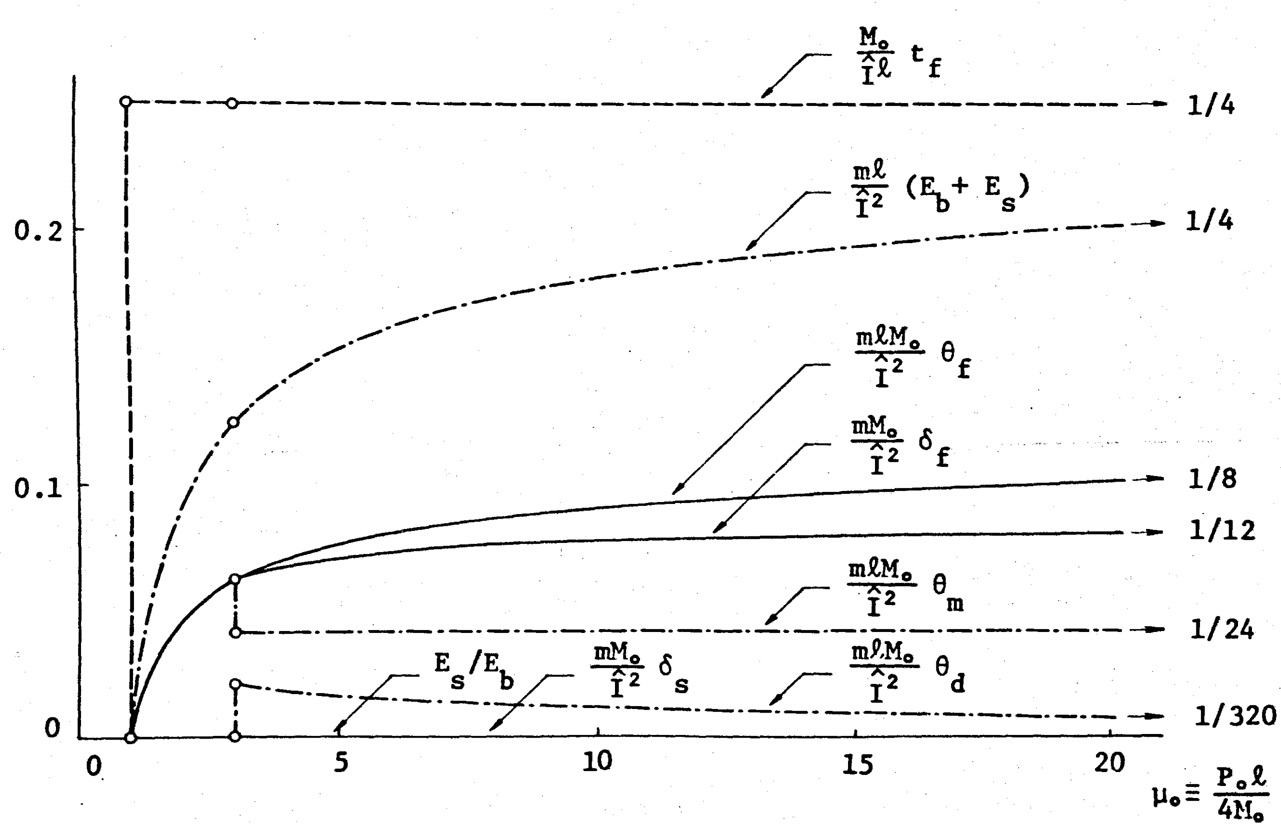

Fig. 15 Deformation parameters of a beam with $\nu = 10$ for rectangular pulse load

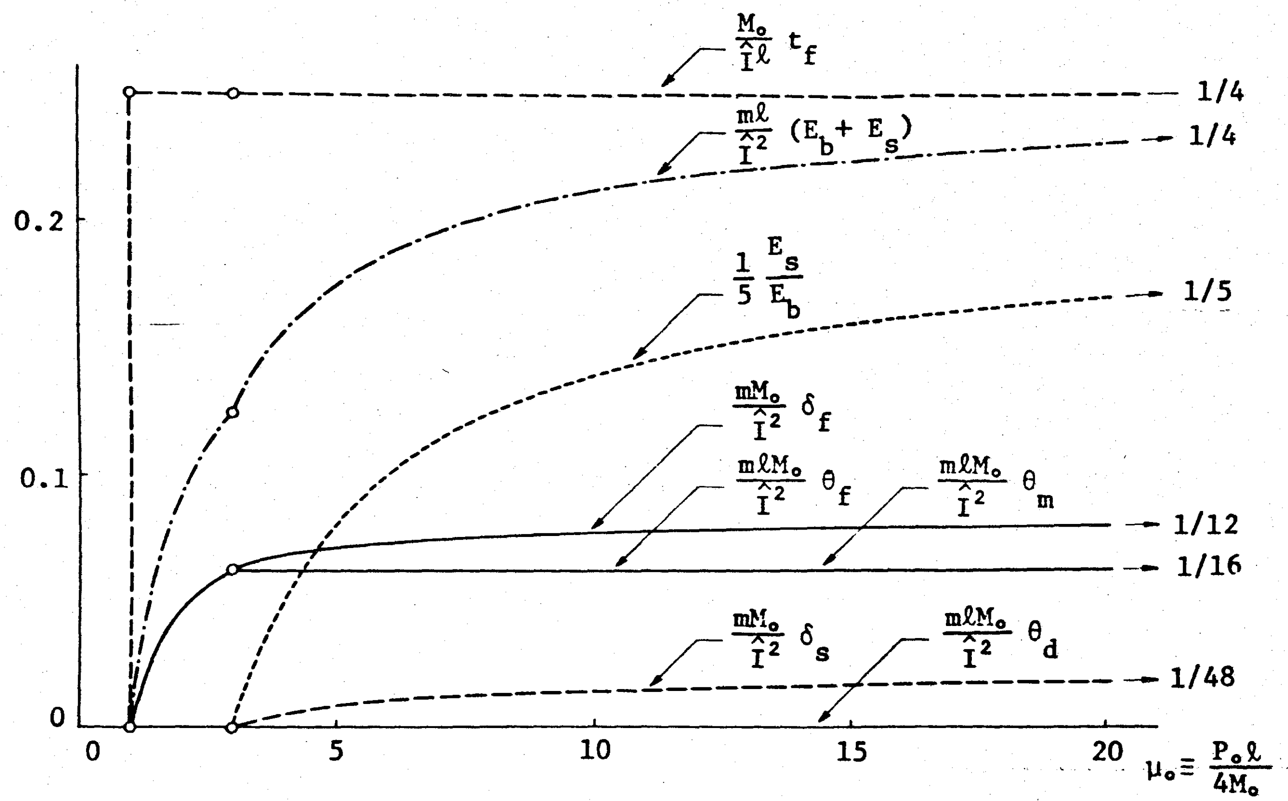

Fig. 16 Deformation parameters of a beam with $\nu = 1.5$ for rectangular pulse load

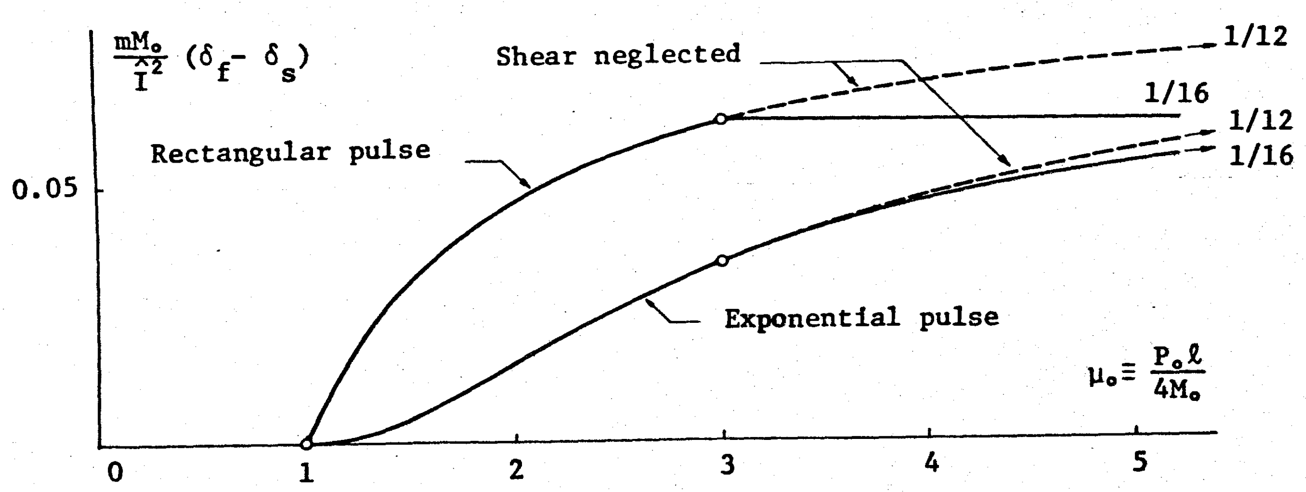

Fig. 17 $\frac{mM_o}{\hat{I}^2} (\delta_f - \delta_s)$ of a beam with $\nu = 1.5$ for rectangular and exponential pulse loads and that faster than for the case of $\nu = 10$. It is thus observed that the bending deformation is well approximated by impulsive loading when μ_0 is of the order of ten or greater, but the shear deformation cannot be determined without taking account of the load magnitude. It is concluded that the plastic deformation increases with μ_0 for the same total impulse, that when ν is of the order of unity, the plastic deformation greatly depends on the values of ν and μ_0, so that the shear deformation should be taken into account and to regard the load as impulsive is not appropriate unless μ_0 is of the order greater than ten. When ν is of the order greater than unity, the effect of shear may be neglected; when μ_0 is of the order less than ten, the load magnitude as well as the total impulse has to be taken into consideration. If ν and μ_0 are of the order greater than unity and ten, respectively, then the plastic deformation is well approximated by neglecting the shear effect and by the idealization of impulsive loading.

4.3 EXPONENTIALLY DECREASING LOADING

If the load decreases exponentially with time as in $P = P_o e^{-t/\tau}$ with the total impulse $\hat{I} = P_o \tau$, then the use of

$$\mu = \mu_0 e^{-t/\tau}, \qquad I = (\hat{I}\, l/4M_0)(1 - e^{-t/\tau}) \tag{71a, b}$$

in the afore-derived formulae determines the dynamic plastic behavior. In Fig. 17 are shown the results for a beam with $\nu = 1.5$, for which $\delta_f - \delta_s = \theta_f l$ is plotted as a function of μ_0 in such a dimensionless form that the ordinate is independent of the total impulse. The afore-introduced curve of rectangular pulse loading is also included for comparison. It is seen that the exponentially decreasing load produces smaller deformation of bending than the rectangular pulse load for the same impulse and peak magnitude. This is because in the former the load in $t \geqq t_f$ does not contribute to deformation whilst in the latter the whole impulse affects deformation for any μ_o not smaller than unity. The difference is significant for small values of μ_o,, since t_f is small for small μ_o, causing a slow rise of the former curve. At $\mu_o = 5$ the deformation caused by the former is 13.6% less than the latter. The difference clearly decreases with μ_o, and tends to vanish as $\mu_o \to \infty$. It is also observed that the effect of shear is smaller for the former than the latter.

5. FURTHER REMARKS

Let us reconsider the validity of the assumed yield condition of Eq. (1). As was observed in the general analysis or in Figs. 5 to 9, the maximum shear magnitude is always attained at the beam ends where the bending moment is zero, while the bending moment is maximum at the middle portion of the beam where the shear force is zero. The compatibility consideration indicates a continuous distribution of the bending moment and shear along the beam length. Hence, the limit moment in pure bending M_o can be attained only at the middle portion, and the limit shear in pure shear Q_o only at the beam ends, when the simply-supported beam is subjected to uniformly distributed load. Between these portions there are both non-zero M and Q, less in magnitude than M_o and Q_o, respectively. For a yield curve smaller than the assumed polygon, there may be a possibility of reaching the yield limit under the M-N interaction. In the first quadrant of Fig. 1 an exact yield curve, if it existed at all, would have had to pass the points B and S of the liming states, and suppose it be the arc BDS, for instance. If the arc BIS, which represents the state of stress of the half beam in Type D or E motion, touches the yield curve BDS somewhere between B and S, then an additional plastic deformation can take place both in shear and bending at the corresponding beam element. The analysis presented in this paper is seen to be valid for any yield curves which between B and S lie outside of the stress curve BIS.

We have found that the importance of the shear effect hinges on the values of the parameter $\nu = Q_o l/(2M_o)$ as well as μ. With d denoting the beam depth, ν is proportional to the quotient l/d. The proportional factor $Q_o d/(2M_o)$ depends only on the shape of the cross section, and takes quite distinct values for a compact cross section such as a rectangular or circular cross section and a non-compact cross section such as an I-, wide flange or box-cross section. With recourse to the yield criterion of maximum shear stress, $Q_o d/(2M_o) = 1$ for a rectangular cross section; by taking the full web for the effective shear area, a rough estimate for a representative wide flange section gives $Q_o d/(2M_o) = 1/7$ [7]. If, for example, the span-depth ratio $2\,l/d = 20$, then $\nu = 10$ for the former and $\nu = 10/7$ for the latter. Thus ν may normally be of the order of ten for a compact cross section, and is of the order of unity for a wide flange or I-section, so that Fig. 15 can be regarded as representing the former and Fig. 16 the latter.

Although the analysis presented herein has dealt with a particular problem, the results obtained are expected to apply, at least qualitatively, for general cases of rigid-plastic beams under impact loading, provided μ and ν are evaluated from proper values of P_b and P_s determined in each case.

6. CONCLUSIONS

Among significant results obtained by analysing a rigid-perfectly plastic simply-supported beam under uniformly distributed blast-type loading in the light of shear-bending interaction, the following seems to be characteristic of general application.

A rigid-plastic beam deforms with various patterns of motion combined by plastic bending and shear sliding for a load of magnitude P_o not smaller than the strength in bending P_b and/or the strength in shear P_s. The shear deformation reduces the bending, part of the kinetic energy being absorbed in shear sliding. The importance of the shear deformation relative to the bending depends on the value of P_s relative to P_b as well as on the value of P_o relative to the beam strength. In terms of the parameters $\nu \equiv P_s/P_b$ and $\mu_o \equiv P_o/P_b$, the shear effect gets larger as ν gets smaller and as μ_o gets larger. For impulsive loading with μ_o tending to infinity, shear slides always take place and this effect becomes maximum among blast-type loads with the same total impulse. For a beam with a non-compact cross section such as an I-section, ν takes a magnitude of the order less than that for a compact cross section. Under normal conditions the shear effect is small for a compact cross section unless the span-depth ratio is small and μ_o is very large, whereas this effect is not negligible for a non-compact cross section when μ_o is of the order greater than unity. In the case of an ordinary load pulse with μ_o of the order greater than ten, the permanent deformation is well approximated by treating the loading as impulsive, which gives the largest plastic deformation for the same total impulse. When μ_o is of the order of ten or less, the finiteness of the load magnitude should be taken into account, and if μ_o is not much larger than unity, the exact load-time relation has to be considered. It is reminded in this connection, that the asymptotic approach to the impulsive loading is accelerated by the inclusion of elasticity effect [10].

ACKNOWLEDGEMENT

The essential part of the material presented in Chapter 7 was prepared while the author was engaged in graduate study at Brown University, under the general guidance of Prof. P.S. Symonds, to whom the author wishes to express his gratitude.

REFERENCES

[1] N. Jones, "A Literature Review of the Dynamic Plastic Response of Structures", The Shock and Vibration Digest, Vol. 7, No. 8, August, 1975, pp. 89-105.

[2] D.G. Eyre, "Inelastic Shear Deflection of Steel Beams", Journal of the Structural Division, Proceedings of American Society of Civil Engineers, Vol. 99, No. ST 10, October, 1973, pp. 1985-1997.

[3] A. Pisanty and Y. Tene, "Analysis of Geometrically Nonlinear Plane Frames Incorporating Shear Deformations", International Journal of Solids and Structures, Vol. 11, 1975, pp. 643-645.

[4] H.H. Bleich and R. Shaw, "Dominance of Shear Stresses in Early Stages of Impulsive Motion of Beams", Journal of Applied Mechanics, Vol. 27, 1960, pp. 132-138.

[5] M.G. Salvadori and P. Weidlinger, "On the Dynamic Strength of Rigid-Plastic Beams under Blast Loads", Journal of the Engineering Mechanics Division, Proceedings of the American Society of Civil Engineers, Vol. 83, No. EM4, October, 1957, pp. 1389-1-1389-34.

[6] B. Karunes and E.T. Onat, "On the Effect of Shear on Plastic Deformation of Beams under Transverse Impact Loading", Journal of Applied Mechanics, Vol. 27, 1960, pp. 107-110.

[7] T. Nonaka, "Some Interaction Effects in a Problem of Plastic Beam Dynamics Part 1: Interaction Analysis of a Rigid, Perfectly Plastic Beam", Journal of Applied Mechanics, Vol. 34, 1967, pp. 623-630; Chapter 8, I of this treatise.

[8] M. Wakabayashi, T. Nonaka and M. Shibata, "Large Plastic Deformation of Structures due to Impact - On the Bending and Shearing Deformation of a Rigid-Plastic Simply Supported Beam -", Disaster Prevention Research Institute Annuals, Kyoto University, Vol. 11A, March, 1973, pp. 587-605 (in Japanese).

[9] P.S. Symonds, "Plastic Shear Deformations in Dynamic Load Problems", Engineering Plasticity edited by J. Heyman and F.A. Leckie, 1968, pp. 647-664.

[10] T. Nonaka,"Some Interaction Effects in a Problem of Plastic Beam Dynamics Part 2: Analysis of a Structure as a System of One Degree of Freedom", Journal of Applied Mechanics, Vol. 34, 1967, pp. 631-637; Chapter 8, II of this treas Chapter 8, II of this treatise.

[11] E.H. Lee and P.S. Symonds, "Large Plastic Deformations of Beams under Transverse Impact", Journal of Applied Mechanics, Vol. 19, 1952, pp. 308-314.

[12] J.A. Seiler, B.A. Cotter and P.S. Symonds, "Impulsive Loading of Elastic-Plastic Beams", Journal of Applied Mechanics, Vol. 23, 1956, pp. 515-521.

[13] N. Perrone, "On a Simplified Method for Solving Impulsively Loaded Structures of Rate-Sensitive Materials", Journal of Applied Mechanics, Vol. 32, 1965, pp. 489-492.

[14] D.C. Drucker, "The Effect of Shear on the Plastic Bending of Beams", Journal of Applied Mechanics, Vol. 23, 1956, pp. 509-514.

[15] B.G. Neal, "The Effect of Shear Forces on the Fully Plastic Moment of an I-Beam", Journal of Mechanical Engineering Science, Vol. 3, 1961, pp. 258-266.

[16] J. Heyman, "The Full Plastic Moment of an I-Beam in the Response of Shear Force", Journal of Mechanics and Physics of Solids, Vol. 18, 1970, pp. 359-365.

[17] P.S. Symonds, "Large Plastic Deformations of Beams under Blast Type Loading", Proceedings of the Second U.S. National Congress of Applied Mechanics, 1954, pp. 505-515.

CHAPTER 8

DYNAMIC PLASTIC BEHAVIOR OF A BEAM WITH SHEAR, BENDING AND AXIAL DEFORMATION

ABSTRACT Theoretical and experimental studies are made for the permanent deformation of clamped beams with constraints against axial displacements at the ends with a boss (attached mass) at the center subjected to large transverse dynamic loading. We take account of the combined action of bending moments, axial forces and shearing forces in the plastic range.

In the first part, the interaction problem is considered for a perfectly plastic material. An analysis is presented to determine the permanent deformation of a rigid-perfectly plastic beam due to impulsive loading applied to the central mass, based on a fixed yield surface or interaction relation. An approximate interaction diagram is adopted. Various patterns of the deformation are found to occur, according to the beam dimensions. Ordinarily shearing deformation predominates at early stages of deformation. When constraints against axial motion are present, axial forces come into effect as the deformation proceeds so that the interaction of bending moment and extension plays an important role, and when the beam acquires a deflection of the order of the beam depth or greater, the deformation is primarily governed by the axial force. The axial constraints reduce the deflection by

a considerable amount when the maximum deflection is of the order of the beam depth or greater; whereas the shear effect is found to be small for ordinary beam span-depth ratios with compact cross-sections unless the mass ratio is small. The shear effect becomes larger for short beams and non-compact sections subjected to impulsive loading. The major portion of the deformation is acquired under a deformation mode of one degree of freedom, with the two halves of the beam rotating about the supports, unless the attached mass is small compared to the mass of the beam.

In the second part of the theoretical approach, the effects of strain-rate sensitivity, elasticity, and duration of load pulse are also taken into account in an approximate manner based on this deformation pattern; the one degree of freedom mode assumption facilitates the inclusion of these effects in the analysis. For the same total impulse, a load with a flatter load-time relation produces a smaller deformation and impulsive loading (duration time approaching zero) gives the largest deformation. The asymptotic approach to the limiting deformation of impulsive loading is faster when the elastic effect is included and also speeded by axial constraints. A rigid-plastic beam undergoes a smaller permanent deformation than an elastic-plastic beam for a flat load pulse but the opposite is true for a load close to impulsive loading with the same total impulse. Plastic strains are assumed to be concentrated in small regions at plastic hinges for the evaluation of the strain-rate, until the transition to the string stage occurs.

Experiments were performed using aluminum alloy 6061-T6 and mild steel specimens, and showed a general agreement with the theoretical predictions from the latter approach. The rigid-perfectly plastic analysis overestimated the deformation but served as a first approximation. A substantial reduction in the permanent deformation due to the axial constraints was confirmed. The localized plastic deformation was observed clearly in the 6061-T6 aluminum alloy specimens, and is displayed in pictures of the deformed specimens.

SOURCE The contents of Chapter 8 are based on the following papers: Taijiro NONAKA, "Some Interaction Effects in a Problem of Plastic Beam Dynamics, Part 1 Interaction Analysis of a Rigid, Perfectly Plastic Beam", Journal of Applied Mechanics, Trans. ASME, Vol. 89, 1967, pp. 623-630; Taijiro NONAKA,"Some Interaction Effects in a Problem of Plastic Beam Dynamics, Part 2 Analysis of a Structure as a System of One Degree of Freedom", Journal of Applied Mechanics, Trans. ASME, Vol. 89, 1967, pp. 631-637; Taijiro NONAKA, "Some Interaction Effects in a Problem of Plastic Beam Dynamics, Part 3 Experimental Study", Journal of Applied Mechanics, Trans. ASME, Vol. 89, 1967, pp. 638-643; Taijiro NONAKA, "Large Plastic Deformation of Structures due to Impact - On an Interaction Problem and the Validity of Rigid-Plastic Analysis -", Disaster Prevention Research Institute Annuals, No. 11A, 1968, pp. 607-616(in Japanese).

Notation

A cross-section area

a_1 $\sqrt{\frac{3(3-\nu)}{\nu\gamma^2}}$

a_2 $\sqrt{\frac{\beta(3-\nu)}{2\alpha\nu a_1}}$

b beam width

c ratio of cross-section area to shear area

D material constant

d distance between longitudinal fiber and neutral axis

E Young's modulus

EI flexural rigidity

F resisting force

$F(\varphi)$ incomplete elliptic integral of the first kind with modulus $\frac{1}{\sqrt{2}}$

f yield function

h beam depth

I impulse

$J(u)$ $\int_0^u \frac{x\,dx}{1+kx^{\frac{1}{p}}}$

j $\frac{4M_o}{\sigma_o A}$

K complete elliptic integral of the first kind with modulus $\frac{1}{\sqrt{2}}$

k $\left(\frac{2M_o}{D\ell\sqrt{N_o m_1}\ell}\right)^{\frac{1}{p}}$

L actual length of half beam

ℓ effective length of half beam

M bending moment

M_o static limit moment in pure bending

M_1 magnitude of bending moment at points adjacent to the boss

M_y dynamic limit moment in pure bending

m mass per unit length

m_1 $m_o + \frac{2}{3} m\ell$

m_o attached mass.

N axial tension

N_o static limit force in pure tension

N_1 axial force at points adjacent to the boss

N_y dynamic limit force in pure tension

p material constant

Q shear

Q_o static limit shear in pure shear

q load due to D'Alembert's force

R reaction

R^* $\frac{2\delta^*}{y_e}$

s length of a plastic region in string stage

T_f load duration time.

t time

u $\frac{\sqrt{N_o m_1 \ell}}{4M_o} \dot{y}$

v_o initial velocity of the attached mass

x coordinate along beam axis

x_h length of a rigid segment

y displacement in y-direction (displacement of the attached mass for Part II)

y_o displacement of the attached mass

y_1 displacement of points adjacent to the boss

y_e elastic limit displacement

y_{er} elastic recovery

z $cn(K-a_2 t)$

α $\dfrac{m_o v_o^2}{12M_o}$

β $\dfrac{m_o}{m\ell}$

γ $\dfrac{N_o \ell}{4M_o}$

$\dot{\gamma}$ shearing strain rate

δ final value of y_1 (plastic displacement of the boss for Part II)

δ^* final plastic displacement of the boss according to rigid-perfectly plastic beam theory for one degree of freedom mode due to impulsive loading

ε extensional strain

η_o $\dfrac{y_o}{\ell}$

η_1 $\dfrac{y_1}{\ell}$

$\varkappa$ curvature

λ $T\sqrt{\dfrac{24EI}{m_1 \ell^3}}$

θ slope angle

θ^* final slope angle at points adjacent to the boss according to rigid-plastic simple bending theory

θ_e final slope angle at end-points according to rigid-plastic simple bending theory

μ Poisson's ratio

ν $\frac{6M_o}{Q_o \ell}$

$\tilde{\nu}$ $\frac{3M_o}{Q_o \ell}$

ξ $\frac{x_h}{\ell}$

σ_o static limit stress in pure tension

σ_y dynamic limit stress in pure tension

τ $\frac{v_o t}{\ell}$

τ_o static limit stress in pure shear

φ $\mathrm{am}(K-a_2\tau)$

ψ $\tan^{-1}(\cot \frac{\lambda}{2})$

ω angular velocity

Subscripts

A   state at A

B   state at B

e   elastic limit state

f   final state

h   state when finite plastic zone shrinks to a hinge

i   approximate initial state

m   maximum value

o   initial state

s   state when shear slide stops

T   state at $t = T$

t   state at the initiation of string stage

Dots denote differentiation with respect to the time t. Primes denote differentiation with respect to τ.

INTRODUCTION

When a structure is subjected to a load greater than its collapse load, no equilibrium state can exist, and an accelerated motion starts. The structure will undergo a large deformation, and may rupture or otherwise become unserviceable if such a loading continues for a sufficiently long time. However, if the time of load application is short enough, the inertial resistance of the structure may be sufficient to prevent excessive deformation. The purpose of a dynamic plastic analysis is to estimate the permanent deformation of a structure under these circumstances.

In the case of beams and framed structures, bending deformation usually predominates. In fact, under statical loading, the effect of shearing force is generally small, and axial force becomes important only in the design of heavily loaded columns, or the calculation of large deflection of beams with axial constraints. Under conditions of dynamical loading, however, the applied loads may be considerably greater than the static collapse loads, so that shear effect might not be negligible, and a finite deflection may cause axial forces to become important. On the other hand, the effect of elastic deformation becomes less important compared to plastic deformation, and rigid-plastic treatment simplifies the analysis.

Problems of the plastic interactions between bending and extension, and between bending and shear in structural dynamics, have been considered separately for several structures. Symonds and Mentel [1] considered the effect of axial constraints for uniform rigid-plastic beams subjected to impulsive uniform pressure. They found that the tensile forces arising from a finite deflection greatly reduce the deflections if loads are such that deflections are of the order of the beam thickness or greater. This was confirmed by experiments performed by Humphreys [2]. Bleich and Shaw [3] showed from an elastic approach using Timoshenko beam theory, that all beams, even those which are statically much stronger in shear than in bending, will begin to yield in shear before yielding in bending when subjected to sufficiently high initial velocity distributions. Salvadori and Weidlinger [4] indicated the possibility of shear sliding and the coupled motion of sliding and bending in a rigid-plastic simply supported beam subjected to a uniform pressure. Karunes and Onat [5] solved the interaction problem of bending and shear for rigid-plastic free-free beams under constant impact velocity at the mid-point. Their analysis is based on the square interaction diagram and shows that the effect of shear deformation is quite appreciable for I-beams, whereas for rectangular cross-sections it becomes important only for very short beams. The present author [6] examined all possible deformations of a rigid-plastic simply-supported beam for general blast type loading uniformly distributed along the beam. They found that under impulsive (very short duration) loading shear slides always take place, and that the shear effect is largest for this case as compared with general dynamic loading. No experiments seem to have been done in order to investigate absorption of energy in shear in dynamic loading.

This chapter aims at solving the interaction problem of bending, extension and shear. The existence of axial constraints is visualized in an interior span of a beam on many supports; conceivable shearing deformation is concerned with large transverse loading. We will determine the permanent deformation of a clamped beam of uniform cross-section whose ends are constrained against axial motions, with an attached mass (boss) at the center, due to large impact loads at the boss. A typical example of the application is the deformation of columns in a portal frame subjected to a dynamic load on the beam level (see Section 1.4). We attempt to solve the problem analytically in order to evaluate the effects of shear and axial forces.

In Part I, the above interaction problem is discussed on the basis of a rigid-perfectly plastic beam for impulsive loading. In Part II, we attempt to make a more realistic calculation for the permanent deformation by taking account of the duration of the load pulse, elastic, and strain-rate effects. A simplifying assumption is made as to the mode of the deformation. Experimental results are compared with the predictions from these theories in Part III.

I. INTERACTION ANALYSIS OF A RIGID-PERFECTLY PLASTIC BEAM

1.1 ASSUMPTIONS

The main assumptions employed in Part I are the following:

1. The beam is composed of rigid, perfectly plastic, ductile material (elastic deformation, strain hardening, strain-rate and delay time effects of yield being ignored). It is believed that elastic strains can be neglected if the energy absorbed in plastic deformation is very large as compared with the maximum strain energy the structure could absorb in an elastic manner.

2. The loading is impulsive, i.e., infinite magnitude of the load is applied for infinitesimal duration, the total impulse being finite. This assumption may be permissible if the load duration is sufficiently short in comparison with the deformation time.*

3. Although finite deflections are considered, it is assumed that the square of the slope is negligibly small in comparison with unity.

4. Longitudinal (axial) stress waves are disregarded; the axial force is assumed constant over the beam length. No out-of-plane deformation occurs.

5. Plastic action can take place only when the state of stress lies on a fixed yield surface. This concept is briefly discussed in the following section.

1.2 YEILD SURFACE

When a structure such as a beam or plate is analyzed, a state of stress is specified at each element in terms of the stress resultants, or generalized

---

*As for the effect of load duration, see Appendix 2.

stresses. According to a general theory of limit analysis [7], there exists some function of the stress resultants (yield function) which characterizes the yield condition. If at a structural element, this yield function takes a value less than a certain critical value, the yield limit is not reached at that element; the critical value cannot be exceeded anywhere in a structure. If the yield function takes the critical value, plastic action can take place according to the associated flow rule. When a state of stress is represented in a stress resultant space, the geometrical configuration of the yield condition serves as a yield surface. The yield surface is the locus of points representing states of stress at the yield limit. The yield surface is assumed to be convex. We superpose the generalized strain rate axes on the corresponding axes of generalized stresses, a generalized strain rate being such that its product with the corresponding generalized stress has dimension of rate of work per unit length. We can then represent the plastic flow by a strain rate vector originating at the corresponding stress point. With the geometrical terminology thus defined, the flow rule states that the plastic strain rate vector is in the direction of the outward normal to the yield surface. At a corner point of the yield surface, if one exists, the flow rule requires that the strain rate vector lies in the region bounded by the normals to the adjacent surfaces.

In a simple beam theory, the bending moment is the only stress resultant (shear is considered to be a reaction), and the condition for perfect plasticity states that an indefinitely large change of curvature can occur under a constant limit moment. The more elaborate theory developed for structures with axial elongation or compression in addition to curvature change, includes axial force. For a rectangular cross-section with bending moment M and axial tension N, the full plastic condition is expressed by two parabolic arcs

(Fig. 1(a))

$$f(\frac{M}{M_o}, \frac{N}{N_o}) = |\frac{M}{M_o}| + (\frac{N}{N_o})^2 - 1 = 0 \tag{1.1}$$

where f is the yield function, M_o and N_o are limit moment in pure bending, and axial tension in pure tension, respectively. For a section with depth h and width b, $M_o = \frac{1}{4} \sigma_o h^2 b$ and $N_o = \sigma_o bh$, where σ_o is the yield stress in pure tension. When this condition is represented in the nondimensional stress resultant plane $(\frac{N}{N_o}, \frac{M}{M_o})$, components of the corresponding strain rate are $N_o \dot{\varepsilon}$ and $M_o \dot{\kappa}$, and the flow rule requires for positive bending moment

$$\frac{N_o \dot{\varepsilon}}{M_o \dot{\kappa}} = \frac{\dfrac{\partial f}{\partial(\frac{N}{N_o})}}{\dfrac{\partial f}{\partial(\frac{M}{M_o})}} = 2 \frac{N}{N_o} \tag{1.2}$$

where $\dot{\varepsilon}$ and $\dot{\kappa}$ are the extensional strain rate at the axis, and the curvature rate, respectively. At the corner points, i.e., when the bending moment vanishes or $|N| = N_o$, the strain rate vector with components $(N_o\dot{\varepsilon}, M_o\dot{\kappa})$ lies between normals to the adjacent curves. This corresponds to the restriction for the plastic action to occur at $|N| = N_o$, that the neutral axis remain outside the cross-section.

For an ideal I-section, which has indefinitely thin web and flanges, the interaction diagram (the yield curve) is composed of four straight line segments as shown by dotted lines in Fig. 1(a). For most structural sections, the diagram falls between those two cases. The relation (1.1) is also a good approximation for other compact sections, but is slightly unconservative for I-sections. The above treatments assume that an element has infinite strength in shear.

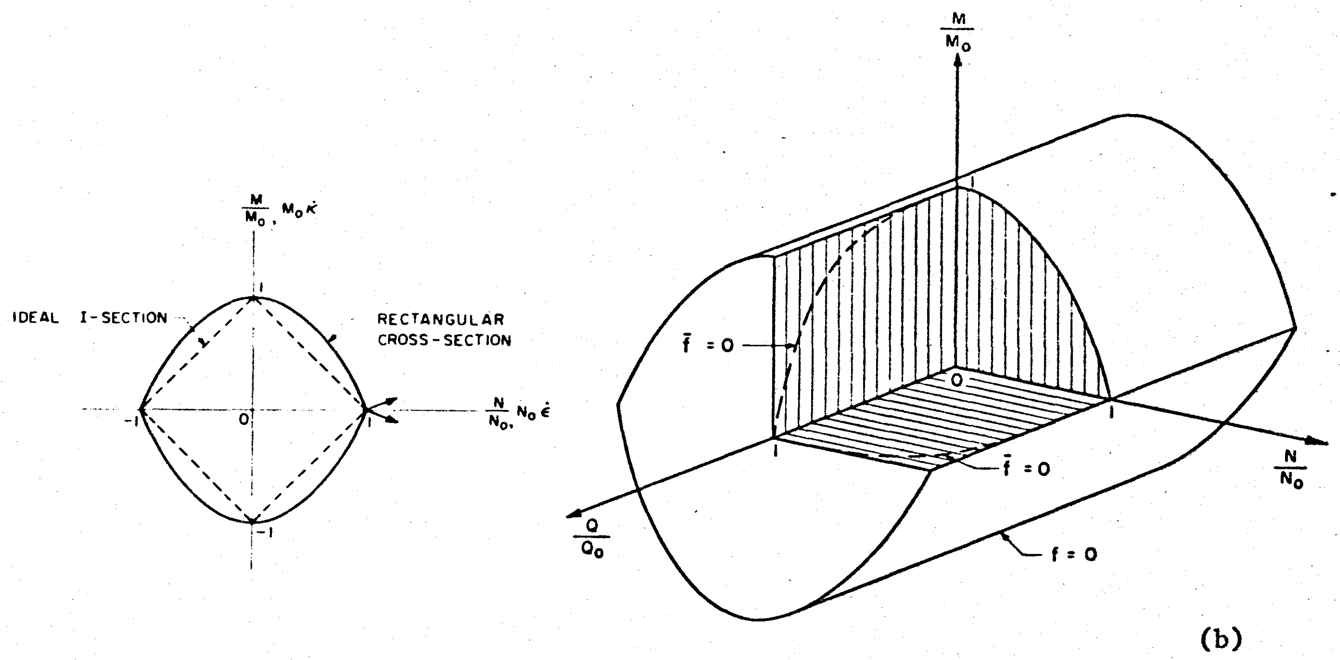

(a)

(b)

$$f \equiv \left\{ \left| \frac{M}{M_o} \right| + \left(\frac{N}{N_o} \right)^2 - 1 \right\} \left\{ \left| \frac{Q}{Q_o} \right| - 1 \right\}$$

$$\bar{f} \equiv \left| \frac{M}{M_o} \right| + \left(\frac{N}{N_o} \right)^2 + \frac{\left(\frac{Q}{Q_o} \right)^4}{1 - \left(\frac{N}{N_o} \right)^2} - 1$$

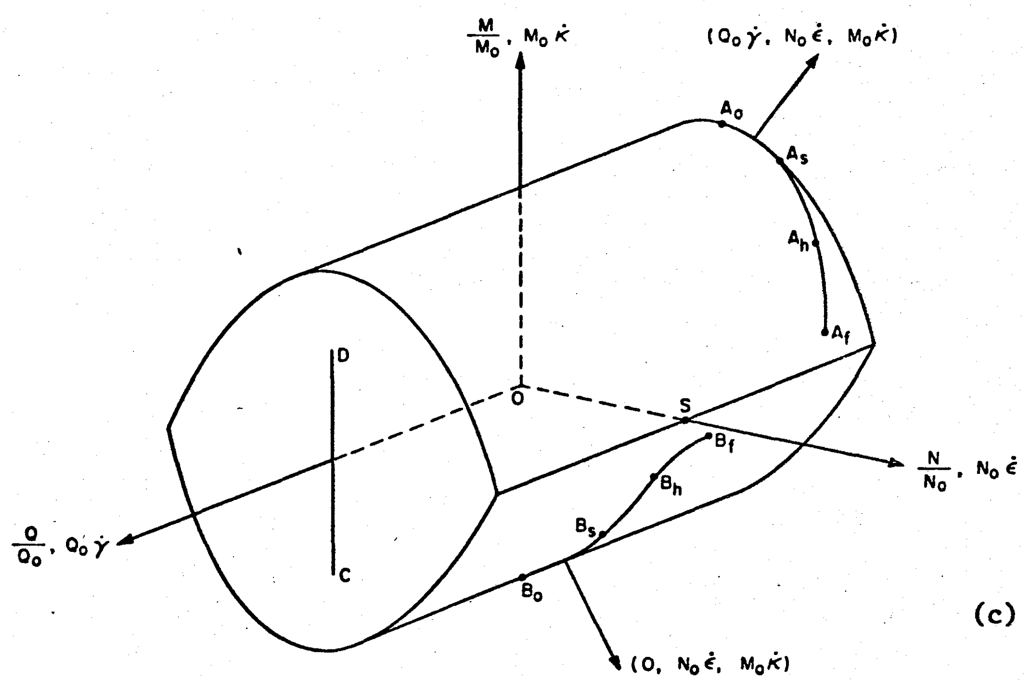

(c)

Fig. 1 Yield surfaces

We now consider the presence of shear forces as well, making use of a three dimensional space with axes $\frac{Q}{Q_o}$, $\frac{N}{N_o}$ and $\frac{M}{M_o}$, where Q and Q_o are shear force and limit shear in pure shear, respectively. The simple beam theory would assume the yield surface of two parallel planes $|\frac{M}{M_o}| = 1$, and the above treatment an infinite cylinder with axis parallel to the $\frac{Q}{Q_o}$-axis. Since $|Q| \leq Q_o$, a finite yield surface is required if the strength of the beam in shear is considered.

In contrast to the interaction of bending and extension, the effect of shear cannot be discussed as a local condition [8]. This is because axial forces and bending moments are both produced by suitable distribution of tensile stress, whereas in the presence of shear stresses, conditions in the adjoining parts of a structure come into effect so that the geometry and loading of the entire structure are important. A local condition for full plasticity is not necessarily compatible with the adjoining parts when there is shearing deformation.

From these considerations we use in the present analysis for the interaction relation the approximation

$$f\left(\frac{Q}{Q_o}, \frac{N}{N_o}, \frac{M}{M_o}\right) = \left\{\left|\frac{M}{M_o}\right| + \left(\frac{N}{N_o}\right)^2 - 1\right\}\left\{\left|\frac{Q}{Q_o}\right| - 1\right\} = 0 \qquad (1.3)$$

The geometrical configuration or the yield surface is shown in Fig. 1(b). In the figure, this approximation is compared with the interaction relation suggested for a rectangular cross-section by Neal [9]

$$\left|\frac{M}{M_o}\right| + \left(\frac{N}{N_o}\right)^2 + \frac{\left(\frac{Q}{Q_o}\right)^4}{1 - \left(\frac{N}{N_o}\right)^2} - 1 = 0. \qquad (1.4)$$

Eq. (1.4), in turn, agrees with a formula proposed by Drucker [8] for the interaction between bending and shear, which is

$$\left|\frac{M}{M_o}\right| + \left(\frac{Q}{Q_o}\right)^4 - 1 = 0 .$$

Thus, Eq. (1.3) may be a reasonably good approximation for compact sections, but is a little unsafe for non-compact sections.

According to the assumption of rigid-perfectly plastic behavior, no deformation occurs at an element when the state of stress of that element corresponds to a point inside the yield surface. Plastic strains can occur only when the state of stress corresponds to a point on the surface, according to the associated normality rule of the strain rate vector with components $(Q_o\dot{\gamma}, N_o\dot{\varepsilon}, M_o\dot{\kappa})$ to the yield surface, where $\dot{\gamma}$ is the shearing strain rate.

1.3 ANALYSIS

Suppose a concentrated mass (boss*) m_o is supported by a uniform beam with length 2ℓ, mass per unit length m, and limit stress resultants M_o, N_o, Q_o whose ends are constrained against both angular and axial motions (Fig. 2). When an impulsive loading with impulse I is applied to the mass it is assumed that the mass moves instantaneously with initial velocity $v_o = \frac{I}{m_o}$ while bending deformation starts (Fig. 3(a)). When a beam is subjected to transverse impulsive loading which has an infinite magnitude during an infinitesimal time period, sliding motion always occurs due to the shear at the point of load application. This happens because the shearing force can have only finite magnitude [6]. This problem of impulsive loading is essentially equivalent to

---

*The dimensions or volume of the boss do not come into the analysis so long as it can be considered as a particle. It is considered perfectly rigid in comparison with the beam, and loads are applied symmetrically about its center.

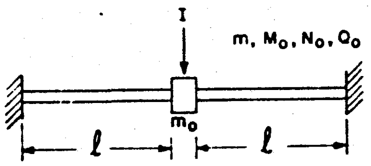

Fig. 2 Structure and loading

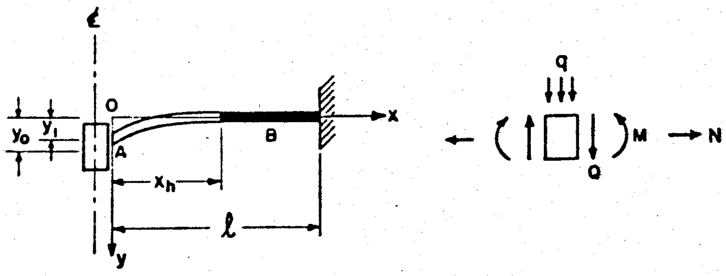

(a) First phase of motion (b) Stress resultants

Fig. 3 Notation

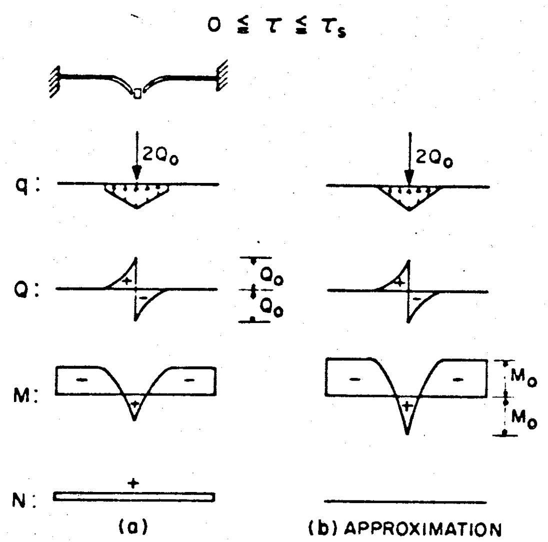

Fig. 4 First phase of motion for $\nu < 1$

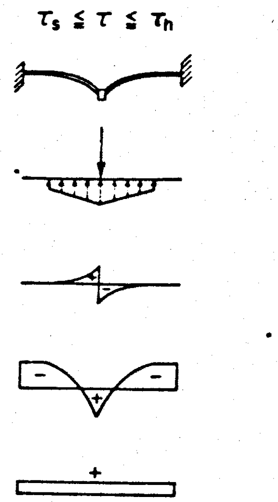

Fig. 5 Second phase of motion for $\nu < 1$

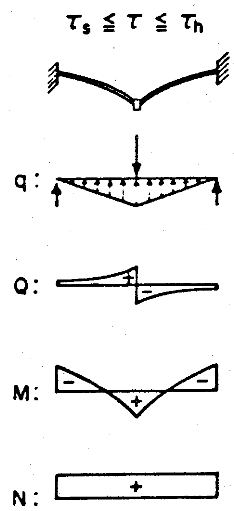

Fig. 6 Third phase of motion for $\nu < 1$; second phase of motion for $1 \leqq \nu \leqq 3$

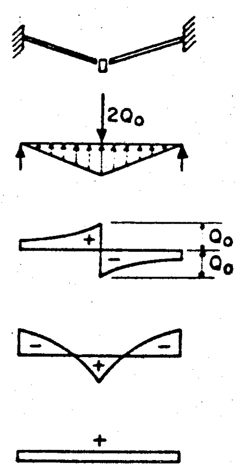

Fig. 7 First phase of motion for $1 \leqq \nu \leqq 3$

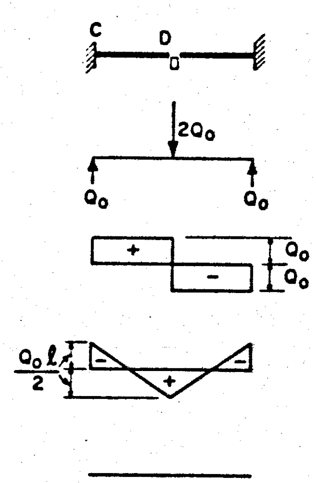

Fig. 8 Pure shear sliding motion for $\nu > 3$

that of a uniform beam struck transversely by a moving particle m_o with velocity v_o at the mid-point, the mass being assumed to become attached instantaneously to the beam. As the displacement acquires a finite magnitude, the axial force comes into effect and finally dominates the deformation. The impulse is assumed to be sufficiently large so that the elastic deformation is negligible in comparison with the plastic and that the extensional deformation is not negligible.

For a beam strong in shear,* the first phase of motion has the pattern shown in Fig. 3(a), which shows the right half of the structure. x- and y-axes are taken as shown in the figure, coordinates (x,y) indicating the position of the beam center line. Two segments of length x_h rotate as rigid bodies about $|x| = x_h$ while the mass moves downward, having plastic hinges at the center just left and right of the boss, and finite plastic zones between ends and rigid segments. The interaction relation Eq. (1.3) is satisfied at each section in these regimes. In Fig. 3(b) are shown directions of positive stress resultants. Fig. 4(a) shows distributions of D'Alembert's force, shearing force, bending moment and axial force. A uniform distribution of axial force follows from assumptions 3 and 4. The plastic regimes at the center and those between ends and rigid segments have the same magnitude of moment with opposite directions, or $M_B = -M_A$, where M_A and M_B are the bending moments at regimes A and B in the right half beam.

Let us consider stress points in Fig. 1(c). All points along the beam axis correspond to stress points on the same plane, $\frac{N}{N_o}$ = constant, at each instant starting from $\frac{N}{N_o} = 0$ toward $\frac{N}{N_o} = 1$. In this phase of motion, the

*It will be shown later that this pattern of deformation holds for a beam with $\nu = \frac{6M_o}{Q_o l} < 1$.

stress point of the plastic regime A just to the right of the boss moves from A_o toward A_s along the corner curve, and that of the plastic regime B in the right half beam between $x = x_h$ to $x = \ell$ moves from B_o toward B_s along the intersection curve of the plane $\frac{Q}{Q_o} = 0$ and the interaction surface. Rigid segments correspond to points inside the surface lying on the plane $\frac{N}{N_o}$ = constant.

The flow rule requires that the strain rate vector at regime B has components $(0, N_o\dot{\varepsilon}, M_o\dot{\varkappa})$ and that the strain rate vector at regime A has components $(Q_o\dot{\gamma}, N_o\dot{\varepsilon}, M_o\dot{\varkappa})$ lying between two normals $(0, N_o\dot{\varepsilon}, M_o\dot{\varkappa})$ and $(Q_o\dot{\gamma}, 0, 0)$ to the adjacent surfaces. The restrictions on the components are that at regime A, from Eq. (1.2)

$$\frac{N_o\dot{\varepsilon}}{M_o\dot{\varkappa}} = 2\,\frac{N}{N_o} \tag{1.5}$$

and $\dot{\gamma} \leq 0$, and that at regime B,

$$\frac{N_o\dot{\varepsilon}}{M_o\dot{\varkappa}} = -\,2\,\frac{N}{N_o}\;. \tag{1.6}$$

Unknowns are the bending moment M_A, axial force N, position of the rigid-plastic interface x_h, displacements y_o and y_1 of the mass and the adjacent points of the beam. The angular velocity of the rigid segments is given from the velocity continuity across the rigid-plastic interfaces as $\frac{\dot{y}_1}{x_h}$. The dot denotes differentation with respect to time. These unknowns are to be determined by equations of motion, the interaction relation and the flow rule.

Assuming loading occurs at time $t = 0$, conservation of momentum for the mass is

$$m_o(\dot{y}_o - v_o) = -\,2Q_o t. \tag{1.7}$$

Conservation of linear momentum and angular momentum of the right-half beam about origin is expressed by

$$\tfrac{1}{2}m\dot{y}_1 x_h = Q_o t \qquad (1.8)$$

and

$$\frac{1}{6}\, m(\dot{y}_1 x_h^2)^{\cdot} = 2M_A + Ny_1 . \qquad (1.9)$$

The interaction relation gives us

$$\frac{M_A}{M_o} + \left(\frac{N}{N_o}\right)^2 = 1. \qquad (1.10)$$

The ratio of the rates, $\frac{\dot{\varepsilon}}{\dot{\kappa}}$ is expressed in terms of the deflection y_1 as $\frac{\dot{\varepsilon}}{\dot{\kappa}} = \frac{y_1}{2}$ [1]* and the flow rule Eq. (1.5) is expressed by

$$\frac{N}{N_o} = \frac{1}{2}\,\frac{N_o \dot{\varepsilon}}{M_o \dot{\kappa}} = \frac{N_o y_1}{4M_o} . \qquad (1.11)$$

We will first consider sufficiently small deformation so that $\frac{N}{N_o} < 1$.

Eliminating M_A and N from Eqs. (1.9), (1.10) and (1.11) and substituting Eq. (1.8) into the result, we have

$$\frac{Q_o}{6M_o}\,\frac{d}{dt}\,(x_h t) = 1 + \left(\frac{N_o y_1}{4M_o}\right)^2 . \qquad (1.12)$$

If we introduce dimensionless quantities

$$\alpha \equiv \frac{m_o v_o^2}{12M_o}, \qquad \beta \equiv \frac{m_o}{m\ell}, \qquad \gamma \equiv \frac{N_o \ell}{4M_o}, \qquad \nu \equiv \frac{6M_o}{Q_o \ell} \qquad (1.13)$$

---

*This is derived as follows: In a small time increment dt, the rigid segment rotates through an angle $d\theta$ while the length of the segment increases by an amount dx_h. The strain ε and curvature κ instantly acquired by an element at x_h are $\varepsilon = y_1 d\theta/2dx_h$ and $\kappa = d\theta/dx_h$. Hence $\varepsilon/\kappa = y_1/2 = \dot{\varepsilon}/\dot{\kappa}$.

$$\xi = \frac{x_h}{\ell}, \quad \eta_o = \frac{y_o}{\ell}, \quad \eta_1 = \frac{y_1}{\ell}, \quad \tau = \frac{v_o t}{\ell}, \tag{1.14}$$

equations (1.7), (1.8) and (1.12) become

$$\eta_o' = 1 - \frac{\tau}{\alpha\nu} \tag{1.15}$$

$$\eta_1' \xi = \frac{\beta\tau}{\alpha\nu} \tag{1.16}$$

$$(\xi\tau)' = \nu(1+\gamma^2\eta_1^2) \tag{1.17}$$

where primes denote differentiation with respect to τ. We have now three unknowns ξ, η_o and η_1 to be determined from Eqs. (1.15), (1.16) and (1.17).

The parameters introduced in Eqs. (1.13) have the following physical meaning. α is related to the load magnitude; $\alpha = \frac{2}{3}\theta^*$, θ^* being the final slope angle at the mid-point calculated from simple bending theory. This is obtained by equating the initial kinetic energy $\frac{1}{2}m_o v_o^2$ to the plastic work done in pure bending which is $2M_o\{\theta^* + (\theta^* - \theta_e) + \theta_e\} = 4M_o\theta^*$ where θ_e is the final slope angle at the clamped ends. β is the ratio of the mass of the attached mass to the mass of the half beam. γ is the length ratio determining the importance of axial deformation. Writing $N_o = \sigma_o A$ and $M_o = \frac{1}{4}\sigma_o A j$, $\gamma = \frac{\ell}{j}$, where A is the cross-section area. For a rectangular section with depth h, $j = h$; for a circular section with diameter h, $j = \frac{8h}{3\pi}$; for an ideal I-section, $j = 2h$; for 8WF40, $j = 1.65h$*. ν indicates the importance of shearing deformation, depending upon the shape of the cross-section and the span-depth ratio. If we write $Q_o = \frac{\tau_o A}{c}$, $\nu = \frac{3c\sigma_o j}{2\tau_o \ell}$. With the yield stress in pure shear $\tau_o = \frac{\sigma_o}{2}$, $\nu = \frac{3cj}{\ell}$, where c depends on the shape of the cross-section. For a compact cross-section, $c = 1$; for an I-section or a wide flange section, c should

---

*It should be borne in mind that the adopted interaction relation Eq. (1.3) is less appropriate for non-compact sections such as I- , wide flange or box-sections.

be the ratio of the gross sectional area to the area of the full web, e.g., for 8WF40, $c = 4.19$. We note that γ and ν are not independent of each other but are related by $\gamma\nu = 3c$. In Table 1 are shown values of the parameters γ and ν in terms of the half span-depth ratio $\frac{\ell}{h}$.

Parameter \ Section	Circular	Rectangular	8WF40
γ	$\frac{3\pi}{8}\ \frac{\ell}{h}$	$\frac{\ell}{h}$	$0.609\ \frac{\ell}{h}$
ν	$\frac{8}{\pi}\ \frac{h}{\ell}$	$3\frac{h}{\ell}$	$20.7\ \frac{h}{\ell}$

Table 1. Parameters γ and ν

Assuming that

$$\gamma^2\eta_1^2 << 1, \tag{1.18}$$

which is equivalent to ignoring axial constraints, in this phase of motion, we have from Eqs. (1.16) and (1.17)

$$\xi = \nu \tag{1.19}$$

$$\eta_1' = \frac{\beta\tau}{\alpha\nu^2} . \tag{1.20}$$

Note that

$$\frac{N}{N_o} = \frac{N_o y_1}{4M_o} = \frac{y_1}{j} = \gamma\eta_1$$

and that relation (1.18) means, e.g., for a rectangular cross-section

$$\left(\frac{N}{N_o}\right)^2 = \left(\frac{y_1}{h}\right)^2 << 1.$$

Eq. (1.19) shows that the position of the rigid-plastic interface is independent of the input, mass ratio, etc. but depends only upon the parameter ν, and that it does not travel along the beam if there is no axial constraint. Thus $M_A = |M_B| \cong M_o$ and D'Alembert's force q is continuous in this approximation (Fig. 4(b)).

Sliding motion stops when $\eta_o' = \eta_1'$ at $\tau = \tau_s$; from Eqs. (1.15) and (1.20),

$$\tau_s = \frac{\alpha\nu^2}{\nu+\beta} \tag{1.21}$$

and the nondimensional velocity and displacements at this instant are

$$\eta_{1s}' \equiv (\eta_1')_{\tau=\tau_s} = \frac{\beta}{\nu+\beta}\ , \tag{1.22}$$

$$\eta_{1s} \equiv (\eta_1)_{\tau=\tau_s} = \frac{\alpha\beta\nu^2}{2(\nu+\beta)^2} \tag{1.23}$$

and

$$\eta_{os} \equiv (\eta_o)_{\tau=\tau_s} = \frac{\alpha\nu^2(\nu+2\beta)}{2(\nu+\beta)^2}\ . \tag{1.24}$$

For τ somewhat larger than τ_s, the second phase of motion occurs as shown in Fig. 5. There is now no relative motion between the mass and the adjacent beam portions and we take account of the effect of axial constraints. For conservation of linear momentum, we have

$$(m_o + mx_h)\dot{y}_1 = m_o v_o \tag{1.25}$$

or

$$\eta_1' = \frac{\beta}{\beta+\xi}\ . \tag{1.26}$$

Notice that the shear is still zero near the clamped ends, but ξ now increases, i.e., the rigid-plastic interfaces move toward the ends.

Eqs. (1.9), (1.10) and (1.11) again hold, but we do not use Ineq. (1.18) so that we obtain

$$\frac{\alpha}{\beta}\,(\eta_1'\xi^2)' = 1 + \gamma^2\eta_1^2. \tag{1.27}$$

From Eqs. (1.26) and (1.27), we have

$$1 + \gamma^2 \eta_1^2 + \alpha\beta\left(\frac{\eta_1''}{\eta_1'^2} - \eta_1''\right) = 0 . \tag{1.28}$$

Integrating this after multiplying by η_1', we get

$$\eta_1 + \frac{\gamma^2}{3}\eta_1^3 + \alpha\beta\left(\log \eta_1' - \frac{\eta_1'^2}{2}\right) = \eta_{1s} + \frac{\gamma^2}{3}\eta_{1s}^3 + \alpha\beta\left(\log \eta_{1s}' - \frac{\eta_{1s}'^2}{2}\right). \tag{1.29}$$

Right hand side of the above equation can be evaluated from Eqs. (1.22) and (1.23).

Eq. (1.29) is valid until $\tau = \tau_h$ corresponding to $\xi = 1$, when η_1' and η_1 attain the values η_{1h}' and η_{1h}, respectively, given by

$$\eta_{1h}' = \frac{\beta}{1+\beta} \tag{1.30}$$

$$\eta_{1h} + \frac{\gamma^2}{3}\eta_{1h}^3 = \eta_{1s} + \frac{\gamma^2}{3}\eta_{1s}^3 + \alpha\beta\left\{\log \frac{\eta_{1s}'}{\eta_{1h}'} + \tfrac{1}{2}(\eta_{1h}'^2 - \eta_{1s}'^2)\right\} . \tag{1.31}$$

For $\tau \geqq \tau_h$, the third phase of motion takes place with the two half beams rotating about the clamped ends, where shear is no longer zero. Let R be the component of the reaction at the ends in the negative y-direction (Fig. 6). Conservation of linear momentum

$$(m_o + m\ell)\ddot{y}_1 = - 2R \tag{1.32}$$

and conservation of angular momentum of a half beam about origin

$$\frac{m\ell^2\ddot{y}_1}{6} = 2M_A + Ny_1 - R\ell \tag{1.33}$$

hold in addition to the interaction relation (1.10) and the flow rule Eq. (1.11). Eliminating R, M_A and N from these four equations we have in terms of non-dimensional quantities

$$\frac{\alpha(2+3\beta)}{\beta}\eta_1'' + 1 + \gamma^2\eta_1^2 = 0. \tag{1.34}$$

Integrating Eq. (1.34) after multiplying by η_1', we obtain

$$\frac{\alpha(2+3\beta)}{2\beta}\eta_1'^2 + \eta_1 + \frac{\gamma^2}{3}\eta_1^3 = \frac{\alpha(2+3\beta)}{2\beta}\eta_{1h}'^2 + \eta_{1h} + \frac{\gamma^2}{3}\eta_{1h}^3. \tag{1.35}$$

Deformation finishes when $\eta_1' = 0$ at $\tau = \tau_f$ and the final value of η_1, η_{1f} is given by

$$\eta_{1f} + \frac{\gamma^2}{3}\eta_{1f}^3 = \frac{\alpha(2+3\beta)}{2\beta}\eta_{1h}'^2 + \eta_{1h} + \frac{\gamma^2}{3}\eta_{1h}^3. \tag{1.36}$$

From Eqs. (1.22), (1.23), (1.30), (1.31) and (1.36), we obtain

$$\eta_{1f} + \frac{\gamma^2}{3}\eta_{1f}^3 = \alpha\beta\left\{\frac{\nu-\beta}{2(\nu+\beta)} + \frac{2+\beta}{2(1+\beta)} + \frac{(\alpha\beta\nu)^2}{24}\left(\frac{\nu}{\nu+\beta}\right)^6 + \log\frac{1+\beta}{\nu+\beta}\right\} \tag{1.37}$$

The final value of η_o, η_{of} is given by

$$\eta_{of} = \eta_{1f} + (\eta_{os} - \eta_{1s}) = \eta_{1f} + \frac{\alpha\nu^2}{2(\nu+\beta)}\,. \tag{1.38}$$

The last term of Eq. (1.38) shows the amount of shear sliding.

As the pattern of motion changes, the stress points on the interaction surface corresponding to plastic regimes A and B move as (Fig. 1(c))

$$A_o \to A_s \to A_h \to A_f; \quad B_o \to B_s \to B_h \to B_f$$

as

$$\tau = 0 \to \tau_s \to \tau_h \to \tau_f.$$

Point A moves inwards from the corner curve at $\tau = \tau_s$, and B from the intersection curve made by the surface and the plane $\frac{Q}{Q_o} = 0$ to negative $\frac{Q}{Q_o}$ -direction on the interaction surface at $\tau = \tau_h$. Both A_s and B_s also lie on the plane $\frac{N}{N_o} = \gamma\eta_{1s}$, and similarly A_h and B_h on $\frac{N}{N_o} = \gamma\eta_{1h}$, A_f

and B_f on $\frac{N}{N_o} = \gamma\eta_{1f}$.

Now, let us check the assumption (1.18) which should hold for $0 \leq \tau \leq \tau_s$ in order for the above analysis to be valid. Using Eq. (1.23),

$$\max_{0 \leq \tau \leq \tau_s} (\gamma^2\eta_1^2) = \gamma^2\eta_{1s}^{\ 2} = \left\{ \frac{\alpha\beta\gamma\nu^2}{2(\nu+\beta)^2} \right\}^2 . \tag{1.39}$$

Since $\alpha\gamma$ has the same order of magnitude as the ratio of the maximum deflection to the depth of the beam*, condition

$$\nu^4 << 1 \tag{1.40}$$

is sufficient for

$$\gamma^2\eta_1^2 << 1 \quad \text{for} \quad 0 \leq \tau \leq \tau_s$$

unless β is too small compared to one. Condition (1.40) can be made weaker if β is large.

To this order of accuracy, the third term in the brackets of the right hand side of Eq. (1.37) is negligible as compared with other terms. Replacing η_{1f} by $\frac{\delta}{\ell}$ where δ is the maximum value of y_1, we have the final result

$$\frac{\delta}{\ell} + \frac{\gamma^2}{3}\left(\frac{\delta}{\ell}\right)^3 = \alpha\beta\left\{\frac{\nu-\beta}{2(\nu+\beta)} + \frac{2+\beta}{2(1+\beta)} + \log\frac{1+\beta}{\nu+\beta}\right\}. \tag{1.41}$$

The condition $\frac{N}{N_o} < 1$ is satisfied if $\frac{N_o\delta}{4M_o} < 1$ or $\frac{\delta}{\ell} < \frac{1}{\gamma}$ or if

$$\alpha\beta\gamma\left\{\frac{\nu-\beta}{2(\nu+\beta)} + \frac{2+\beta}{2(1+\beta)} + \log\frac{1+\beta}{\nu+\beta}\right\} < \frac{4}{3} .$$

Eq. (1.41) can be written in other forms. Introducing the nondimensional deformation $\frac{N_o\delta}{4M_o}$ instead of $\frac{\delta}{\ell}$, and writing $\nu = \frac{3c}{\gamma}$, Eq. (1.41) becomes

$$\frac{N_o\delta}{4M_o} + \frac{1}{3}\left(\frac{N_o\delta}{4M_o}\right)^3 = \alpha\beta\gamma\left\{\frac{3c-\beta\gamma}{2(3c+\beta\gamma)} + \frac{2+\beta}{2(1+\beta)} + \log\frac{\gamma(1+\beta)}{3c+\beta\gamma}\right\}. \tag{1.41a}$$

---

*Note that $\alpha\gamma = \frac{2\theta^*\ell}{3j}$. We are interested in a deformation such that the final deflection is of the order of the beam depth.

This equation shows explicitly that for a given cross-section $\frac{N_o \delta}{4M_o} = \frac{\delta}{j}$ is a function of α, β and γ. For a beam with infinite strength in shear substitution of $c = 0$ gives

$$\frac{N_o \delta}{4M_o} + \frac{1}{3}\left(\frac{N_o \delta}{4M_o}\right)^3 = \alpha\beta\gamma \left\{ \frac{1}{2(1+\beta)} + \log \frac{1+\beta}{\beta} \right\}$$

which shows that $\frac{N_o \delta}{4M_o}$ is a function of two parameters $\alpha\gamma$ and β; whereas substitution of $\nu = 0$ in Eq. (1.41) gives a relation showing that $\frac{\delta}{\ell}$ is a function of three parameters α, β and γ (see Eq. (1.69)). Hence $\frac{N_o \delta}{4M_o}$ is used for the nondimensional displacement instead of $\frac{\delta}{\ell}$ in the analysis of Part II where the shear effect is neglected. Incidentally, for a rectangular cross-section Eq. (1.41a) becomes

$$\frac{\delta}{h} + \frac{1}{3}\left(\frac{\delta}{h}\right)^3 = \alpha\beta\gamma \left\{ \frac{3-\beta\gamma}{2(3+\beta\gamma)} + \frac{2+\beta}{2(1+\beta)} + \log \frac{\gamma(1+\beta)}{3+\beta\gamma} \right\}. \tag{1.41b}$$

On the other hand Eq. (1.41) is more convenient to eliminate the effect of axial constraints. Substitution of $\gamma = 0$ in Eq. (1.41) gives the result immediately for a clamped beam without axial constraints. For this reason the form of Eq. (1.41) is kept in Part I.

It should be noticed that the effect of axial constraints appears only in the left hand side of the above equations for the final deformation. This effect can be neglected if $\frac{1}{3}\left(\frac{\delta}{j}\right)^2 << 1$ or roughly if $\left(\frac{\delta}{h}\right)^2 << 1$. If there is no axial constraint, $\frac{\delta}{\ell}$ is proportional to the parameter α as we see in Eq. (1.41). The effect of shear, on the other hand, is associated with both ν and β. The shear effect can be neglected if $\frac{\nu}{\beta} << 1$. It should be kept in mind that we are considering pure impulsive loading and the shear effect is therefore overestimated for actual loading of finite duration time.

So far we have been referring to small ν or beams strong in shear. We will now consider cases where $\nu \geqq 1$. Eq. (1.19) shows that plastic regime B shrinks to a hinge for $\nu = 1$. The pattern of the first phase of motion is that two halves of the beam rotate as rigid bodies about the clamped ends with angular velocity $\frac{\dot{y}_1}{\ell}$ while the central mass moves downwards with velocity $\dot{y}_o$ (Fig. 7). This turns out to be the case for $1 \leqq \nu \leqq 3$. (For $\nu > 3$, the limit moment is not reached at the ends.) The equation of motion for the mass is again Eq. (1.8) or Eq. (1.15); the equations of motion for each half beam are

$$\frac{m\ell\ddot{y}_1}{2} = Q_o - R \tag{1.42}$$

and

$$\frac{m\ell^2\ddot{y}_1}{6} = 2M_A + Ny_1 - R\ell . \tag{1.43}$$

Combining with the interaction relation (1.10) and the flow rule (1.11) using notations in Eqs. (1.13) and (1.14) we obtain

$$\frac{2\alpha}{\beta}\eta_1'' + 1 - \frac{3}{\nu} + \gamma^2\eta_1^2 = 0. \tag{1.44}$$

The last term in this equation should not be neglected any more since Inequality (1.40) is not satisfied. This is because the beam is weak in shear and η_1 attains an appreciable value before shear sliding stops, so that now the effect of axial constraints is not negligible even in the first phase of motion.

Integrating Eq. (1.44) after multiplying by η_1', we obtain

$$\frac{\alpha}{\beta}\eta_1'^2 + (1 - \frac{3}{\nu})\eta_1 + \frac{1}{3}\gamma^2\eta_1^3 = 0 \tag{1.45}$$

or

$$\tau = \sqrt{\frac{\alpha\,\nu}{\beta(3-\nu)}} \int_0^{\eta_1} \frac{d\eta}{\sqrt{\eta\left(1-\frac{\eta^2}{a_1^2}\right)}} \tag{1.46}$$

where

$$a_1^2 \equiv \frac{3(3-\nu)}{\nu\gamma^2}\,. \tag{1.47}$$

Setting

$$\eta = a_1 z^2$$

and

$$z = \cos\varphi\,,$$

the integral

$$\int_0^{\eta_1} \frac{d\eta}{\sqrt{\eta\left(1-\frac{\eta^2}{a_1^2}\right)}} = 2\sqrt{a_1}\int_0^z \frac{dz}{\sqrt{1-z^4}}$$

$$= -\sqrt{2a_1}\int_{\frac{\pi}{2}}^{\varphi} \frac{d\varphi}{\sqrt{1-\frac{1}{2}\sin^2\varphi}}$$

$$= \sqrt{2a_1}\left\{K - F(\varphi)\right\}\,, \tag{1.48}$$

where K is the complete elliptic integral of the first kind with modulus $\frac{1}{\sqrt{2}}$ and $F(\varphi)$ is the incomplete elliptic integral of the first kind with modulus $\frac{1}{\sqrt{2}}$, amplitude φ, i.e.,

$$K \equiv \int_0^{\frac{\pi}{2}} \frac{d\varphi}{\sqrt{1-\frac{1}{2}\sin^2\varphi}} \tag{1.49}$$

$$F(\varphi) \equiv \int_0^{\varphi} \frac{d\varphi}{\sqrt{1-\frac{1}{2}\sin^2\varphi}} \; . \tag{1.50}$$

Hence,

$$a_2\tau = K - F(\varphi) \tag{1.51}$$

where

$$a_2 \equiv \sqrt{\frac{\beta(3-\nu)}{2\alpha\nu a_1}} = \sqrt{\frac{\beta\gamma}{2\alpha}}\sqrt[4]{\frac{3-\nu}{3\nu}} \, , \tag{1.52}$$

and

$$\varphi = \operatorname{am}(K-a_2\tau) \tag{1.53}$$

$$z = \operatorname{cn}(K-a_2\tau) \tag{1.54}$$

$$\eta_1 = a_1\operatorname{cn}^2(K-a_2\tau) \tag{1.55}$$

$$\eta_1' = 2a_1a_2\operatorname{sn}(K-a_2\tau)\ \operatorname{cn}(K-a_2\tau)\ \operatorname{dn}(K-a_2\tau). \tag{1.56}$$

This phase of motion stops at $\tau = \tau_s$ when shear sliding stops or $\eta_o' = \eta_1'$, τ_s being obtained from

$$\tau_s + 2\alpha\nu a_1a_2\operatorname{sn}(K-a_2\tau_s)\cdot\operatorname{cn}(K-a_2\tau_s)\cdot\operatorname{dn}(K-a_2\tau_s) = \alpha\nu \tag{1.57}$$

and

$$\eta_{1s} = a_1 cn^2(K-a_2\tau_s), \tag{1.58}$$

$$\eta_{os} = \tau_s - \frac{\tau_s^2}{2\alpha\nu} , \tag{1.59}$$

$$\eta'_{1s} = 1 - \frac{\tau_s}{\alpha\nu} . \tag{1.60}$$

For $\tau \geqq \tau_s$, the pattern of motion is just the same as the third phase of motion in the preceding case, as shown in Fig. 6. Therefore, Eq. (1.34) again holds; with initial condition at $\tau = \tau_s$, we get

$$\eta_{1f} + \frac{\gamma^2}{3}\eta_{1f}^3 = \eta_{1s} + \frac{\gamma^2}{3}\eta_{1s}^3 + \frac{\alpha(2+3\beta)}{2\beta}\eta_{1s}'^2 . \tag{1.61}$$

From Eq. (1.45),

$$\eta_{1s} + \frac{\gamma^2}{3}\eta_{1s}^3 = \frac{3}{\nu}\eta_{1s} - \frac{\alpha}{\beta}\eta_{1s}'^2 . \tag{1.62}$$

Substituting this into Eq. (1.61) and using Eqs. (1.58), (1.59) and (1.60), we obtain

$$\eta_{1f} + \frac{\gamma^2}{3}\eta_{1f}^3 = \frac{3}{2\alpha}\left(\frac{\alpha\nu-\tau_s}{\nu}\right)^2 + \frac{3a_1}{\nu} cn^2(K-a_2\tau_s) \tag{1.63}$$

$$\eta_{of} = \eta_{1f} + (\eta_{os} - \eta_{1s}) = \eta_{1f} - a_1 cn^2(K-a_2\tau_s) + \tau_s - \frac{1}{2\alpha\nu}\tau_s^2 . \tag{1.64}$$

For later convenience Eq. (1.63) is rewritten as:

$$\frac{\delta}{\ell} + \frac{\gamma^2}{3}\left(\frac{\delta}{\ell}\right)^3 = \frac{3}{2\alpha}\left(\frac{\alpha\nu-\tau_s}{\nu}\right)^2 + \frac{3a_1}{\nu} cn^2(K-a_2\tau_s). \tag{1.65}$$

If the beam is so weak in shear that

$$Q_o\ell < 2M_o \qquad \text{or} \qquad \nu > 3, \tag{1.66}$$

then no bending deformation takes place; the central mass moves transversely while the half beams suffer no deformation (Fig. 8). It is of interest that shearing deformation always occurs in the case of impulsive loading whereas bending deformation does not take place under certain circumstances [6].

Plastic regime CD of the left half beam corresponds to the line CD on the interaction surface in Fig. 1(c). The occurrence of shear sliding at any position other than the center would violate the shear plasticity condition. Equation of motion (1.7) or (1.15) holds until $\tau = \tau_f$ when $\eta_o' = 0$ yielding

$$\eta_{of} = \frac{\alpha\nu}{2}\,. \tag{1.67}$$

In this type of motion, of course

$$\eta_{1f} = 0 \quad \text{or} \quad \delta = 0\,. \tag{1.68}$$

To summarize, the final displacement $\delta = \eta_{1f}\ell$ at sections adjacent to the central mass is obtained under the condition that $\frac{\delta}{\ell} < \frac{1}{\gamma}$ as the solution of

Eq. (1.41) if $\nu < 1$;

Eq. (1.65) if $1 \leqq \nu \leqq 3$;

and

Eq. (1.68) if $3 < \nu$.

If we neglect the shearing deformation altogether or for $\nu = 0$, Eq. (1.41) becomes

$$\frac{\delta}{\ell} + \frac{\gamma^2}{3}\left(\frac{\delta}{\ell}\right)^3 = \alpha\beta\left\{\frac{1}{2(1+\beta)} + \log\frac{1+\beta}{\beta}\right\}. \tag{1.69}$$

Furthermore, if we also neglect the effect of axial constraints, and set $\gamma = \nu = 0$, we have

$$\frac{\delta}{\ell} = \alpha\beta\left\{\frac{1}{2(1+\beta)} + \log\frac{1+\beta}{\beta}\right\}. \tag{1.70}$$

This is the solution obtained from simple bending theory. Here $\frac{\delta}{\alpha\ell}$ depends only on the mass ratio β; as $\beta \to \infty$, $\frac{\delta}{\ell} \to \theta^* = \frac{3}{2}\alpha$. In simple bending theory, our problem is equivalent to a cantilever of length ℓ, mass per unit length m and yield moment $2M_o$, with tip mass $\frac{m_o}{2}$ subjected to initial velocity v_o. Parkes first solved this problem [10]; Eq. (1.70) is equivalent to his solution and the deformation of the whole beam can be obtained very easily in the simple bending theory (Parkes also included the present clamped beam in another paper on the basis of rigid-plastic simple beam theory [11]).

If the deformation attains the value such that $\frac{N}{N_o} = 1$, the beam reaches the state in which bending moment is zero throughout the beam and it behaves like a plastic string.* The flow rule states that the strain rate vector at $\frac{N}{N_o} = 1$ lies between two normals to the adjacent surfaces. However, if we assume that the vector lies in the plane $\frac{M}{M_o} = 0$ or just in the middle of those normals, then $\dot{\kappa} = 0$ or the beam extends along its axis without any change in curvature. This assumption corresponds to assuming that all fibers undergo the same axial elongation at the string stage. All points of the beam have the stress point S with coordinates (0,1,0) in Fig. 1(c) and stay there.

The remaining kinetic energy at the transition, $\tau = \tau_t$, is spent in work of pure extension under constant axial force N_o. Total work done in the string stage is twice the integral

$$N_o \int_{y_{1t}}^{\delta} d\left(\sqrt{\ell^2+y_1^2}\right) = N_o\left(\sqrt{\ell^2+\delta^2} - \sqrt{\ell^2+y_{1t}^2}\right) \tag{1.71}$$

where $y_{1t} \equiv (y_1)_{\tau=\tau_t}$. Assuming the transition occurs in the last phase of

*This does not occur if $\nu > 3$, for which $y_1 = 0$.

motion*, Fig. 6, the remaining kinetic energy at the transition is

$$\left(\frac{m_o}{2} + \frac{m\ell}{3}\right) \dot{y}_{1t}^{2} \tag{1.72}$$

where $\dot{y}_{1t} = (\dot{y}_1)_{\tau=\tau_t}$. Hence, by equating the remaining kinetic energy to the work done we have

$$\frac{\alpha(2+3\beta)}{2\beta} \eta_{1t}'^{2} = 2\left(\sqrt{\gamma^2+\gamma^2\eta_{1f}^2} - \sqrt{\gamma^2+1}\right) \tag{1.73}$$

where $\eta_{1t}' \equiv (\eta_1')_{\tau=\tau_t}$ is obtained by setting $(\eta_1)_{\tau=\tau_t} = \frac{1}{\gamma}$ in Eq. (1.35) if $\nu < 1$ and in Eqs. (1.55) and (1.56) if $1 \leqq \nu \leqq 3$. Thus, we have for $\frac{\delta}{\ell} \geqq \frac{1}{\gamma}$,

$$\left(\frac{\delta}{\ell}\right)^2 = \begin{cases} \frac{1}{\gamma^2}\left[\sqrt{1+\gamma^2} - \frac{2}{3\gamma} + \frac{\alpha\beta}{2}\left\{\frac{\nu-\beta}{2(\nu+\beta)} + \frac{2+\beta}{2(1+\beta)} + \log\frac{1+\beta}{\nu+\beta}\right\}\right]^2 - 1 & \text{if } \nu < 1 \\ \frac{1}{\gamma^2}\left[\sqrt{1+\gamma^2} - \frac{2}{3\gamma} + \frac{3}{4\alpha}\left(\frac{\alpha\nu-\tau_s}{\nu}\right)^2 + \frac{3a_1}{2\nu}\,\mathrm{cn}^2(K-a_2\tau_s)\right]^2 - 1 & \text{if } 1 \leqq \nu \leqq 3 \\ 0 & \text{if } 3 < \nu \end{cases} \tag{1.74}$$

1.4 EXAMPLES AND APPLICATION

Examples are given for compact cross-sections with parameters:

$$\beta \equiv \frac{m_o}{m\ell}: \quad 0.1, \quad 1.0, \quad 10, \quad 100$$

$$\gamma \equiv \frac{N_o \ell}{4M_o}: \quad 5, \quad 10, \quad 15.$$

*This happens generally for impulses causing deformation of the order of beam depth, for ordinary beam dimensions and for mass ratio β of the order of one or more.

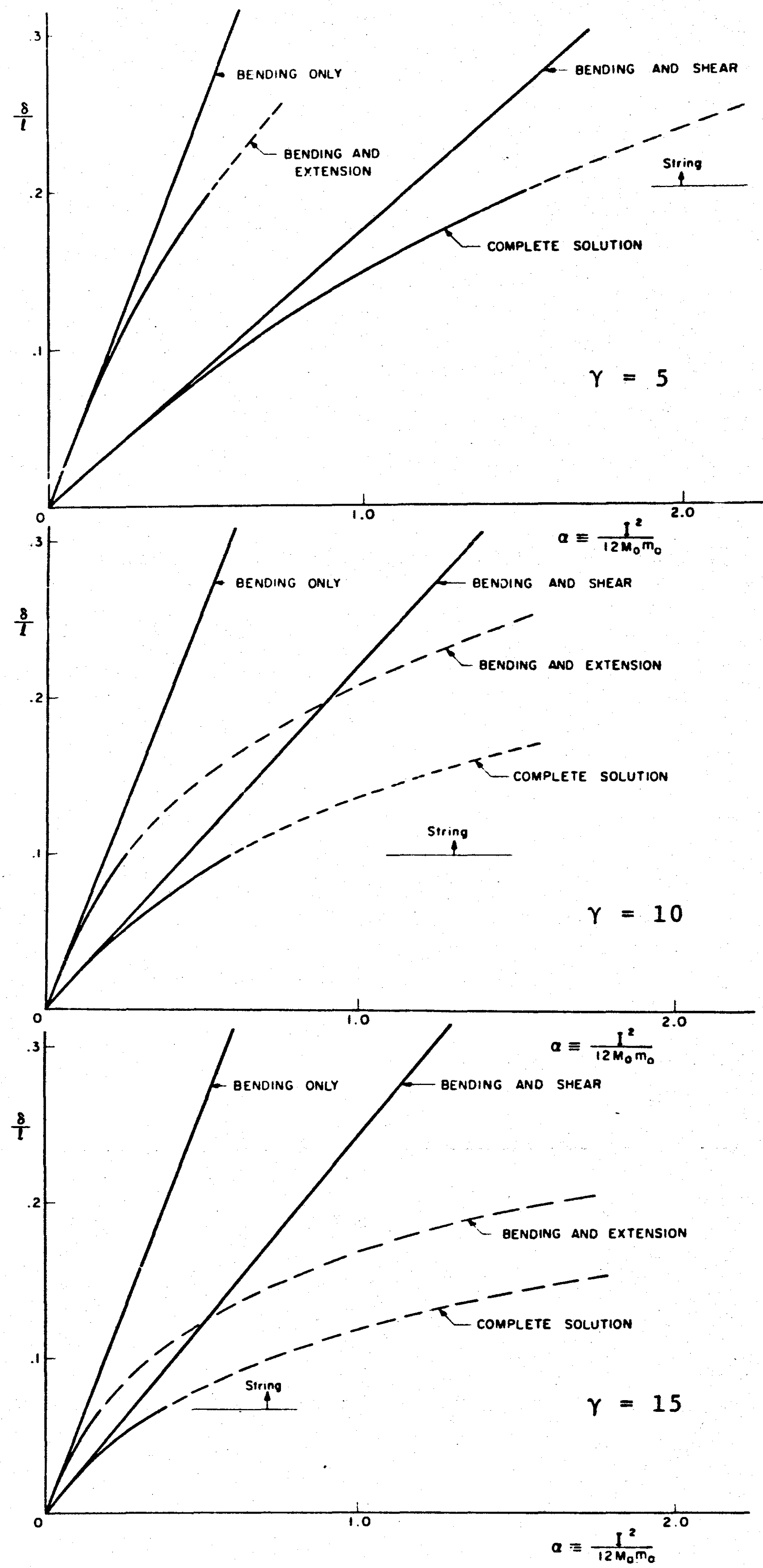

Fig. 9(a) Compact cross section of $\beta = 0.1$

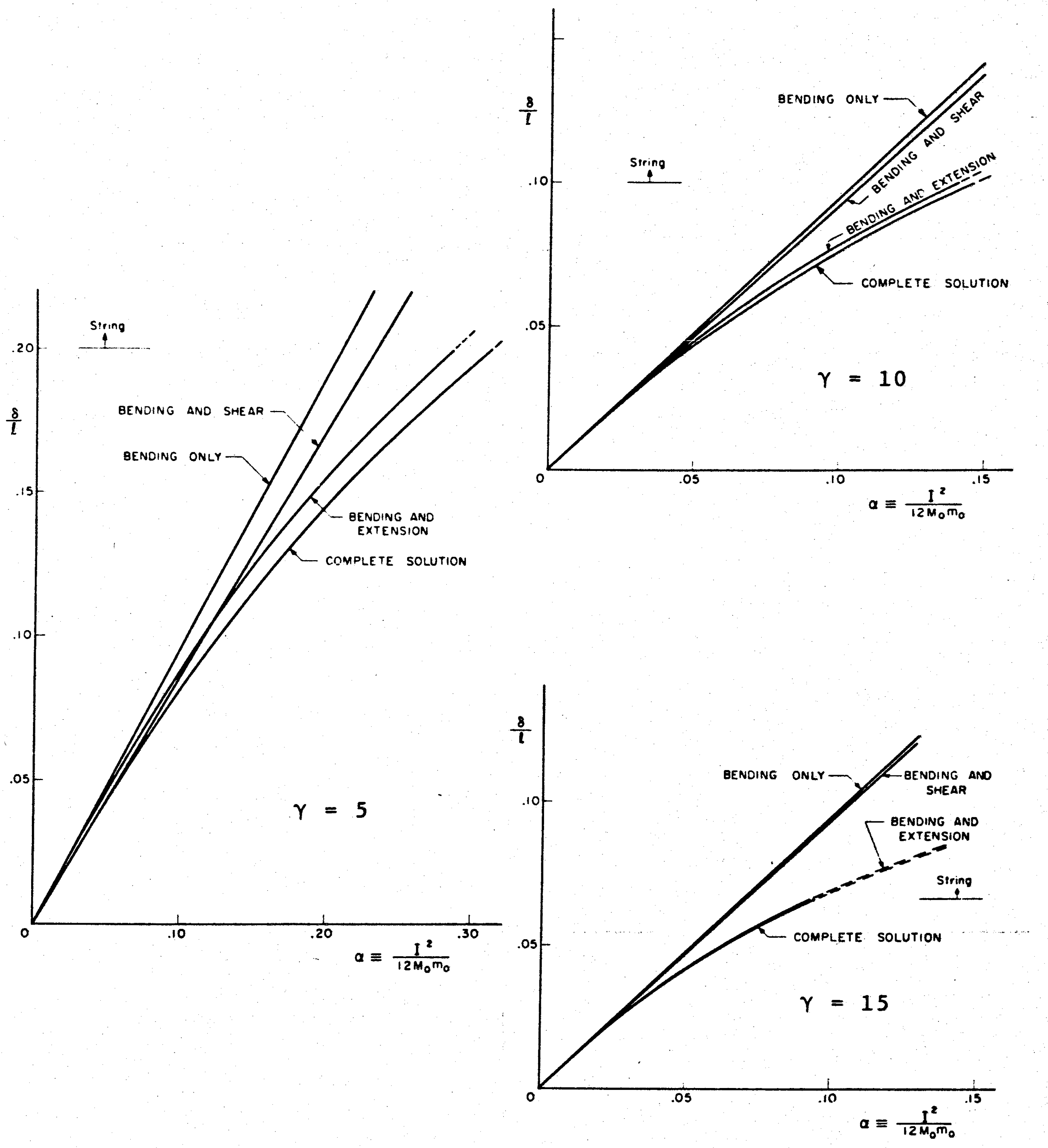

Fig. 9(b) Compact cross section of $\beta = 1$

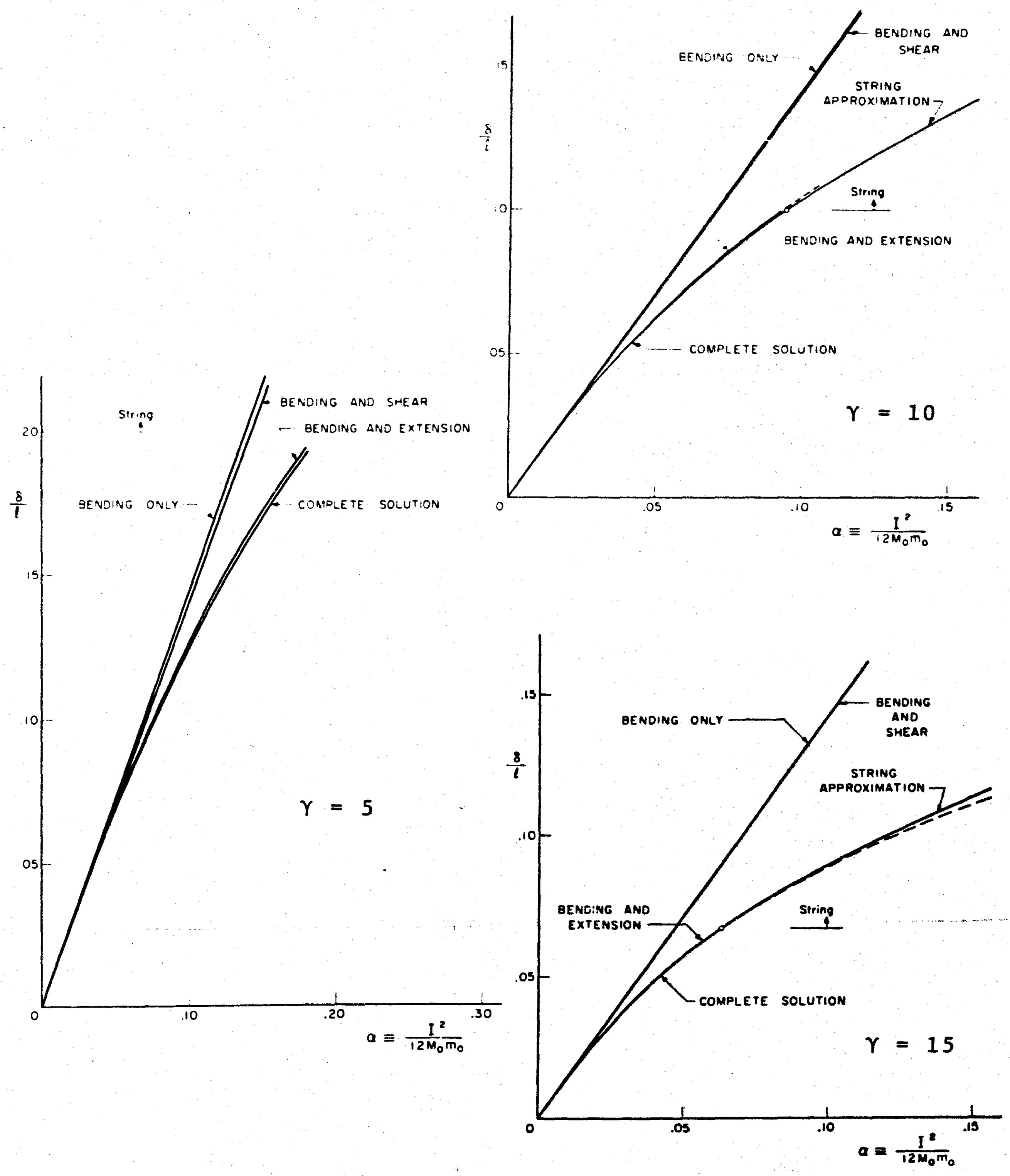

Fig. 9(c) Compact cross section of $\beta = 10$

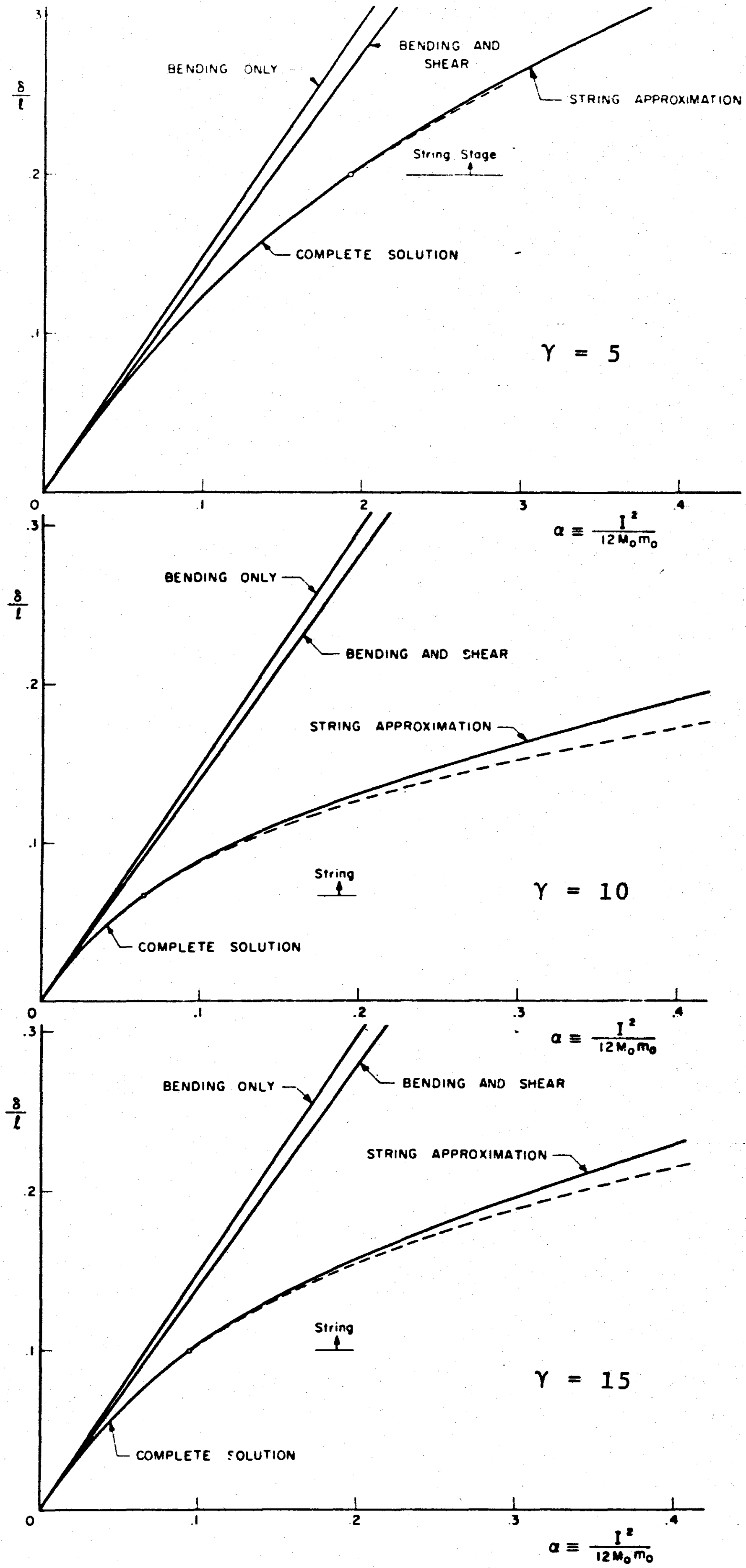

Fig. 9(d) Compact cross section of β = 100

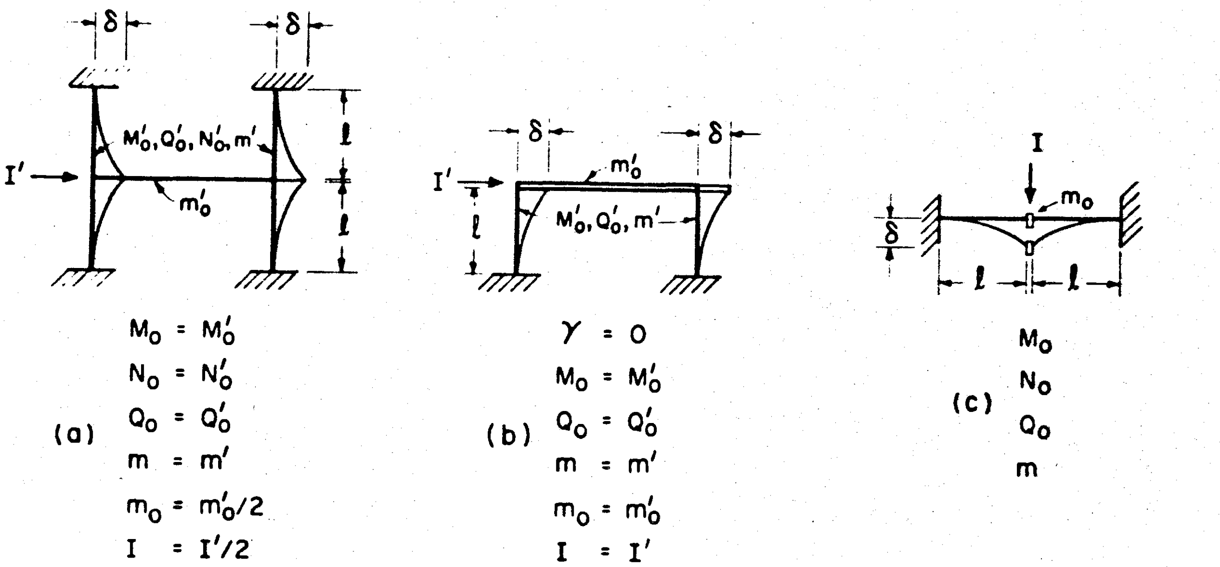

Fig. 10 Examples of application and correspondence to the problem

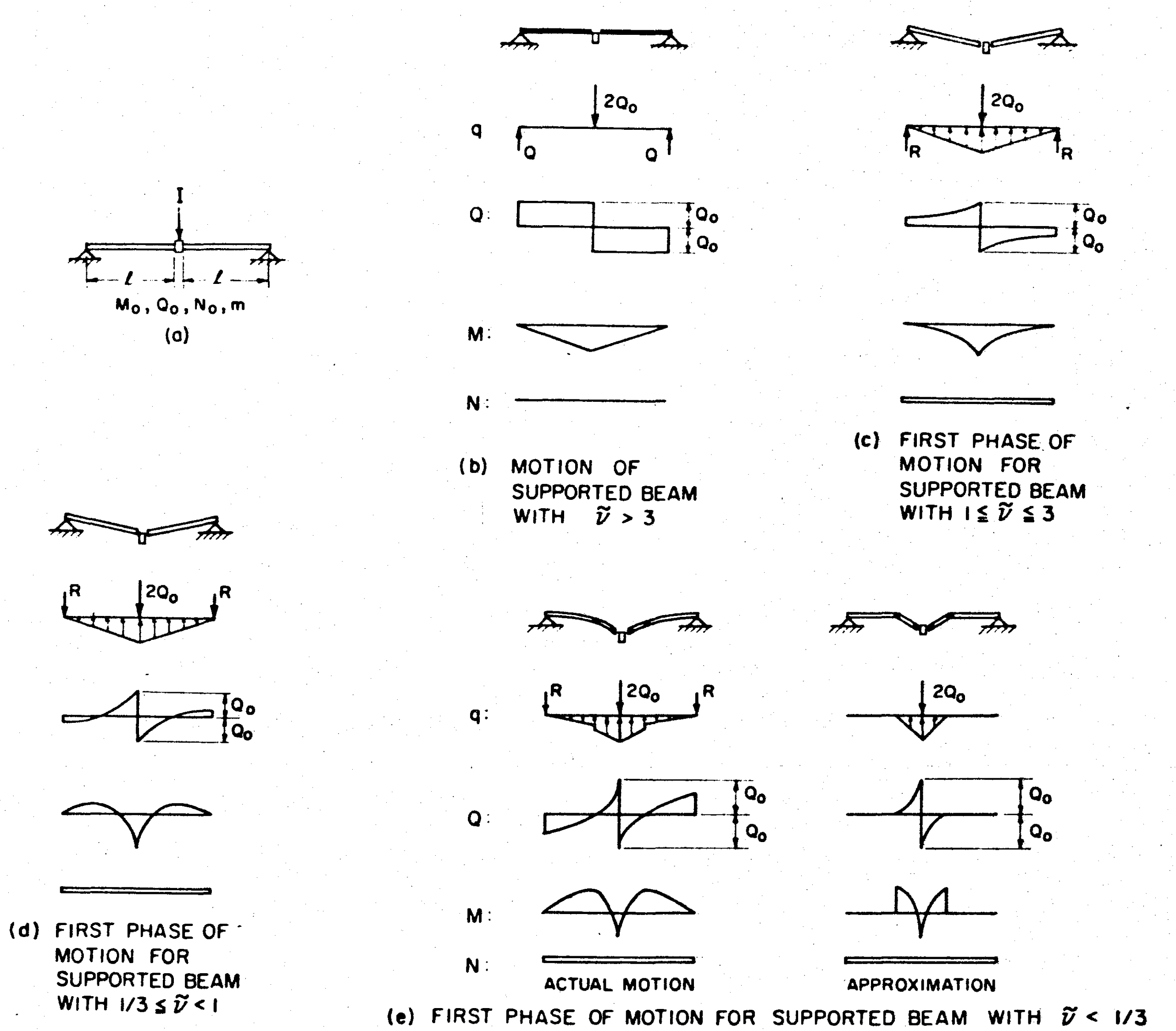

Fig. 11 Supported beam

Note that γ specifies the value of parameter ν also by relation $\nu = \frac{3}{\gamma}$. In Fig. 9 are drawn curves of $\frac{\delta}{\ell}$ as functions of α for each combination of the above values of parameters.

It is seen that both plastic shear deformation and axial constraints reduce the value of $\frac{\delta}{\ell}$. The effect of the former is relatively small except for small values of the mass ratio whereas the latter causes a substantial reduction for finite deformations. It should be kept in mind that these examples are for compact cross-sections subjected to impulsive loading. The effect of shear deformation is larger for non-compact cross-sections and smaller for actual loading which has finite load magnitude with finite duration.

Figs.10(a) and (b) show examples for application of the present problem to rigid-jointed frames. The beam in the example (b) is assumed to be rigid compared with columns. Correspondence of the related quantities is also shown in the figures.

Let us consider the interaction problem of a rigid-plastic simply supported beam. Suppose both ends of our clamped beam are replaced by hinged supports and otherwise the same (Fig. 11(a)). Noting that the force $2Q_o$ is transmitted by shear to the beam, we see that no bending or extensional deformation occurs if $M_o > Q_o\ell$ or parameter $\tilde{\nu} \equiv \frac{3M_o}{Q_o\ell} > 3$ (Fig. 11(b)). For $\tilde{\nu}$ somewhat smaller than 3, motion of the type shown in Fig. 11(c) first occurs, which was the case for the clamped beam with $\nu \equiv \frac{6M_o}{Q_o\ell}$ such that $1 \leq \nu \leq 3$. Equations of motion for this supported beam are obtained simply by replacing $2M_o$ in those for the clamped beam by M_o; the reaction at the supports becomes zero when $\tilde{\nu} = 1$ corresponding to $\nu = 1$ in the clamped beam. For $\tilde{\nu}$ smaller than one, the reaction reverses the direction as shown in Fig. 11(d). When $\tilde{\nu} = \frac{1}{3}$, the maximum magnitude of the negative moment reaches limit moment at certain points between ends and the mid-point.

The flow rule for a supported beam is written as $\frac{N}{N_o} = \frac{N_o y_1}{2M_o}$ [1], which would be obtained by replacing $2M_o$ in the flow rule for the clamped beam by M_o. For $\tilde{\nu} < \frac{1}{3}$ the pattern of the first phase of motion for the supported beam is shown in Fig. 11(e). The angle of rotation of the outer rigid segments is usually small in the first phase of motion. If we neglect the motion of the outer segments in comparison with the motion of the inner segments for the first phase of motion, we again get equations of motion which are obtained by replacing $2M_o$ by M_o in those for the clamped beam. Replacement of $2M_o$ by M_o is also valid for later phases of motion. Therefore, the final deformation for the supported beam with and without axial constraints is obtained by replacing $2M_o$ in the foregoing results for the clamped beam by M_o; the correspondence is as follows:

$$\tilde{\nu} < \frac{1}{3} \quad : \quad \nu < 1$$

$$\frac{1}{3} \leq \tilde{\nu} \leq 3 \quad : \quad 1 \leq \nu \leq 3$$

$$3 < \tilde{\nu} \quad : \quad 3 < \nu$$

Treatment of the type to be introduced in Part II can also be done and the results for the supported beam are obtained again by replacing $2M_o$ in those for the clamped beam by M_o. Examples for the application of the supported beam corresponding to Fig. 10(a) and (b) are obvious.

1.5 ADDITIONAL REMARKS

The criterion for elastic deformation to be negligible requires that the plastic work done is sufficiently large as compared with the maximum possible strain energy which could be stored in the structure [12][13]. The plastic work done equals the initial kinetic energy $\frac{1}{2}m_o v_o^2$ less the total energy of elastic vibration. In the presence of axial force and shear as well as bending moment the maximum strain energy should be calculated to maximize the possible elastic energy without violating a yield condition. In ordinary structural theory, non-zero stress components are a normal stress and a shear stress, and in the state of plane stress two normal stresses and a shear stress. The von Mises yield criterion, for example, gives the maximum strain energy for the beam length 2ℓ, $\frac{N_o^2\ell}{EA}$ and $2(1-\mu)\frac{N_o^2\ell}{EA}$ for those two cases[14], where E is the Young's modulus and μ is the Poisson's ratio; both coincide for an incompressible material, $\mu = \frac{1}{2}$. Thus, it is necessary according to the criterion that

$$\frac{m_o v_o^2}{2} \gg \frac{N_o^2 \ell}{EA} .$$

The value of shear parameter ν is small for a compact cross-section except for very short beams. The effect of shear may therefore be negligible unless the mass ratio β is small for compact cross-sections with ordinary beam dimensions. It is surmised that for a large mass ratio the major portion of the deformation occurs during the last phase of motion, i.e., with the pattern in which two halves of the beam rotate about the clamped ends. Hence, the deformation during earlier phases of motion may be neglected for beams with compact cross-section and large mass ratio .

Suppose the two half beams begin to rotate about their ends from the instant of the impulsive loading with impulse $m_o v_o$ (this motion has only one degree of freedom). Then equations for $\tau_h \leqq \tau$ are valid, and the final non-dimensional deflection η_{1f} is obtained so long as $\eta_{1f} \leqq \frac{1}{\gamma}$ from Eq. (1.36) by setting $\eta_{1h} = 0$ and replacing η'_{1h} by η'_{1i}:

$$\eta_{1f} + \frac{\gamma^2}{3}\eta_{1f}^3 = \frac{\alpha(2+3\beta)}{2\beta}\eta_{1i}'^2$$

where $\eta'_{1i} \equiv (\eta'_1)_{\tau=0}$ is the non-dimensional initial velocity of the mid-point due to the impulse. By equating the moment of the half of the impulse to the change in moment of momentum of the half beam plus half the central mass with respect to the clamped end, we have

$$\eta'_{1i} = \frac{3\beta}{2+3\beta} .$$

We, therefore, obtain the relation

$$\eta_{1f} + \frac{\gamma^2}{3}\eta_{1f}^3 = \frac{9\alpha\beta}{2(2+3\beta)} .$$

For example, if $\beta = 10$, $\gamma = 15$ (hence $\nu = \frac{1}{5}$), the right hand side of the above equation is only 4% larger than that of the complete solution, Eq. (1.41). If the deformation is larger so that the string stage is reached, this one degree of freedom approximation must give a result closer to that of the preceding sections.

The above mode assumption makes the analysis extremely simple and may make it sufficiently tractable so as to allow us to take other important effects such as elastic vibration, strain rate sensitivity, etc., into account. This is attempted in Part II.

II. ANALYSIS OF A STRUCTURE AS A SYSTEM OF ONE DEGREE OF FREEDOM

2.1 ASSUMPTIONS AND FORMULATION

We have seen in Part I that the major portion of the deformation occurs in the pattern such that the two halves of the beam rotate about the clamped ends; this is true for all compact cross-sections except for cases of short beams and small mass ratio. The analysis was based on the assumptions of rigid-perfectly plastic behavior and pure impulsive loading. Effects of high strain rate, elasticity and load duration were neglected. Several investigators have reported that the inclusion of a strain rate dependent yield stress in theoretical predictions is essential in order to obtain agreement with experiment for the permanent deformation of beams and rings [11][15]-[18]. Strain rate dependent analyses have been made for a number of cases of bending deformation [11][15]-[21]. We will now make an attempt to include the strain rate effect in the presence of axial force as well as bending moment by assuming the above mentioned pattern of deformation. We will also take account of the load duration and the elastic behavior in an approximate manner.

We assume that two halves of the beam rotate as straight bars about the clamped ends as if connected by hinges to the attached mass which is subjected to the transverse load $P(t)$ (Fig. 12). This neglects the deformation due to shear and the existence of finite plastic zones*. On this mode assumption, the mass of the half beams appears in the analysis just as an addition to the central mass m_o by amount $\frac{2}{3} m \ell$. This is clear when we consider the angular momentum of the half beam plus half the central mass with respect to a support (see Appendix 2(a)). Hence, we can regard the modified central mass.

*According to rigid-plastic simple beam theory, finite zones do not occur and this one degree of freedom type deformation takes place if $1 \leqq \frac{P\ell}{4M_o} \leqq 3(1 + \frac{m_o}{m\ell})$ (see Appendix 2(a)).

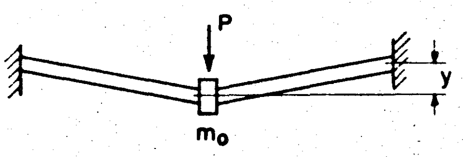

Fig. 12 Mode assumption

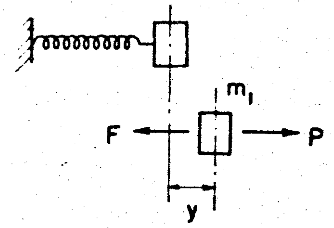

Fig. 13 One degree of freedom model

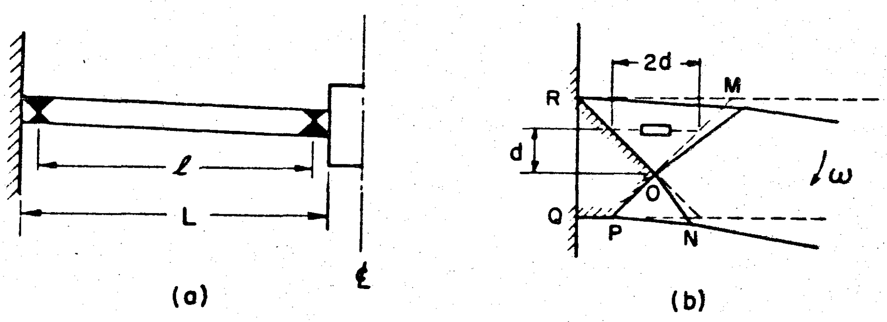

Fig. 14 Assumed plastic regions and relative motion

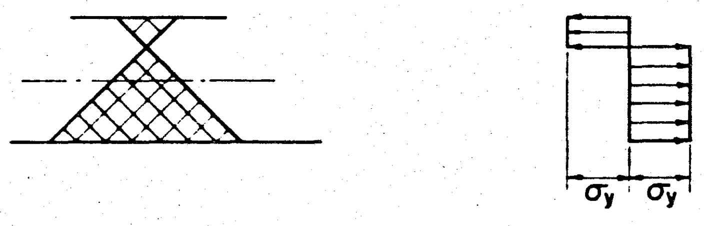

Fig. 15 Slip line field and stress distribution

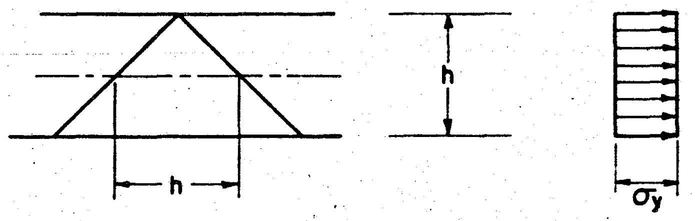

Fig. 16 Initiation of string stage

$$m_1 = m_o + \frac{2}{3} m\ell \qquad (2.1)$$

as supported by a massless beam of length 2ℓ, and as displaced by an amount y due to the load P. This problem is equivalent to the one degree of freedom model with non-linear rate dependent behavior as shown in Fig. 13. A resisting force F in the model corresponds in our structure to the vertical component (opposite to the direction of loading) of the force exerted on the mass by the beam and hence F is equal to twice the shear of the beam at the adjacent points; F is dependent on the rate of displacement $\dot{y}$ as well as the displacement y. Thus, our problem reduces to solving the ordinary differential equation

$$m_1\ddot{y} + F(y,\dot{y}) = P(t). \qquad (2.2)$$

It is assumed that the beam is composed of ductile material having elastic visco-plastic behavior with no strain-hardening, that the effect of shear stresses is negligible, and that the beam is so supported that lateral buckling or any other failure due to instability is prevented.

We will hereafter restrict ourselves to rectangular cross-sections only.

2.2 RESISTING FORCE

(1) Elastic range

On the basis of one degree of freedom mode assumption, it is permissible to find the resisting force from equilibrium consideration of each half beam. Neglecting both inertia and extensional deformation*, the shear at the end of a beam with length ℓ with infinitesimal transverse relative displacement y and zero slope angle at both ends is

$$Q_1 = \frac{2M_1}{\ell} = \frac{12EI\,y}{\ell^3} \qquad (2.3)$$

*The effect of axial constraints in elastic range is estimated in Appendix 1.

where EI is the flexural rigidity, and M_1 and Q_1 are the magnitudes of the moment and the shear at the ends, respectively. Hence,

$$F = 2Q_1 = \frac{24EI\ y}{\ell^3} . \tag{2.4}$$

This relation holds until y reaches the elastic limit displacement y_e, which we take to correspond to reaching the full plastic moment M_o and hence,

$$y_e = \frac{M_o \ell^2}{6EI} . \tag{2.5}$$

The plastic component δ of the displacement y is obtained by subtracting the elastic recovery y_{er} from the maximum displacement. y_{er} is the elastic limit displacement of a rigid frame with two inclined straight members as in Fig. 12. If we again consider only bending deformation, the difference between y_{er} and y_e arises only from the difference in the length of each straight member and its horizontal projection. Hence we can approximate

$$y_{er} \cong y_e \tag{2.6}$$

when elastic deformation itself is a small fraction of the total deformation.

(2) Interaction stage

As the deformation develops, the full plastic condition is first reached at the end points and points adjacent to the central mass. Axial forces arising from the constraints against axial motion of the ends may not be ignored in the plastic range due to finite deflection.

During an impact test, the strain rate is not uniform with time and with space and a complete inclusion of stress-strain rate relations in the analysis is extremely difficult owing to the complexity of the governing equations.

In the interaction problem of bending and extension, it might be permissible to make the common assumption that plane sections remain plane, and in this way to relate the dynamic bending moment and axial force to the curvature rate and extensional strain rate. However, this approach leads to cumbersome relations between the four quantities, and the analysis is intractable. Another possible starting point might be to assume that the static interaction relation for full plasticity keeps its form relating the resultant stresses M and N in dynamic action to dynamic yield resultant stresses in pure bending and pure tension, M_y and N_y, i.e.,

$$\left|\frac{M}{M_y}\right| + \left(\frac{N}{N_y}\right)^2 = 1 \tag{2.7}$$

where

$$M_y = \tfrac{1}{4}\sigma_y bh^2, \qquad N_y = \sigma_y bh \tag{2.8}$$

and σ_y is the dynamic yield stress in pure tension to be determined from the extensional strain rate $\dot{\varepsilon}$.

Alternatively, if we assume that plastic strains occur uniformly in triangular regions* as in Fig. 14(a), then a uniform stress distribution in both tension and compression sides follows and so does the interaction relation, Eq. (2.7). On the basis of the mode assumption there is an angular rotation ω of each rigid segment, with point O on the neutral axis indicating the axis of rotation (Fig. 14(b)). Velocity fields are assumed in the triangular regions so as to match this relative rotation. The figures show the section of the plastic hinge perpendicular to the axis of rotation. The assumed plastic region is composed of two isoceles right triangles, ORM and ONP, the larger one on the tension side. The region OPQR is taken as rigid; O

*This idea was first suggested by the upper bound theorem of limit analysis and the slip line field for a cantilever presented by Onat and Shield [22], and encouraged by the appearance of deformed aluminum specimens (see Fig. 26) during the experiment.

is the trace of the axis of rotation. The extensional strain rate $\dot{\varepsilon}$ of a horizontal element in tension side at distance d from the neutral axis is obtained as the ratio of the relative velocity component ωd in the horizontal direction to the length 2d to be $\frac{\omega}{2}$. Similarly in compression side $\dot{\varepsilon}$ is $-\frac{\omega}{2}$. These uniform extensional strain rates provide uniform dynamic stresses. If we adopt a constitutive relation for strain rate sensitive material of type

$$\dot{\varepsilon} = D\left(\frac{\sigma_y}{\sigma_o} - 1\right)^p \tag{2.9}$$

then the dynamic yield stress σ_y is obtained from

$$\frac{\omega}{2} = D\left(\frac{\sigma_y}{\sigma_o} - 1\right)^p \tag{2.10}$$

where D and p are material constants.

The above assumption of uniform strain rate has, however, some theoretical defects. First, the stress is not continuous across the rigid-plastic interfaces, i.e., the stress in the plastic region has a magnitude larger than the static limit stress σ_o while that in the rigid segments cannot exceed σ_o. This requires discontinuities in both shear stress parallel to the interface and normal stress perpendicular to the interface. Second, the inertia of the plastic regions must be ignored in assuming fields of uniform stress. Third, from the standpoint of the quasi-static slip line theory in plane strain, the above assumption is equivalent to the uniform slip line field of Fig. 15 and this cannot transmit any shear*.

Despite these theoretical defects, we shall use the assumption because of its simplicity. We note that the assumption gives the relation

$$\frac{M_y}{M_o} = \frac{N_y}{N_o} = \frac{\sigma_y}{\sigma_o} . \tag{2.11}$$

*Gillis applies a similar slip line field independently for the pure bending deformation of a cantilever beam with a tip mass subjected to dynamic loading and discusses difficulties of the assumption from slip line theory [23] .

On this assumption we regard the small rigid region between a support and the adjacent plastic region as belonging to the support rather than being a part of the beam (and also the region between the central boss and the adjacent plastic region as belonging to the boss). It may be appropriate to use an approximate effective length of the half beam as

$$\ell = L - h \tag{2.12}$$

where L is the real length between the support and the central boss. We use this value as the half beam length throughout the analysis in Part II.

The shear at the ends of the massless half beam is

$$Q_1 = \frac{2M_1 + N_1 y}{\ell} . \tag{2.13}$$

The axial force N_1 and the bending moment M_1 of the plastic hinges must satisfy the plasticity condition Eq. (2.7) or

$$\frac{M_1}{M_y} + \left(\frac{N_1}{N_y}\right)^2 = 1 \tag{2.14}$$

and the normality condition

$$\frac{N_1}{N_y} = \frac{N_y y}{4M_y} = \frac{N_o y}{4M_o} . \tag{2.15}$$

Using Eqs. (2.13), (2.14) and (2.15), we obtain

$$F = 2Q_1 = \frac{4M_y}{\ell} \left\{ 1 + \left(\frac{N_o y}{4M_o}\right)^2 \right\} . \tag{2.16}$$

From Eqs. (2.10), (2.11) and (2.16), and the relation $\omega = \frac{\dot{y}}{\ell}$, we find

$$F = \frac{4M_o}{\ell} \left\{ 1 + \left(\frac{\dot{y}}{2D\ell}\right)^{\frac{1}{p}} \right\} \left\{ 1 + \left(\frac{N_o y}{4M_o}\right)^2 \right\} . \tag{2.17}$$

As deformation develops the neutral axis at the extensible hinge approaches the extreme fiber of the beam and finally the entire cross-section is subjected to tensile stress, with $\frac{N_1}{N_y} = \frac{N_o y}{4M_o} = 1$ as in Fig. 16 ($\frac{N_o y}{4M_o} = 1$ implies $y = h$). Hence, Eq. (2.17) holds only for

$$\frac{N_o y}{4M_o} \leqq 1 . \tag{2.18}$$

(3) String stage

The axial force $N_1 = N_y$ for deformation such that $\frac{N_o y}{4M_o} \geqq 1$, N_y depending upon the rate of extensional strain. On our assumption, plastic deformation has been concentrated in hinges so far. At the initiation of the string stage, extensional strain of the beam axis is concentrated within the length h (see Fig. 16). As the deformation develops and the beam is stretched, this plastic regime may increase in length. Let the length of a plastic regime in the string stage be s. Then the strain increment is

$$d\varepsilon = \frac{d(\sqrt{\ell^2 + y^2})}{2s} = \frac{y dy}{2s\sqrt{\ell^2 + y^2}} . \tag{2.19}$$

Notice that $s = h = y$ at the initiation of the string stage. Considering that s increases as y does, we make the drastic assumption

$$s \cong y \tag{2.20}$$

until the plastic regimes extend to the whole beam. This assumption may be permissible because of weak dependence of dynamic yield stresses on strain-rate. To this accuracy, we approximate $\sqrt{\ell^2 + y^2} \cong \ell$. Thus, for the estimation of strain rate, we use

$$\dot{\varepsilon} = \frac{\dot{y}}{2\ell} . \tag{2.21}$$

Note that the above ad hoc assumption gives a continuous transition for the strain rate $\dot{\varepsilon}$ of the beam axis and that pure extension or $\dot{\kappa} = 0$ is permitted by the flow rule. Thus, Eqs. (2.9) (2.11) and (2.21) give

$$N_1 = N_y = N_o \left\{ 1 + \left(\frac{\dot{y}}{2D\ell}\right)^{\frac{1}{p}} \right\}. \tag{2.22}$$

The plastic regimes extend over the whole beam length when $2s = \ell$ or $\frac{y}{\ell} \cong \frac{1}{2}$ according to Eq. (2.20). Deformation beyond this point is of less interest because most structural metals would fracture before reaching this large a deformation (note that large strains occur in small regions).

The resisting force F equals twice the vertical component of the axial force and hence

$$F = 2N_o \left\{ 1 + \left(\frac{\dot{y}}{2D\ell}\right)^{\frac{1}{p}} \right\} \frac{y}{\sqrt{\ell^2 + y^2}} . \tag{2.23}$$

Formulas, Eqs. (2.17) and (2.23) for the resisting force do not apply for the unloading condition or for $\dot{y} \leqq 0$.

2.3 SOLUTION

We now solve Eq. (2.2) in which F is given for $\dot{y} \geqq 0$ by

$$F = \begin{cases} \dfrac{24EIy}{\ell^3} & \text{if } 0 \leqq \dfrac{N_o y}{4M_o} < \dfrac{N_o y_e}{4M_o} \\ \dfrac{4M_o}{\ell} \left\{ 1 + \left(\dfrac{\dot{y}}{2D\ell}\right)^{\frac{1}{p}} \right\} \left\{ 1 + \left(\dfrac{N_o y}{4M_o}\right)^2 \right\} & \text{if } \dfrac{N_o y_e}{4M_o} \leqq \dfrac{N_o y}{4M_o} \leqq 1 \\ 2N_o \left\{ 1 + \left(\dfrac{\dot{y}}{2D\ell}\right)^{\frac{1}{p}} \right\} \dfrac{y}{\sqrt{\ell^2+y^2}} & \text{if } 1 < \dfrac{N_o y}{4M_o} \end{cases} \tag{2.24}$$

where $\frac{N_o y_e}{4M_o}$ is the elastic parameter given from Eq. (2.5) as

$$\frac{N_o y_e}{4M_o} = \frac{N_o \ell^2}{24EI} . \tag{2.25}$$

It is convenient to use $\frac{N_o y}{4M_o}$ for a nondimensional displacement $\left(\frac{N_o y}{4M_o} = \frac{y}{h}\right)$. The final plastic displacement δ is obtained from the maximum displacement y_m as

$$\frac{N_o\delta}{4M_o} = \frac{N_o y_m}{4M_o} - \frac{N_o y_{er}}{4M_o} \simeq \frac{N_o y_m}{4M_o} - \frac{N_o y_e}{4M_o} . \qquad (2.26)$$

Let us consider rectangular pulse loading with magnitude P_o, duration time T starting at $t = 0$:

$$P(t) = P_o\{ H(t) - H(t-T)\} \qquad (2.27)$$

where $H(t)$ is Heaviside's unit step function. P_o is large and T is small but both are finite. We assume that T is so small that the load application is completed before the elastic limit displacement is reached.

We introduce two nondimensional loading parameters $\frac{P_o \ell}{4M_o}$ and $\frac{N_o\delta*}{4M_o}$ instead of P_o and T. The former is related to the magnitude of the load and the latter to the total impulse. δ^* is the final plastic displacement obtained from the rigid-plastic simple bending theory based on the one degree of freedom mode in case the impulse P_oT is applied impulsively; this is obtained by equating the initial kinetic energy $\frac{(P_oT)^2}{2m_1}$ to the plastic work done $\frac{4M_o\delta^*}{\ell}$ to be

$$\delta^* = \frac{(P_oT)^2\ell}{8M_o m_1} . \qquad (2.28)$$

Parameter $\frac{P_o\ell}{4M_o}$ is the ratio of the load magnitude to the plastic collapse load for the clamped beam. It is noted that $\frac{N_o\delta^*}{4M_o} = \frac{\delta^*}{h}$.

We define energy ratio R^* to be the ratio of the plastic work done for the displacement δ^* under constant limit resisting force F_e to the maximum elastic energy

$$R^* \equiv \frac{F_e\delta^*}{\frac{1}{2}F_e y_e} = \frac{2\delta^*}{y_e} . \qquad (2.29)$$

Let t_e, t_t and t_m be the times at which the elastic limit displacement, string stage and maximum displacement are reached, respectively, under condition that $\dot{y} \geqq 0$.

Solution of Eqs. (2.2), (2.24) and (2.27) for $0 \leq t \leq T$ is

$$\frac{N_o y}{4M_o} = \frac{P_o \ell}{4M_o} \frac{N_o y_e}{4M_o} \left(1-\cos \lambda \frac{t}{T}\right) \tag{2.30}$$

and for $T \leq t \leq t_e$ is

$$\frac{N_o y}{4M_o} = 2 \frac{P_o \ell}{4M_o} \frac{N_o y_e}{4M_o} \quad \sin \frac{\lambda}{2} \cos \left\{ \lambda \left(\frac{t}{T} -1\right) - \psi \right\} \tag{2.31}$$

where

$$\lambda \equiv T \sqrt{\frac{24EI}{m_1 \ell^3}} = \frac{4M_o}{P_o \ell} \sqrt{2 \frac{\delta^*}{y_e}} = \frac{4M_o}{P_o \ell} \sqrt{R^*} \tag{2.32}$$

$$\tan \psi \equiv \frac{\sin \lambda}{1-\cos \lambda} = \cot \frac{\lambda}{2} . \tag{2.33}$$

The condition $(y)_{t=T} \leq y_e$ requires

$$\frac{P_o \ell}{4M_o} (1-\cos \lambda) \leq 1 . \tag{2.34}$$

If the condition

$$2 \frac{P_o \ell}{4M_o} \sin \frac{\lambda}{2} > 1 \tag{2.35}$$

is satisfied, plastic deformation takes place. Introducing the nondimensional velocity

$$u \equiv \frac{\sqrt{N_o m_1 \ell}}{4M_o} \dot{y}, \tag{2.36}$$

$u_e \equiv (u)_{t=t_e}$ is obtained from

$$u_e^2 = \frac{N_o y_e}{4M_o} \left\{ \left(2 \frac{P_o \ell}{4M_o} \sin \frac{\lambda}{2}\right)^2 - 1 \right\}. \tag{2.37}$$

The solution for $t_e \leq t \leq t_t$ is obtained from

$$J(u) + \frac{N_o y}{4M_o} + \frac{1}{3}\left(\frac{N_o y}{4M_o}\right)^3 = J(u_e) + \frac{N_o y_e}{4M_o} + \frac{1}{3}\left(\frac{N_o y_e}{4M_o}\right)^3 \tag{2.38}$$

where

$$J(u) \equiv \int_0^u \frac{x\,dx}{1+kx^{\frac{1}{p}}}, \qquad k \equiv \left(\frac{2M_o}{D\ell\sqrt{N_o m_1 \ell}}\right)^{\frac{1}{p}}. \tag{2.39}$$

When p is an integer, the integral $J(u)$ can be easily evaluated by the substitution of $x^{\frac{1}{p}}$ by another variable of integration.

The maximum displacement y_m is obtained from Eq. (2.38) by setting $u = 0$ as

$$\frac{N_o y_m}{4M_o} + \frac{1}{3}\left(\frac{N_o y_m}{4M_o}\right)^3 = J(u_e) + \frac{N_o y_e}{4M_o} + \frac{1}{3}\left(\frac{N_o y_e}{4M_o}\right)^3 \tag{2.40}$$

so long as $\frac{N_o y_m}{4M_o} \leqq 1$ or

$$J(u_e) + \frac{N_o y_e}{4M_o} + \frac{1}{3}\left(\frac{N_o y_e}{4M_o}\right)^3 \leqq \frac{4}{3}. \tag{2.41}$$

If Inequality (2.41) is not satisfied, then the string stage is reached and u takes the value u_t at $t = t_t$ given by

$$J(u_t) = J(u_e) + \frac{N_o y_e}{4M_o} + \frac{1}{3}\left(\frac{N_o y_e}{4M_o}\right)^3 - \frac{4}{3}. \tag{2.42}$$

The solution for $t_t \leqq t \leqq t_m$ is obtained from

$$\frac{1}{2}\frac{4M_o}{N_o\ell}J(u) + \sqrt{\left(\frac{N_o\ell}{4M_o}\right)^2 + \left(\frac{N_o y}{4M_o}\right)^2} = \frac{1}{2}\frac{4M_o}{N_o\ell}J(u_t) + \sqrt{\left(\frac{N_o\ell}{4M_o}\right)^2 + 1} \tag{4.43}$$

and y_m is obtained from

$$\left(\frac{N_o y_m}{4M_o}\right)^2 = \left\{\frac{1}{2}\frac{4M_o}{N_o\ell}J(u_t) + \sqrt{\left(\frac{N_o\ell}{4M_o}\right)^2 + 1}\right\}^2 - \left(\frac{N_o\ell}{4M_o}\right)^2 \tag{4.44}$$

so long as

$$1 \leqq \frac{N_o y_m}{4M_o} \leqq \frac{1}{2}\frac{N_o\ell}{4M_o}. \tag{4.45}$$

It should be recalled that $\frac{N_o\ell}{4M_o} \equiv \gamma = \frac{\ell}{h}$.

For a strain-rate insensitive material, $k = 0$ and

$$J(u) = \frac{u^2}{2}. \tag{2.46}$$

For the clamped beam without axial constraints, by omitting the cubic terms in Eq. (2.40) we have

$$\frac{N_o y_m}{4M_o} - \frac{N_o y_e}{4M_o} = J(u_e). \tag{2.47}$$

For impulsive loading, taking the limit $\frac{P_o \ell}{4M_o} \rightarrow \infty$ in Eq. (2.37) we obtain

$$u_e^2 = 2\frac{N_o \delta^*}{4M_o} - \frac{N_o y_e}{4M_o} = \frac{N_o y_e}{4M_o}(R^*-1). \tag{2.48}$$

For a strain-rate insensitive beam without axial constraints under impulsive loading, from Eqs. (2.46), (2.47) and (2.48), we have

$$\frac{N_o y_m}{4M_o} - \frac{N_o y_e}{4M_o} = \frac{u_e^2}{2} = \frac{N_o \delta^*}{4M_o} - \frac{1}{2}\frac{N_o y_e}{4M_o} = \frac{1}{2}\frac{N_o y_e}{4M_o}(R^*-1). \tag{2.49}$$

For a rigid-perfectly plastic fully clamped beam subjected to impulsive loading

$$y_e = k = 0, \qquad \delta = y_m, \qquad J(u_e) = \frac{N_o \delta^*}{4M_o}$$

and Eq. (2.40) becomes

$$\frac{N_o \delta}{4M_o} + \frac{1}{3}\left(\frac{N_o \delta}{4M_o}\right)^3 = \frac{N_o \delta^*}{4M_o} \tag{2.50}$$

This is equivalent to the last equation of Part I because

$$\frac{N_o \delta^*}{4M_o} = \frac{9\alpha\beta\gamma}{2(2+3\beta)}. \tag{2.51}$$

2.4 EXAMPLE

If input parameter $\frac{N_o \delta^*}{4M_o} = 2$, load magnitude parameter $\frac{P_o \ell}{4M_o} = 10$, elastic parameter $\frac{N_o y_e}{4M_o} = \frac{N_o y_{er}}{4M_o} = \frac{1}{5}$, strain rate parameter $k = 1$ and the power $p = 5$, then from Eq. (2.32)

$$\lambda = \frac{4M_o}{P_o \ell} \sqrt{2 \frac{N_o \delta^*}{4M_o} \frac{4M_o}{N_o y_e}} = 0.447.$$

Condition (2.34) is satisfied because

$$\frac{P_o \ell}{4M_o} (1-\cos\lambda) = 0.983 < 1.$$

Eq. (2.37) gives

$$u_e^2 = \frac{N_o y_e}{4M_o} \left\{ \left(2 \frac{P_o \ell}{4M_o} \sin \frac{\lambda}{2}\right)^2 - 1 \right\} = 3.74$$

or

$$u_e = 1.93.$$

From Eq. (2.39)

$$J(u_e) = \int_0^{u_e} \frac{x dx}{1+x^{\frac{1}{5}}} = 0.900.$$

From Eq. (2.40)

$$\frac{N_o y_m}{4M_o} + \frac{1}{3}\left(\frac{N_o y_m}{4M_o}\right)^3 = J(u_e) + \frac{N_o y_e}{4M_o} + \frac{1}{3}\left(\frac{N_o y_e}{4M_o}\right)^3 = 1.103.$$

Hence,

$$\frac{N_o y_m}{4M_o} = 0.878 < 1.$$

Therefore, Eq. (2.26) gives

$$\frac{N_o \delta}{4M_o} = \frac{N_o y_m}{4M_o} - \frac{N_o y_e}{4M_o} = 0.678.$$

If we neglect the effect of axial constraint, Eq. (2.47) gives

$$\frac{N_o \delta}{4M_o} = J(u_e) = 0.900.$$

If the strain rate effect is neglected, from Eq. (2.46)

$$J(u_e) = \frac{u_e^2}{2} = 1.86.$$

Since it is clear that

$$\frac{N_o y_m}{4M_o} > 1,$$

string stage is considered to be reached and another parameter $\frac{N_o \ell}{4M_o}$ is needed. We take, say, $\frac{N_o \ell}{4M_o} = 10$. Eq. (2.42) gives

$$J(u_t) = J(u_e) + \frac{N_o y_e}{4M_o} + \frac{1}{3}\left(\frac{N_o y_e}{4M_o}\right)^3 - \frac{4}{3} = 0.73.$$

Hence, Eq. (2.44) gives

$$\left(\frac{N_o y_m}{4M_o}\right)^2 = \left\{\sqrt{\left(\frac{N_o \ell}{4M_o}\right)^2 + 1} + \frac{1}{2}\,\frac{4M_o}{P_o \ell}\,J(u_t)\right\}^2 - \left(\frac{N_o \ell}{4M_o}\right)^2 = 1.74$$

or

$$\frac{N_o y_m}{4M_o} = 1.32 < \frac{1}{2}\,\frac{N_o \ell}{4M_o}\ .$$

Thus, we have

$$\frac{N_o \delta}{4M_o} = 1.12.$$

If we neglect the effects of axial constraint and strain rate, from Eqs. (2.46) and (2.47) we have

$$\frac{N_o \delta}{4M_o} = J(u_e) = 1.86.$$

III. EXPERIMENTAL STUDY

3.1 DESCRIPTION OF THE EXPERIMENT

(1) Scope of the tests

The test program employed clamped beams of rectangular cross-section, with and without axial constraint, with a boss at the center. Tests were made with the mass ratio $\beta \equiv \frac{m_o}{m\ell} = 10$ and the length ratio $\gamma \equiv \frac{N_o \ell}{4M_o} = 15$. A total of thirty specimens of aluminum alloy 6061-T6 and hot rolled mild steel 1020 were tested and compared with the theories developed.

(2) General arrangement

The schematic diagram Fig. 17 shows the general arrangement of the experiment. A specimen was held on a ballistic pendulum through a specimen holder which was designed to obtain the desired boundary conditions. The pendulum served as a means of measuring the applied impulse, and was assumed to be a simple pendulum. The load, produced by detonating an electric blasting cap, is assumed to be impulsively applied to the specimen and the pendulum. It is treated as a pure impulse, neglecting the deformation time in comparison with the natural period of the pendulum. The impulse was calculated from the measured values of the amplitude, period and weight of the pendulum.

(3) Equipment

Fig. 18 shows the specimen holder. A fully clamped end condition was produced by means of serrated surfaces which were made of oil-hardened tool steel. For the constraint against rotation but not axial motion, the serrated surfaces were covered by two steel blocks at each support, and teflon sheets were placed between the specimen and the steel blocks in order to permit free axial motion. The upper part of the specimen holder had a hole through which a blasting cap and its container were mounted at the center of the central boss of the specimen, and this was held on the lower part by

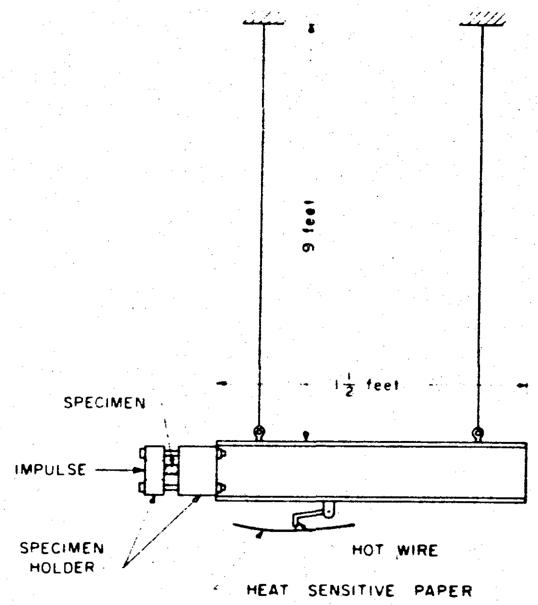

Fig. 17 Schematic diagram for ballistic pendulum

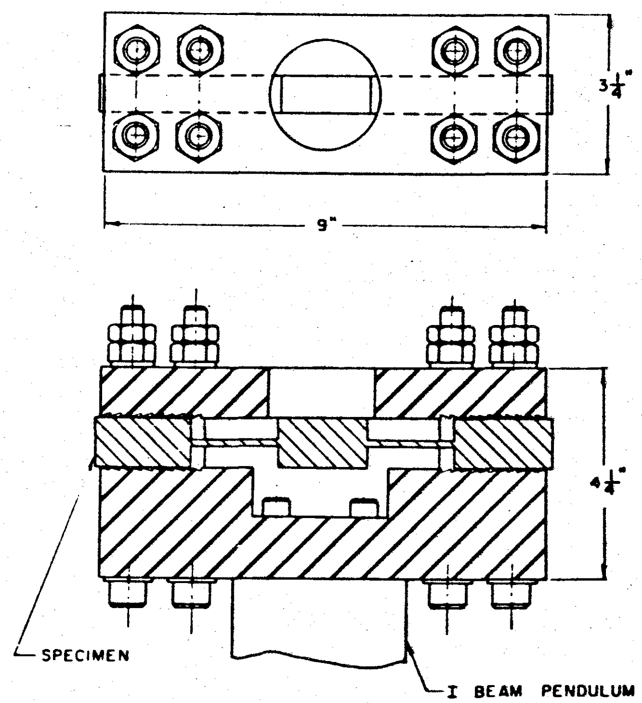

Fig. 18 Specimen holder

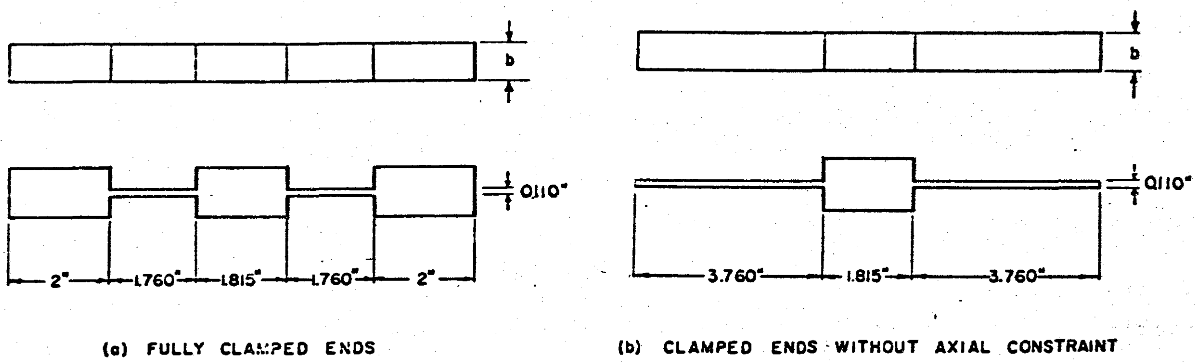

Fig. 19 Specimens

eight bolts.

The amplitude of the pendulum swing was recorded by means of an attached hot wire passing over stationary heat sensitive paper.

(4) Specimen and material properties

The shape of specimens is shown in Fig. 19. The beam specimen, ends, and the central mass were machined from a single block of metal, in order to have the desired end conditions, continuity, and mass ratio. The block was taken from plate stock so that the beam axis lay in the direction of rolling. There was no heat treatment. It is assumed that the size of the central mass does not affect the deformation so long as it can be taken as rigid and does not rotate. For beams without axial constraint the beam parts of the specimen were extended towards both supports and for fully constrained beams the supported parts were made much thicker than the beam parts so that the deformation at the supports would be negligible in comparison with that in the beam sections.

The beam depth was chosen as $h = 0.110$ inch. Other dimensions of the specimen were chosen to give the length ratio $\gamma = 15$ and the mass ratio $\beta = 10$. The actual half beam length L was made larger than the effective length ℓ by an amount equal to the beam depth h. The width of the beam was varied from 0.470 inch to 1.000 inch to obtain a suitable range of the input parameter $(\frac{N_o \delta^*}{4M_o} = 21.1\alpha)$.

Standard $\frac{1}{2}$ inch round tension test specimens (0.505 inch diameter) were taken from four corners of the plate stock (for both the 6061-T6 aluminum alloy and the mild steel). Stress-strain curves obtained in the tension test are shown in Figs. 20 and 21. These were recorded by Riehle testing machine. The aluminum alloy appears to have characteristics close to elastic-perfectly plastic material in the static test, whereas the mild steel shows appreciable strain-hardening. Average values of yield stresses

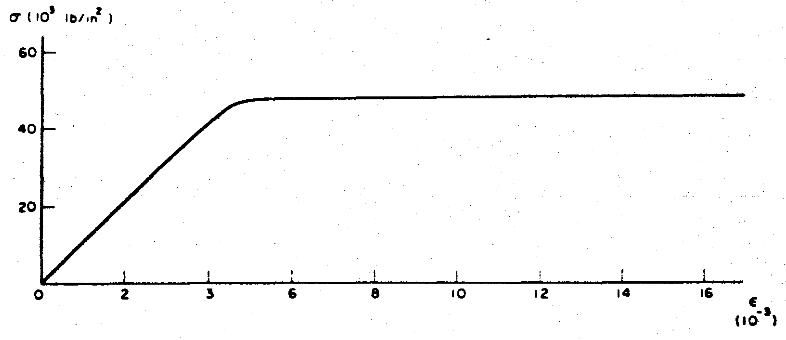

Fig. 20 Stress-strain curve for 6061-T6 aluminum alloy

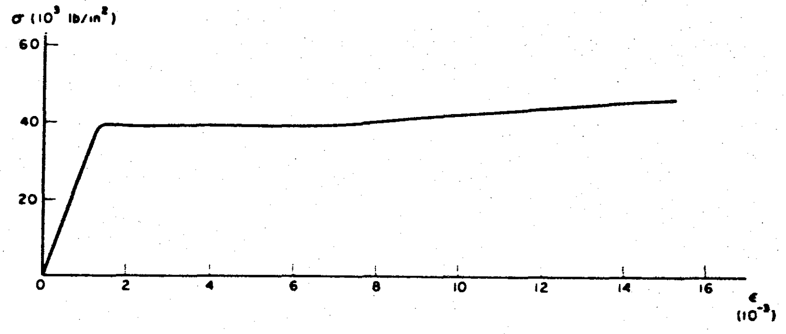

Fig. 21 Stress-strain curve for 1020 mild steel

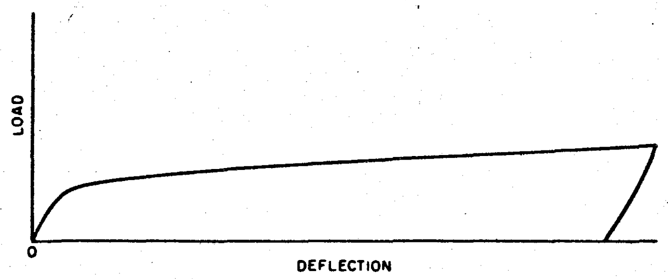

STATIC LOAD-DEFLECTION RELATION FOR CLAMPED BEAM OF MILD STEEL

Fig. 22

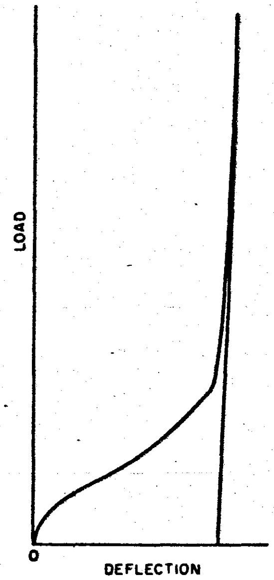

STATIC LOAD-DEFLECTION RELATION FOR FULLY CLAMPED BEAM OF MILD STEEL

Fig. 23

are listed in Table 2. In Figs. 22 and 23 are shown load-deflection relations in static tests for beams with and without axial constraint of mild steel for comparison with the dynamic test results. We see in Fig. 23 the transition behavior from elastic bending toward string stage. No difference in the shape of deformation was observed between static and dynamic tests.

Table 2. Properties and Classification of Specimens

(1) Common properties for 6061-T6 aluminum alloy specimens

$E = 10.25 \times 10^6$ lb/in^2

$\sigma_o = 46,550$ lb/in^2

density $= 0.0984$ lb/in^3

$$\frac{N_o y_e}{4M_o} = \frac{y_e}{h} = \frac{1}{2}\frac{\sigma_o}{E}\left(\frac{\ell}{h}\right)^2 = 0.509$$

(2) Common properties for 1020 mild steel specimens

$E = 30.1 \times 10^6$ lb/in^2

$\sigma_o = 39,700$ lb/in^2

density $= 0.283$ lb/in^3

$$\frac{N_o y_e}{4M_o} = 0.149$$

(3) Classification of specimens

$\beta = 10$	Aluminum alloy	Fully clamped beam	: A1
$\gamma = 15$		Clamped beam	: A2
	Mild steel	Fully clamped beam	: S1
		Clamped beam	: S2

(5) Loading

Dupont Instantaneous Electric Blasting Caps, type E-3B and E 77, were used in order to get the desired impulse for various specimen widths.

Attention was paid to the possibility that some of the impulse caught by the pendulum directly reaches the specimen holder or the pendulum without being applied to the specimen. In order to avoid this possibility, a blasting cap was held by an aluminum cylinder (container) which was cemented on the central boss and then a small plug (pellet) of some $\frac{1}{8}$ inch length with the diameter of the blasting cap was placed in the hole between the blasting cap and the boss. The lightest cylinder which would not break on explosion was used. It was hoped that this device would give a concentrated load on the central boss. The aluminum cylinder and the plug detached instantly on explosion from the specimen and hence it was believed that they did not affect the mass of the specimen.

The measurement of the load-time relation was not attempted. The applied impulse was calculated from the relation for a simple pendulum:

$$I = \frac{2\pi W a_o}{g T_o}$$

where W is the weight of the pendulum (including the specimen and its holder), a_o the amplitude (determined at each test) and T_o the period of the pendulum. The amplitude a_o of an undamped pendulum was determined by extrapolation from measurement of the amplitude of several swings. In our tests the following values were used: $T_o = 3.37$ sec., $W = 32.1$ to 33.4 lbs. and $2a_o = 2.03$ to 11.69 in.

(6) Deflection measurement

The specimen was taken off the holder after testing and placed on a surface plate. The relative displacement at the distance of the effective length was measured for each half beam by a dial gage mounted on a height gage, which was placed on the surface plate. The average value of the relative displacement between both halves was taken as the plastic deflection δ.

3.2 RESULTS AND DISCUSSION

Figs. 24, 25, 26(a) and 26(b) show typical shapes of the specimens after tests. The beam parts of the specimen have remained essentially straight except for small regions adjacent to the supports and the central boss. Figs. 26(a) and (b)* show clearly how the deformation is concentrated at those regions, which seem to have a triangular shape as assumed in Part II. Somewhat larger and less distinct deformation regions were observed in mild steel (see Fig. 25).

Test results are listed in Table 3 and are compared with the theoretical predictions in Figs. 27 and 28 using the dimensionless parameters introduced in Part II. Solid curves are drawn from the theory in Part II and dotted curves in Part I. As for the strain rate effect, the constitutive equations of Bodner and Symonds [16][17]

---

*These specimen have values: $\beta = 1.0$ and $\gamma = 5$; this series of tests was originally planned but the loading impulse was not measured successfully because of small central boss. For this amount of deformation, the string stage is not yet reached ($\delta < h$).

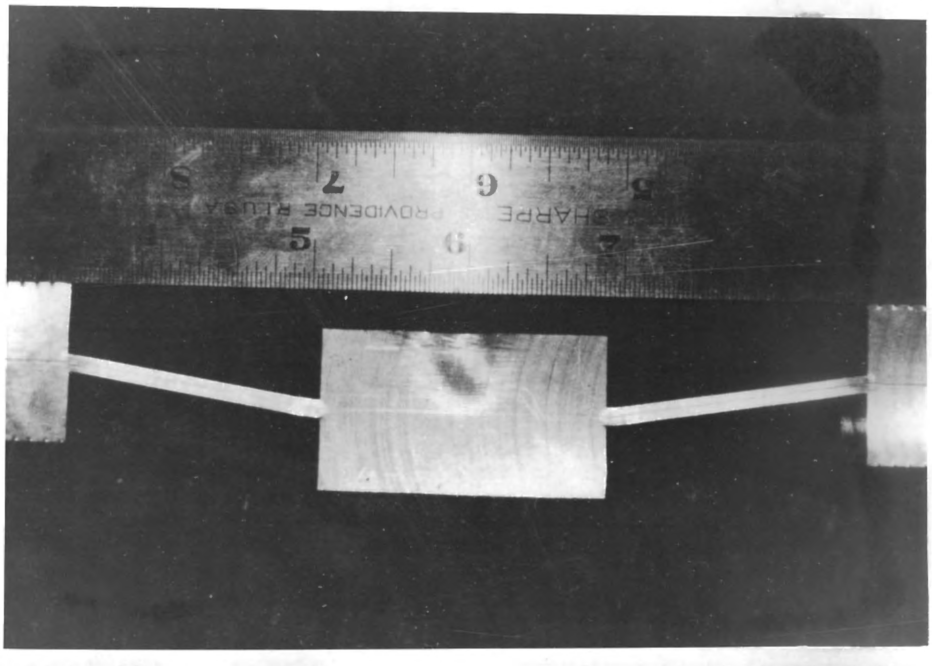

Fig. 24 Aluminum specimen of fully clamped beam after test

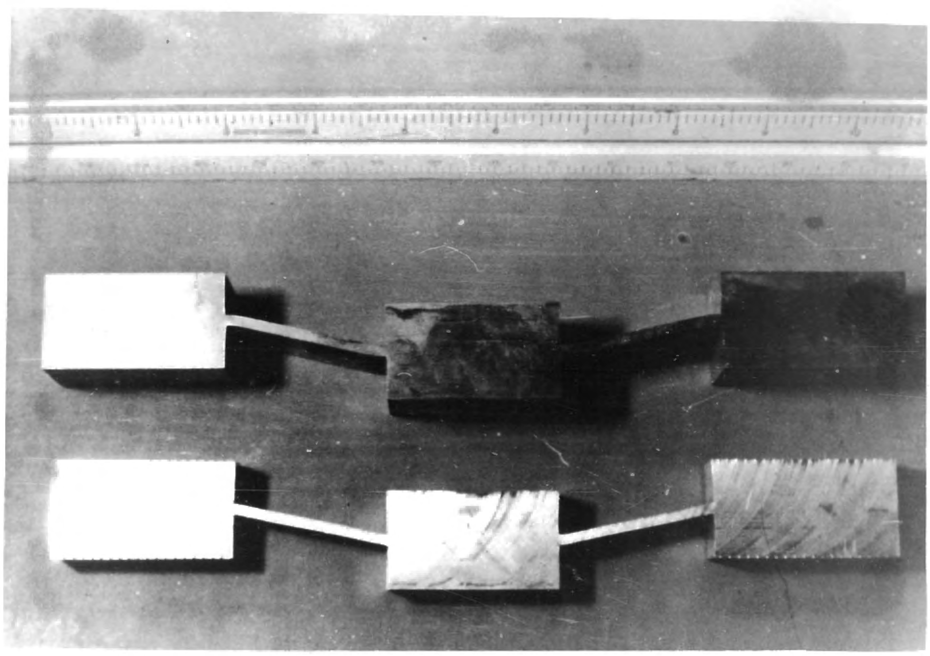

Fig. 25 Specimens after test; mild steel(above) and aluminum(below)

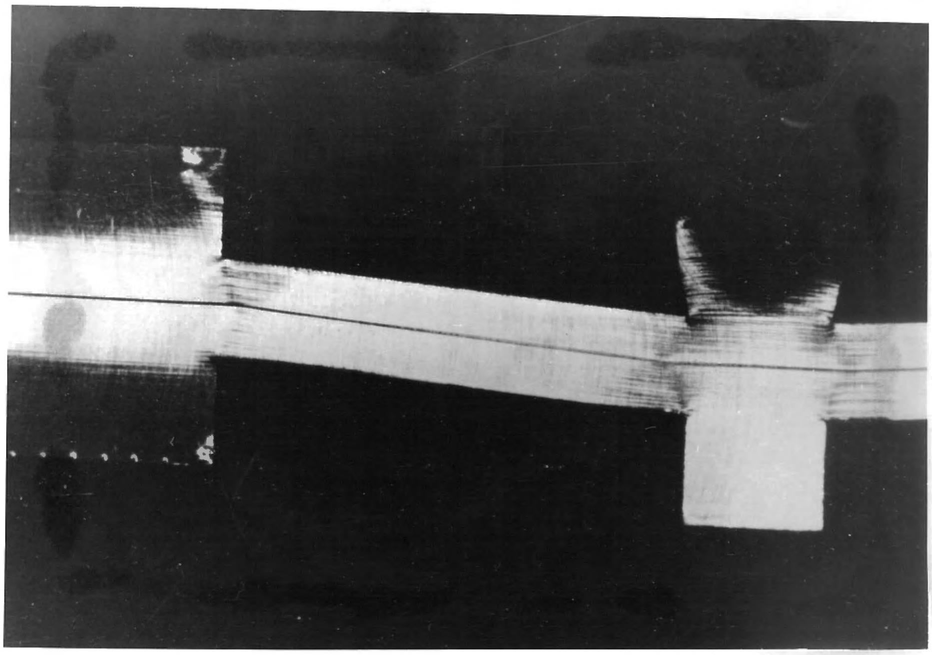

(a)

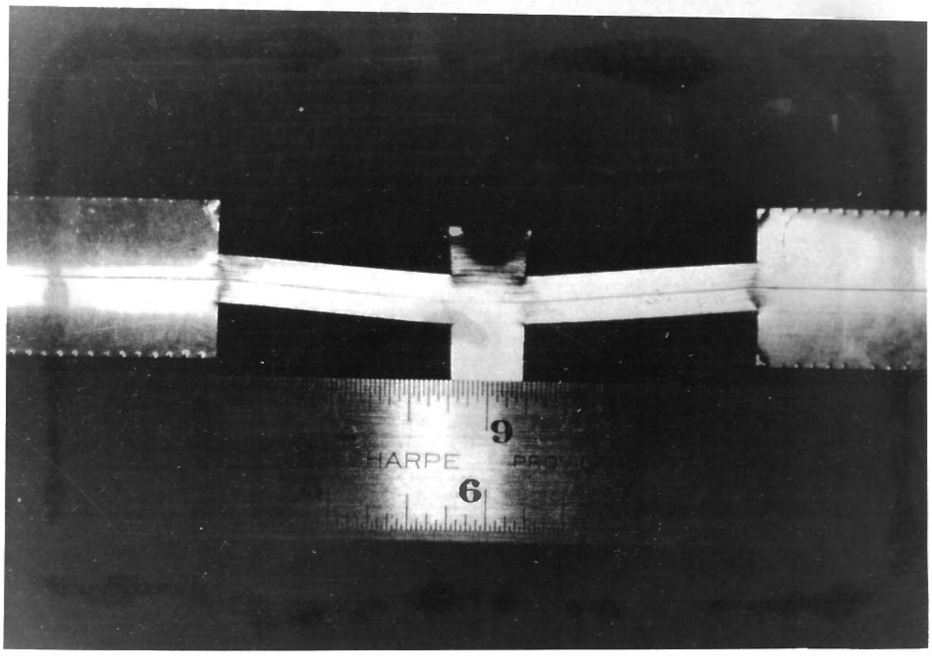

(b)

Fig. 26 Deformation pattern of aluminum specimens

$$\dot{\varepsilon} = 6500 \left(\frac{\sigma_y}{\sigma_o} - 1\right)^4 \qquad \text{for 6061-T6 aluminum alloy}$$

$$\dot{\varepsilon} = 40.4 \left(\frac{\sigma_y}{\sigma_o} - 1\right)^5 \qquad \text{for mild steel}$$

were used where $\dot{\varepsilon}$ is extensional strain-rate in sec^{-1}. In this calculation, the load was taken as impulsive. The effect of load shape is found to be small when elastic effect is taken account (see Appendix 2(b)).

Most significant consequence is that considerable effects of axial constraint are observed both in theory and experiment. In general, experimental results agree quite well for the permanent deformation with the theoretical predictions in Part II which takes account of the strain-rate and elastic effects. A satisfactory agreement is seen for the aluminum specimens (Fig. 27). For the mild steel specimens the experimental results for the fully clamped beams lie consistently a little below the theoretical curve. The reason for this may be that the deformation is not localized in mild steel as much as in aluminum alloy (so that the assumption of concentrated plastic regions or one degree of freedom mode is less appropriate for mild steel) and also that the strain-hardening is neglected in the theory.

Apparently rigid-plastic theory may well be used as a first approximation for large deformations. (Rigid plastic theory will improve when load shape is taken into account, see Appendix 2(a).)

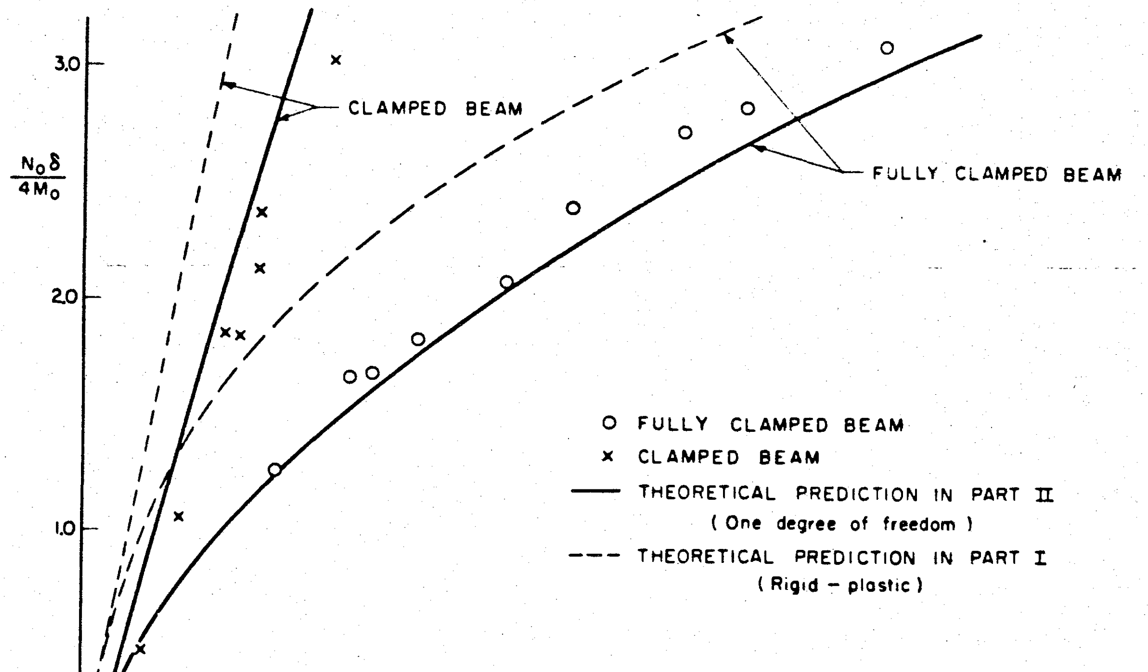

FIG. 27 TEST RESULTS — 6061-T6 ALUMINUM ALLOY

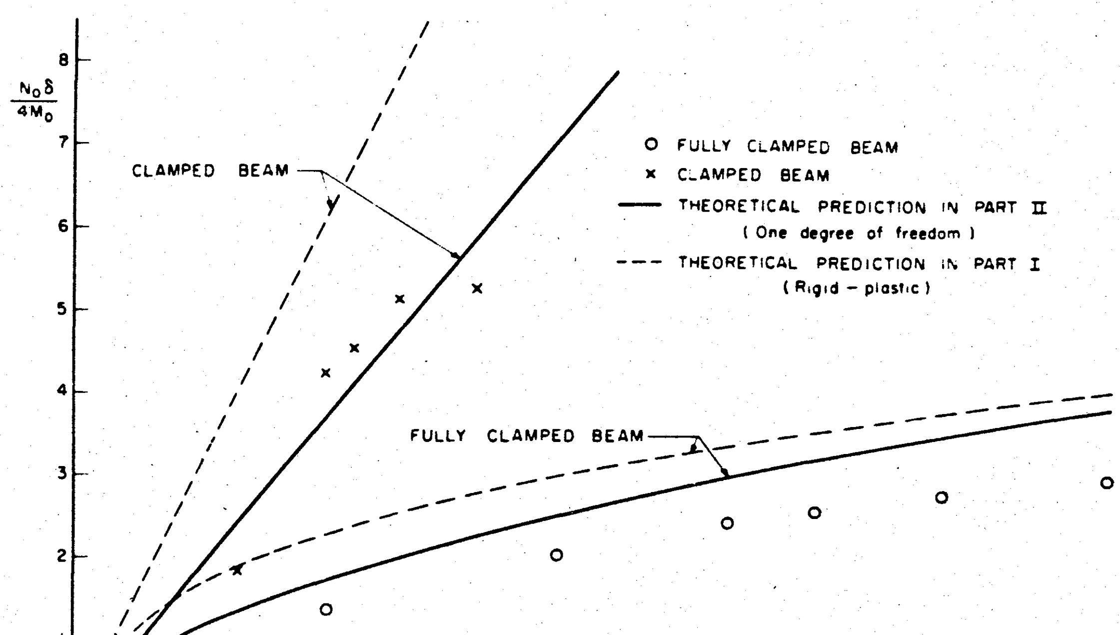

FIG 28 TEST RESULTS — MILD STEEL

Table 3. Experimental Results

Number	h in.	ℓ in.	b in.	I lb. sec.	δ in.	$\frac{N_o\delta^*}{4M_o} = \frac{\delta^*}{h}$	$\frac{N_o\delta}{4M_o} = \frac{\delta}{h}$	$R^* = \frac{2\delta^*}{y_e}$
A1-1	0.110	1.650	1.000	0.394	0.138	4.18	1.26	16.4
2	"	"	0.470	0.218	0.184	5.76	1.67	22.6
3	"	"	0.740	0.370	0.184	6.23	1.68	24.5
4	"	"	1.000	0.516	0.201	7.20	1.83	28.3
5	"	"	0.470	0.273	0.230	9.10	2.08	35.7
6	"	"	0.740	0.463	0.264	10.6	2.40	41.4
7	"	"	0.610	0.423	0.301	12.9	2.93	50.8
8	"	"	0.610	0.444	0.313	14.3	2.84	55.9
9	"	"	0.530	0.425	0.341	17.3	3.11	67.9
A2-1	"	"	0.740	0.164	0.031	1.31	0.28	5.1
2	"	"	1.000	0.284	0.116	2.11	1.06	8.3
3	"	"	0.740	0.252	0.202	3.10	1.85	12.2
4	"	"	1.000	0.356	0.202	3.40	1.84	13.4
5	"	"	0.610	0.231	0.261	3.84	2.37	15.1
6	"	"	0.740	0.280	0.234	3.84	2.13	15.1
7	"	"	0.470	0.203	0.333	5.38	3.03	21.1
S1-1	"	"	0.810	0.408	0.077	2.78	0.700	37.3
2	"	"	0.661	0.339	0.080	2.87	0.727	38.5
3	"	"	1.150	0.646	0.103	3.45	0.938	46.3
4	"	"	0.610	0.460	0.150	6.22	1.36	83.5
5	"	"	0.929	0.964	0.212	11.8	2.02	158
6	"	"	0.808	0.980	0.263	16.0	2.41	215
7	"	"	0.710	0.913	0.279	18.2	2.54	244
8	"	"	0.660	0.920	0.299	21.3	2.72	286
9	"	"	0.568	0.864	0.313	25.3	2.85	340
S2-1	"	"	1.150	0.697	0.200	4.03	1.82	54.8
2	"	"	0.810	0.603	0.464	6.08	4.22	81.7
3	"	"	0.812	0.641	0.498	6.83	4.53	91.7
4	"	"	0.719	0.612	0.565	7.93	5.13	106
5	"	"	0.660	0.626	0.580	9.83	5.27	132

CONCLUSIONS

It has been found both in theory and experiment that the permanent deformation is considerably reduced by the constraints against axial displacement for beams subjected to large dynamic loading or loads such that the deflection is an appreciable fraction of the beam depth. When the deflection is of the order of beam thickness or greater, the treatment as a beam becomes unrealistic and deformations are primarily governed by axial forces as pointed out by Symonds and Mentel [1]. However, shear effects are small for beams of compact cross-section with ordinary beam dimensions, unless the mass ratio is small. Shear effects become larger for short beams, noncompact sections (e.g., I-section, wide flange or box beams) subjected to impulsive loading.

The one degree of freedom mode assumption facilitates including the effects of elasticity, strain rate and load pulse in the analysis. The concept of plastic hinge or extensible plastic hinge appears to be applicable for dynamic behavior of structures. The simple estimate of strain-rate effects based on this concept was reasonably well confirmed by the experiment, the closest agreement being found for aluminum alloy 6061-T6.

The simple rigid-plastic analysis overestimates the deformation, but serves as a first approximation for large deformations. Consideration of load duration seems to improve the simple rigid-plastic theory.

The effects of load pulse or the finiteness of the load magnitude and duration become smaller when elastic vibration is taken account so that the assumption of impulsive loading becomes better when the elastic effect is considered, even if the elastic effect itself is small.

NOTES

The work presented in this chapter has been followed by not a few investigations into the dynamic plastic behavior of beams with the stretching effect taken into account. Having recourse to numerical scheme or approximation on the basis of bounding procedures or of mode assumptions, analyses have resulted invariably in the importance of the favourable effect due to the axial constraints for deflections of the order of beam thickness. It is to be noted, however, by way of causion for design purposes that a remarkably small axial displacement at the supports can change the response from that of an axially restrained beam, with considerable reserve strengthening beyond the plastic limit load for moderate lateral deflections, to that of a freely supported beam with no increase in strength beyond the limit load, which is derived in a static analysis [24].

Experiments were also conducted, utilizing the gripping device with serrated surfaces which the author of this treatise had designed as described herein. It is reported that this device ensures a fully clamped end condition with axial constraints for specimens [25].

ACKNOWLEDGEMENT

The results of this chapter were obtainded while the author was engaged in his graduate work for the degree of Doctor of Philosophy at Brown University, U.S.A. between 1961 to 1964. He wishes to take this opportunity to express gratidude to Professor Paul S. Symonds for general guidance and encouragement, and also to express appreciation for the experimental facilities made available as well as for invaluable assistance he received from the staff of the University.

REFERENCES

[1] P. S. Symonds and T. J. Mentel, "Impulsive Loading of Plastic Beams with Axial Constraints," Journal of the Mechanics and Physics of Solids, Vol. 6, 1958, pp. 186-202.

[2] J. S. Humphreys, "Plastic Deformation of Impulsively Loaded Straight Clamped Beams," Journal of Applied Mechanics, Vol. 32, March, 1965, pp. 7-10.

[3] H, H. Bleich and R. Shaw, "Dominance of Shear Stresses in Early Stages of Impulsive Motion of Beams," Journal of Applied Mechanics, Vol. 27, March, 1960, pp. 132-138.

[4] M. G. Salvadori and P. Weidlinger, "On the Dynamic Strength of Rigid-Plastic Beams under Blast Loads," Journal of the Engineering Mechanics Division, Vol. 83, No. EM 4, October, 1957.

[5] B. Karunes and E. T. Onat, "On the Effect of Shear on Plastic Deformation of Beams under Transverse Impact Loading," Journal of Applied Mechanics, Vol. 27, March, 1960, pp. 107-110.

[6] T. Nonaka, "Shear and Bending Response of a Rigid-Plastic Beam to Blast-Type Loading," to be published; Chapter 7 of this treatise.

[7] W. Prager, "The General Theory of Limit Design", Proceedings of the Eighth International Congress of Applied Mechanics, Vol. 2, Istanbul, 1952, pp. 65-72.

[8] D. C. Drucher, "The Effect of Shear on the Plastic Bending of Beams," Journal of Applied Mechanics, Vol. 23, Dec., 1956, pp. 506-514.

[9] B. G. Neal, "The Effect of Shear and Normal Forces on the Fully Plastic Moment of a Beam of Rectangular Cross-Section," Journal of Applied Mechanics, Vol. 28, June, 1961, pp. 269-275.

[10] E. W. Parkes, "The Permanent Deformation of a Cantilever Struck Trans-

versely at Its Tip," Proceedings of the Royal Society, Series A, Vol. 228, 1955, pp. 462-476.

[11] E. W. Parkes, "The Permanent Deformation of an Encastrè Beam Struck Transversely at any Point in Its Span," Proceedings of the Institution of Civil Engineers, Vol. 10, July 1958, pp. 277-304.

[12] E. H. Lee and P. S. Symonds, "Large Plastic Deformations of Beams under Transverse Impact," Journal of Applied Mechanics, Vol. 19, Sept., 1952, pp. 308-314.

[13] J. A. Seiler, B. A. Cotter and P. S. Symonds, "Impulsive Loading of Elastic-Plastic Beams," Journal of Applied Mechanics, Vol. 23, Dec., 1956, pp. 515-521.

[14] T. Nonaka, "Large Plastic Deformation of Structures due to Impact - On an Interaction Problem and the Validity of Rigid-Plastic Analysis-", Annuals, Disaster Prevention Research Institute, No. 11A., March, 1968, pp. 607-616 (in Japanese).

[15] T. J. Mentel, "The Plastic Deformation due to Impact of a Cantilever Beam with an Attached Tip Mass," Journal of Applied Mechanics, Vol. 25, Dec., 1958, pp. 515-524.

[16] S. R. Bodner and P. S. Symonds, "Plastic Deformations in Impact and Impulsive Loading of Beams," Plasticity, Pergamon Press, 1960, pp. 488 -500.

[17] S. R. Bodner and P. S. Symonds, "Experimental and Theoretical Investigation of the Plastic Deformation of Cantilever Beams Subjected to Impulsive Loading," Journal of Applied Mechanics, Vol. 29, Dec., 1962, pp. 719-728.

[18] D. P. Updike, "Dynamic-Plastic Deformations of a Ring with Attached Masses," Report, Division of Engineering, Brown University, NSF-GP1115/2, July, 1963.

[19] G. R. Cowper and P. S. Symonds, "Strain Hardening and Strain-Rate Effects in the Impact Loading of Cantilever Beams," Report C11-28 of Brown University, Division of Applied Mathematics to Office of Naval Research, Contract Nonr 562(10), Sept., 1957.

[20] T.C.T. Ting, "The Plastic Deformation of a Cantilever Beam with Strain Rate Sensitivity Under Impulsive Loading," Journal of Applied Mechanics, Vol. 31, March, 1964, pp. 38-42.

[21] T.C.T. Ting and P. S. Symonds, "Impact of a Cantilever Beam with Strain Rate Sensitivity," Proceedings of the 4th U. S. National Congress of Applied Mechanics, pp. 1153-1165.

[22] E. T. Onat and R. T. Shield, "The Influence of Shearing Forces on the Plastic Bending of Wide Beams," Proceedings of the Second U. S. National Congress of Applied Mechanics, June, 1954, pp. 535-537.

[23] P. F. Gillis, "An Estimation of Strain Rate Effects in Cantilever Beams under Impact," Thesis for the Degree of Master of Science, Brown University, 1961.

[24] N. Jones, "Influence of In-Plane Displacements at the Boundaries of Rigid-Plastic Beams and Plates", International Journal of Mechanical Sciences, Vol. 15, 1973, pp. 547-561.

[25] P. S. Symonds and N. Jones, "Impulsive Loading of Fully Clamped Beams with Finite Plastic Deflections and Strain-Rate Sensitivity", International Journal of Mechanical Sciences, Vol. 14, 1972, pp. 49-69.

APPENDIX 1. Effect of Axial Constraints in Elastic Range

In the analysis of Part II, we have disregarded the extensional deformation for the elastic range, and approximated the resisting force as

$$F = 2Q_1 = \frac{4M_1}{\ell} = \frac{24EIy}{\ell^3} \tag{A.1}$$

and the elastic limit displacement as

$$y_e = \frac{M_o \ell^2}{6EI} . \tag{A.2}$$

This was based on the infinitesimal bending theory of a massless clamped beam with length ℓ subjected to transverse relative movement y. However, the presence of axial constraints modifies both F and y_e for finite deflection. We will now estimate the effect of axial constraints on these quantities. The resisting force F^c for a fully clamped beam is (Fig. 29)

$$F^c = 2Q_1 = 2\,\frac{2M_1+N_1y}{\ell} . \tag{A.3}$$

The infinitesimal deflection v at distance x from the fixed end is

$$v = y\left(\frac{x}{\ell}\right)^2\left(3-2\,\frac{x}{\ell}\right). \tag{A.4}$$

The magnitude M_1 of the bending moment at the ends of the beam is

$$M_1 = \frac{6EIy}{\ell^2} . \tag{A.5}$$

N_1 is taken to be the average axial force, i.e.,

$$N_1 = AE\varepsilon_{av} \tag{A.6}$$

where ε_{av} is the average axial strain and taken as

$$\varepsilon_{av} = \frac{1}{\ell}\int_0^\ell \frac{1}{2}\left(\frac{dv}{dx}\right)^2 dx = \frac{3}{5}\left(\frac{y}{\ell}\right)^2 . \tag{A.7}$$

Hence, the ratio of the resisting forces

$$\frac{F^c}{F} = 1 + \frac{N_1 y}{2M_1} = 1 + \frac{3}{5}\left(\frac{y}{h}\right)^2. \tag{A.8}$$

Here, the relation $I = \frac{Ah^2}{12}$ is used.

The elastic limit y_e^c is taken approximately as corresponding to full plasticity for the fully clamped beam, and is obtained as the deflection which satisfies the relation

$$\frac{M_1}{M_o} + \left(\frac{N_1}{N_o}\right)^2 = 1. \tag{A.9}$$

Noting that

$$\frac{y_e}{h} = \frac{1}{2}\,\frac{\sigma_o}{E}\left(\frac{\ell}{h}\right)^2, \tag{A.10}$$

the ratio $\frac{y_e^c}{y_e}$ of the elastic limit deflections is obtained from

$$\frac{y_e^c}{y_e} = \frac{M_1}{M_o} = 1 - \left(\frac{N_1}{N_o}\right)^2 = 1 - \left\{\frac{3}{10}\,\frac{h}{y_e}\left(\frac{y_e^c}{h}\right)^2\right\}^2. \tag{A.11}$$

If we approximate $y_e^c \cong y_e$ in the extreme right-hand side of Eq. (A.11), we have

$$\frac{y_e^c}{y_e} \cong 1 - \left(\frac{3}{10}\,\frac{y_e}{h}\right)^2. \tag{A.12}$$

Let F_e^c and F_e be elastic limit resisting forces for cases with and without axial constraints, respectively. The maximum elastic work or strain energy for the latter is $W_e = \frac{1}{2}F_e y_e$, and for the former is $W_e^c \cong \frac{1}{2}F_e^c y_e^c$; the ratio

$$\frac{W_e^c}{W_e} \cong \left\{1 + \frac{3}{5}\left(\frac{y_e^c}{h}\right)^2\right\}\left\{1 - \left(\frac{3}{10}\,\frac{y_e}{h}\right)^2\right\} \cong 1 - \frac{1}{2}\left(\frac{y_e}{h}\right)^2. \tag{A.13}$$

For example, if $y_e = \frac{1}{2}h$,

$$1 \leq \frac{F^c}{F} \leq \frac{F_e^c}{F_e} \cong 1 + \frac{3}{20}, \qquad \frac{y_e^c}{y_e} \cong 1 - \left(\frac{3}{20}\right)^2$$

and

$$\frac{W_e^c}{W_e} \cong 1 - \frac{1}{8} \, .$$

Thus, we see that

$$F^c \cong F, \quad y_e^c \cong y_e, \quad W_e^c \cong W_e \tag{A.14}$$

with an error of less than 15 per cent. Thus the effect of axial constraints can be neglected in the elastic range when the elastic deformation is a small fraction of the plastic.

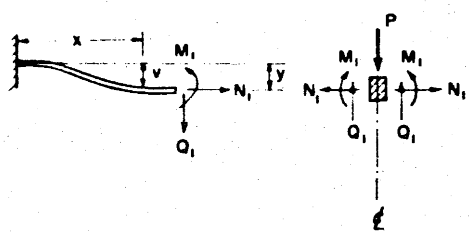

Fig. 29

APPENDIX 2. Effects of Load Duration and Elastic Vibration

In Part I, the load was assumed to be impulsive. A pure impulsive load is an idealization of a load with large magnitude applied for a short time duration and of course no actual load is strictly impulsive. It is worth while to consider how the load shape affects the permanent deformation of the beam for the same total impulse. We will first consider rigid-perfectly plastic beams with and without axial constraints and then include the elastic effect in an approximate manner for the beam without axial constraint, based upon the one degree of freedom mode assumption. We neglect strain-rate effects and shear deformation.

(a) Rigid-perfectly plastic beams

We assume the pattern of motion as shown in Fig. 6 under load $P(t)$. We consider only small deformation so that the string stage is not reached. An equation corresponding to Eq. (2.2) can be readily obtained by modifying Eq. (1.34). We write the displacement of the central mass as y.

The equations of motion

$$(m_o+m\ell)\ddot{y} = P - 2R \tag{A.15}$$

and

$$\frac{m\ell^2\ddot{y}}{6} = 2M_A + Ny - R\ell \tag{A.16}$$

combine to give

$$(m_o+\frac{2}{3}m\ell)\ddot{y} = P - \frac{2}{\ell}(2M_A+Ny). \tag{A.17}$$

The interaction relation

$$\frac{M_A}{M_o} + \left(\frac{N}{N_o}\right)^2 = 1 \tag{A.18}$$

and the flow rule

$$\frac{N}{N_o} = \frac{N_o y}{4M_o} \tag{A.19}$$

together with Eq. (A.17) give

$$(m_o+\frac{2}{3}m\ell)\ddot{y} = P - \frac{4M_o}{\ell}\left\{1 + \left(\frac{N_o y}{4M_o}\right)^2\right\}. \tag{A.20}$$

Multiplying both sides by $\dot{y}$ and integrating, we get

$$\frac{1}{2}(m_o+\frac{2}{3}m\ell)\dot{y}^2 = \int_0^t P\dot{y}dt - \frac{4M_o}{\ell}\left\{y + \frac{1}{3}\left(\frac{N_o}{4M_o}\right)^2 y^3\right\}. \tag{A.21}$$

Deformation finishes when $\dot{y} = 0$ at $t = t_f$ and the final deformation is obtained from

$$\delta\left\{1 + \frac{1}{3}\left(\frac{N_o\delta}{4M_o}\right)^2\right\} = \int_0^{t_f} \frac{P\ell\dot{y}}{4M_o}\,dt\,. \tag{A.22}$$

If the load is a rectangular pulse:

$$P(t) = P_o \left\{ H(t) - H(t-T) \right\} \tag{A.23}$$

then

$$\int_0^{t_f} \frac{P\ell \dot{y}}{4M_o} dt = \begin{cases} \dfrac{P_o \ell}{4M_o} \displaystyle\int_0^T \dot{y} dt = \dfrac{P_o \ell}{4M_o} y_T & \text{if} \quad T \leq t_f \\ \dfrac{P_o \ell}{4M_o} \displaystyle\int_0^{t_f} \dot{y} dt = \dfrac{P_o \ell}{4M_o} \delta & \text{if} \quad T \geq t_f \end{cases} \tag{A.24}$$

The latter case is possible only for a beam with axial constraints. $y_T \equiv (y)_{t=T}$ is obtained by direct integration of Eq. (A.21) which is rewritten as

$$t = \sqrt{\frac{m_1 \ell}{8M_o}} \int_0^y \frac{dy}{\sqrt{y \left\{ \frac{P_o \ell}{4M_o} - 1 - \frac{1}{3} \left(\frac{N_o y}{4M_o} \right)^2 \right\}}} \tag{A.25}$$

where

$$m_1 \equiv m_o + \frac{2}{3} m \ell. \tag{A.26}$$

Writing

$$A \equiv \frac{4M_o}{N_o} \sqrt{3 \left(\frac{P_o \ell}{4M_o} - 1 \right)} \tag{A.27}$$

and

$$y = A \cos^2 \Phi \tag{A.28}$$

we obtain from Eq. (A.25)

$$t = -\sqrt{\frac{m_1 \ell A}{4M_o(\frac{P_o \ell}{4M_o} - 1)}} \int_{\frac{\pi}{2}}^{\Phi} \frac{d\Phi}{\sqrt{1-\frac{1}{2}\sin^2\Phi}} \tag{A.29}$$

or

$$Bt = K - F(\Phi) \tag{A.30}$$

where

$$B = \sqrt{\frac{4M_o(\frac{P_o \ell}{4M_o} - 1)}{m_1 \ell A}} = \sqrt{\frac{N_o}{m_1 \ell}} \sqrt[4]{\frac{1}{3}(\frac{P_o \ell}{4M_o} - 1)}. \tag{A.31}$$

Hence,

$$\Phi = \mathrm{am}(K-Bt), \tag{A.32}$$

$$y = A\,\mathrm{cn}^2(K-Bt) \tag{A.33}$$

and

$$y_T = A\,\mathrm{cn}^2(K-BT) \tag{A.34}$$

Eqs. (A.22) and (A.24) now give

$$\frac{N_o \delta}{4M_o} = \sqrt{3(\frac{P_o \ell}{4M_o} - 1)}, \qquad \text{if} \quad T \geqq t_f$$

and (A.35)

$$\frac{N_o \delta}{4M_o} + \frac{1}{3}(\frac{N_o \delta}{4M_o})^3 = \frac{P_o \ell}{4M_o} \sqrt{3(\frac{P_o \ell}{4M_o} - 1)}\ \mathrm{cn}^2(K-BT), \qquad \text{if} \quad T \leqq t_f .$$

Inequalities $T \gtreqless t_f$ correspond to inequalities $BT \gtreqless K$ and both equations are checked to coincide when $T = t_f$ or $BT = K$.

Using the notation

$$\delta^* = \frac{(P_oT)^2 \ell}{8M_o m_1} \tag{A.36}$$

we get

$$BT = \frac{4M_o}{P_o \ell}\sqrt{\frac{2}{3}\frac{N_o\delta^*}{4M_o}}\ \sqrt[4]{3\left(\frac{P_o\ell}{4M_o} - 1\right)}. \tag{A.37}$$

For pure impulsive loading, the limit $\frac{P_o\ell}{4M_o} \to \infty$ gives

$$\frac{N_o\delta}{4M_o} + \frac{1}{3}\left(\frac{N_o\delta}{4M_o}\right)^3 = \frac{N_o\delta^*}{4M_o} \tag{A.38}$$

which is nothing but Eq. (2.50).

Clearly the deformation for the beam without axial constraint is obtained by omitting the cubic term in the above equations.

Curves are drawn in Fig. 30 for the nondimensional permanent deformation $\frac{N_o\delta}{4M_o}$ as a function of nondimensional load magnitude $\frac{P_o\ell}{4M_o}$ for the case $\frac{N_o\delta^*}{4M_o} = 1$. It is seen that larger magnitude of the load causes larger deformation for the same total impulse. The asymtote for the clamped beam without axial constraint is $\frac{N_o\delta}{4M_o} = 1$ and for the fully clamped beam is the solution of Eq. (A.38): $\frac{N_o\delta}{4M_o} = 0.819$ as $\frac{P_o\ell}{4M_o}$ tends to infinity. The figure shows that the asymptotic approach to the limiting case is speeded by the axial constraint. In both cases, the error due to the assumption of impulsive loading is less than 10 per cent when the load magnitude is larger than 10 times the plastic collapse load.

The condition that the reaction $R \geq 0$ at $t = 0$ gives

$$\frac{P_o\ell}{4M_o} \leq 3\left(\frac{m_o}{m\ell} + 1\right).$$

If

$$\frac{P_o\ell}{4M_o} > 3\left(\frac{m_o}{m\ell} + 1\right) \tag{A.39}$$

the plastic hinges at the ends spread into finite plastic zones. Condition $\dot{y} \geqq 0$ at $t = 0$ gives

$$\frac{P_o \ell}{4M_o} \geqq 1.$$

Thus, the validity of the one degree of freedom type deformation requires

$$1 \leqq \frac{P_o \ell}{4M_o} \leqq 3(\frac{m_o}{m\ell} + 1) \tag{A.40}$$

according to rigid-plastic beam theory. Cases with finite plastic zones are not considered here.

(b) Elastic-perfectly plastic clamped beam without axial constraint

We now consider how the effect of load duration changes when the elastic effect is taken account for the clamped beam without axial constraint. We again use the approximation adopted in the analysis of Part II; that is, the mass of the beam is distributed linearly along the axis but the elastic component of the stress resultants occurs just as in statical loading or in the massless beam. This approximation is equivalent to taking the massless beam as attached by the central mass $m_1 = m_o + \frac{2}{3}m\ell$. We consider the rectangular pulse load. We also assume that the elastic recovery y_{er} is equal to the elastic limit displacement y_e.

If $T \leqq t_e$, eliminating terms due to axial constraints and to the strain-rate in the result in Part II, we have

$$\frac{M_o \delta}{4M_o} = \frac{N_o y_m}{4M_o} - \frac{N_o y_e}{4M_o} = \frac{u_e^2}{2} \tag{A.41}$$

where

$$u_e^2 = \frac{N_o y_e}{4M_o} \left\{ (2 \frac{P_o \ell}{4M_o} \sin \frac{\lambda}{2})^2 - 1 \right\} \tag{A.42}$$

$$\lambda = \frac{4M_o}{P_o \ell} \sqrt{2 \frac{\delta^*}{y_e}} . \tag{A.43}$$

If $T \geqq t_e$, we have equations of motion

$$m_1\ddot{y} + \frac{24EI}{\ell^3} y = P_o \qquad \text{for } 0 \leqq t \leqq t_e,$$

$$m_1\ddot{y} + \frac{4M_o}{\ell} = P_o \qquad \text{for } t_e \leqq t \leqq T, \tag{A.44}$$

and

$$m_1\ddot{y} + \frac{4M_o}{\ell} = 0 \qquad \text{for } T \leqq t \leqq t_m.$$

The solution for the above equations is given in the following nondimensional form:

$$\frac{N_o\delta}{4M_o} = \frac{1}{2}\left\{(u_e + \sqrt{2\frac{N_o\delta^*}{4M_o} - \frac{P_o\ell}{4M_o}\tau_e})^2 - \frac{4M_o}{P_o\ell}(\sqrt{2\frac{N_o\delta^*}{4M_o} - \frac{P_o\ell}{4M_o}\tau_e})^2\right\} \tag{A.45}$$

where

$$u_e^2 = (\frac{P_o\ell}{4M_o})^2 \frac{N_o y_e}{4M_o}\left\{1 - (1-\frac{4M_o}{P_o\ell})^2\right\}, \tag{A.46}$$

$$\tau_e \equiv \sqrt{\frac{N_o}{m_1\ell}}\, t_e = \sqrt{\frac{N_o y_e}{4M_o}} \cos^{-1}(1-\frac{4M_o}{P_o\ell}). \tag{A.47}$$

When $T = t_e$,

$$\sqrt{2\frac{N_o\delta^*}{4M_o}} = \frac{P_o\ell}{4M_o}\tau_e$$

and Eqs. (A.41) and (A.45) coincide.

The above relations are shown in Fig. 31 for $\frac{N_o\delta^*}{4M_o} = 1$ and $\frac{N_o y_e}{4M_o} = \frac{1}{5}(R^* = 2\frac{\delta^*}{y_e} = 10)$. In the figure also included is the curve for a rigid-plastic beam introduced in Fig. 30.

Note that the plastic deformation occurs for $\frac{P_o\ell}{4M_o} > \frac{1}{2}$ when elastic deformations are taken account. We see that the elastic-plastic analysis gives a faster asymptotic approach to the limiting case of impulsive loading, and that it gives a larger deformation than the rigid-plastic analysis for small values of $\frac{P_o \ell}{4M_o}$ and a smaller deformation for large value of $\frac{P_o \ell}{4M_o}$, for the same total impulse. We conclude that the error due to the assumption of impulsive loading decreases when the elastic effect is included.

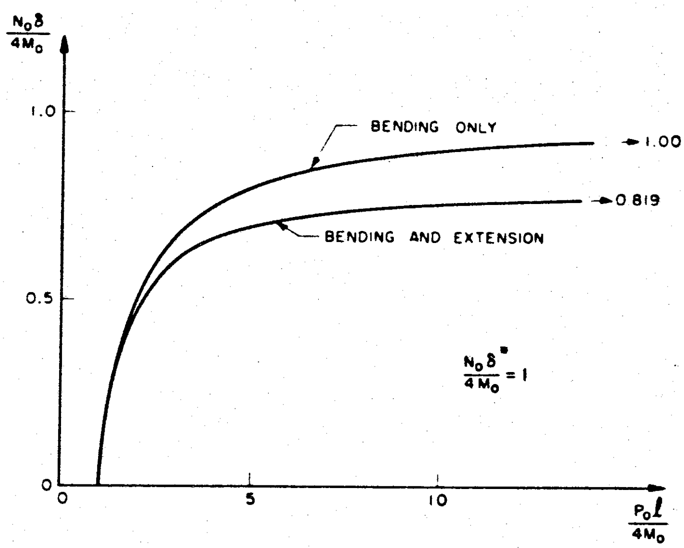

Fig. 30 Effect of load pulse for constant total impulse

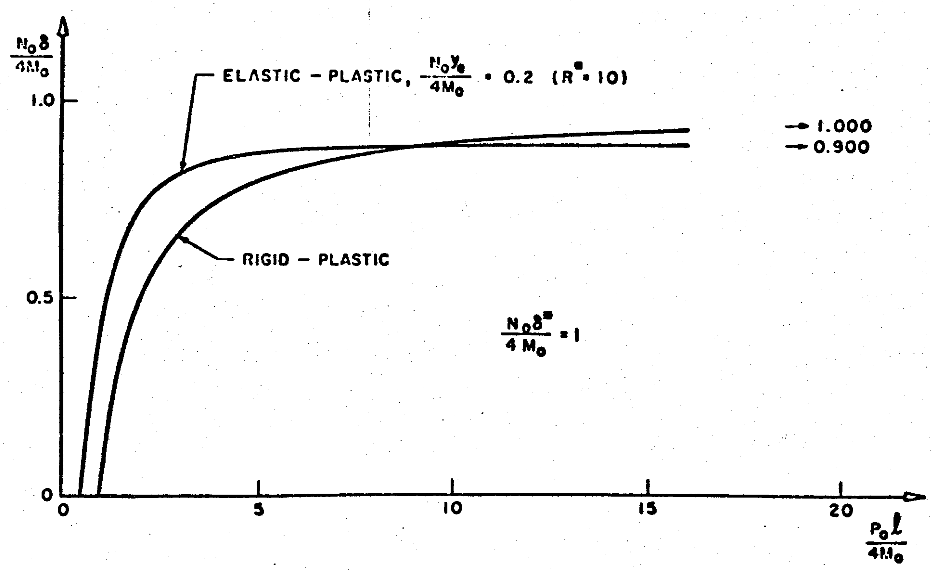

Fig. 31 Effects of load pulse and elasticity